Universitat Autònoma de Barcelona

NOVEL APPROACHES TOWARDS PRECISION MEDICINE IN ACUTE AND CHRONIC HEART FAILURE

Oriol Iborra Egea

Novel Approaches towards Precision Medicine in Acute and Chronic Heart Failure

PhD Thesis by

Oriol Iborra Egea

PhD Program in Medicine

Department of Medicine

NOVEL APPROACHES TOWARDS PRECISION MEDICINE IN ACUTE AND CHRONIC HEART FAILURE

Noves aproximacions a la medicina de precisió en insuficiència cardíaca aguda i crònica

Thesis presented by Oriol Iborra Egea to qualify for the PhD degree by the Universitat Autònoma de Barcelona.

The presented work has been performed in the Insuficiència Cardíaca i REgeneració Cardíaca group (ICREC), at the Germans Trias i Pujol Health Sciences Research Institute (IGTP) and directed by Professor Antoni Bayés Genís, Dra. Carolina Gálvez Montón and Dr. Santiago Roura Ferrer.

Barcelona, 03rd September 2019

Oriol Iborra Egea

(PhD candidate)

Prof. Antoni Bayés Genís (Director and Tutor)

Dra. Carolina Gálvez Montón (Director)

Dr. Santiago Roura Ferrer (Director)

“He who would make accurate forecasts as to those who will recover, and those who will die, and whether the disease will last a greater or less number of days, must understand all the symptoms thoroughly and be able to appreciate them, estimating their powers when they are compared with one another, as I have set forth.”

Hippocrates, Prognostic XXV (Jones, 1923-31)

ABBREVIATION LIST

ACE: angiotensin converter enzyme

AI: artificial intelligence

ALDOB: fructose-bisphosphate aldolase B

Ang-1 and Ang-2: angiopoietin-1 and -2

ANN: artificial neural network

AT1R: angiotensin II type 1 receptor

AUC: area under the curve

B2MG: beta-2-microglobulin

BIRC5: baculoviral IAP repeat-containing protein 5

BNP: brain natriuretic peptide

CAD: coronary artery disease

CS: cardiogenic shock

cTn: cardiac troponins

CTRL: control

CVD: cardiovascular disease

CysC: cystatin C

DM: diabetes mellitus

ECM: extracellular matrix

ESC: European Society of Cardiology

EVs: extracellular vesicles.

FC: fold-change

FDR: false discovery rate

FGF23: fibroblast growth factor 23

GA: genetic algorithms

G-CSF: granulocyte colony stimulating factor

GDF15: growth-differentiation factor 15

GO: gene ontology

GWAS: genome-wide association studies

HF: heart failure

HFrEF: heart failure with reduced ejection fraction

IC1: SerpinG1

IFG: impaired fasting glucose level

IL-1: interleukin-1

INF-γ: interferon gamma

KIM1: kidney injury molecule 1

L-FABP: liver fatty-acid-binding protein

LIMMA: linear models for microarray analysis

LncRNAs: long non-coding RNAs

LVEF: left ventricular ejection fraction

LVECMR: left ventricular extracellular matrix remodeling

MCP-1β: monocyte chemoattractant protein-1β

MHC: major histocompatibility complex

MI: myocardial infarction

MIP-1β: macrophage inflammatory protein-1β

miRNA: microRNA

MnSOD: manganese superoxide dismutase

MoA: mechanism of action.

NGAL: neutrophil gelatinase-associated lipocalin

NHE1: sodium-hydrogen exchanger-1

NT-ProBNP: N-terminal prohormone of brain natriuretic peptide

OPG: osteoprotegerin

PCA: principal component analysis

pPCI: primary percutaneous coronary intervention

PPI: protein-protein interaction

RANTES-403G/A: regulated on activation, normal T cell expressed and secreted polymorphism

RBH: reciprocal best hits

RNAseq: RNA sequencing

SD: standard deviation

SGLT2: sodium/glucose co-transporter

ST2: interleukin-1 receptor-like 1

STEMI: ST elevation myocardial infarction

TNF-α: tumor necrosis factor α

TPMS: therapeutic performance mapping system

XIa: factor XI or plasma thromboplastin antecedent

XIAP: X-linked inhibitor of apoptosis

XIIa: coagulation factor XII, also known as Hageman factor

INDEX

THESIS SUMMARY

Myocardial infarction (MI) is caused by a sudden stop of coronary blood flow that can lead to local ischemia in the heart and causes a pathologic remodeling, which ultimately gives rise to heart failure (HF). Although it might present as a static event, this is a complex and dynamic process.

In this thesis, we aimed to assess HF considering the whole spectrum of the disease. From the acute phase, in which a patient suddenly falls victim to a drastic illness, to investigate the molecular transition towards its chronification and elucidate the mechanisms of action (MoA) of the most novel pharmaceutical therapies in chronic HF. Moreover, growing evidence supports the idea that specific biological processes are likely influenced by their biological context—for example, a specific tissue or a certain disease. This approach constantly generates vast amounts of data, such that putting together, analyzing, and interpreting this information constitutes an overwhelming task.

Consequently, we harnessed artificial intelligence techniques to combine molecular data with clinical responses observed in patients, thus generating a mathematical model capable of both reproducing existing knowledge and discern MoAs hidden under thousands of molecular interactions, otherwise inaccessible.

First, we analyzed the two drugs that are revolutionizing HF management: sacubitril/valsartan, which showed a reduction in the number of deaths and admissions by 22% in recent clinical trials, and Empagliflozin (a SGLT2 inhibitor indicated for type2 diabetes mellitus (DM) patients) that showed an unexpected 32% slash in development of new HF cases in the EMPAREG trial.

Our first study revealed that Sacubitril/Valsartan acts synergistically by blocking both cell death and the pathological makeover of the extracellular matrix (ECM) of cardiac cells. Most importantly, we discovered a core of 8 proteins that emerge as key players in this process.

Secondly, the MoA of Empagliflozin was deciphered using deep learning analyses, which achieved 94.7% accuracy and showed an amelioration of cardiomyocyte cell death by restoring the activity of two genes suppressed during HF, XIAP and BIRC5. These results were confirmed in an in vivo rat model, and proved independent of the presence of DM, suggesting that Empagliflozin may emerge as a new standalone treatment in HF.

Although both drugs have very distinct indications and intrinsic MoAs, their benefits in slowing HF progression were remarkably similar, evidencing a key role for ventricular remodeling.

Thus, next we aimed to explore cardiac remodeling to delineate a structured and clear picture of the complete post-MI remodeling process towards HF. Here, we identified those altered proteins most related to cardiac remodeling in both MI and HF, and used them to look for processes with sustained enrichment throughout MI progression. Once we established which processes are affected at different stages and their evolution during MI, we finally sought to identify the key proteins driving these signaling cascades.

Chronic HF is the leading cause of inter-hospital mortality worldwide, which constitutes an authentic pandemic. However, many of these patients either develop HF derived from an acute event or experience a drastic worsening of the condition during the recurrent hospitalizations. Indeed, acute HF is the leading cause of intra-hospital mortality in more-developed countries, in which cardiogenic shock (CS) represents its most aggressive form. Yet, acute HF receives little attention compared to the chronic form of the disease

By using transcriptomic and advanced proteomics techniques, we first investigated new potential biomarkers to aid CS management. Assessing microRNA and proteins differentially expressed in afflicted patients, we describe the current status of biomarker research in CS, as well as a new molecular score, the CS4P, to reliably predict the prognostic outcomes of these patients.

RESUM DE LA TESI

L'infart de miocardi (IM) és causat per una aturada sobtada del flux sanguini coronari que pot provocar isquèmia local al cor i desencadenar un remodelat patològic, que en última instància pot desenvolupar insuficiència cardíaca (IC). Tot i que pot presentar-se com un esdeveniment estàtic, aquest és un procés complex i dinàmic.

En aquesta tesi, s'ha abordat la IC tenint en compte tot l'espectre de la malaltia. A més, estudis recents donen suport a la idea que processos biològics específics probablement estiguin influïts pel context biològic (p. ex: un teixit específic o una determinada malaltia). Aquesta aproximació constantment genera grans quantitats de dades, de manera que el recull, l'anàlisi i la interpretació d'aquesta informació constitueixen una tasca aclaparadora.

En conseqüència, vam utilitzar tècniques d'intel·ligència artificial per combinar dades moleculars amb respostes clíniques observades en pacients, generant així un model matemàtic capaç de discernir els mecanismes d'acció ocults en milers d'interaccions moleculars, altrament inaccessibles.

Primer, vam voler analitzar els dos fàrmacs que estan revolucionant la gestió de la IC: sacubitril/valsartan, que ha demostrat una reducció del nombre de morts i ingressos en un 22% en assajos clínics recents, i Empagliflozina (un inhibidor de SGLT2 indicat per a pacients amb diabetis mellitus tipus 2) que va sorprendre amb una disminució del 32% en el desenvolupament de nous casos de IC a l'assaig EMPAREG.

El nostre primer estudi va revelar que Sacubitril/Valsartan actua de manera sinèrgica bloquejant tant la mort cel·lular com el remodelat patològic de la matriu extracel·lular dels cardiomiòcits. Addicionalment, vam descobrir un nucli de 8 proteïnes que es posicionen com a actors clau en aquest procés.

En segon lloc, el mecanisme d'acció d'Empagliflozina suggeria una millora de la mort cardiomiocítica mitjançant la restauració de l'activitat de dos gens suprimits durant la IC, XIAP i BIRC5. Aquests resultats es van confirmar en un model de rata in vivo i van demostrar ser independents de la presència de diabetis, indicant que Empagliflozina podria establir-se com a nou tractament en el maneig de la IC.

Tot i que ambdós fàrmacs presenten indicacions i mecanismes moleculars molt diferents, els seus beneficis en la reducció de la progressió de la IC eren notablement similars, evidenciant un paper clau sobre el remodelat ventricular advers.

Així doncs, a continuació vam voler explorar aquest remodelat per delinear una imatge estructurada i clara del procés complet post-IM. Aquí, vam identificar aquelles proteïnes alterades més relacionades amb el remodelat cardíac tant en l'IM com en la IC, i les vam utilitzar per buscar processos amb un enriquiment sostingut al llarg de la progressió de l'infart. Un cop establerts quins processos es veuen afectats en diferents etapes i la seva evolució durant l'IM, finalment vam identificar les proteïnes clau que impulsen aquestes cascades de senyalització.

La IC crònica és la principal causa de mortalitat interhospitalària a tot el món, i es constitueix com a autèntica pandèmia. Tot i això, molts d'aquests pacients o bé desenvolupen IC derivat d'un esdeveniment agut o experimenten un deteriorament dràstic de la condició durant les hospitalitzacions recurrents. De fet, la IC aguda és la principal causa de mortalitat intrahospitalària en països més desenvolupats, i el xoc cardiogènic (CS) representa la seva forma més agressiva. No obstant això, la IC aguda rep poca atenció en comparació amb la forma crònica de la malaltia

Mitjançant tècniques de proteòmica i transcriptòmica avançades, primer vam investigar nous biomarcadors per ajudar a la gestió del CS. Avaluant els microRNAs i les proteïnes expressades diferencialment en pacients afectats, hem descrit l'estat actual de la investigació sobre biomarcadors en CS, així com desenvolupat un nou test molecular, el CS4P, per predir de forma fiable els resultats pronòstics d'aquests pacients.

INTRODUCTION

CARDIOVASCULAR DISEASES - A HEARTED HISTORY

Pharaoh Merenptah, the fourth pharaoh of the nineteenth dynasty of ancient Egypt, died in the year 1203 BC afflicted by atherosclerosis.

In 2009, researchers attending the American Heart Association meeting in Orlando (FL, USA), presented their results showing that 3,500 years old Egyptian mummies had evidence of cardiovascular disease (CVD)— specifically atherosclerosis — in several arteries of the body (1,2). In their work, the authors theorized that diet could be involved, as prominent Egyptians may have eaten large quantities of fatty meats from cattle, ducks, and geese. This study raised some interesting questions, but also shed light on the prevalence and evolution of CVDs in human history.

Early Attention to the Heart – Puzzling Out a Structured Organ

To say exactly when civilization first became aware of CVDs is difficult.

During most of our history as established societies, before the use of the scientific method to understand the world around us, religion and spirituality were the main drivers of medical research.

***Figure 1**. Ebers Papyrus. Source: U.S. National Library of Medicine/National Institutes of Health.*

In the Ebers Papyrus, the oldest anatomical manuscript in the world, we can find detailed cures, ailments and anatomical observations from the ancient Egypt (3500 BC) (**Figure 1**). In its pages, we find a treatise on the heart, which established the heart as the center of the body, mind and soul, responsible for blood supply, but also for all other fluids of the human body—air, tears, urine, feces and semen (3,4). Although it does not appear that ancient Egyptians identified specific structures within the heart, they were able to relate the peripheral pulse with the beating of the heart (4).

Certainly, they were not the only ones. Around 2600 BC, the Chinese society was also investigating the human body and its illnesses. They identified the heart as the organ regulating blood circulation (5,6), also connected to the pulse and responsible to distribute the qi (氣, the life force in ancient Chinese culture) throughout the body via what we now know as the left and right carotid arteries.

There are no records of increasing knowledge of the cardiovascular system for almost two millennia, until 500 BC. Alcmaeon, a pupil of Pythagoras in the ancient Greece, performed a series of anatomical studies that led him to differentiate between veins and arteries, as well as to differ from his predecessors and stated that the mind and consciousness resides in the brain, and not the heart (7,8). Fifty years later, in the Greek island of Kos, one of the greatest revolutions in the history of medicine took place. It started the Hippocratic era. Son of Heraclides and student of Democritus and Gorgias,

Hippocrates led the doctrine that stated, for the first time, that diseases and illnesses occur naturally, rather than being caused by divine punishments. Hippocrates separated medicine from religion and beliefs, and ensured that physicians and scientists based their opinions on scientific evidence and analytical thinking (9–11). This new methodology grounded the anatomical basis of the cardiovascular system, embodied in Hippocrates book “On the Heart” (12). Here, the heart is described as a strong, ovoid muscle located on the left side of the chest surrounded by the lungs. Hippocrates also described for the first time a membrane covering the organ (the pericardium), and the heart as having two ventricles, the left ventricle having thicker walls, and two atria, all separated by the interventricular septum and connected by valves. Not only that, but he also was the first to identify and differentiate the pulmonary artery and vein.

In the following decades, several generations of physicians built upon this knowledge and improved the description mainly of blood vessels and heart valves. In Alexandria (300 BC), Herophilus and Eristratus established the characteristics of arteries and veins, focusing in the aorta and vena cava, and detailed the structure of valves, considering the heart a four-chambered double pump (13,14). During the Roman Era (130 AD), Galen described the muscular fibers responsible for heart contraction and noticed the discordance between inlet and outlet valve aperture; when one set of valves closed, the other set opened (8). Around 1000 AD, anatomists in the medieval Islamic era, such as Haly Abbas and Avicenna, described in great detail the movements and pauses of peripheral pulse and the location, structure and function of coronary arteries, stating that the only way for blood to pass between the two sides of the heart was through pulmonary circulation (15,16). Finally, during the medieval European era (1400 AD), Leonardo Da Vinci managed to incorporate all this knowledge and came with a very accurate

anatomical description of the heart, which established the basics of modern cardiac anatomy (17).

From here, William Harvey and Niel Stensen pioneered the inclusion of the heart's physiology to explain its anatomy (18,19). In the eighteenth century, Raymond Vieussens, Adam Christian Thebesius and Antonio Scarpa followed their steps and described the heart's complex innervation system and established a relationship between anatomy and function of the heart structures (20–22). Finally, between 1839 and 1893, His and Purkinje described the electrical conducting system, which was completed by contributions from Tawara after dissecting the heart and revealed the anatomical details of the atrioventricular conducting system in 1906 (23). These last discoveries led Robert Anderson to describe the morphological changes that occur during congenital malformations within the heart and the location of the conductive system (24).

Learning to Detect Cardiovascular Diseases

It was not until more recent times that heart diseases were diagnosed by carefully interpreting its anatomy and physiology in the appropriate environmental context.

Angina Pectoris — chest pain and/or discomfort that often indicates cardiac ischemic damage caused by insufficient blood flow — had many physicians troubled in the 18th and 19th centuries.

William Heberden (1710-1801) was the first to thoroughly describe angina pathophysiology in 1768, which was believed to be caused by problems in blood circulation in the coronary arteries (25). Following him, William Osler (1849-1919) reported on cardiac arrhythmia, unusual auscultation findings, congenital deformities, and endocarditis. However, lately in his career, Osler also worked extensively on angina,

noting coronary artery spasm and coronary stenosis as a possible cause of angina, which led him to indicate that angina was a symptom as much as a disease in itself (26).

Still, it was not until 1912 that James B. Herrick (1861-1954) differentiated clinical manifestations of coronary obstruction and concluded that the slow, gradual narrowing of the coronary arteries, which impeded a correct blood supply and dismantled the heart's functional integrity, could be a cause of angina (27).

The 20th century marked a period of increased interest, research and understanding of cardiovascular diseases. In 1915, physicians and social workers in the field of cardiology came together in New York City and formed an organization called the Association for the Prevention and Relief of Heart Disease. In 1924, this and other similar organizations became the American Heart Association with the aim of encouraging cardiovascular research to tackle series of diseases that had patients with little hope for treatment or a fulfilling life. Prior to the first world congress of cardiology, which was held in Paris, Europe followed suit and, in 1950, the European Society of Cardiology (ESC) was born.

A few years later, after the American Heart Association came into existence, German physician Werner Forssmann (1904–1979), thanks to contributions from the Portuguese physician Egas Moniz (1874–1955), began to explore the coronary arteries using catheters (28,29); These procedures would lay the foundation of what would become angiographies and cardiac catheterization.

This revolution would come from the hand of a pediatric cardiologist, F. Mason Sones (1918–1985) in 1958, whom developed coronary angiography by injecting small amounts of contrast directly into coronary arteries, producing high-quality diagnostic images capable of accurately identify arterial blockages for the first time. The new technique made possible the development of the most important tools that cardiologists today have

at their disposal to treat cardiac ischemic injuries: coronary artery bypass surgery and interventional cardiology (30–32).

Nevertheless, not every breakthrough came in the form of surgical practices.

Electrophysiology, the proceeding of studying the electrical properties of cells and tissues, led Willem Einthoven (1860-1927) to develop a string galvanometer capable of recording, somewhat precisely, the electrical activity of the beating heart. This first electrocardiographic device, allowed him to describe the alterations on the electrical current as indicators of several cardiovascular diseases, including complete coronary blockage, ventricular hypertrophy, and atrial fibrillation and flutter (33–35).

The field of cardiac imaging was also experimenting its own revolution at the same time. During World War II (1939-1945), sonars harnessing ultrasound technology improved rapidly to detect enemy submarines. Then, Inge Edler (1911-2001) and Hellmuth Hertz (1920-1990) used an adapted military sonar device to record cardiac echoes from Hertz's own heart (35). In 1954, their invention allowed them to monitor the movement of cardiac walls, which then helped physicians interpret the patient’s cardiac function non-invasively (36,37).

All of these improvements in diagnosis also accompanied and shaped patient management, which ultimately have greatly influenced mortality rates worldwide.

From Past to Current Clinical Management

It was in the 1960s and 1970s, when mortality rates of coronary heart disease peaked in 1968 (38,39), that procedures like bypass surgery and percutaneous coronary interventions were first used to help treat cardiovascular diseases by re-establishing blood flow to the injured heart (40–43).

These procedures were followed closely by the introduction of self-expanding, stainless steel wire-mesh structured stents in the 1980s, which helped keep open a narrowed artery for several months (44). Today, revascularization procedures, such as primary percutaneous coronary intervention (pPCI) with stenting, are the intervention of choice to restore arterial blood flow to heart tissue and prevent angina, MI and death.

Indeed, diagnostic assessment of patients with obstructive CAD is crucial to identify which specific conditions are likely to benefit from myocardial revascularization. In this regard, non-invasive diagnostic approaches aimed to assess ischemia and evaluate myocardial viability in patients with local wall motion abnormalities or reduced ejection fraction are recommended as the first-line test in all major clinical guidelines (45). Surely, the detection of a large area of myocardial ischemia by functional imaging is associated with impaired prognosis and thus helps identify which scenarios would benefit the most from revascularization therapies (46,47).

The indications for such therapies in patients with stable CAD are the persistence of symptoms despite medical treatment and/or the improvement of prognosis.

Hence, patients with advanced symptoms but viable myocardium should first undergo revascularization with coronary artery bypass grafting or pPCI before being considered for mechanical circulatory support or heart transplantation.

All of these discoveries, add up to compose the picture for modern clinical cardiology. And it has been a story of great achievements that have improved the life expentancy and quality of live beyond what was thought possible.

However, there is still room for much improvement.

It is acknowledged that the biggest impact on cardiovascular diseases prevalence comes by reducing risk factors and increasing healthy habits. In fact, is estimated that up to 80%

of cardiovascular disease diagnostics are underlined by lifestyle habits (48–51). Thus, physicians are also looking to change some misconceptions about healthy lifestyles, but this is certainly an effort for the whole society to carry, via regulatory and clinical managements, scientific dissemination and individual resolution.

In the meantime, a paradigm shift has been drifting during the past two decades, which aims to understand, and possibly treat pathologies at their most elementary level: the genetic code and its molecular pathways.

A Revolution at the Molecular Level

The biological understanding of how life works at the most fundamental basis, following the explosion of new technologies that made these advances possible, allowed scientists to think about pathologies in a totally different manner. What once was though that diseases and malfunctions were the result of structural variances between individuals, was suddenly transformed in something far more complex. Not only some traits were strongly inherited and thus passes over generations, but also the environmental context in which these elemental building blocks, the genes and their corresponding transcripts and proteins, were fitted also determined their degree of activity. Now, having a specific change in one gene, what we call a mutation, did not translate into the absolute certainty of developing a specific disease. However, the opposite was also true. The presence of one additional mutation, or even an external factor such as an infection, or smoking or your diet, could act as a second hit to trigger the development of a pathology.

Specifically, molecular cardiology aims to apply all this newly found biological features for the mechanistic investigation, diagnosis, prevention, and treatment of cardiovascular diseases, with great interest in the identification of novel circulating factors that regulate cardiac biology.

Subsequently, there have been numerous attempts to apply these novel techniques to the clinical setting (**Figure 2**).

However, routine molecular genetic testing or DNA analysis is not available in most hospitals or clinical chemistry laboratories. In addition, there are few powerful molecular biology tests and gene therapy protocols established for treating cardiovascular diseases, mainly due to a lack of dependable techniques. Thus, there is an urgent demand for the advancement of efficient and dependable molecular cardiology techniques.

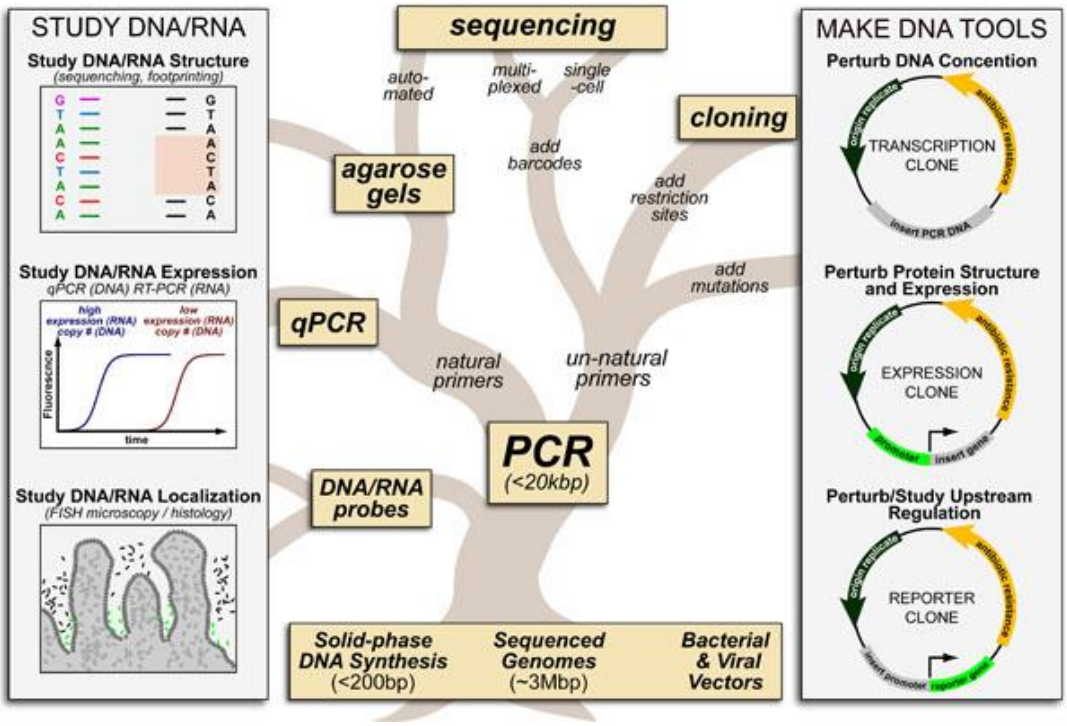

***Figure 2**. Molecular biology has evolved as a vertically integrated discipline, and many techniques share common mechanisms built upon: (1) chemical synthesis of short oligonucleotides, (2) fully sequenced genomes and (3) vectors derived from bacteria and viruses. Source: https://www.practicallyscience.com.*

Several advances have already contributed significantly to the molecular cardiology field. These include the discovery of specific restriction endonucleases to manipulate DNA and reverse transcriptase to amplify specific regions of these molecules, the development of cloning techniques and vector technology and the availability of rapid DNA sequencing.

All of these advances help us to better understand the gene regulation of cardiac and vascular biology, pinpoint genes causing cardiovascular illnesses, diagnose karyotype-related problems and develop gene therapy approaches.

Changes in gene expression are certainly related to the development of cardiovascular disease. However, it is crucial to determine if these changes are the cause underneath a specific cardiovascular issue or are just secondary to it.

Microarray gene expression analysis is a useful tool for mapping gene expression profiles in the injured heart. Moreover, apoptosis is known to play a key role in MI and atherosclerosis, and its modulation could improve several conditions.

Indeed, transcriptomics is an emerging and growing field in biomarker discovery and drug safety assessment. More importantly, transcriptomics has the potential to provide significant insight into the understanding of the disease pathogenesis (52). The most widely analyzed components in transcriptomics are microRNAs (miRNAs) and long non-coding RNAs (lncRNAs), two major families of non-protein-coding transcripts differentiated by their length and specific targets, which can regulate fundamental cellular processes and play critical roles in the pathogenesis of human diseases (53).

MiRNAs, ~22 nucleotides in length, may be obtained in many biological fluids and display promising characteristics of circulating biomarkers, such as robust stability to temperature changes and resistance to degradation by endogenous RNAase activity (54).

Of note, changes in messenger RNA expression levels do not necessarily reflect changes in protein expression levels. Therefore, it is important to determine the functional protein expression. The recent application of proteomic techniques has greatly increased our understanding of the heart disease process. Mass spectrometry has been used for the identification of proteins and their post-translational modifications (55,56). In addition,

functional proteomics provides structural and functional assessments of multiprotein complexes. Thus, cardiovascular proteomics has emerged as a new discipline that will have a great impact on the diagnosis and treatment of cardiovascular disease.

Molecular cardiology has initiated new and exciting approaches to the study of cardiovascular diseases. These new approaches have contributed to traditional cardiology in many ways, including disease pathogenesis, diagnosis and treatment. Gene analysis and transgenic techniques have provided a new understanding of cardiovascular disease pathogenesis. Gene therapy and stem cell therapy have provided physicians and scientists with novel ideas for the treatment of heart diseases, although there is a lack of clinical success at this time.

These technological advances facilitate the study of many biomedical disciplines, including degenerative diseases, cancer and, of course, cardiovascular diseases. Nonetheless, this excitement becomes even more apparent in heart failure (HF), in which an injured heart, usually stemming from a MI, tries to compensate the lost function with burdening consequences for the patient and the whole healthcare industry.

HEART FAILURE - THE END-STAGE FOR A SCARRED HEART

HF is a clinical syndrome characterized at the myocardial level by a pathological ventricular remodeling and dysfunction (57,58), and clinically by breathlessness, lower limb swelling, fatigue, pump failure and sudden death. Usually, HF is a derivative from a structural and/or functional cardiac abnormality, which results in a reduced cardiac output and/or elevated intracardiac pressures.

The principal causes of HF in more industrialized countries are coronary artery disease (CAD) and MI, but the current definition of HF in the clinical guidelines of reference

restricts it to stages at which clinical symptoms are apparent. Nonetheless, patients often display asymptomatic stages induced by already present cardiac irregularities before clinical symptoms become apparent, which are precursors of HF. Thus, the identification of these precursor stages of the disease is important to place preventive activities or start specific treatments early on, which has been shown to reduce mortality (59,60).

Interestingly, a significant number of patients with HF are revealed to have normal left ventricular ejection fraction (LVEF) when examined using an echocardiogram. Thus, HF is categorized based on measurement of the LVEF, which comprises a wide range of patients, from those with normal (or preserved) LVEF (HFpEF; typically considered as ≥50%) to those with reduced LVEF (HFrEF; typically considered as <40%). Patients with an LVEF in the range of 40–49% are more uncertain, and are defined as HF with mid range EF (HFmrEF). These differences are important to determine the underlying etiologies, demographics, co-morbidities and response to therapies.

Chronic Heart Failure – A Broken Heart

Epidemiology, etiology and natural history of heart failure

Symptoms	Signs
Typical	**More specific**
Breathlessness Orthopnoea Paroxysmal nocturnal dyspnoea Reduced exercise tolerance Fatigue, tiredness, increased time to recover after exercise Ankle swelling	Elevated jugular venous pressure Hepatojugular reflux Third heart sound (gallop rhythm) Laterally displaced apical impulse
Less typical	**Less specific**
Nocturnal cough Wheezing Bloated feeling Loss of appetite Confusion (especially in the elderly) Depression Palpitations Dizziness Syncope Bendopnea[53]	Weight gain (>2 kg/week) Weight loss (in advanced HF) Tissue wasting (cachexia) Cardiac murmur Peripheral oedema (ankle, sacral, scrotal) Pulmonary crepitations Reduced air entry and dullness to percussion at lung bases (pleural effusion) Tachycardia Irregular pulse Tachypnoea Cheyne Stokes respiration Hepatomegaly Ascites Cold extremities Oliguria Narrow pulse pressure

***Figure 3**. Symptoms and signs typical of heart failure. Source: 2016 ESC Guidelines for the diagnosis and treatment of acute and chronic heart failure: The Task Force for the diagnosis and treatment of acute and chronic heart failure of the European Society of Cardiology (ESC).*

In general, clinicians use the term HF to refer specifically to the chronic form of the condition. Thus, when not specified, it is meant to discuss chronic HF, which is the most common form as can be derived from many cardiovascular conditions, postulating as a true pandemic illness.

HF prevalence is approximately 1–2% of the adult population in highly developed countries, increasing to ≥10% among people over 70 years of age (61–63), and presenting a lifetime risk of 33% and 28% for men and women respectively, at age 55.

The etiology of HF is very diverse between populations, countries and even continents. As such, patients can develop several pathologies—cardiovascular and non-cardiovascular—that cooperate to precipitate HF. In addition, differentiating between *de novo* cases and inherited cardiomyopathies remains difficult. In most patients, once diagnosed with HF, genetic testing is not further implemented to guide a specific diagnosis, but genetic counselling is recommended in some cases, such as hypertrophic cardiomyopathy, dilated cardiomyopathy or arrhythmogenic right ventricular cardiomyopathy.

Over the last decades, improvements in treatments and their subsequent implementation have enhanced survival and reduced the hospitalization rate in patients with HF. Indeed, 12-months all-cause mortality for hospitalized and stable HF patients have decreased dramatically to 17% and 7%, respectively, and hospitalization rates during the same period are 44% and 32%, respectively, according to the ESC-HF Pilot Study (64). Here, most deaths are mainly attributable to sudden death and worsening HF, with patients suffering from reduced ejection fraction being at higher risk (64,65). Interestingly, hospitalizations are often due to a non-cardiovascular cause, which speaks of the many comorbidities that afflict cardiovascular patients.

Symptoms and signs

As discussed previously, HF is a highly heterogenic, very complex syndrome. As such, symptoms are often non-specific, which difficult the diagnostic and management (**Figure 3**) (66–70). For instance, symptomatology caused by fluid retention can be resolved quickly with diuretic therapy. However, elevated venous pressure and displacement of the apical impulse, although are considered more specific signs, are much harder to detect, leading to mediocre reproducibility (70–72). Moreover, these symptoms can be further masked, and thus become even more challenging to interpret, in the presence of common comorbidities, such as obesity, older age and chronic lung disease (73–75). HF is unusual in the absence of a relevant medical history or a potential cause of cardiac damage. However, the opposite is also true. Various features, specifically previous MI, greatly increase the likelihood of developing HF (66–69). Hence, a detailed medical history is necessary to manage appropriately each patient.

Symptoms and signs are important in monitoring a patient's response to treatment and stability over time. Persistence of symptoms despite treatment usually indicates the need

for additional therapy, and worsening of symptoms is a serious development, which requires prompt medical attention.

Prognosis

There are several reasons why prognostic factors are important in the medical setting. First, by determining which variables are prognostic of outcomes we gain insights on the biology and natural history of the disease. Second, appropriate treatment strategies may be optimized based on the prognostic factors of an individual patient. Third, prognostic factors are often used in the design, conduct, and analysis of clinical trials. Lastly, patients and their families can be informed about the risk of recurrence or death, which can help them cope with the disease evolution.

Various prognostic factors and risk scores of mortality and hospitalization have been identified for HF (65,76–80). However, their clinical application is debatable and accurate risk stratification remains challenging.

Multivariable risk scores have shown some successes in predicting mortality in patients with HF, but fall apart when inferring the probability of a subsequent hospitalization (76,77). Here, a systematic review, which examined a large number of prognostic models, revealed a modest accuracy for models predicting mortality, whereas models designed to predict the combined endpoint of death or hospitalization, or only hospitalization, largely disappointed in their discriminative ability.

Essential initial investigations: natriuretic peptides, electrocardiogram and echocardiography

The plasma concentration of natriuretic peptides, hormones secreted by the heart with functions in blood pressure, natriuretic, diuretic and/or kaliuretic processes, inhibition of the renin–angiotensin system, sympathetic outflow, and vascular smooth muscle and

endothelial cell proliferation, are useful as an initial diagnostic test, especially in the non-acute setting when echocardiography is not immediately available. High levels of natriuretic peptides help identify those patients that may require further investigation with a negative predicting value; in this regard, patients with values below the cut-off mark are usually excluded from additional testing. Thus, patients with normal plasma concentrations are unlikely to develop HF.

It is important to note that several other conditions can cause elevated levels, which weakens their diagnostic convenience. Among them, age and renal failure are the most important confounding factors (81).

To rule out the diagnosis of HF, electrocardiogram readings are routinely used. Although it carries little specificity values, an abnormal electrocardiogram has been shown to increase the likelihood of the diagnosis (70,71,82,83). Moreover, a thorough interpretation of these readings can provide information on etiology or facilitate indications for specific therapies.

Finally, echocardiography is the most useful, widely available test in patients with suspected HF to diagnosis establishment. This methodology provides both immediate and accurate information on crucial variables to establish the diagnosis and the appropriate treatment, including chamber volumes, ventricular systolic and diastolic function, wall thickness, valve function and pulmonary hypertension (84–91). After the echocardiography, magnetic resonance imaging techniques can be used to further improve on the structural detailing of the cardiac irregularities leading to HF.

Acute Heart Failure - Cardiogenic Shock

Definition and classification

Acute HF may present itself as a first occurrence event, but more frequently develops because of an aggressive decompensation of an already established HF condition, which can be caused by a primary cardiac dysfunction or precipitated by extrinsic factors. These include severe infections, uncontrolled hypertension, rhythm disturbances or non-adherence with drugs/diet.

As such, it is a life-threatening condition, which requires urgent admission into the intensive care unit to provide highly experienced technical care.

It exists a large number of classifications for acute HF (92–95), but the most utilized are those based on clinical presentation at admission. This allow clinicians to identify patients at high risk of complications and to direct management at specific targets, which creates a pathway for personalized care in the acute HF setting, according the ESC (96).

In most cases, clinicians first identify the systolic blood pressure of entering patients. According to reports, only 5–8% of all patients show low systolic blood pressure (i.e. <90 mmHg), which has been associated with poor prognosis, particularly when accompanied by hypoperfusion.

Other precipitants, which are feared to lead to decompensation and need to be corrected urgently, include hypertensive emergencies, rapid arrhythmias or severe bradycardia and conduction disturbances, acute mechanical causes and acute pulmonary embolism.

Physical examination on the bedside can also help to identify clinical symptoms of congestion, usually as a result of high left ventricular diastolic pressure rather than to low

cardiac output ('wet' vs. 'dry' if present vs. absent), and/or peripheral hypoperfusion ('cold' vs. 'warm' if present vs. absent) (**Figure 4**) (97,98).

Using this classification, we can specify four groups: warm and wet (well perfused but congested) —the most commonly present; cold and wet (hypoperfused and congested) — which bears the worst outcomes; cold and dry (hypoperfused but without congestion); and warm and dry (compensated, well perfused and without congestion) —which holds the most hopeful outcomes.

In regards of HF caused by MI, patients can be classified according to the severity of the condition, primarily by using the Killip class system (99). Here, class I equals to having no clinically relevant signs; class II includes individuals with rales or crackles in the lungs and elevated jugular venous pressure; class III includes patients with acute pulmonary edema; finally, class IV describes individuals in cardiogenic shock (CS), hypotension and evidence of peripheral vasoconstriction such as oliguria, cyanosis and diaphoresis.

Cardiogenic Shock - A Growing Epidemic

CS is a low-cardiac-output state, caused by left, right or biventricular dysfunction, resulting in a life-threatening state of critical end-organ hypoperfusion and hypoxia. Its most frequently caused by acute MI with left ventricular dysfunction, but other causes include myocarditis, and acute decompensation of HF (100).

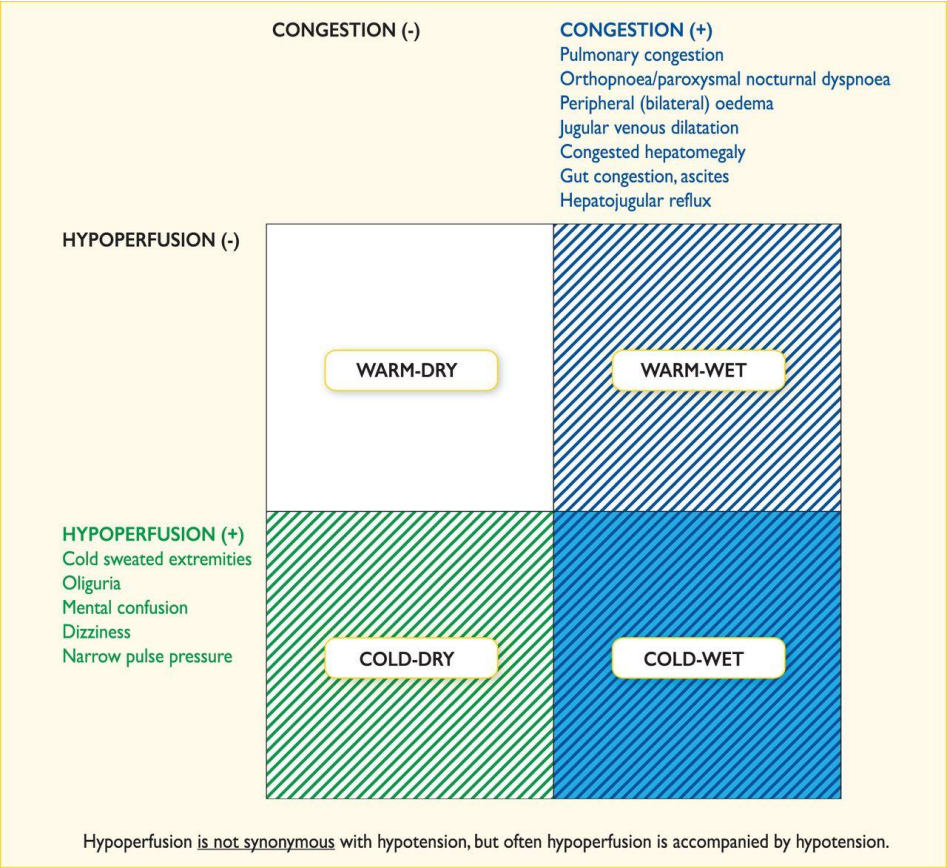

***Figure 4**. Clinical profiles of patients with acute heart failure based on the presence/absence of congestion and/or hypoperfusion. Source: 2016 ESC Guidelines for the diagnosis and treatment of acute and chronic HF: The Task Force for the diagnosis and treatment of acute and chronic HF of the European Society of Cardiology (ESC).*

The incidence of CS has increased remarkably over the past decade, in part associated with an aging population. Acute MI-derived CS increased from 6.5% in 2003 to 10.1% in 2010, with a greater increase among patients older than 75 years (101). Among patients with congestive HF not preceded by acute MI, its incidence rose from 0.5% to 1.0%. During the same period, in-hospital mortality decreased from 62% to 48%, likely due to significant advances in revascularization and supportive care, such as use of mechanical circulatory support. Nevertheless, mortality remains unacceptably high despite recent

advances in the disease management in modern times, with close to one out of two patients dead at 90 days.

CS is not simply a sudden fall in cardiac contractile function. It is also a multi-organ dysfunction syndrome, often complicated by a systemic inflammatory response with severe cellular and metabolic dysregulations (100). Such multi-organ failure, source of countless circulating molecules has been and will be of great value in CS characterization. Indeed, contemporary advances in –omics technologies provide new insight into a more holistic molecular signature of the condition, including myocardial, inflammatory, and end-organ failure.

Diagnosis and Prognostic Evaluation

As the first step in the diagnostic of acute HF, clinicians need to previously exclude alternative causes for the patient's symptoms (i.e. pulmonary infection, severe anemia, acute renal failure). If a diagnostic of acute HF is confirmed, clinical evaluation will lead further management.

The initial diagnosis should be based on the patient’s prior cardiovascular history and potential cardiac and non-cardiac precipitants.

Current diagnostic practices include laboratory studies (biochemical profile and stress-related cardiac enzymes), imaging studies (echocardiography, radiography, angiography…), electrocardiography and invasive hemodynamic monitoring.

It is important to assess the signs and symptoms of congestion, hypoperfusion and seek for diagnosis confirmation using electrocardiogram, chest X-ray, laboratory assessment (with specific biomarkers) and echocardiography evaluations.

These symptoms and signs typically reflect fluid overload (pulmonary congestion and/or peripheral edema) or, less often, reduced cardiac output with peripheral hypoperfusion. Although chest X-ray can be a useful, findings suggest that up to 20% of patients with display a normal test (102). Nonetheless, X-ray can also be useful to identify alternative non-cardiac diseases that may cause or contribute to the patient's symptoms.

Of note, the electrocardiogram on these patients is rarely normal (103), but can also be helpful in identifying underlying cardiac disease and potential precipitants.

Management

As stated previously, acute HF is a life-threatening medical condition, which requires admission to an intensive care setting and fluid resuscitation to correct hypovolemia and hypotension. Although it’s very scarce, patients also need prompt initiation of pharmacologic therapy to maintain blood pressure and cardiac output (aspirin/heparin, diuretics and inotropic and/or vasopressor drug therapy) and early restoration of coronary blood flow (but these procedures are highly invasive, such as pPCI, stenting and using ventricular assisting devices).

Of course, early diagnosis is important in acute HF. Therefore, all patients should have a diagnostic workup and appropriate pharmacological and non-pharmacological treatment started as promptly as possible.

Initial evaluation and continued non-invasive monitoring of the patient's vital cardiorespiratory functions, including pulse oximetry, blood pressure, respiratory rate and a continuous electrocardiogram instituted within minutes, is essential to evaluate whether ventilation, peripheral perfusion, oxygenation, heart rate and blood pressure are adequate (**Figure 5**).

Oxygen therapy and/or ventilatory support

Oxygen therapy, which should not be used routinely in non-hypoxemic patients due vasoconstriction and a reduction in cardiac output (104,105), is usually performed with both continuous positive airway pressure and bi-level positive pressure ventilation.

Congestion affects lung function and increases intrapulmonary shunting, resulting in hypoxemia. Non-invasive positive pressure ventilation reduces respiratory distress and may decrease intubation and mortality rates (106–109).

Pharmacological therapy

Diuretics

Diuretics are a cornerstone in the treatment of patients with acute HF and signs of fluid overload and congestion. These drugs act by increasing renal salt and water excretion and have some vasodilatory effect. The initial approach to congestion management involves intravenous diuretics with the addition of vasodilators for dyspnea relief.

Vasodilators

Intravenous vasodilators are the second most often used agents in acute HF for symptomatic relief; however, there is no robust evidence confirming their beneficial effects.

They have dual benefit by decreasing venous tone (to optimize preload) and arterial tone (decrease afterload). Consequently, they may also increase stroke volume. Vasodilators

are especially useful in patients with hypertensive acute HF, whereas they should be avoided in patients with CS.

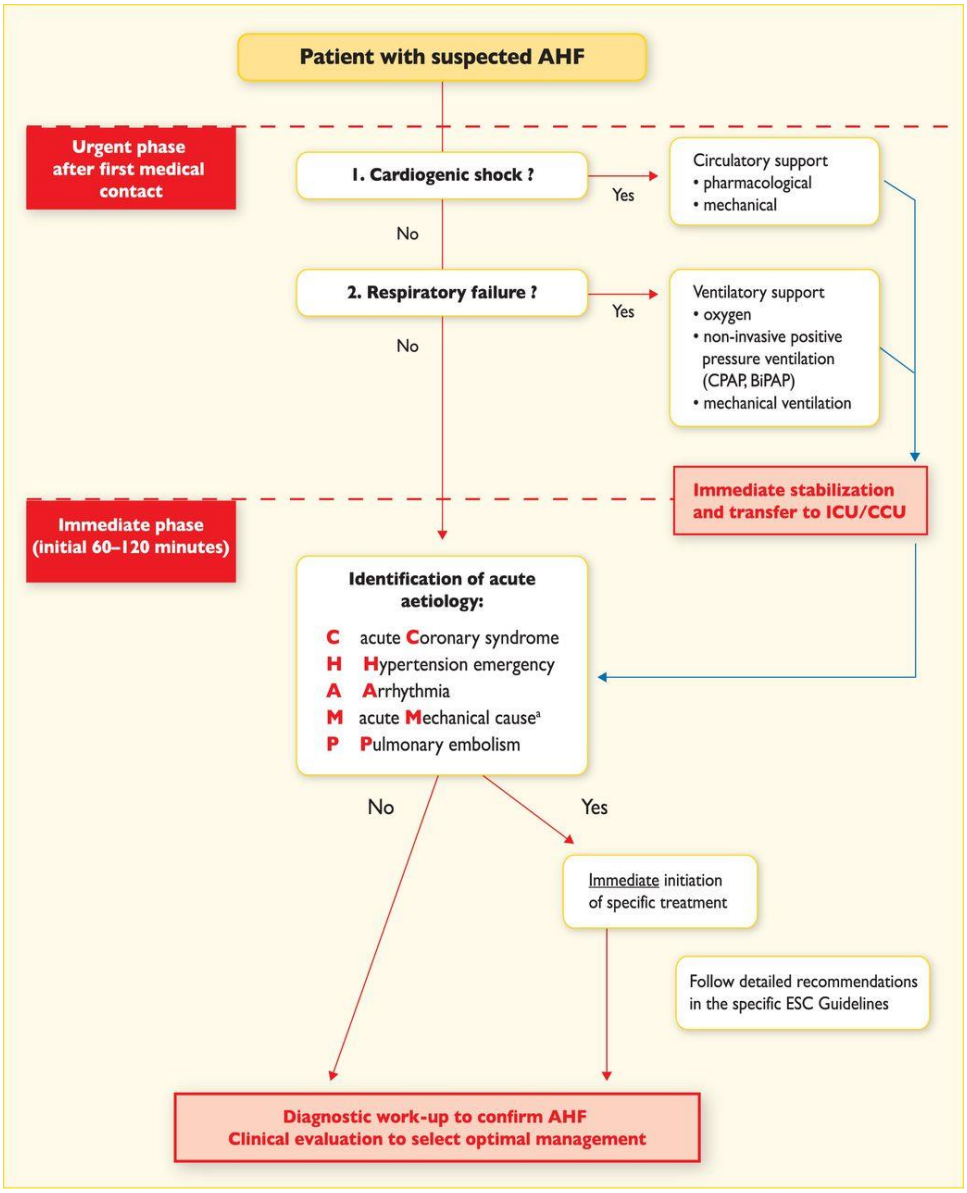

Figure 5. Initial management of a patient with acute heart failure. Acute mechanical cause: myocardial rupture complicating acute coronary syndrome (free wall rupture, ventricular septal defect, acute mitral regurgitation), chest trauma or cardiac intervention, acute native or prosthetic valve incompetence secondary to endocarditis, aortic dissection or thrombosis. Source: 2016 ESC Guidelines for the diagnosis and treatment of acute and chronic heart failure: The Task Force for the diagnosis and treatment of acute and chronic heart failure of the European

Vasopressors

Drugs with prominent peripheral arterial vasoconstrictor action are given to patients with marked hypotension. These agents are given to raise blood pressure and redistribute blood to the vital organs. However, this is at the expense of an increase in left ventricular afterload.

Thromboembolism prophylaxis

Thromboembolism prophylaxis with anticoagulants is recommended unless contraindicated or unnecessary.

Vasopressin antagonists

Vasopressin antagonists block the action of arginine vasopressin in renal tubules and promote aquaresis, which may be used to treat patients with volume overload and resistant hyponatremia.

Opiates

Opiates relieve dyspnea and anxiety in patients with severe dyspnea and pulmonary edema.

Mechanical assist devices

Intra-aortic balloon pump

The conventional indications for an intra-aortic balloon pump are to support the circulation before surgical correction of specific acute mechanical problems (e.g. interventricular septal rupture and acute mitral regurgitation), during severe acute myocarditis and in selected patients with acute myocardial ischemia or infarction before, during and after percutaneous or surgical revascularization.

PRECISION MEDICINE – IT IS WEIRD NOT TO BE WEIRD

If this thesis were to end here, we would imagine our response to HF as being in the pinnacle of the possible treatments. Certainly, if we combine our prowess in biomarker strategy to detect cardiovascular irregularities early on, with all the interventional advances to rapidly restore blood flow guided by imaging techniques and our best drug therapies to counteract the physiological decompensation occurring after such aggressive conditions, we can rejoice; we have come a long way. However, HF still amounts a large toll on global mortality, albeit far smaller than it could have been if not for the abovementioned breakthroughs, and remains one of the most heterogenic and complex illnesses to burden our healthcare systems.

In addition, we still encounter one final problem.

Up until now, all our treatments have been tested and stressed in randomized clinical trials, which ideally include a large number of patients and as much diversity as possible within our research of interest. On the surface this is the best possible way down the research line, and it has absolutely helped in determining which therapies and interventions could help the larger number of patients; the majority.

However, this may not be the best strategy anymore.

A Tailored Approach for Personalized Treatment and Prevention

The addition of multiple variables in research drives further away individuals from the average than for any single measurement alone, which increases diagnostic sophistication make diseases become more dissimilar as a result. This phenomenon is known as the curse of dimensionality.

All the advances discussed here, from interpreting the pathophysiology of cardiovascular diseases in terms of structural and physiological abnormalities, to understanding their underlying molecular mechanisms according to individual variability among patients both, in the biological and environmental contexts, follow a line of thinking that has produced spectacular results in the clinical and pre-clinical setting. And the aftermath of such investigations over the last decade allows for a tailored approach to each person. This is what we know as precision medicine. Nonetheless, failure to consider the curse of dimensionality will ultimately lead to inherent limits on the degree to which precision medicine can extend the advances of evidence-based medicine for selecting suitable treatments (110).

Suddenly, we can start thinking on those patients in clinical trials that did responded to a specific therapy, but saw their improvements vanish because overall it was not helping a larger group of people.

Not only that, but we can design much more specific and flexible clinical trials that could be adjusted depending solely on the response of specific members of the cohort under study. Certainly, this could massively help close the last gap in HF management.

Succinctly, this strategy allows doctors and researchers to predict more accurately which treatment and prevention strategies for a particular disease will work in which groups of people. It is in contrast to a one-size-fits-all approach, in which disease treatment and prevention strategies are developed for the average person, with less consideration for the differences between individuals.

The underlying concept of precision medicine is not new. For example, transfusion patients have been matched with donors according to blood type for more than a century (111,112). However, advances in molecular biology, and the growing availability of

health data, present an opportunity to make precise personalized patient care a clinical reality.

Nonetheless, there are many challenges to overcome prior to fulfil this vision.

At its core, precision medicine is powered by patient data. Health records, genetic codes and gene/protein expression of patients, healthy volunteers and molecular biology understanding, including protein-protein interactions and other forms of molecular activity, are vital to get a complete picture of the disease and the best way to tackle it. However, all of this information amounts to vast quantities of data that need to be analyzed and integrated seamlessly, which a human could never do by itself.

SYSTEMS BIOLOGY AND ARTIFICIAL INTELLIGENCE- RISE OF THE MACHINES

Growing evidence supports the idea that specific biological processes (e.g., protein–protein interactions or epigenetic regulations) are likely influenced by the biological context—for example, a specific tissue or a certain disease.

In current research, *in silico* and *in vitro* modelling are widely extended as the initial phases on any biological investigation. When faced with positive outcomes, this scales up into animal models in pre-clinical testing. Of note, compared to small animal models, large experimental animal models more closely resemble human cardiac physiology, function, and anatomy, and thus their use constitutes a key step in translating experimentally obtained information into clinical use (**Figure 6**). During all these stages and beyond, including clinical trials, vast amounts of data are constantly being generated worldwide, such that putting together, analyzing, and interpreting this information as a whole constitutes an overwhelming task. For this purpose, new technologies are rapidly

emerging, which combine different engineering approaches and bioinformatics. Within this context, systems biology arises as an interdisciplinary field of study, which aims to unravel the key interactions within complex biological networks following a holistic approach based on computational and mathematical models.

This new field of research explores the adoption of machines capable of "intelligent" behavior. To do so, artificial intelligence, and more specifically machine learning and deep learning, attempt to mimic human cognition using proxy reasoning and deduction skills and natural language processing. This approach has already made large contributions to the medical field in the short span of its existence.

In medical imaging diagnosis, computer analysis has achieved autonomous interpretation of X-Ray on par with highly trained physicians, by improving image reconstruction, noise reduction, quality assurance, triage, segmentation, computer-aided detection and computer-aided classification (113). Here, ~5% of image interpretations rendered by radiologists contain clinically important errors, with inter- and intra-observer variability rates as high as 37%, depending on the imaging modality (114–116). In stark contrast, machine learning algorithms approach a ~2% error rate (117).

Another major contribution of artificial intelligence involves re-shaping the whole industry behind drug discovery. While much of the healthcare industry is largely based on trial and error methods to discover new drug sites, drug components and re-positioning already existing treatments, drug discovery stands out as a relatively straightforward economic value for machine learning applications. By integrating as much data as possible about each component of the drug-therapy combination, modern algorithms can simulate almost every interaction between each component as well as to predict the best scenario for this interaction to occur. This new approach creates a data-driven hypothesis

that pharmaceutical companies can pursue to minimize risk and time, and economical losses.

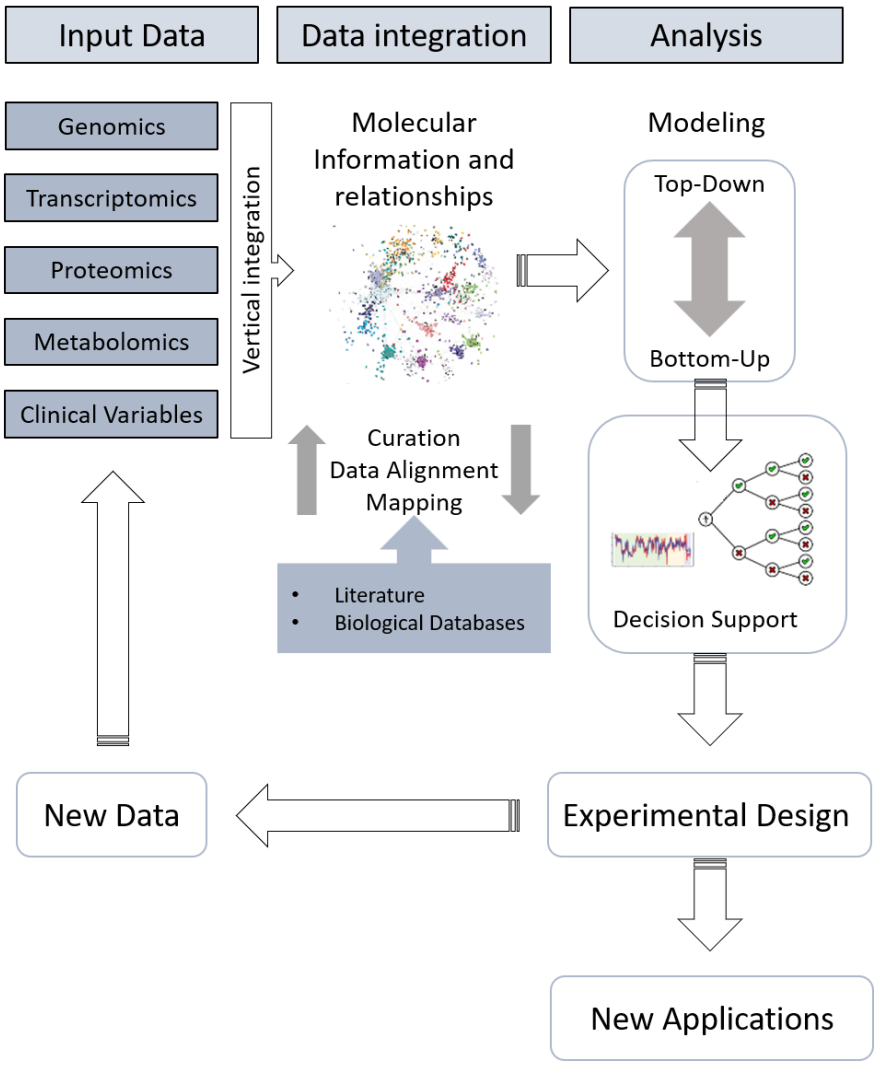

***Figure 6**. Schematic flowchart of a systems biology approach.*

Additionally, artificial intelligence is not only useful to predict outcomes. In the advent of the big data era, in which incommensurable amounts of data are generated in each step of the research line, artificial intelligence can be used as a descriptive tool to integrate these datasets and gain insight in the structure and classification of the data. In doing so, researchers can fit very complex datasets and generate a clear picture representative of the whole system (e.g., a complex disease), which considered every variable possible.

This application is what could directly impact patient management. By virtue of this analyses, drug and dose prescription could be fined tuned for each patient, but also the decision of incurring in invasive treatments or procedures can also be assisted by understanding the whole condition as one but with specific differences between patients.

However, medicine is more than math.

A researcher or a physician is not just an advanced mathematical model considering data entries and elaborating out the most likely diagnosis. Healthcare professionals are constantly evaluating streams of information that machines today are incapable of replicating. The look on a patient's face, their behavior and nervousness, their body language and way of talk or what their relatives and acquaintances inform about their behavioral changes. Thus, although very helpful, replacing the job of said professionals – at least for general diagnosis, assessing biological relevance and management – is inconceivable.

Indeed, while machine learning can support diagnosis and decision-making, a physician judgement will still be needed to factor in the specific context of each patient. Nonetheless, from the technical standpoint, an artificial intelligence algorithm properly trained can easily surpass any human expertise in managing large variables.

PROLOGUE

In this thesis, we considered this preamble sufficient to educate the reader towards a better understanding on the history of cardiovascular research, but also in what HF is, why it poses a burden for the whole society, how can we currently manage it and what could we do in the future to keep slowing its progression.

Onwards, we present the results obtained after implementing machine learning and deep learning techniques to investigate two of the most revolutionary drugs posed to change chronic HF management and elucidate their common mechanism involving adverse cardiac remodeling, which describe the evolution of MI towards HF. Furthermore, we also describe our approach to improve acute HF diagnostic and prognostic prospects by using advanced targeted proteomic and transcriptomic analyses.

HYPOTHESIS

By using a systems biology approach, we can combine transcriptomic, proteomic and big data information to assess both acute and chronic HF and obtain new molecular candidates to improve understanding, prognosis and patient management.

OBJECTIVES

Main Objective

Implement OMICs technologies and artificial intelligence models to impact prognosis and patient management in acute and chronic HF.

Secondary Objectives

Chronic HF

1. Elucidate the molecular mechanism of action (MoA) of novel pharmacological therapies (sacubitril/valsartan and empagliflozin) in HF patients (with and without diabetes mellitus (DM)).
2. Complete molecular characterization of post-MI remodeling towards HF using artificial intelligence

Acute HF (Cardiogenic Shock)

3. Use transcriptomic analysis to search for new potential biomarkers to aid CS prognosis – microRNAs.
4. Investigate the current state of biomarker research in CS and use proteomic analysis to search for new potential biomarker candidates to aid CS prognosis.

MATERIALS & METHODS

Chronic Heart Failure

Artificial Intelligence Models

Compilation of transcriptomic data

Transcriptomic information was derived from a series of well-characterized cohorts for each independent study, including a microarray gene-expression pattern obtained in vivo after infarct induction in a swine model to explore post-myocardial infarction (MI) remodeling. It also contained publicly available RNA sequencing (RNA seq) datasets (public data available in GEO, accession GSE57345, subseries GSE57338; GSE57345, subseries GSE57338; and GSE26887), from failing and non-failing hearts, to explore heart failure (HF) ventricular remodeling, and myocardial tissue data derived from heart failure with reduced ejection fraction (HFrEF) with (118) or without DM (119) to model the molecular effects of Sacubitril/valsartan and empagliflozin respectively in each scenario (119,120).

First, the datasets were filtered to discard all entries showing contradictory information (i.e., two entries for the same gene name with negative and positive ratio values), and to identify the number of unique altered genes. Next, whenever including animal data into the models, it is required to be translated to their human equivalents via Reciprocal Best Hits (RBH) with BLAST and Gene Name Correspondence (i.e.; the swine transcriptomic information). Pig-to-human RBH were identified using the InParanoid database (121). If RBH were not found for a protein, we used the reviewed UniProt entry for the human protein with a matching gene name as a correspondence (Supplementary Table 1).

Then, the proteins were labelled with a certain "state" based on whether the protein is activated or inhibited under physiological conditions (defined by FDR > 0.01 and logFC > 0.25), and this information was used as baseline. Finally, proteins with human UniProt IDs within each cohort were used as molecular restrictions for our models.

Microarray data was processed using the GEO2R tool (122), and compiled and processed using the neqc method for normalization (123) and Linear Models for Microarray Analysis (LIMMA) (124,125). Both methods allowed identification of differential expression and calculation of fold-change (FC). The P values obtained for each probe were adjusted using the Benjamini-Hochberg FDR at a significance level of 0.01 (126,127). We only considered genes with an adjusted P value of <0.01, and logFC > 0.25. For introduction into the protein network, gene information was mapped one-to-one with proteins.

Molecular characterization of pathologies and drugs

In brief, we integrated published data with our results defining a set of molecular profiles characterizing MI, HF, adverse myocardial remodeling and DM, as well as the described molecular interactions of Sacubitril/Valsartan and Empagliflozin for each independent

study, which were used to build the protein network and the subsequent mathematical model.

When a specific molecular information describing the condition was found, the articles were thoroughly reviewed to identify protein/gene candidates to feed the mathematical models. When the evidence of the implication of a candidate in the condition was judged not consistent enough to be assigned as an effector, an additional search was performed specifically for the candidate, including all the protein names according to UniProtKB. No text-mining tools were used to avoid intrinsic technical biases, and only English-language articles were included, which accounted for more than 6509 items reviewed.

Moreover, pharmacological data and molecular relationships described for MI, HF and DM were expanded by integrating massive, publicly available databases such as Drugbank, Reactome, MINT and BioGrid. All this information accounted for more than 350.000 interactions in each case (Figure 10), in which gene information was one-to-one mapped to proteins for introduction into the protein network,.

To study the effects of Sacubitril/Valsartan, we included a list of 6739 proteins (4737 for MI and 2002 for HF), with 672 overlapping proteins (**Figure 7**). To investigate the evolution of MI towards HF, we used the gene expression data of a post-infarction model in swine at 6, 30, and 45 days of evolution. We used samples from the infarct core area (hereafter termed C6, C30 and C45, which included 4737, 4730, and 4203 differentially expressed proteins, respectively) and from the remote area surrounding the infarct localization (hereafter termed R6, R30, and R45, which included 122, 117, and 21 differentially expressed proteins respectively).

By using this data, we identified the main pathophysiological processes that were altered in MI and cardiac remodeling. We then further characterized them at the protein level,

ultimately using a set of 136 unique proteins reported to play a role in cardiac remodeling to study Sacubitril/Valsartan (Supplementary Table 3), 280 proteins of interest to study empagliflozin (Supplementary Table 9) and 202 unique proteins (121 related to MI and 136 to cardiac remodeling) to assess the progression of MI towards HF.

This collection of experimental pathophysiological signals was used as a list of principles, termed a truth table, which apply to a specific condition (i.e. some proteins are overexpressed only in HF patients with DM) (128) and allow to delineate the molecular behavior of each situation.

Therapeutic performance mapping system (TPMS) technology

TPMS (129–132) uses as input a combination of biological information drawn from manual curation of the literature and public and private databases (e.g. Reactome, MINT, BioGrid) and experimental information about the disease under study. Then, TPMS creates mathematical models of the patients (either real, when using clinical data, or objective of treatment/study, when using preclinical data), which displays the mechanistically-based result that explain the observable clinical outcomes, in this case adverse cardiac remodeling (output). A simple example of input-output pair would be drug-indication, as for example acetylsalicylic acid, and headache; both clinical terms are then translated to the protein level (i.e. acetylsalicylic acid's molecular target, and the whole set of proteins and genes whose function modulations have been associated with headache). Typical results of TPMS are: a compound's MoA, a molecular mechanism of a gene/protein function modulation or combinations thereof, repositioning of compound, finding of therapeutic targets for a given disease, mechanistically-rooted biomarkers, clinical prediction of the efficacy and safety of a compound.

Generation of mathematical models

The mathematical models were constructed through TPMS technology. Through the use of artificial intelligence and pattern recognition techniques (based on optimization methods of genetic algorithms (GA), where GAs differ from traditional methods by working with a coding of the parameter set (instead of the parameters themselves), searching from a population of points, using payoff (objective function), and probabilistic transition rules.) (133–135), this technology generates mathematical models that integrate all the available biological, pharmacological and medical knowledge and are able to suggest mechanistic hypotheses that are consistent with actual biological processes, e.g. to simulate human physiology in silico(136–141) (Supplementary Table 5 and Supplementary Table 6). This goal is achieved by compiling information about the drug (Sacubitril/Valsartan or Empagliflozin) and/or the disease under study (post-MI, HF, ventricular remodeling or DM), and then incorporating it into the Biological Effectors Database (BED) (130). TPMS BED, is a hand-curated database that relates biological processes (adverse drug reactions, indications, diseases and molecular pathways) to their molecular effectors, i.e. each one of the proteins involved in the physiological process (Supplementary Figure 2).

The models are able to weight the relative value of each protein (node). However, the large number of links exponentially increases the number of parameters that have to be solved. Different approaches and optimization systems can be called upon in this scenario. These may be based on randomized systems (such as a Montecarlo based system) (142), or use information derived from the topology of the network.

Generating a molecular model of cardiac remodeling

With these model already set up, and starting from the differential proteins for each cohort, to study the progression of MI towards HF we performed a relationship analysis to identify proteins that were mechanistically related to cardiac remodeling. Proteins having a predictive value of >50% (corresponding to a ~20% probability of accepting false positives) were included for further evaluation (**Table 1**). Thus, we were able to construct a molecular model specifically trained to bear the analysis of the remodeling occurring after MI.

Upon identifying the differential proteins more closely related to cardiac remodeling, two analyses were performed. A gene set enrichment analysis (GSEA) method, based on functional annotation of the differentially expressed genes, was used to identify relevant biological processes (KEGG pathways, GO function, and GO process terms) (143,144). We also applied triggering proteins analysis to identify the key proteins in a network, which strongly affected the rest of the dataset (i.e., the proteins triggering the observed output). These proteins were further investigated, and sampling methods were used to explore their exact relationship to cardiac remodeling.

Protein localization	*C6*	*C30*	*C45*	*R6*	*R30*	*R45*
# of proteins mechanistically related to cardiac remodeling	3302	3267	2930	83	77	13

***Table 1**. Number of proteins found to be mechanistically related to cardiac remodeling. C: infarct core area; R: remote area; 6: 6 days after infarction; 30: 30 days after infarction; 45: 45 days after infarction.*

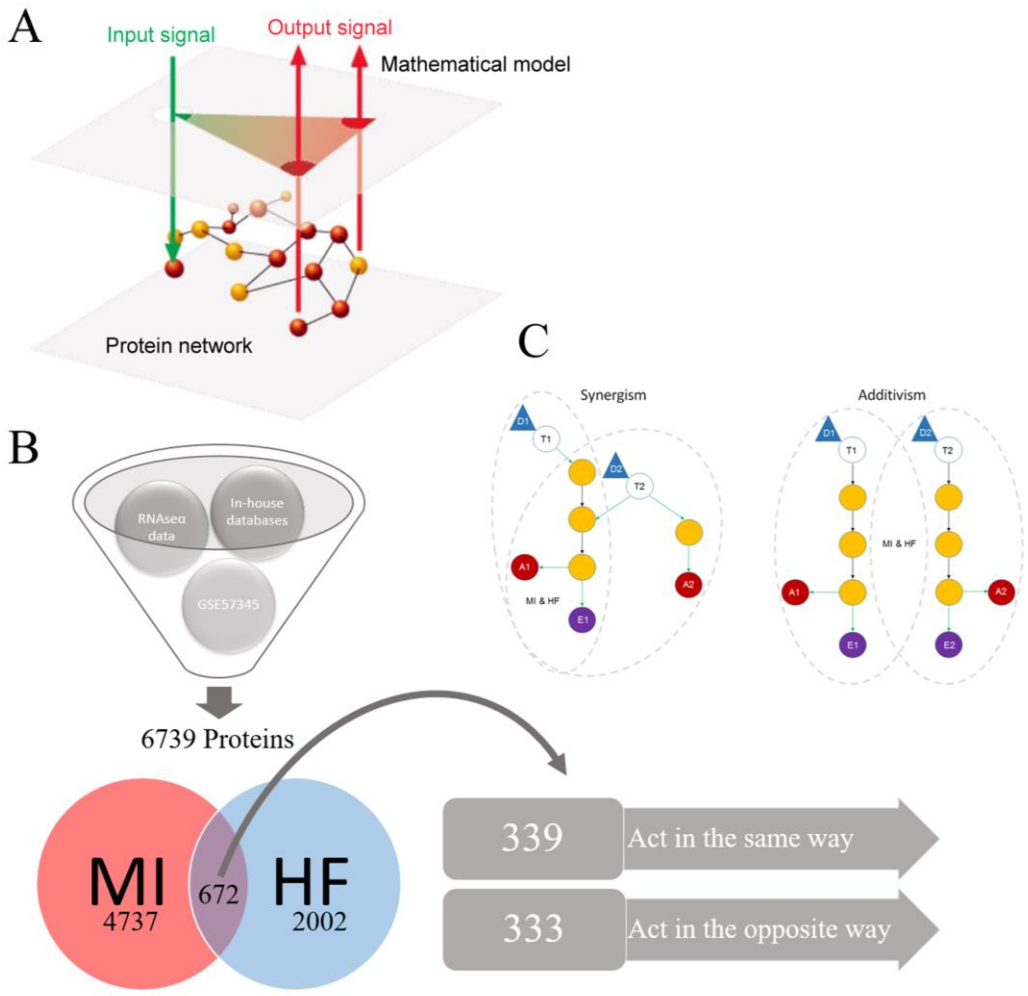

***Figure 7**. Schematic representation of the mathematical model workflow. A) Illustration of the input/output data flow. Once all the information available around Sacubitril/Valsartan targets (eg. Drugbank), the pathophysiology of both conditions (MI and HF) (input signals, green arrows) and its links to cardiac remodeling (output signals; red arrows) have been identified and characterized at the protein level, the protein network is built. Then the models are trained with all this information and emit how the system is more likely to respond at the protein level (whether by up-regulation or down-regulation) after a certain treatment. Thus, we can elucidate one MoA that is able to explain how the system goes from the stimulus (input) to the observable clinical response (output). B) Depiction of data processing using TPMS technology. C) Synergism/additivism schemes. Triangular shapes represent drug administration. Void circles act as the drug targets. Yellow circles represent downstream proteins participating on the cascade. Red and purple circles refer to different types of effects. Grey dotted-line patterns show the pathways of each condition, marking if there is a common share. MI= myocardial infarction; HF= Heart*

Solving the mathematical models

TPMS technology includes two different and complementary strategies to solve mathematical models:

- Artificial Neural Networks (ANNs): ANNs are supervised algorithms which identify relations between drug targets and clinical elements of the network (130,145). This strategy is able to identify relationships among regions of the network by inferring the probability of the existence of a specific relationship between two or more protein sets (relationship between Sacubitril/Valsartan protein targets and cardiac remodeling pathway), based on a validation of the predictive capacity of the model towards the truth table. The creation, validation, refinement and checking of the mathematical model that explains the behavior of the network is done by using known data (Known Input) about targets, mechanisms of action of drugs (Hidden MoA), and their clinical observable effects contained in truth table (Known Output) (Supplementary Figure 3).

The raw information that is fed into the network is known as Input layer. The learning methodology used consisted in an architecture of stratified ensembles of neural networks as a model, trained with a gradient descent algorithm to approximate the values of the given truth table. In order to correctly predict the effect of a drug independently of the number of targets, different ensemble of neural networks are trained for different subset of drugs according to their number of targets (drugs with 1 target, 2 targets, 3 targets…). Then, the predictions for a query drug are calculated by all the ensembles, and pondered according to the number of targets of the query drug.

Specifically, the neural network model used is a Multilayer Perceptron (MLP) Neural Network classifier (146–148). MLP gradient descent training depends on randomization initialization. In this way each training process, applying exactly the same truth table, can

give slightly different resulting models. In order to generate each of the ensembles, 1000 MLPs (Multilayer Perceptrons) are trained with the training subset. The best 100 ones are used as ensemble. When a new drug-indication pair has to be classified as probable or false, the features describing the topological relation between targets and indication effectors are classified with each of the ensembles; in order to obtain the most accurate prediction, the difference between the number of targets of the query (number of targets of Sacubitril and/or Valsartan) and the number of targets of the drugs used to calculate each ensemble is used to ponder the result of each ensemble. The higher the difference between the numbers of targets, the less weight the results for this ensemble of neural networks have in the final prediction calculation. The output is one node which corresponds to the relationship between a certain drug and its adverse effect (AEs) or indication (Yes-1 or No-0).

- Sampling Methods: This second strategy is used to describe all plausible relationship between sets of proteins previously identified with ANNs as suggested by experimental work, where each parameter corresponds to the relative weight of a link, connecting nodes (genes/proteins) in a graph (protein map). Thus, this approach does not provide a single solution, but rather identifies a universe of possible solutions that satisfy the biological restrictions of the truth table. However, not all solutions are used for the analysis. The accuracy is calculated by checking how much the models comply with the truth table, and it is defined as the percentage of true positives (correct predictions respect the knowledge stored in the truth table) of the mathematical solution respect the total of parameters to evaluate. The solutions used in subsequent analysis present accuracy higher than 95%. That is, only MoAs that are plausible from the standpoint of currently accepted scientific understanding were considered in the analysis. Once a response (in this case cardiac remodeling) is identified to a specific stimulus (Valsartan, Sacubitril or

empagliflozin), it is possible to analyze the molecular mechanisms that justify this association using the sampling methods strategy (Supplementary Figure 4). Through this methodology, TPMS technology generates models that comply with the biological restrictions of the truth table. By tracing the changes occurred in the model after applying known pairs of stimulus-response signals, we are able to assess how perturbations are transmitted across the network, thereby adding a dynamic component to an otherwise static model.

Biomarker identification

We performed multivariate analysis, evaluating combinations of proteins to identify those that best classified either the solutions of the models or the experimental data. To assess the probability of correctly predicting and classifying the set of samples of high-throughput data, we used a "leave one out" strategy, which involved analyzing a subset of samples that were not previously included with models that were not previously used.

The combinations were obtained through four strategies. To classify the solutions of the models, we used a model-based strategy and a model/HT-based strategy. Both strategies identified the protein combinations that better classified the solutions of the models to their corresponding cohort. The model/HT-based strategy additionally filtered the protein combinations using the high-throughput data (i.e., what was measured in the microarray), reducing the universe of proteins, and thus facilitating the identification of a combination with higher generalization capability.

To classify the transcriptomic experiments, we used an HT-based strategy and a HT/model-based strategy. Both strategies identified the combinations of proteins that better classified the microarray experiments to their corresponding cohort. The HT-based

strategy did not use the information from the disease models, while the HT/model-based strategy filtered the combinations by the proteins found to be relevant in the models.

Data integration

We integrated the in silico analysis of the microarray gene expression data to identify relationships across signature datasets, providing an independent assessment and functional validation. To cross-validate our findings, we used several complementary methods for complex data integration. The Metascape bioinformatic tool (149) was used for pathway analyses, the Perseus software platform (150) for high-dimensional omics data analysis, and the STRING (151) online tool to explore relevant protein–protein interactions (PPI) at 0.9 confidence.

Data Generation and In Vivo Models

Post-infarct in vivo swine model

In order to obtain the cardiac samples necessary to establish specific gene expression patterns with which to feed the mathematical models, a swine model of MI was set up. Here, female Landrace × Large White pigs (n= 9) were intramuscularly (IM) premedicated with azaperone (10mg/kg), and then administered intravenous (IV) pentobarbital sodium (15mg/kg). These pigs underwent endotracheal intubation, with 2% inhaled isoflurane used for the anesthesia. During the procedure, IV fentanyl (0.75mg/kg/45 min) was administered as analgesic, and IV atracurium besylate (bolus of 1.5mg/kg) was used to induce muscular relaxation. After left lateral thoracotomy, MI was induced via permanent ligation of the circumflex artery, as previously described18. IM tulathromicin (2.5mg/kg) was administered as antibiotic prophylaxis, and a transdermal fentanyl patch was applied to facilitate post-operative analgesic care. These surgical

interventions were monitored by electrocardiogram (ECG), capnography, and pulse oximetry, and by non-invasive arterial blood pressure and temperature measurements.

At 6 days (n= 3), 30 days (n= 3), or 45 days (n= 3) after MI, animals were randomly sacrificed using an IV overdose infusion of potassium chloride solution. At each temporal stage, we analyzed three paired myocardial samples from infarct core and non-infarcted remote myocardium. As a physiological control, we also analyzed myocardial samples from healthy animals (n= 3).

Post-infarct heart failure (MI-HF) in vivo rat model

In order to validate the in silico results obtained in the analysis of the mechanism of action of empagliflozin, a rat model was set up. A total of 74 rats were used for the experimental validations. The non-diabetic, MI-HF study was performed in male Sprague Dawley rats weighing 250-280g obtained from ENVIGO (The Netherlands). The diabetic MI-HF study (MI-HF-DM) was performed in male Wistar rats weighing 160-200g obtained from ENVIGO (Barcelona, Spain).

Animals were housed in group under standard laboratory condition at 12h light/dark cycle. All animals received food and water ad libitum during the study (N=7-12 per group).

Induction of diabetes mellitus (DM) in Wistar rats

DM was induced via a single intraperitoneal injection of streptozotocin (STZ, S0130 Sigma-Aldrich, St. Louis, MO, USA) (50 mg/kg/body weight), dissolved in freshly prepared 0.1M citrate buffer (pH 4.5, 71402 Sigma-Aldrich, St. Louis, MO, USA). In order to prevent hypoglycemia in the first 24h following STZ injection, rats were allowed

to have free access to water with 5% glucose. Three days after STZ- injection, rats with blood glucose levels greater than 300 mg/dl were considered diabetic.

Induction of myocardial infarction (MI) in rats

Initially, animals were anesthetized with intraperitoneal ketamine (75 mg/kg) and medetomidine (0.5 mg/kg), before being intubated and ventilated under 2% isoflurane anesthesia. Rats were randomly allocated to myocardial infarction (MI) or sham surgery as described before (152). Left-sided thoracotomy was performed by a small incision between the third and fourth intercostal spaces. The pericardial sac surrounding the heart was cut open, but the heart was not exteriorized. The infarction was performed by ligation of the left anterior descending coronary artery. Visible blanching and cyanosis of the anterior wall of the left ventricle and swelling of the left atrium were taken as indicative of successful ligation. Sham surgery was identical to the MI surgery, but without any ligation.

In vivo Experimental design and study protocol in rats

Two weeks after surgery, non-diabetic rats (N=40) were fed either with standard rat chow (R/M-H V1534-70, Ssniff, Germany) or empagliflozin containing chow (BI 10773; in concentration of 200 mg/kg/day to reach dose 30 mg/kg/day), and this was continued for a period of 12 weeks. After 12 weeks, hearts were rapidly excised, weighed and processed for further analysis. Animals were divided into four groups: Group 1 (n=7): Sham rats receiving vehicle treatment; Group 2 (n=10): Sham rats receiving empagliflozin; Group 3 (n=12): Infarcted rats receiving vehicle treatment; Group 4: Infarcted rats receiving empagliflozin.

Immediately after inducing diabetes, Wistar rats were treated with empagliflozin (10 mg/kg/day) (N=34). This treatment was maintained for 4 weeks before the induction of

myocardial infarction and was continued for a period of 4 weeks post-MI. After 4 weeks, hearts were rapidly excised, weighed and processed for further analysis. Animals were divided into four groups: Group 1 (n=8): Diabetic sham rats receiving PBS for 56 days; Group 2 (n=9): Diabetic sham rats receiving empagliflozin for 56 days; Group 3 (n=7): Diabetic infarcted rats receiving PBS for 56 days; Group 4 (n=10): Diabetic infarcted rats receiving empagliflozin for 56 days.

In Vitro Analyses and Validations

RNA Extraction and Processing

Following sternotomy in the swine model, hearts were washed in ice-cold buffered saline solution to remove blood residue. Biopsies were obtained from infarct core (center of the scar on the left ventricle), remote myocardium (non-infarcted interventricular septum), and control myocardium (healthy animals). To ensure RNA stabilization, biopsies were preserved in Allprotect Tissue Reagent (Qiagen) at room temperature. Total RNA was isolated using the RNeasy Fibrous Tissue Mini Kit (Qiagen). RNA purity and integrity were assessed by spectrophotometry (NanoDrop ND-1000, NanoDrop Technologies) and nanoelectrophoresis (2100 Bioanalyzer, Agilent Technologies).

Microarray gene expression analyses

We obtained the microarray expression profiles using the GeneChip® Porcine Genome Array (Affymetrix). From each sample, 200ng of total RNA was processed, labeled, fragmented, and hybridized to the GeneChip® following the manufacturer's User Manual. Arrays were scanned using an Affymetrix GeneChip® Scanner 3000 7 G. The raw expression values were pre-processed using the robust multi-chip average (RMA)-normalization method (153), yielding 24,123 probe sets on a log2 basis.

Real time PCR

Total RNA from tissues were isolated by the TRIzol RNA isolation protocol. cDNA was further isolated from RNA using QuantiTecht RT kit (Qiagen), following manufacturer's instruction. Quantitative real-time pCR (qRT-PCR) on a BioRad CFX384 real time system using SYBR Green mix (Thermo Fischer Scientific) was used to determine the relative gene expression. Gene expression was determined by correcting the reference gene (36B4) and the calculated values are expressed relative to the control group per experiment. The primers for BIRC5 and XIAP qRT-PCR used in this study can be found in Supplementary Table 10.

Statistical Analysis

After empagliflozin treatment, gene expression was determined by correcting the reference gene (36B4) and the calculated values are expressed relative to the control group per experiment. The '2-ΔΔCT method' for comparing relative expression results between treatments in real-time PCR was applied. To compare normally distributed parameters, one-way analysis of variance (ANOVA) followed by Tukey's post-hoc test was used. When data were not normally distributed, a non-parametric Kruskal–Wallis test followed by a Mann–Whitney U test with correction for multiple comparisons was used. To compare EMPA and vehicle treatment, an independent t-test or a Mann – Whitney U test was used, where appropriate. Two-sided tests yielding a $p<0.05$ was considered statistically significant. SPSS statistics for Windows, version 23.0 (IBM Corp., Armonk, NY, USA) was used to perform all statistical analysis.

Ethical Declaration

All experiments involving animal models were conducted in accordance with the NIH Guide for the Care and Use of Laboratory Animals and were approved by the Committee for Animal Experiments. The protocols complied with all guidelines concerning the use of animals in research and teaching, as defined by the Guide For the Care and Use of Laboratory Animals (NIH Publication No. 80-23, revised 1996).

Acute Heart Failure – Cardiogenic Shock

Patients and Cohorts

To investigate transcriptomic biomarkers in CS, we performed a prospective observational study, which included consecutive STEMI patients complicated with CS admitted to a single center within a primary percutaneous coronary intervention (pPCI) network between February 2011 and March 2015. In particular, inclusion criteria were systolic blood pressure <90 mmHg (or >90 mmHg with vasopressors for >30 min), signs of poor peripheral perfusion, signs of pulmonary congestion, and lack of rapid resolution after pPCI. Patients with mechanical complications were excluded in order to warrant a more homogenous sample, as in these patients death can be led by other factors than heart failure (e.g. surgical technical issues, availability of emergent surgery…). Patients with out-of-hospital cardiac arrest were excluded if CPR was not initiated in the first 15 minutes after collapse or if duration of arrest was longer than 45 minutes.

Baseline demographics and clinical data were recorded during admission.

RNA Extraction and Processing

Serum samples were obtained at three specified time points (on admission immediately after pPCI, at 12h, and at 24h), and stored at -80ºC until analysis. Total RNA was

extracted from 200 µl of serum samples using miRCURY RNA Isolation Kit (Exiqon, Vedbaek, Denmark). A synthetic C elegans miRNA Cel-miR-39 (Qiagen, Hilden, Germany) was spiked in to the samples to correct for extraction efficiency (154). Reverse transcription of RNA was performed with miScript II RT Kit (Qiagen) and quantification of miR-21, miR-122a, miR-320a and miR-423-5p levels was performed using miScript SYBR Green PCR kit (Qiagen) and miRNA-specific miScript primer sets (Qiagen) on Roche LightCycler 480.

MicroRNA Quantification

Quantification of miR-21, miR-122a, miR-320a and miR-423-5p levels was performed using miScript SYBR Green PCR kit (Qiagen) and miRNA-specific miScript primer sets (Qiagen) on Roche LightCycler 480.

Statistical Analysis

The primary end-point of this study was determined as all-cause of death at 30 days. Post-discharge deaths were identified by telephone contacts and from electronic patient records. The local ethics committee approved the study and all participants provided informed consent according to the declaration of Helsinki.

Categorical variables were expressed as percentages, continuous variables as mean (standard deviation [SD]) or median (interquartile range) for normal and non-normal distributions, respectively. Differences between groups (survivors vs. non-survivors at 30 days) were assessed by the chi-squared test, Student's t-test, and Mann–Whitney U test as appropriate. We also performed univariate and multivariate logistic regression analyses (backward step method) with 30-day all-cause death as the dependent variable and miRNA after logarithmic transformation (per 1 SD). In the multivariate analysis, significant variables in the comparison between survivors and non-survivors, as well as

clinically significant variables, were included as covariates. Statistical analyses were performed with SPSS 15 (SPSS Inc., Chicago, IL). Two-sided $p<0.05$ was considered significant.

RESULTS

CHRONIC HEART FAILURE

HF is characterized at the myocardial level by ventricular remodeling and dysfunction (57,58), and clinically, by pump failure and sudden death. The principal causes of HF in western countries are coronary artery disease and MI (155). Important advances have been accomplished in HF management, as the better understanding of neurohormonal activation and agents to block it demonstrated value in improving symptoms and prolonging life expectancy (156).

In this thesis, we aimed to study the mechanism of action of the two pharmacological treatments that have disrupted the field of HF: A) Sacubitril/valsartan (previously known as LCZ696, and marketed by Novartis® under the name of Entresto®), a novel combination drug 1:1, has proven to be superior to conventional angiotensin-converting-enzyme (ACE) inhibition in reducing cardiovascular deaths and HF readmissions, in a large prospective randomized clinical trial (157). B) Empagliflozin, a new class of oral antidiabetic inhibiting the sodium/glucose co-transporter (SGLT2), which in the EMPA-REG OUTCOME trial, patients with type 2 DM who were at high risk for cardiovascular events and who received empagliflozin in addition to standard care showed drastically lower rates of the following compared to those who received placebo: primary composite cardiovascular outcome (death from cardiovascular causes, nonfatal myocardial infarction or nonfatal stroke); HF-related hospitalizations; death from cardiovascular causes; and death from any cause (158). This marked the first time a pharmacological drug of this characteristics improved cardiovascular outcomes, which came as a great surprise to the medical community.

Nonetheless, these treatments are on the cutting edge of HF management, and despite their big impact and massive interest baked into their potential, still little research has been done to understand their molecular insights. Additionally, even though both drugs

have very distinct purposes and implied mechanisms of action, their benefits are strikingly similar, which lead us to investigate their molecular cascades in further detail.

Here, growing evidence supports the idea that specific biological processes (e.g., protein–protein interactions or epigenetic regulations) are likely influenced by the biological context—for example, a specific tissue or a certain disease (159). However, in order to be able to consider such bewildering number of variables, vast amounts of data are constantly being generated, such that putting together, analyzing, and interpreting this information as a whole constitutes an overwhelming task.

For this purpose, new technologies are rapidly emerging, which combine different engineering approaches and bioinformatics. Within this context, systems biology arises as an interdisciplinary field of study that aims to unravel the key interactions within complex biological networks following a holistic approach based on computational and mathematical models.

Thus, we harnessed artificial intelligence technologies to endow us with the capabilities to analyze the mechanisms of action of Sacubitril/valsartan and Empagliflozin at the molecular level, by integrating transcriptomic and publicly available information regarding both drugs and the diseases under study.

Mechanisms of action of sacubitril/valsartan on cardiac remodeling: a systems biology approach

Given Sacubitril/valsartan success, both the AHA/ACC and the ESC HF guidelines have rapidly incorporated Sacubitril/valsartan into their recommendations for HF with reduced left ventricular ejection fraction (96,160). While the mechanism of action for this

combination drug is likely to involve the regulation of adverse tissue remodeling, the molecular mechanisms underlying the beneficial effects of Sacubitril/valsartan (a salt complex at a 1:1 molar ratio) (161,162), are, at present, incompletely characterized. Individually, the Sacubitril metabolite LBQ657 inhibits neprilysin, while Valsartan imposes a blockade of the angiotensin II type 1 receptor (AT1R).

Accordingly, we used the backbone of the mathematical models constructed previously and modified it to explore the intricate mechanisms of action of Sacubitril/valsartan as compared to either Sacubitril or Valsartan alone.

To that end, a myocardial transcriptome obtained in response to MI in swine was analyzed to address post-infarction ventricular remodeling (120). HF remodeling was studied using public data available in GEO (119). A dedicated database and a series of mathematical models, adjusted to known physiological processes, were then used to predict the precise molecular effects of Sacubitril/valsartan upon the myocardium and vasculature.

Transcriptome analyses revealed 4737 proteins in the post-infarction cohort (MI), and 2002 proteins comprising the HF disease signature (according to RNAseq data). Collectively, the MI/HF disease signatures shared 672 proteins, of which 339 (50.5%) were directly correlated (e.g. both activated or inhibited in either condition), and 333 (49.5%) exhibited inversely correlated activities (e.g. activated in one condition and inhibited in the other) (**Figure 7b**).

Valsartan and Sacubitril act synergistically to prevent cardiomyocyte cell death and matrix remodeling

An ANN was generated to identify the relationships between each drug (Sacubitril, Valsartan, and their combination (e.g. LCZ696)) and the clinical condition under study, e.g. cardiac remodeling. This allowed an assessment of whether Sacubitril/valsartan acts synergistically or in an additive manner (**Figure 7c**). As shown in **Table 2**, the molecular mechanisms of Valsartan are strongly associated with the prevention of hypertrophy. In contrast, Sacubitril acts by preventing the breakdown of endogenous vasoactive peptides, including natriuretic peptides (ANP, BNP, and CNP), thereby limiting myocardial cell death. In the combination drug, molecular synergy may reverse or reduce left ventricular extracellular matrix remodeling (LVEMR), reduce cardiomyocyte cell death, and, via Valsartan, enhance the effects of Sacubitril. Remarkably, the molecular mechanisms of

Remodeling parameters	*Sacubitril*	*Valsartan*	*LCZ696*	*>20% max*	*>addition*
Cardiomyocyte cell death	48.00%	15.00%	61.00%	✓	Ø
Hypertrophy	31.00%	96.00%	80.00%	Ø	Ø
Impaired myocyte contractility	5.00%	14.00%	8.00%	Ø	Ø
LVEMR	21.00%	14.00%	42.00%	✓	✓

Table 2*. Relationships between the drugs and pathologies under study. The columns Sacubitril, Valsartan, and LCZ696 (Sacubitril/valsartan), indicate, as a percentage score, the degree of relationship between these drugs and the condition under study; the higher the value, the closer the relationship. The two last columns indicate if the value for their combination exceeds the maximal value achieved by either drug alone with a 20% premium (LCZ696 >120% max (Sacubitril, Valsartan), or exceeds the sum of both individual drugs (e.g. LCZ696 > addition (Sacubitril, Valsartan). These columns therefore indicate if the combination drug acts synergistically or simply adds the effects of both components. LVEMR: left ventricular extracellular matrix remodeling.*

Sacubitril and Valsartan alone are not associated with LVEMR, and it is only their combination that activates these molecular processes.

Mechanism of action of Sacubitril/valsartan on myocardial remodeling

Based on our TPMS analyses, the model was able to generate a network displaying the mechanisms of action (MoA) that could explain Sacubitril/valsartan's beneficial effects (**Figure 8**). The same synergistic MoA was identified in the two cohorts, post-MI and HF, with many pathways corroborating the notion that Valsartan potentiates the effects of Sacubitril.

The MoA included 46 proteins, 8 acting synergistically (Supplementary Table 7), with 18 protein effectors of cardiac remodeling: 6 involved in hypertrophy, 4 in LVEMR, 6 in cardiomyocyte cell death, and 2 in impaired myocyte contractility (**Table 3**). The MoA contains 23 proteins from microarray data derived from MI, and 10 from HF; 17 of the 23 proteins linked to MI are modulated by the administration of Sacubitril/valsartan in an opposite fashion to that induced by infarction (as indicated by transcriptome data), indicating the drug's beneficial effects. In the case of HF restriction, this effect was observed in 8 of 10 proteins.

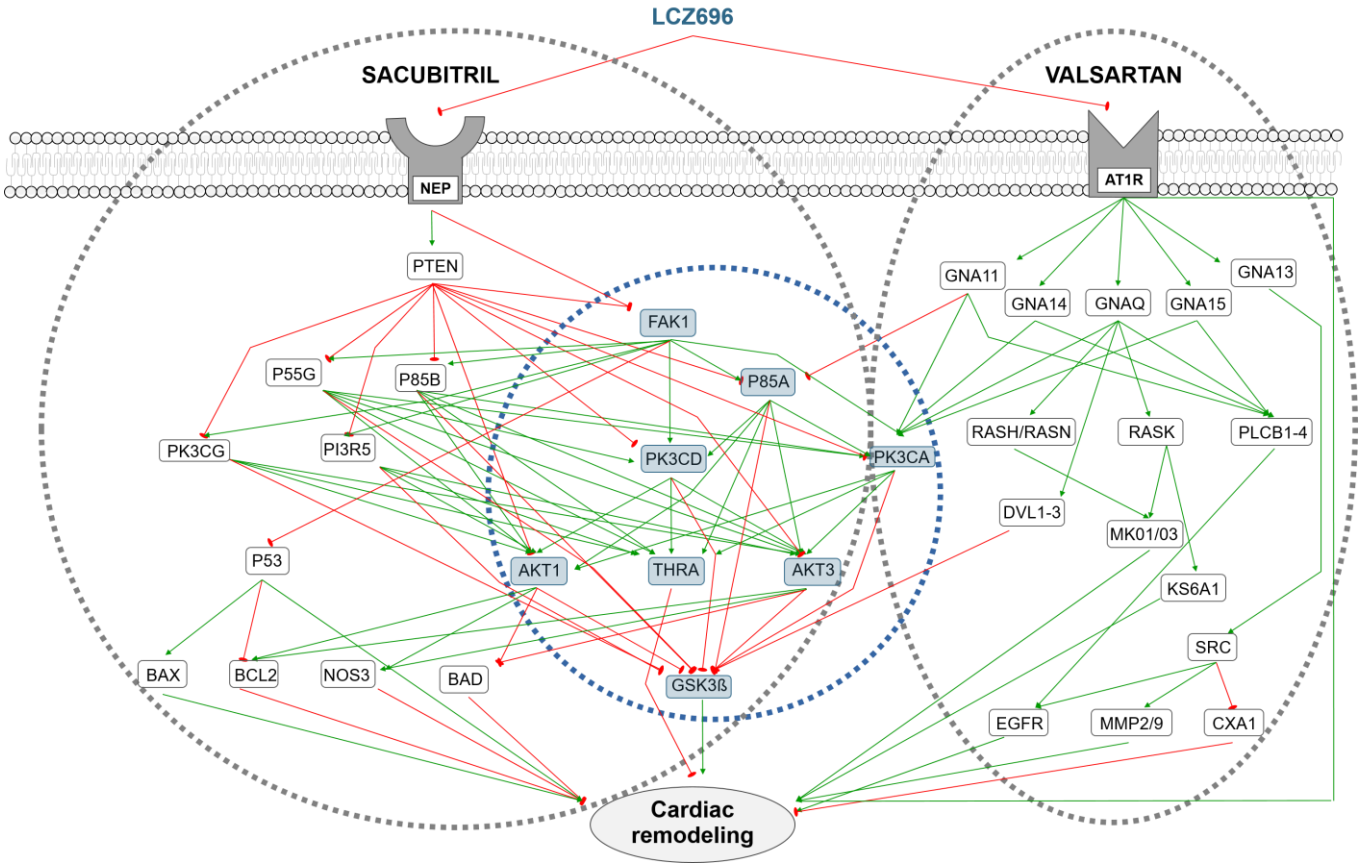

Figure 8. *Sacubitril/valsartan's mechanisms of action (MoA). Every relationship depicted represents a mechanism by which the drug could directly or indirectly (via downstream effectors) improve or reverse pathological cardiac remodeling, either through the activation (green arrows) or inhibition (red arrows) of downstream proteins. The same synergistic MoA was identified for both, MI and HF, cohorts; therefore, the depiction applies for both of them. Grey dotted-line circles encompass the proteins affected either by Sacubitril, Valsartan, or both. Blue dotted-line circle encompass the core of eight proteins that the mathematical models predict to act synergistically, by being related to both, Sacubitril and Valsartan, pathways in some manner.*

Uniprot	*Displayed Name*	*Protein name*	*Synergistic node*	*Remodeling effector*
P00533	EGFR	Epidermal growth factor receptor	×	Hypertrophy
P09038	FGF2	Fibroblast growth factor 2	✓	Hypertrophy
P28482	MAPK1	Mitogen-activated protein kinase 1	×	Hypertrophy
P27361	MAPK3	Mitogen-activated protein kinase 3	×	Hypertrophy
Q15418	RPS6KA1	Ribosomal protein S6 kinase alpha-1	×	Hypertrophy
P30556	AGTR1	Type-1 angiotensin II receptor	×	Hypertrophy
P17302	GJA1	Gap junction alpha-1 protein	×	Left ventricle extracellular matrix remodeling
P08253	MMP2	72 kDa type IV collagenase	×	Left ventricle extracellular matrix remodeling
P14780	MMP9	Matrix metalloproteinase-9	✓	Left ventricle extracellular matrix remodeling
P01137	TGFB1	Transforming growth factor beta-1	✓	Left ventricle extracellular matrix remodeling
Q13490	BIRC2	Baculoviral IAP repeat-containing protein 2	✓	Cardiomyocyte cell death
Q92934	BAD	Bcl2-associated agonist of cell death	×	Cardiomyocyte cell death
P04637	TP53	Cellular tumor antigen p53	×	Cardiomyocyte cell death
P49841	GSK3B	Glycogen synthase kinase-3 beta	✓	Cardiomyocyte cell death
Q07812	BAX	Apoptosis regulator	×	Cardiomyocyte cell death
P10415	BCL2	Apoptosis regulator	×	Cardiomyocyte cell death
P29474	NOS3	Nitric oxide synthase, endothelial	×	Impaired myocyte contractility
P10827	THRA	Thyroid hormone receptor alpha	✓	Impaired myocyte contractility

***Table 3**. Protein effectors of cardiac remodeling included in the MoA representation.*

Valsartan improves cardiac remodeling by inhibiting guanine nucleotide-binding proteins

The inhibition of AT1R seems to inactivate or reduce the activity of a series of cascades that participate in cardiac remodeling, via inhibition of different subunits of guanine nucleotide-binding proteins. For example, inhibition of guanine nucleotide-binding protein G(q) subunit alpha (GNAQ) blocks the ERK1/2 pathway, and the ribosomal protein S6 kinase alpha-1 (KS6A1) (**Figure 8**). These are both effectors of cardiac hypertrophy through their inhibition of Ras GTPase superfamily members (RASH, RASN, and KRAS) (Supplementary Figure 5). The model indicates that ERK signaling is also a potential synergistic pathway for Sacubitril/valsartan's effects on cardiac remodeling, possibly acting via FAK1, downstream of Sacubitril binding (Supplementary Figure 6).

Valsartan also contributes to the synergistic effects mediated downstream of Sacubitril via its regulation of glycogen synthase kinase-3 beta (GSK3B) and the activities of the segment polarity protein disheveled homologs DVL-1, 2, and 3 (Figure 8) (Supplementary Figure 5).

Inhibition of the guanine nucleotide-binding protein subunit alpha-13 (GNA13) induces the inactivation or attenuation of the activity of the proto-oncogene Scr kinase, thus producing a reduction of LVEMR through inhibition of matrix metalloproteases-2 and 9 (MMP-2 and MMP-9), and gap junction alpha-1 protein (CXA1). At the same time, a reduction of hypertrophy is achieved through inhibition of the epidermal growth factor receptor (EGFR) (Supplementary Figure 5). Inhibition of guanine nucleotide-binding protein subunit alpha-11, 14, and 15 (GNA-11,14,15), along with

GNAQ, inhibits 1-phosphatidylinositol 4,5-bisphosphate phosphodiesterase beta-1, 2, 3, and 4, thus reducing cardiac hypertrophy through EGFR blockade.

Additionally, inhibition of GNA11 is one of Valsartan's pathways involved in the synergistic effects of Sacubitril/valsartan. This is achieved through activation of phosphatidylinositol 3-kinase regulatory subunit alpha (P85A), and phosphatidylinositol 4,5-bisphosphate 3-kinase catalytic subunit alpha isoform (PK3CA), whose activities affect different pathways involved in cardiomyocyte cell death, hypertrophy, and impaired myocyte contractility.

Sacubitril attenuates cardiomyocyte cell death, hypertrophy, and impaired myocyte contractility by inhibiting PTEN

The inhibition of PTEN mediated by Sacubitril's effect on neprilysin appears to be the initiator of a series of cascades that participate in cardiac remodeling by inducing the activation of different potential synergistic nodes (**Figure 8**). Sacubitril's downstream effects include attenuation or inhibition of cardiomyocyte cell death through activation of p53, which regulates the activity of Bcl2 and Bax. It also helps to reduce hypertrophy and enhance myocyte contractility through the activation of AKT1 and AKT3, which inhibit the endothelial nitric oxide synthase (NOS3), and activation of the thyroid hormone receptor alpha (THRA) (Supplementary Figure 7).

Specific molecular mechanisms of Sacubitril/valsartan in reducing myocardial remodeling in myocardial infarction

Interestingly, although our model indicates that the MoA network is the same between MI and HF, specific proteins associated only with the efficacy of Sacubitril/valsartan for MI patients have been identified (Supplementary Table 8). These include fractalkine, involved in angiogenesis, wound healing, inflammatory processes, and responses to

hypoxic conditioning (163,164). The C-type lectin domain family 7 member A (CLEC7A), is necessary for TLR2-mediated activation of NF-Kβ, mediates inflammatory processes, the production of reactive oxygen species, and plays a role in carbohydrate mediated signaling (165–168). Urokinase plasminogen activator surface receptor (uPAR) is involved in blood coagulation, apoptosis and cellular metabolism (169–172).

Although MYH6 was included as a biological determinant in the HF but not infarction model (according to microarray data), this protein ultimately does not seem to participate in Sacubitril/valsartan efficacy in HF, but may play a role in MI instead. In the case of MYH7, this protein was not included as a determinant in any model, but is involved in the efficacy of Sacubitril/valsartan's action in both the MI and HF models (173,174).

Gene ontology and enrichment analyses pinpoint potentially relevant pathways affected by Sacubitril/valsartan

An enrichment analysis of the proteins shared by the Valsartan and Sacubitril networks identified additional pathways that could be involved in their synergistic effects. As a first approach, we focused our analyses on those pathways where all the relevant activities were present in that set of shared proteins. This approach revealed that the regulation of free fatty acids that modulate insulin secretion, the orexinergic system (Orexin and neuropeptides FF and QRFP), and angiotensin metabolism (target pathway of Valsartan), are the most enriched pathways. Then, we expanded our analyses by focusing on the most relevant pathways according to p-value. This approach added, GPCR downstream signaling, the gastrin-CREB signaling pathway via PKC and MAPK, plasma membrane estrogen receptor signaling, PAR1 and PAR4-mediated thrombin signaling events, and calcium signaling and platelet activation. Interestingly, the ACE inhibition pathway was also identified. The P2Y receptors

pathway, which could constitute a therapeutic target with which to regulate cardiac remodeling and post-ischemic revascularization (175), was also enriched.

To complement this study, a gene ontology (GO) analysis was then performed to map our list of shared proteins and pathways in MI and HF to biological processes, allowing us to generate a detailed map of the potential mechanisms of action of Sacubitril/valsartan. This analysis confirmed the GPCR signaling pathway to be the most relevant, according to p-value, and displayed processes related to blood circulation, the regulation of systemic arterial blood pressure, and wound healing as highly affected.

SUMMARY FIGURE

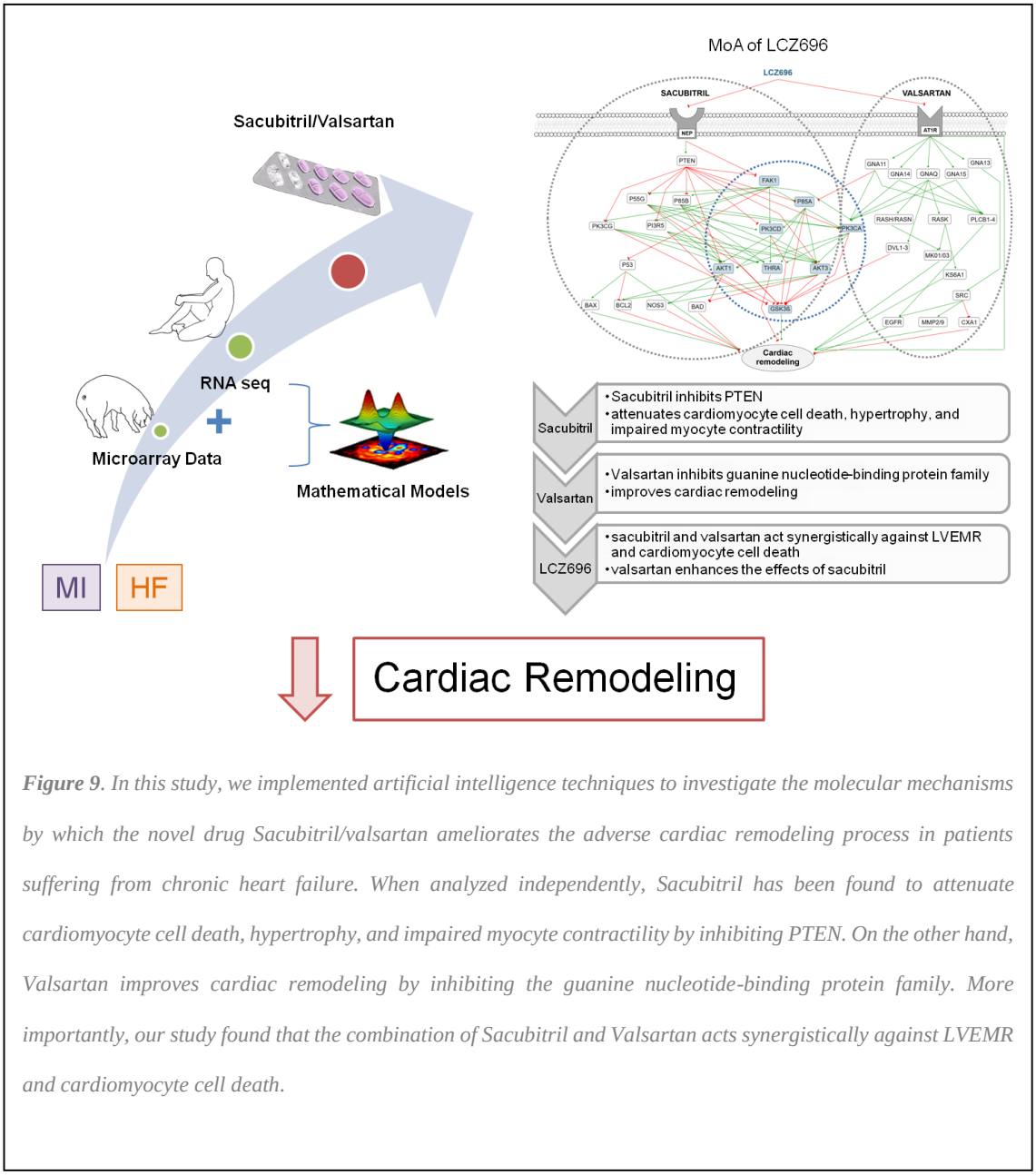

***Figure 9**. In this study, we implemented artificial intelligence techniques to investigate the molecular mechanisms by which the novel drug Sacubitril/valsartan ameliorates the adverse cardiac remodeling process in patients suffering from chronic heart failure. When analyzed independently, Sacubitril has been found to attenuate cardiomyocyte cell death, hypertrophy, and impaired myocyte contractility by inhibiting PTEN. On the other hand, Valsartan improves cardiac remodeling by inhibiting the guanine nucleotide-binding protein family. More importantly, our study found that the combination of Sacubitril and Valsartan acts synergistically against LVEMR and cardiomyocyte cell death.*

Unravelling the molecular mechanism of action of empagliflozin in heart failure with reduced ejection fraction with or without diabetes

Both type 1 and type 2 DM are major risk factors for the development of cardiovascular diseases, increasing morbidity and mortality (176). For decades, long-term clinical studies in DM have shown value in reducing glycemic levels, without a substantial effect on cardiovascular outcomes and certainly no benefit in HF (177). The advent of a new class of agents, SGLT2is, heralds a new era and may represent a turning point. Indeed, in the EMPA-REG OUTCOME trial, Empagliflozin demonstrated to reduce cardiovascular mortality and HF-related hospitalizations (158). Similar results with other SGLT2is have been reported subsequently by both randomized clinical trials and observational studies (178,179).

SGLT2 receptors are located in the proximal renal tubule and are responsible for 90% of glucose reabsorption into the bloodstream. Inhibition of SGLT2 receptors causes glycosuria and reduces glycemic levels (180). However, control of glycemic levels in response to SGLTis alone seems insufficient to explain the reported cardiovascular benefits. In fact, the EMPA-TROPISM trial is an ongoing trial that aims to elucidate whether the benefits obtained in the EMPA-REG OUTCOME trial were mediated, at least in part, by a glucose-independent mechanism (181). A recent viewpoint postulated the hypothesis that the benefit of SGLTis in HF may be mediated by the sodium-hydrogen exchanger (NHE) rather than by the effect on glucose reabsorption (182); however, a comprehensive mechanistic explanation of the extra-renal cardioprotective SGLTi effects remains elusive.

Having experimented the prowess of the systems biology approach used in the previous work, we could confirm that was particularly well-suited for investigating the mechanisms underlying the effects of drugs, including SGLTis. Accordingly, we used deep learning analysis to investigate what the key cardiac mechanisms may be by which empagliflozin exerts its effects in HFrEF with or without DM (**Figure 10**). Machine learning-driven pathways were validated in an *in vivo* empagliflozin-treated post-infarct HF (MI-HF) rat model.

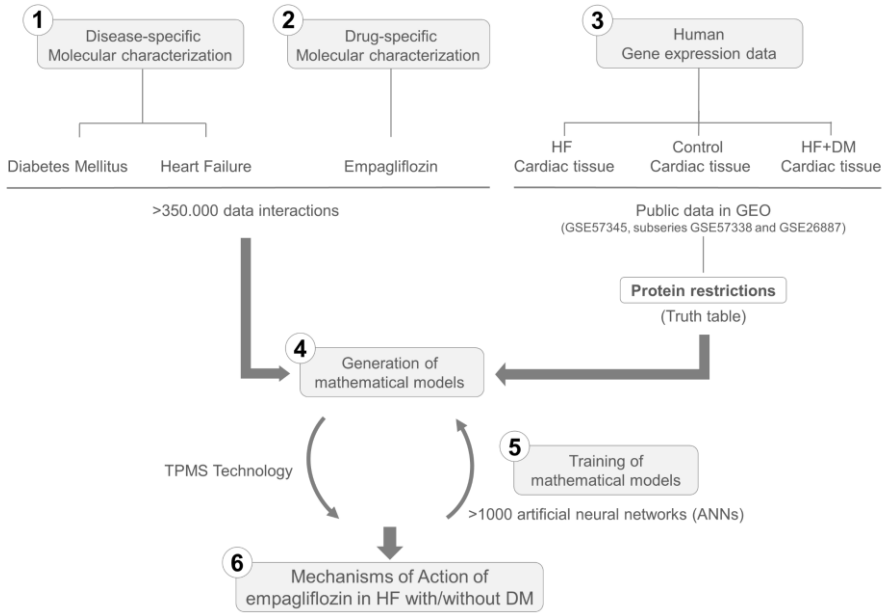

***Figure 10**. Flow chart depicting the machine learning approach used in this study. DM: Diabetes Mellitus; HF: Heart Failure; GEO: Gene Expression Omnibus database; TPMS: Therapeutic Performance Mapping System.*

Empagliflozin acts upon a specific HF-related pathological signature

First, the protein signatures of HFrEF and empagliflozin were defined and an ANN analysis identified the processes most likely associated with the beneficial effects of empagliflozin observed in HFrEF (Supplementary Table 9). Obesity, hypertension and hyperuricemia contributed the most to the HF pathological signature, and encompassed the possible effects of empagliflozin, with 140, 42 and 16 proteins of interest, respectively. For each of these three disorders, a series of mechanisms and the involved proteins were established (**Table 4**).

Pathology	Pathological mechanisms	Implicated Proteins, n
HEART FAILURE		106
	Heart hypertrophy	33
	Cardiomyocyte cell death	47
	Inefficient myocardial fuel metabolism	7
	Oxidative stress	8
	Inflammation	11
OBESITY		140
	Hyperphagia and dysregulated appetite	135
	White adipose tissue formation	5
HYPERTENSION		42
	Retention of sodium	42
HYPERURICEMIA		16
	Decreased renal excretion of uric acid	16

***Table 4**. Summary of the mechanisms involved in heart failure and associated conditions considered in the mechanistic study. The rightmost column indicates the number of implicated proteins in each mechanism.*

The efficacy analysis identified 3 complementary strategies to follow:

1. Considering sodium/glucose cotransporter 2, Na(+)/glucose cotransporter 2 (SGLT2).
2. Considering sodium/hydrogen exchanger 1 and 3 (NHE1 and NHE3)
3. Considering Empagliflozin bioflags; Those proteins known to be modulated by the drug (**Table 5**)

Gene Name	*Protein name*	*Reference (PMID)*
STAT3	Signal transducer and activator of transcription 3	29311992
NOS2	Nitric oxide synthase, inducible	29311992
IL6	Interleukin-6	29311992
BDH1	D-beta-hydroxybutyrate dehydrogenase, mitochondrial	27289126
IFNG	Interferon gamma	29311992
ALDH2	Aldehyde dehydrogenase, mitochondrial	29311992
GCG	Glucagon	26590679
INS	Insulin	27289126
ACE2	Angiotensin-converting enzyme 2	26880444
BDNF	Brain-derived neurotrophic factor	25344694
HDAC1	Histone deacetylase 1	27829948
HDAC2	Histone deacetylase 2	27829948
HDAC3	Histone deacetylase 3	27829948
HDAC8	Histone deacetylase 8	27829948

***Table 5**.Proteins known to be modulated by empagliflozin.*

ANNs evaluate the relations among protein sets inside the network providing a predictive score. Once the pathological signatures were identified, the possible relation between empagliflozin and heart failure, including associated processes, were evaluated by ANN analyses. Thus, the study of the MoA of empagliflozin was focused on the specific pathways (motives) of the diseases affected by the treatment.

1. None of the evaluated diseases and motives is strongly related to SGLT2 according to the established criterion (p-value > 0.3)
2. Considering NHE1 and NHE3 as effectors, two conditions appear as highly (>75%) related to empaglifozin's complete target profile:
    - Hypertension: Retention of sodium is the main motive identified, with a predictive score of 80%.
    - Heart Failure: Heart hypertrophy and Cardiomyocyte cell death are the main motives identified, with a predictive score of 75,6%.
3. Three conditions appear as highly (>75%) related to empaglifozin's bioflags:

- Hyperuricemia: Decreased renal excretion of uric acid is the motive most related to empagliflozin, with 77 % of predictive score.
- Obesity: the most related motives are Hyperphagia and dysregulated appetite and White adipose tissue formation.
- Heart Failure: the most related motives are Energy inefficient myocardial fuel metabolism, Oxidative stress and Inflammation.

NHE1 is responsible for the cardiac effects of empagliflozin in HFrEF with or without DM

By using the differentially expressed proteins found to be related to HF and the specific motives affected during the pharmacological treatment, the mathematical models determined the molecular mechanisms involved in the heart-focused beneficial effects of empagliflozin over heart failure in DM and non-DM patients.

Mathematical models	Stimulus	Response	Restrictions
HF with DM	Cardiac NHE1	Cardiomyocyte cell death, Hypertrophy, Inflammation	Truth Table + GSE57345 subseries GSE57338 dataset
HF without DM			Truth Table + GSE26887 dataset

Table 6*.Mathematical models generated in this study. The stimulus, response and restrictions included in each model are shown. HF, heart failure; DM, diabetes mellitus; NHE1, sodium-hydrogen exchanger-1.*

The most robust MoA identified in this study involved the NHE1 with 94.7% accuracy (**Figure 11**, Supplementary Table 11), which was similar for DM and non-DM patients, indicating a DM-independent mechanism (**Table 6**). This approach describes mainly the mitigation of cell death, but also the prevention of heart hypertrophy and the improvement

upon an inefficient myocardial fuel metabolism as the potential heart-mediated mechanisms by which empagliflozin might counteract heart failure.

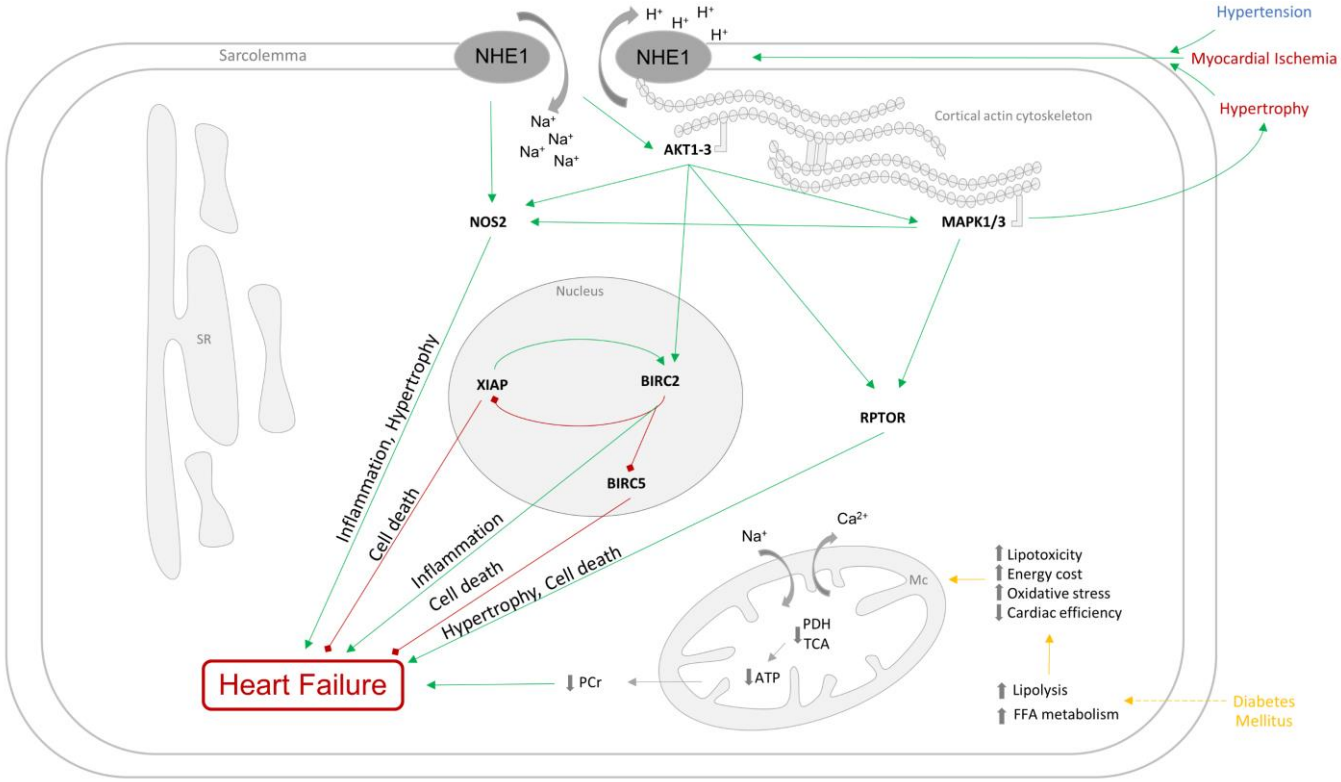

Figure 11. *NHE1 identified signalling pathways in cardiomyocytes in heart failure (HF). Each relationship represents a mechanism that may directly or indirectly (via downstream effectors) impact on HF, either through the activation (green arrows) or inhibition (red arrows) of downstream proteins. NHE1, sodium/hydrogen exchanger 1; NOS2, nitric oxide synthase, inducible; AKT1, RAC-alpha serine/threonine-protein kinase 1; AKT2, RAC-beta serine/threonine-protein kinase 2; AKT3, RAC-gamma serine/threonine-protein kinase 3; MAPK1, mitogen-activated protein kinase 1; MAPK3, mitogen-activated protein kinase 3; BIRC2, baculoviral IAP repeat-containing protein 2; BIRC5, baculoviral IAP repeat-containing protein 5; XIAP, E3 ubiquitin-protein ligase XIAP; RPTOR, regulatory-associated protein of mTOR; LEP, leptin; PDH, pyruvate dehydrogenase; TCA, tricarboxylic acid; ATP, adenosine triphosphate; PCr, phosphocreatine. SR, sarcoplasmic reticulum; MC, mitochondria.*

Direct empagliflozin-driven NHE1 blockade ameliorates cardiomyocyte cell death

In this scenario, the amelioration of cardiomyocyte cell death was established as the main driver of empagliflozin beneficial effects in HFrEF. In the absence of empagliflozin, protein kinases B (AKTs; referred to as AKT1-3 in **Figure 11**) were identified as downstream effectors of NHE1 activation responsible for the induction of baculoviral IAP repeat-containing protein 2 (BIRC2), which in turn induced degradation of proteasome-mediated X-linked inhibitor of apoptosis (XIAP) and BIRC5 and prompted HFrEF progression. In empagliflozin-enriched models, by inhibiting NHE1, repressed AKT1-3 and BIRC2 allowed the expression of the anti-apoptotic mediators XIAP and BIRC5, ultimately halting HFrEF progression.

To validate these data obtained *in silico*, mRNA levels of XIAP and BIRC5, as last effectors of the pathway, were examined *in vivo* in an empagliflozin-treated post-infarct HF (MI-HF) rat model. Confirming *in silico* findings, gene expression of XIAP and BIRC5 fell 45% and 36% in vehicle-treated MI-HF animals as compared to sham controls ($p<0.01$ for both, respectively). Remarkably, empagliflozin-treated MI-HF animals without DM showed upregulation of XIAP and BIRC5 mRNA expression similar to sham controls and significantly higher than vehicle-treated MI-HF counterparts ($p=0.003$ and $p=0.05$ respectively) (**Figure 12**). More importantly, these changes in gene expression occurred ubiquitously irrespective of DM presence, further strengthening the *in silico* predictions. Indeed, empagliflozin-treated MI-HF-DM animals showed upregulation of XIAP and BIRC5 mRNA expression similar to sham controls and significantly higher than vehicle-treated MI-HF-DM counterparts ($p=0.01$ and $p=0.005$, respectively) (**Figure 12).** Thus, empagliflozin-driven NHE1 inhibition ultimately counteracts XIAP and BIRC5 reduced function.

Additionally, our analyses also suggested that empagliflozin could further ameliorate cardiomyocyte cell death by inhibiting the AKT-dependent regulatory-associated protein of mTOR (RPTOR) and by downregulation of nitric oxide synthase (NOS2)-inducible actions (**Figure 11**).

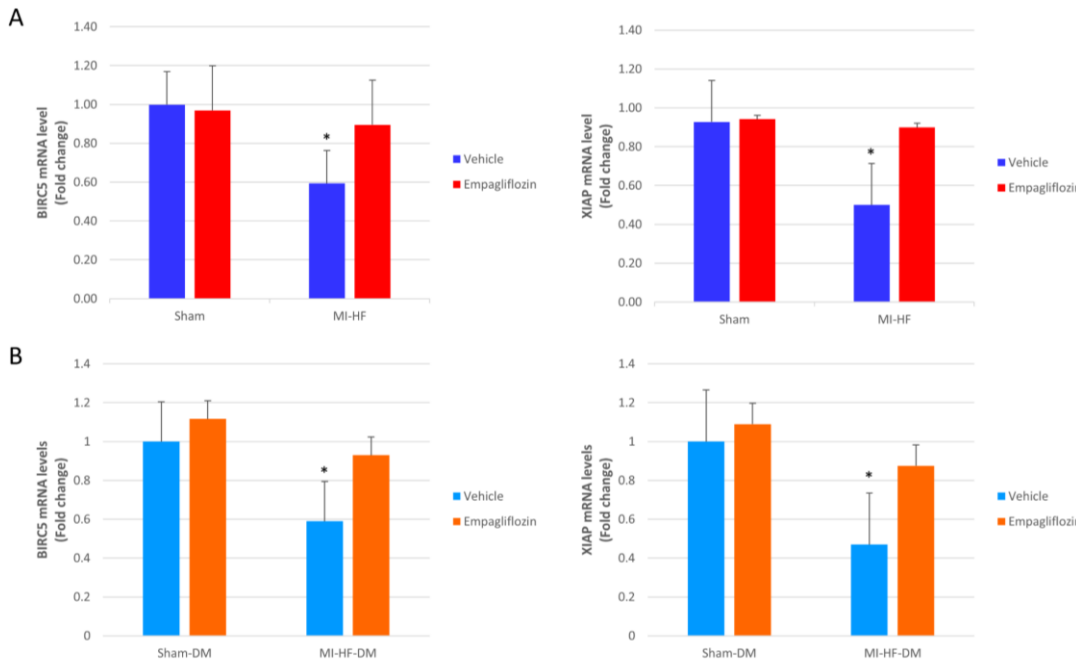

***Figure 12**. mRNA levels of anti-apoptotic proteins XIAP and BIRC5 in vivo. Upper panels (A) show non-diabetic rats. Lower panels (B) show diabetic rats. Data presented as mean ± SEM. * $p < 0.05$ vs. Empagliflozin-MI and Vehicle-Sham. One-way ANOVA followed by Tukey's post Hoc test was used for normally distributed data, while Kruskal-Wallis followed by Mann-Whitney U test was used for non-normally distributed data.*

SUMMARY FIGURE

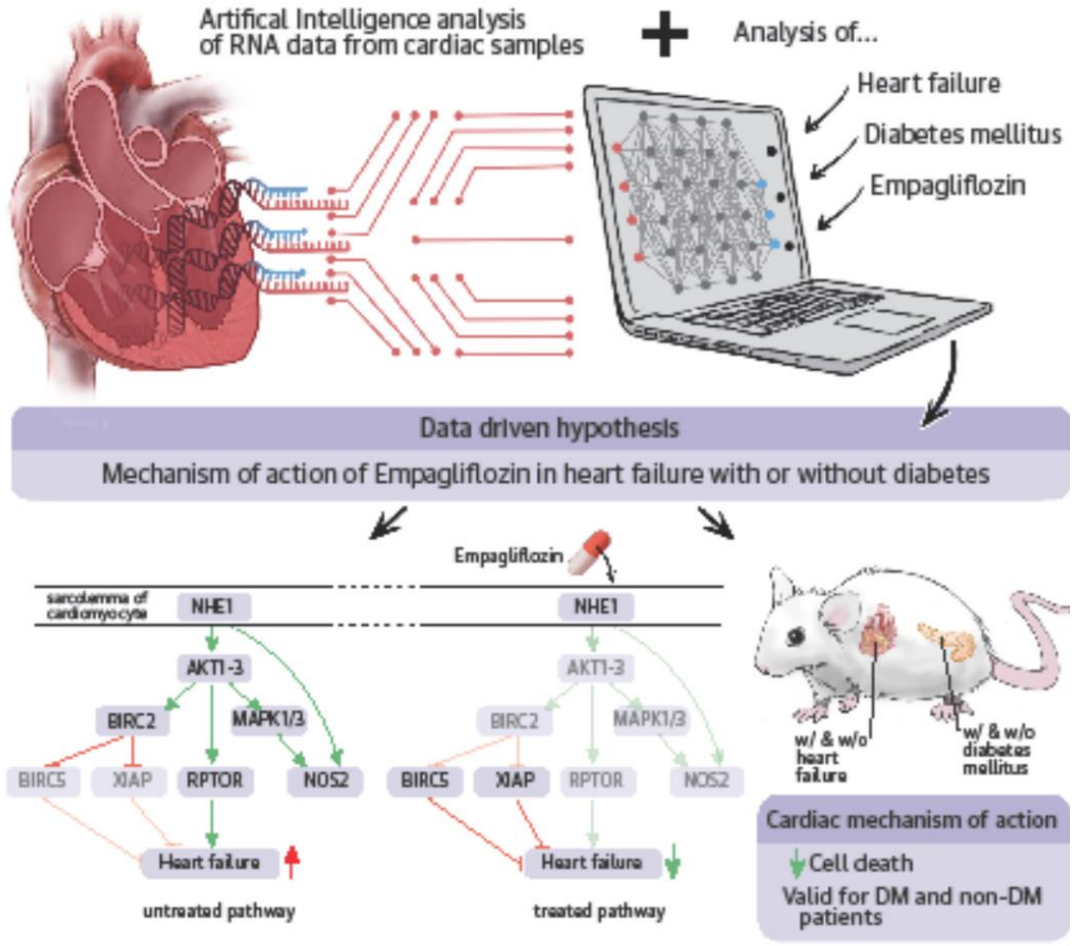

***Figure 13**. In this study, we have applied machine learning techniques to assess the molecular mechanism by which Empagliflozin, a new class of antidiabetic drugs, could be reducing cardiac injury in HF patients. Our analyses predicted Empagliflozin would inhibit NHE1, which would lead to the restoring of antiapoptotic activity by the last effectors XIAP and BIRC5, thus reducing cardiomyocyte death. These results were confirmed in a rat model of post-MI with or without diabetes. Most importantly, our work revealed that Empagliflozin would ameliorate cardiac damage independently of the glycemic status of the patient, suggesting that this therapy could be implemented regularly in HF patients.*

The results obtained after assessing both Sacubitril/valsartan and Empagliflozin treatments indicate a strong role for cardiac remodeling and the LVEM in the amelioration of HF progression. Definitely, this is not a static process, and cardiac remodeling secondary to MI is a well-defined course that may ultimately lead to HF (183,184). Thus, increasing our knowledge on this issue would help advancing our opportunities on slowing HF development on the first place, instead of treating it when it is already established.

Understandably, this process has been examined in a large number of studies. However, the large majority of them used small experimental animal models, mainly providing data about individual genes or proteins (185–188). Although these investigations have certainly and indisputably provided valuable information regarding cardiac remodeling, they have been insufficient to capture this complex development as a whole. Furthermore, the specific dynamic molecular mechanisms underlying this progression are not yet fully characterized, difficulting its understanding.

In this next stage, we wanted to adapt our mathematical models to perform as a descriptive tool, necessary to incorporate the extensive number of variables and molecular data points present in MI evolution, instead of as a prediction tool to generate new hypothesis.

Evolution of post-myocardial infarction remodeling towards heart failure: a complete molecular characterization

First, our group generated transcriptomic information from infarcted and remote in vivo swine heart tissues, and reported the identification of temporal and region-specific myocardial gene expression patterns in response to MI (120). To identify the underlying molecular explanation for the observed cardiac remodeling, we incorporated this transcriptomic data into a deep learning model—the Therapeutic Performance Mapping

System (TPMS) (189) (**Figure 14**). TPMS applies artificial intelligence and pattern recognition techniques to combine interactomic data with molecular and clinical responses observed in patients. First, the interactomic information is used to generate the skeleton for computational models, which act as a network of potential mechanistic interactions. Second, this network is fitted into a deep learning model and trained using clinical and molecular responses observed in patients. This ultimately results in the generation of a mathematical model capable of both reproducing existing knowledge and discerning MoA hidden under thousands of molecular interactions that are otherwise inaccessible.

Thus, we aimed to incorporate transcriptomic data obtained from infarcted porcine hearts at different time-points and human cardiac remodeling RNA sequencing (RNAseq) information into their corresponding mathematical configurations, to gain insights into the molecular evolution of MI over time and its development into HF.

High-dimensional data integration of microarray gene expression during 6 weeks of MI progression

At 6, 30, and 45 days after MI, we analyzed infarcted core tissue (C6, C30, and C45) and remote tissue (R6, R30, and R45). Each distinct tissue dataset revealed substantial changes over 6 weeks of MI progression.

To determine whether these changes were consistent across data types, and to validate their time-dependent evolution in functional pathways, we adopted three independent strategies.

We first sought to assess the internal structure of the data in a way that best explained the variance contained therein. Due to the high complexity of the datasets, we used the Perseus platform to perform principal component analysis (PCA) tests for dimensionality

reduction. This approach clearly separated the core infarcted area from the remote area and the control (CTRL) group, which clustered together (**Figure 15a**).

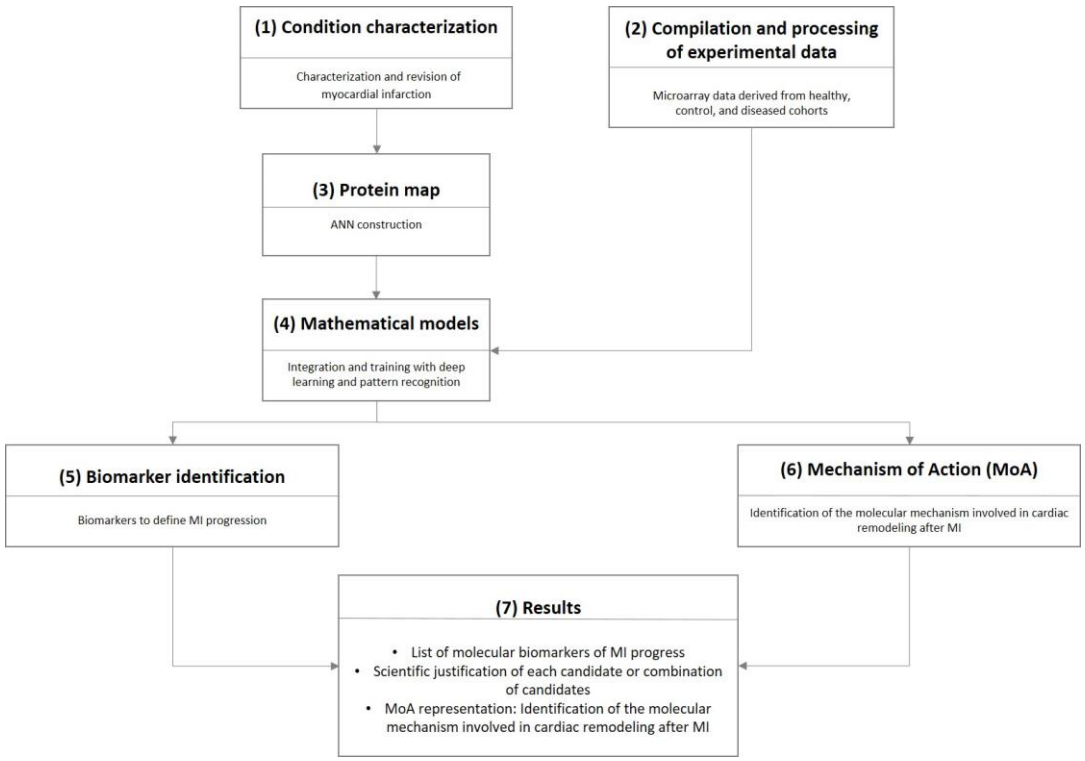

***Figure 14**. Schematic representation of the implemented systems biology workflow. (1) First, we characterized myocardial infarction (MI) at the molecular level via manual curation of the literature and using a compendium of massive public databases describing the molecular interactions of interest. (2) In parallel, we used experimental transcriptomic data to define the molecular behavior of MI at each time-point. (3) Using the information obtained during the first step, we generated a protein map regulated by the obtained experimental data. (4) We then fed the mathematical models to identify patterns in the data, (5) to identify key regulatory proteins, and (6) to predict new MoAs. (7) The final result includes a scientific justification of every prediction. ANN: artificial neural network; MoA: mechanism of action.*

Second, we employed Metascape algorithms to sort out the most affected pathways in the gene set according to their gene ontology (GO) terms (**Figure 16a**). We were further able to robustly cluster them according to their biological significance and associated *P* value (**Figure 16b,c**). These data suggested that MI progression was accompanied by great

affectation of mitochondrial metabolism, as well as marked regulation of adipogenesis, fatty acid metabolism, and epithelial mesenchymal transition processes.

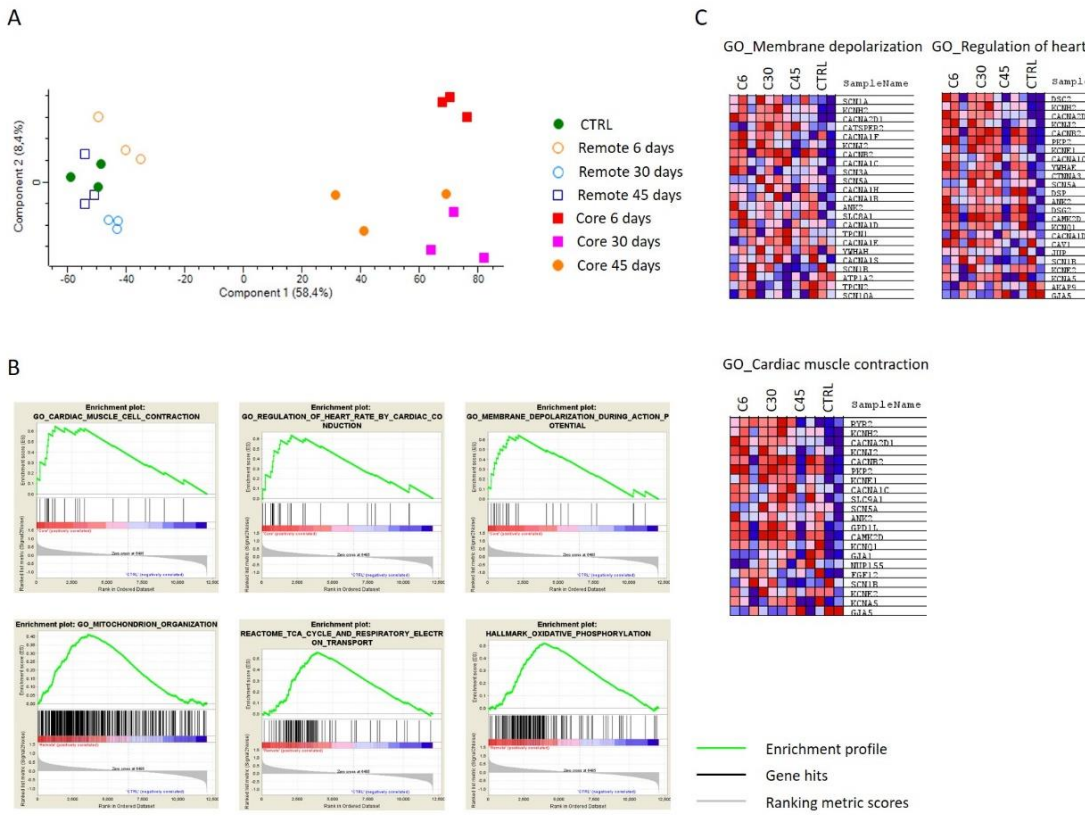

Figure 15. *Principal component analysis, enrichment and overlap analysis, and heat-map clustering. (a) The visual output of principal component analysis (PCA), showing perfect separation of the six groups, and the two different regions (upper left plot) (b) Results of enrichment and overlap analysis. Upper panels: infarct core region. Lower panels: remote myocardium region. The enrichment score (ES) reflects the degree to which a gene set is overrepresented at the top or bottom of a ranked list of genes, with a positive or negative ES indicating gene set enrichment at the top or bottom of the list, respectively. ES is calculated by walking down the ranked list of genes, increasing a running-sum statistic when a gene is in the gene set, and decreasing it when it is absent. The magnitude of the increment depends on the correlation of the gene with the phenotype. The ES is the maximum deviation from zero encountered in walking the list. (c,d) Heat-map clustering. (c) The clustered genes in the leading-edge subsets on the upper panels in b (core region). (d) shows the clustered genes in the leading-edge subsets on the lower panels in b (remote region). Expression values are represented as colors, with red, pink, light blue, and dark blue indicating high, moderate, low, and lowest expression values, respectively.*

Finally, GSEA enrichment and overlapping tests allowed contextualizing of this information, and distribution of the GO terms across the Core vs CTRL, and Remote vs CTRL datasets. This revealed the intrinsic differences between the core and remote

regions of the heart after MI (**Figure 15b-d**). Specifically, the core region showed higher affectation of cardiac contraction, depolarization during action potentials, and heart rate regulation (**Figure 15b**, upper panels), while the remote region showed heavy enrichment of cellular respiration processes (**Figure 15b**, lower panels).

Time-dependent identification of MI-derived biomarkers strongly related to cardiac remodeling

To specifically investigate the adverse cardiac remodeling processes occurring after MI, we integrated the high-throughput microarray data with molecular information available in the literature, and generated an ANN. Analysis of all tissues (infarcted core and remote) and time-points (6, 30, and 45 days) yielded identification of 105 proteins (**Figure 17b**) (Supplementary Table 2).

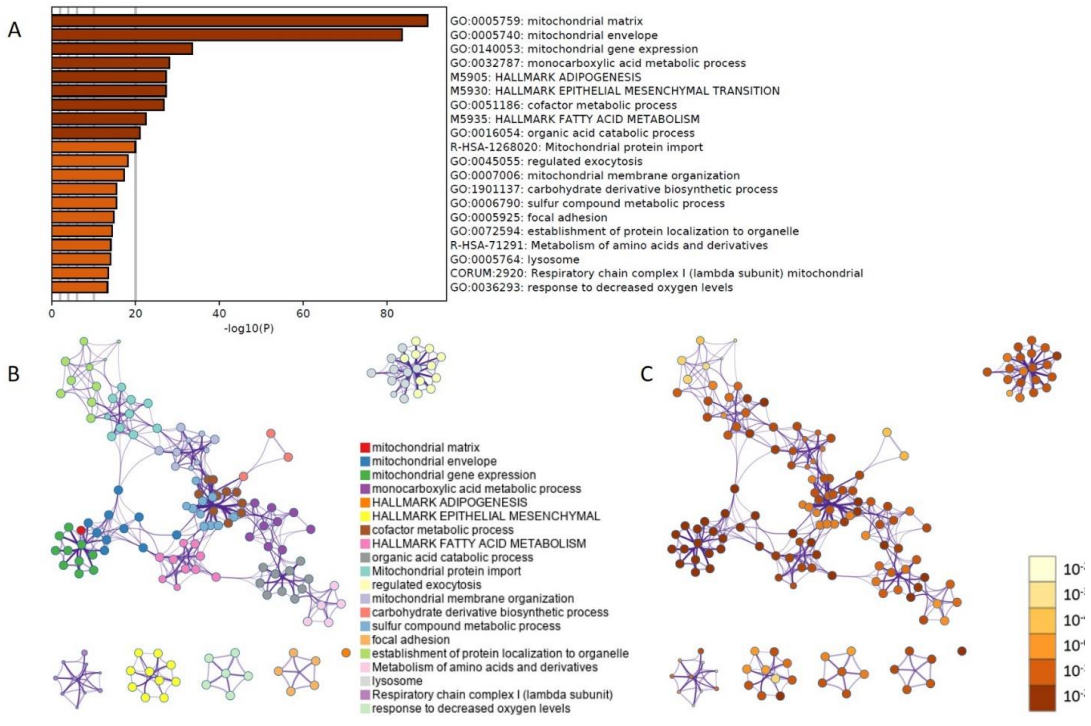

Figure 16*. Functional validation of the integration of gene expression data over 6 weeks after myocardial infarction. Using Metascape algorithms, we identified the most affected biological processes according to their GO terminology (a). These processes were then clearly clustered using a network analysis based on their biological significance (b) and their P value (c).*

Of these, 41 (40%) were previously described in the literature as related to MI, showing associations with adverse remodeling (DPP4, TNR1A, IRAK4), apoptosis and survival (IQGA1, RICTR, p38, JNK, FADD, FOXO1, CASP8, ACINU, CSN3), inflammation and anti-inflammatory processes (LYAM2, TCAM2, AKT3, CCL5, C3, NFKB1, TF65, TNR1A, CXCL7, IRAK4, FOXO4, TLR4, S10A2, LST8), fibrosis (ERK, PGS2, SMAD6, SMAD2, LST8), impaired contractility (ML12A), regeneration and cell proliferation (HMMR, KI67, SMAD1, CSN3), heart development (SMAD6, PRDM1), metabolism shift (AAPK2), and cardiac hypertrophy (CATB, IQGA1, CSN3).

Protein information		*Identification method*	*Identified as classifier*						*Secreted*	*MI*
UniProt	Protein name		C6	C30	C45	R6	R30	R45		
P27487	DPP4	Models, Models/HT	1	1	1	–	1	1	1	1
Q6R327	RICTR	Models	1	1	1	–	–	1	0	1
Q15759	MK11	Models	1	1	1	–	–	–	1	1
P53778	MK12	Models, Models/HT, HT/Models	1	–	1	1	1	–	1	1
P07585	PGS2	Models	–	1	1	1	–	1	1	1
O75676	KS6A4	Models	–	1	1	1	–	–	1	0
Q9UKL0	RCOR1	Models	–	–	1	1	1	–	1	0

Table 7*. Proteins identified as overlapping between the different analyzed time-points, regardless of the myocardial region. Models: the combinations of proteins that better classify the solutions of the models to their corresponding cohort; Models/HT: the combinations of proteins that better classify the solutions of the models to their corresponding cohort, filtered by the proteins acting according to the high-throughput (HT) data; HT/Models: the combinations of proteins that better classify the microarray experiments to their corresponding cohort, filtered by the proteins relevant in the models; 1: detected/positive; 0: negative; –: not detected.*

Notably, seven proteins were identified as overlapping between the different time-points, regardless of the myocardial region (**Table 7**). Of the 105 proteins, 52 (~49.5%) were recognized by both the models and the transcriptomic data analysis (Models/HT or HT/Models identification method). Since these proteins were identified in both models of the pathology and the experimental data, they were considered more robust.

Moreover, we found two distinct combinations of proteins from the infarct core data at each time-point, which had generalization capabilities and accuracies of 100% ($P \leq 0.05$) (**Table 8**). No reliable combinations were achieved using remote myocardium data.

C6	*Uniprot*	*Protein name*	*Generalization capability*	*Accuracy*	*Secreted*[a]	*MI*[b]
Combination 1	P19838	NFKB1	100%	100%	✓	✓
	O14641	DVL2			✓	×
	Q06187	BTK			✓	×
	P01100	FOS			✓	✓
	P61981	1433G			✓	×
Combination 2	P53778	MAPK12	100%	100%	✓	✓
	Q9Y243	AKT3			✓	✓
	P28482	MAPK01			✓	✓
	P19838	NFKB1			✓	✓
	P45984	MAPK09			✓	✓
C30						
Combination 1	P62942	FKB1A	100%	100%	✓	✓
	Q14790	CASP8			✓	✓
Combination 2	P62942	FKB1A	100%	100%	✓	✓
	P30559	OXYR			✓	✓
C45						
Combination 1	P27487	DPP4	100%	100%	✓	✓
	O75330	HMMR			✓	✓
	P03952	KLKB1				
	P07203	GPX1				
	P31645	SLC6A4				
Combination 2	P62942	FKB1A	100%	100%	✓	✓
	P03952	KLKB1			✓	✓

***Table 8**. Best combinations classifying infarcted from non-infarcted hearts, using data from C6, C30, and C45. [a]Indicates if the protein is secreted and/or has been detected in plasma. [b]Indicates if there is a previously known relationship between the protein and MI. Models/HT: the combinations of proteins that better classify the solutions of the models to their corresponding cohort, filtered by the proteins according to the high-throughput (HT) data; MI: myocardial infarction; C6: infarct core area 6 days after infarction; C30: infarct core area 30 days after infarction; C45: infarct core area 45 days after infarction.*

Description of the molecular mechanistic relationships defining MI evolution

Using the differentially expressed proteins found to be related to cardiac remodeling, we performed enrichment analysis to identify and understand the MoA of cardiac remodeling in the infarct core at each time-point. We identified a total of 355 processes as being altered in the infarct core region during at least one time-point: 221 processes upregulated and 134 downregulated. As shown in Figure 17a, there was substantial overlap between the processes altered in the infarct core region at all three time-points (C6, C30, and C45), including 8 KEGG Pathways, 21 GO Function terms, and 72 GO Processes terms. Other processes were specifically altered at one time-point, or two time-points—mainly during the C6-C30 and C30-C45 transitions, although 6 GO Processes terms overlapped between C6 and C45.

Importantly, we found that 101 processes were altered in the infarct core throughout the progression from infarction to 45 days post-infarction. Most of the upregulated processes were related to ECM formation (organization, assembly, and adhesion) and to ECM components (hyaluronic, heparin, collagen, and glycosaminoglycan-related processes). We also detected alterations in processes related to muscle contraction, with upregulation of actin- and calcium-related processes, and downregulation of cardiac muscle contraction. Most of the down-regulated processes were related to metabolism.

Moreover, some of the altered processes exhibited time-dependent behavior. Inflammation clearly appeared to be up-regulated at 6 days post-MI, and decreased in later stages. Processes related to angiogenesis, cell proliferation, and morphogenesis started to increase at 30 days post-MI, and become more relevant at 45 days post-MI. Apoptosis also appeared to gain importance in the late stages. The upregulated pathways at 45 days suggested some normalization of metabolism, although several processes remain altered (**Figure 18**).

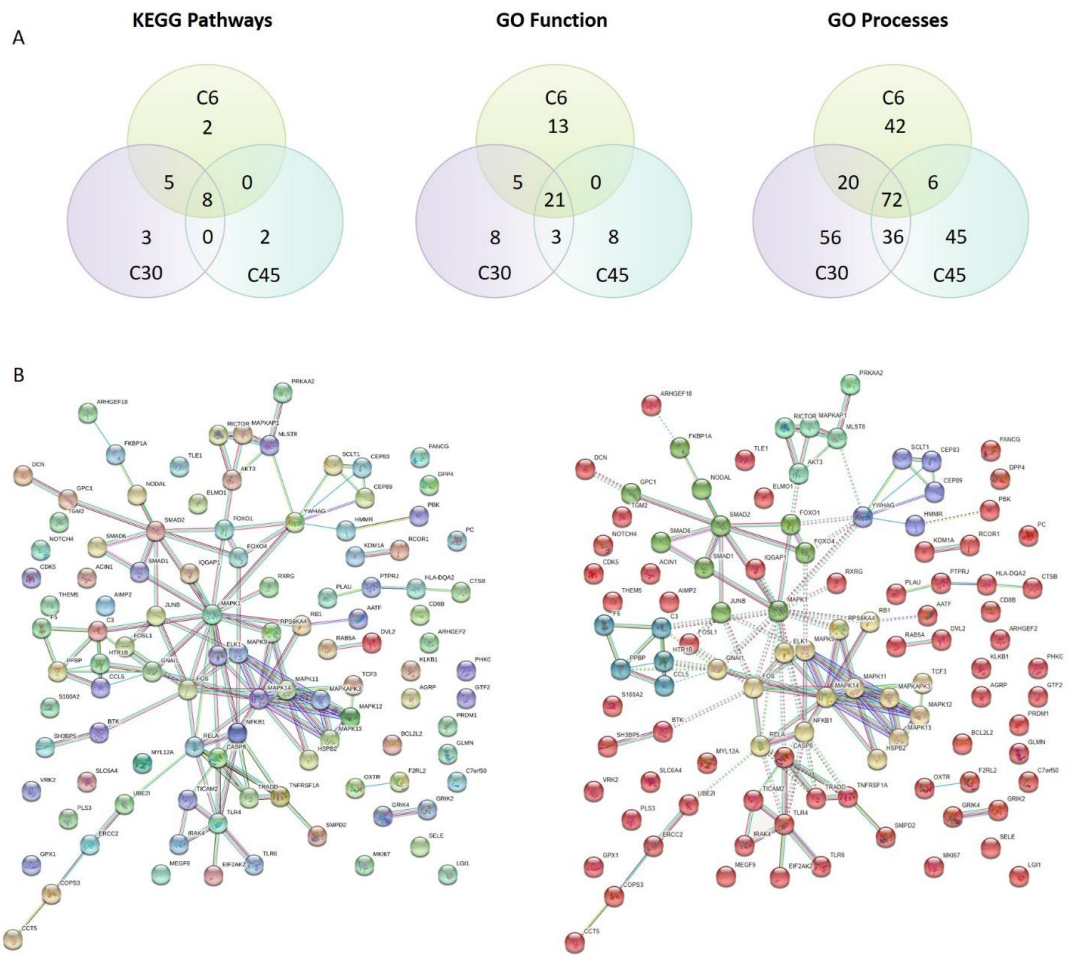

Figure 17. *Protein-protein interaction network analysis. (**a**) Venn diagram depicting the common enriched pathways (KEGG, GO Function, and GO Processes) between the three different time-points. (**b**) Network analysis using the STRING software, including the 105 protein candidates identified by artificial intelligence analysis techniques. Bottom left panel: the cloud of interactions at 0.9 confidence. Bottom right panel: the same interactions clustered by k-means for vector quantization at K= 6. Number of nodes: 105; number of edges: 128; average node degree: 2.44; average local clustering coefficient: 0.469; expected number of edges: 62; PPI enrichment P value: 1.32e^{-13}.*

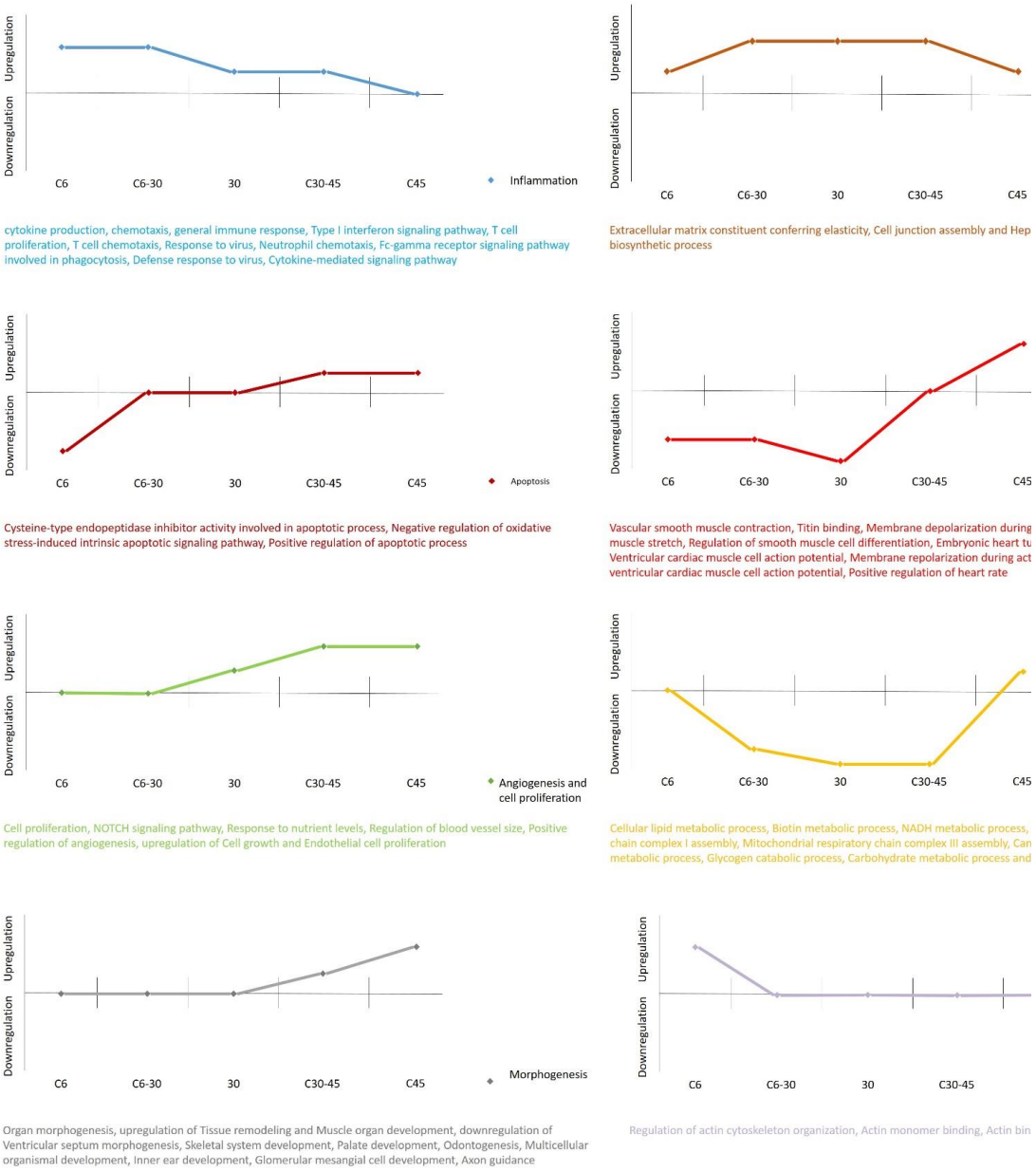

***Figure 18**. Graphic representation of the evolution of affected processes throughout myocardial infarction progression. Values on the X axis show time evolution. Values on the Y axis display upregulation (values above 0), downregulation (values below 0), or lack of differential expression (values of exactly 0 and matching the X axis).*

Identification of the key proteins acting as main drivers of post-MI alterations

Once the mechanistically affected pathways were identified, we used a triggering protein analysis, which allowed specific explanation of the mechanistic relationship between paired sets of proteins. Each analyzed time-point presented a list of particular source proteins (**Table 9**), with some degree of overlap between the different cohorts.

	C6	*C30*	*C45*
Proteins available for analysis[a]	1182	1150	1033
Maximum % of proteins explained by other differential proteins[b]	49%	48%	48%
Number of source proteins[c]	16	18	11
% of explainable proteins explained by triggering proteins[d]	92%	93%	89%

Table 9*. Identification of time-dependent source proteins to explain the molecular mechanism of action of myocardial infarction. Proteins were identified by triggering protein analysis.* [a]*The number of differential proteins related to cardiac remodeling available to be analyzed for each time-point.* [b]*The percentage of evaluable proteins that are linked to another of the evaluated proteins (and are thus explainable by other proteins).* [c]*The number of source proteins selected.* [d]*The percentage of the explainable proteins (i.e., proteins in the second row) that are explained by or linked to the selected source proteins. C: infarcted core region.*

Overall, the transcriptomic experiments in the infarct core region identified 20 proteins (which are primarily involved in growth factor signaling) as the main drivers (source proteins) of post-MI alterations. KPCA, PTN11, JAK2, 1433B, ERBB2, VEGFA, JUN, RAF1, and IGF1R were identified as source proteins at all three time-points. MAPK03, SRC, STAT1, NGF, RAC1, and TF65 were identified as common sources in C6 and C30. CBLB was common for C6 and C45, although its activity changed from day 6 (activated) to 45 (inhibited). GCR, CDC42, and GRB2 were identified as sources only in C30, while MAPK01 was found specifically in C45.

Unraveling the molecular MoA relating the source proteins to cardiac remodeling

Mechanistic analysis of the relationship between the identified source proteins and cardiac remodeling revealed overlap between the different time-points. The common pathways between the protein sources and cardiac remodeling (**Figure 19**) involved IGF1R, RAF1, KPCA, JUN, and PTN11. Analysis of the downstream signaling of these proteins revealed a MoA potentially involving 18 proteins, 15 of which were detected as differentially expressed during at least one time-point (**Table 10**). The ERK kinases MAPK01 and MAPK03 were apparently activated by PTPN11 and PKCA, respectively, and both were upregulated at all three time-points. The other upstream proteins (IGF1R and RAF1) were inhibited. Additionally, PTPN11 was functionally inhibited by MAPK03, resulting in a reduction of MAPK01 activity.

Entry name	*UniProt Code*	*Log Ratio C6*	*Log Ratio C30*	*Log Ratio C45*
TNFA	P01375	-	-	-
RAF1	P04049	−0.69	−0.90	−0.71
P53	P04637	0.82	0.84	-
JUN	P05412	−1.49	−1.46	−1.36
IGF1R	P08069	−1.61	−0.993	−1.54
THB	P10828	−1.59	−2.30	−1.44
KPCA9	P17252	2.61	2.30	1.79
SLC9A1	P19634	-	−0.56	-
MAPK03	P27361	0.60	0.84	-
MAPK01	P28482	-	-	−0.78
MTOR	P42345	−0.57	−0.7	−0.59
TSC2	P49815	-	-	0.75
MMP14	P50281	1.32	1.74	1.40
RPS6KA3	P51812	-	-	−0.49
PTNP11	Q06124	0.86	0.58	0.64
RPS6KA2	Q15349	-	-	-
RPS6KA1	Q15418	-	-	-
BAD	Q92934	0.90	1.07	0.81

***Table 10**. Proteins involved in the common mechanism of action between time-points for the infarct core region, and their log ratio values at each time-point. C6: infarct core area 6 days after infarction; C30: infarct core area 30 days after infarction; C45: infarct core area 45 days after infarction.*

With regards to cellular proliferation, survival, and differentiation, we found that TSC2 was upregulated at C45. We also detected heavy upregulation of the ECM remodeling protein MMP14, and of BAD and P53, which are key components of apoptosis and survival. Accordingly, at all three time-points, we detected downregulation of MTOR, SL9A1 (hypertrophy-related), and THB (impaired myocyte contractility).

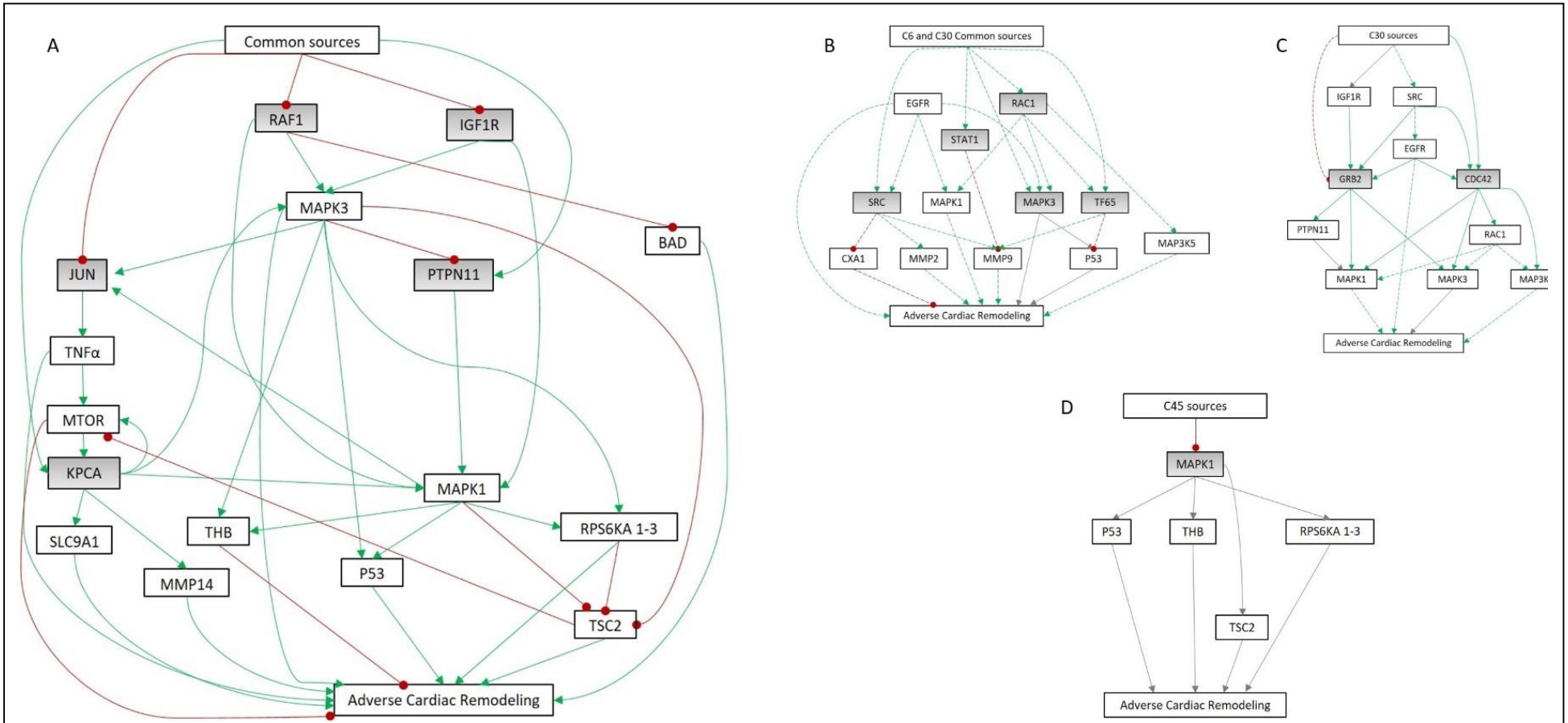

Figure 19. *MoA determined by artificial neural network analysis (ANN). (**a**) Common mechanistic relationship between cardiac remodeling and the common source proteins (in grey: IGF1R, RAF1, KPCA, JUN, and PTN11) identified at all three analyzed time-points in the infarct core region. (**b–d**) Mechanistic representation of (**b**) C6–C30 common source proteins (SRC, STAT1, MK03, RAC1, and TF65), (**c**) C30 source proteins (GRB2 and CDC42), and (**d**) C45 source proteins (MK01). Continuous colored lines depict links present only in one cohort. Discontinued lines depict links present in two cohorts. Continuous grey lines depict links present at all time-points. C6: infarct core area 6 days after infarction; C30: infarct core area 30 days after infarction; C45: infarct core area 45 days after infarction.*

SUMMARY FIGURE

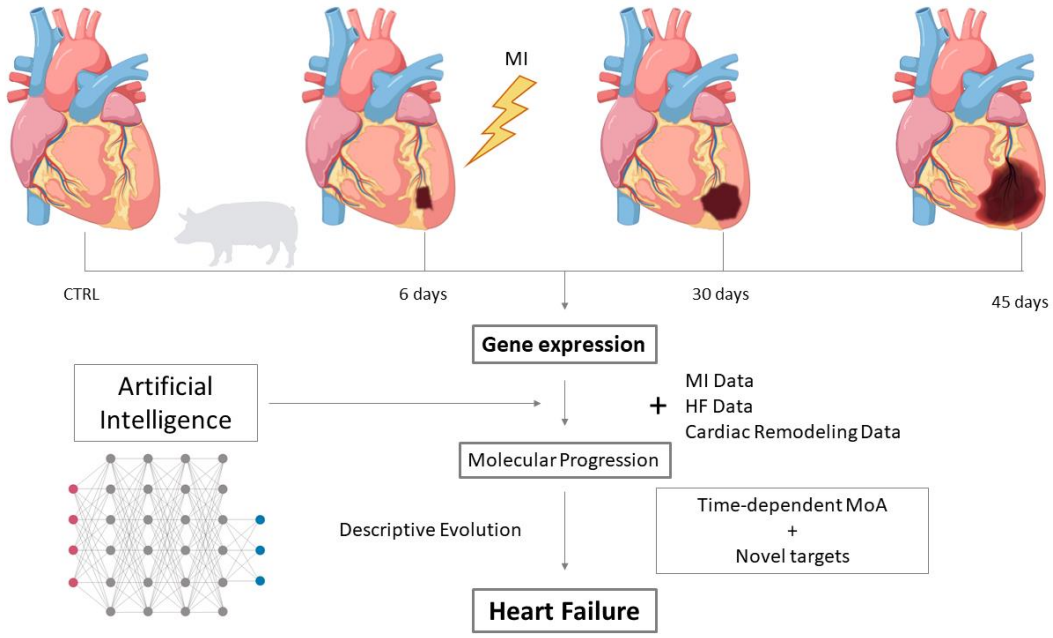

Figure 20. In this work, we aimed to use gene expression data from a pre-clinical model of MI in swine to delineate its molecular evolution towards heart failure. By combining microarray information of MI at 6, 30 and 45 days with publicly available data on MI, HF and cardiac remodeling, we were able to use artificial intelligence techniques to analyze this vast amounts of datapoints and unravel hidden mechanisms and time-dependent patterns. This approach allowed us to clearly delineate the progression of MI towards HF at the molecular level with striking detail. Thus, we describe the complete progression of specific signaling pathways at each stage of the disease and its subsequent targets to halt this process.

ACUTE HEART FAILURE -

CARDIOGENIC SHOCK

Chronic HF is the leading cause of inter-hospital mortality worldwide, which constitutes an authentic pandemic. However, many of these patients either develop HF derived from an acute event or experience a drastic worsening of the condition during the recurrent hospitalizations. Indeed, acute HF is the leading cause of intra-hospital mortality in more-developed countries. More specifically, the most aggressive form of acute HF is CS, a low-cardiac-output state, caused by left, right or biventricular dysfunction, resulting in a life-threatening state of critical end-organ hypoperfusion and hypoxia. Acute MI with left ventricular dysfunction is the most frequent cause of CS, but acute decompensation of HF is also a common originator (100).

Yet, acute HF receives little attention compared to the chronic form of the disease, which has caused this field of research to hold relegated for a long time. This is especially accurate for its prognosis, usually guided by circulating biomarkers, which lacks clinical implementation of new tools for several decades now.

Consequently, in the second part of this thesis we aimed to review the current situation of the biomarker-related research in CS, and build upon it to develop new transcriptomic and/or proteomic scores to aid CS prognosis.

Molecular Signature of Cardiogenic Shock

The incidence of CS has increased remarkably over the past decade, in part associated with an aging population. Acute myocardial infarction-derived CS increased from 6.5% in 2003 to 10.1% in 2010 ($p< 0.001$), with a greater increase among patients older than 75 years (101). Among patients with congestive heart failure not preceded by acute myocardial infarction, the incidence of CS rose from 0.5% to 1.0% ($P<0.001$). Mandawat

and Rao queried the 2004 to 2014 Nationwide Inpatient Sample databases to identify all patients with CS (CS; International Classification of Diseases-Ninth Revision [ICD-9] CM 785.51) and found that the overall incidence of CS increased from 55,123 discharges in 2004 to 126,555 discharges in 2014 (Ptrend=0.002). During the same time period, in-hospital mortality decreased from 62% in 2004 to 48% in 2014 (Ptrend=0.02), likely due to significant advances in revascularization and supportive care, such as use of mechanical circulatory support. Nevertheless, mortality remains unacceptably high despite recent advances in CS management in modern times, with close to one out of two patients dead at 90 days.

CS is not simply a sudden fall in cardiac contractile function. It is also a multiorgan dysfunction syndrome, often complicated by a systemic inflammatory response with severe cellular and metabolic dysregulations (100). Such multi-organ failure, source of countless circulating molecules, has been and will be of great value in CS characterization. Indeed, contemporary advances in –omics technologies provide new insight into a more holistic molecular signature of CS, including myocardial, inflammatory, and end-organ failure. Here, we first wanted to review the biochemical manifestations of CS elaborating on current gold standard biomarkers and novel candidates from the molecular signature of CS.

Current biomarkers: glucose and lactate

Knowledge of elevated lactate and/or glucose levels goes back decades in acute illnesses and has long been used in CS management. Although they are not included in the required diagnostic CS criteria in the most recent ESC guidelines, they did emerge as independent predictors of short-term mortality in contemporary risk scores. The CardShock risk score, published in 2015, only incorporated blood lactate > 4 mmol/L with 2 points out of a

maximum of nine ; the IABP-Shock risk score, published in 2017, incorporated both arterial lactate >5 mmol/L with 2 points, and glucose >10.6 mmol/L (191 mg/dl) with 1 point, also out of a maximum of 9 (190).

Claude Bernard, in his book “Leçons sur le diabète et la glycogenèse animale” published in 1877, was the first to report the occurrence of glycosuria following acute injury, and hyperglycemia is now recognized as a frequent concomitant of acute illness or injury irrespective of the patients’ history of DM (191,192). In brief, the current concept of the pathogenesis of hyperglycemia in the critically ill is that it represents a response to inflammatory mediators, such as interleukin-1 (IL-1) and tumor necrosis factor α (TNF-α) – that suppress insulin secretion relative to blood glucose concentrations (193) and increase the release of counter-regulatory hormones, including cortisol, catecholamines, glucagon, and growth hormone. This dysregulation leads to insulin resistance, thereby inducing hyperglycemia.

Marked hyperglycemia is unequivocally toxic and associated with numerous deleterious effects (192). In CS, data from observational studies, mainly retrospective, suggest an association between glucose levels and prognosis. In 2004, Zeller M *et al.* evaluated in-hospital outcomes after AMI relative to the Impaired Fasting Glucose level (IFG). High fasting blood glucose measures after admission showed a significant increase in cardiogenic shock (12% vs 6%, P=0.011) and ventricular arrhythmia (15% vs 9%, P=0.035) between IFG and Non-IFG groups after adjustment for confounding factors, including age, sex, anterior location, and LVEF (194). Indeed, results from the CardShock registry including patients with CS of different etiologies investigated the association of blood glucose level at time of admission and short-term mortality in CS (195). This study found an independent prognostic role of blood glucose levels on admission, when adjusted for other factors and specifically DM. Similar results were obtained in a sub-

analysis of the IABP-Shock study. The authors also found a relationship between high admission glucose levels and mortality in a cohort of patients presenting acute myocardial infarction-derived CS, again, irrespective of whether the patients were previously glucose tolerant (196). Nonetheless, other groups describe a small increase in predictive power for blood glucose, but only among patients without DM (197).

Lactate was discovered in 1780 by the Swedish chemist Karl William Scheele, although it was not introduced into medicine until 1843 when the German physician Johann Joseph Scherer isolated it in the blood of a woman who died from postpartum septic shock (198). Lactate, easy and quick to measure, has since been considered a marker of tissue hypoperfusion or hypoxia in critical illnesses. Lactate is a key substrate in glucose metabolism with a widely known prognostic impact in patients with acute heart failure and CS. Lactate is created in the muscles and peripheral tissues and then transported into the liver and kidneys where it is transformed into glucose *via* gluconeogenesis (199). In CS hyperlactatemia is primarily caused by an increase in lactate production, rather than mediated by dysfunctional use or clearance in the tissue.

Schmiechen et al first presented the analysis of lactate as a potential prognostic biomarker for cardiac diseases (200), establishing a threshold of 2.2mmol/l with a sensitivity of 96% and a specificity of 55% in diagnosing acute MI. Since then, several studies have evaluated the prognostic value of lactate in acute myocardial infarction and CS. Mavric *et al.* reported that lactate is a strong predictor of shock occurrence during in-hospital stay, irrespective of initial clinical signs in patients with acute myocardial infarction (201). Vermeulen *et al.* reported that raised lactate concentration >1.8 mmol/l was associated with hypotension, increased heart rate, distal coronary embolization, DM, non-smoking, greater enzymatic area of ischemia, more frequent use of intra-aortic balloon pump, and 30-day mortality in patients with ST-elevation myocardial infarction (202).

Moreover, lactate also displays prognostic potential in emergency settings independent of classically interpreted physical signs (heart rate, blood pressure) when assessed in capillary blood, and may be useful in risk stratification at one-year after MI (199).

Understandably, lactate concentration has been used in the majority of trials to analyze the potential benefit of mechanical support devices in CS. However, in a systematic review and collaborative meta-analysis of randomized trials (203), Thiele *et al.* recently concluded that despite the positive impact of mechanical circulatory support on hemodynamic parameters in the form of increased mean arterial pressure and reduced lactate levels, it did not reduce 30-day mortality compared to the control group.

Taken together, glucose and lactate, both more than centenarian, fall short and may be too imprecise to truly aid in CS diagnosis and prognosis (**Table 11**). Clinicians are used to measuring them in their local protocols, but little to no action is taken based on their circulating levels. There is a need for novel biomarkers, derived from contemporary -omics technologies, to better refine CS risk prediction and stratification for a more tailored therapy (204).

Genomics biomarkers for CS

Genotype based risk prediction is fixed from birth, allows early risk prediction, is less susceptible to biological variation over life and is easy to obtain with minimal measurement error. Unfortunately, there are very few data on genes influencing CS (**Table 11**), and nothing has been reported on genome-wide association studies (GWAS) and CS.

Cytokine and chemokine production are massive and deleterious in CS, having received the name of “the tomb markers” of the intensive cardiac care unit. Chemokine RANTES (regulated on activation, normal T cell expressed and secreted), is a member of the group

of inflammatory cytokines that play an important role in immune reactivity. Lipkova *et al.* evaluated the role of RANTES-403G/A polymorphism in HF and CS.

Omics	*Tests*	*Current Applications*	*Current Candidates*	*Clinical Value*
Metabolomics	Biochemical Tests	Follow-Up and Risk Scores	Glucose and Lactate	Indicators of disease severity
Genomics	GWAs and Sequencing	Genotype-based risk prediction and Discovery of gene candidates	RANTES-403G/A, TNF-α308a>g, IFN-γ874t>a, MnSOD Ala16Val	Association to disease developing and evolution
Transcriptomics	RNAseq and Microarrays	Biomarker discovery and Drug safety assessment	miRNAs and LncRNAs	No predictive value (To date)
Peptides & proteins	ELISA assays	Biomarker discovery and Pathogenesis	BNP, NT-ProBNP, cTn, ST2, INF-γ, TNF-α, MIP-1β, G-CSF, MCP-1β, Ang-1 and Ang-2, Th17/Treg, FGF-23, OPG, GDF-15, CS4P	Indicators of disease severity, Prognosis and Clinical outcomes
Secretomics (Extracellular Vesicles)	Ultracentrifugation and Size-Exclusion Chromatography	Biomarker discovery and Pathogenesis	Leukocyte and Platelet-derived EVs	Potential indicators of disease severity

***Table 11**. Review of current high-throughput disciplines and candidate biomarkers that can play an important role in the present and future of CS management. GWAs: Genome-Wide Association studies; RANTES-403G/A: regulated on activation, normal T cell expressed and secreted polymorphism; INF-γ: Interferon gamma; MnSOD: manganese superoxide dismutase; miRNAs: microRNAs; LncRNAs: Long non-coding RNAs; BNP: brain natriuretic peptide; NT-ProBNP: N-terminal prohormone of brain natriuretic peptide; cTn: cardiac troponins; ST2: Interleukin-1 receptor-like 1; TNF-α: tumor necrosis factor alpa; MIP-1β: macrophage inflammatory protein-1β; G-CSF: granulocyte colony stimulating factor; MCP-1β: monocyte chemoattractant protein-1β; Ang-1 and Ang-2: angiopoietin-1 and -2; FGF23: fibroblast growth factor 23; OPG: osteoprotegerin; GDF15: growth-differentiation factor 15; CS4P: Biomarker panel including Beta-2-microglobulin (B2M), Aldolase B (ALDOB), Fatty acid-binding protein, Liver (L-FABP), and Plasma protease C1 inhibitor (IC1); EVs: extracellular vesicles.*

The authors found an association between RANTES-403G/A promoter polymorphism and acute HF and ejection fraction at 3 months of follow-up (205). Appoloni *et al.* explored the association between TNF-α and interferon (IFN)-gamma cytokine polymorphisms in CS. There were no significant differences in TNF-α polymorphism (within the promoter at position 308 A→G between patients with CS and healthy controls, but IFN-gamma polymorphism (at intron 1 at position + 874 T→A) was less common in CS. Patients with the TNF-2 allele had no greater risk of CS, but a better survival rate when it develops (206).

Cardiomyocytes are protected against metabolic oxidative stress by several enzymatic and non-enzymatic defense systems, including manganese superoxide dismutase (MnSOD). Several MnSOD polymorphisms have been described, but only Ala16Val has been demonstrated to have functional significance. In the setting of CS, Charniot *et al.* found that MnSOD dimorphism (Ala16Val) was significantly correlated with the severity and prognosis of CS due to dilated cardiomyopathy (207).

The predictive performance of these preliminary genomic polymorphisms in CS has not been tested, and it should be considered as pathophysiological insight only, without likelihood of entering the clinical realm in the short term.

Transcriptomics biomarkers for CS

Transcriptomics is an emerging and growing field in biomarker discovery and drug safety assessment. More importantly, transcriptomics has the potential to provide significant insight into the understanding of the disease pathogenesis (52). To the best of our knowledge, there are no data at present evaluating the value of lncRNAs in CS, even

though lncRNAs have been found associated with the genetic predisposition to develop coronary artery disease and HF.

MiRNAs may be obtained in many biological fluids and display promising characteristics of circulating biomarkers, such as robust stability to temperature changes and resistance to degradation by endogenous RNAase activity (54). However, transcriptomics has not been used in CS beyond some preliminary studies, and only a handful of miRNAs have been investigated as potential biomarkers. Goldbergova *et al.* found that circulating levels of miR-1, miR-133 and miR-124a were elevated in CS, but could not be correlated to the extent of injury, progress of the disease, or prognosis of patient outcome (209). More specifically, miR-21, miR-122a, miR-320a, and miR-423-5p have been previously linked to cardiac remodeling and heart HF in different studies (210–213). Therefore, we sought to assess the expression dynamics of these miRNAs during the first 24h in patients with ST elevation myocardial infarction (STEMI) complicated with CS, as well as their prognostic value at 30 days.

Circulating MiRNA Dynamics in ST-Segment Elevation Myocardial Infarction-driven Cardiogenic Shock

Out of 1,265 STEMI patients admitted, 51 (4.0%) developed CS and were recruited for this study. 43 patients fulfilled the inclusion criteria; 6 were excluded due to mechanical complications and 2 were not analyzed because of technical issues. All-cause of death at 30 days was 44.2% (n=19) (**Table 12**).

		No.
Age, years	67.8 ± 13.3	43
Male	28 (65)	43
Risk factors		
Smoking current/past	13 (30) / 11 (25)	43
Hypertension	27 (63)	43
Diabetes	19 (44)	43
Dyslipidemia	23 (53)	43
Previous MI	3 (7)	43
Previous PCI	5 (12)	43
Presentation		
Anterior STEMI	28 (65)	43
SBP, mmHg	96.8 ± 31.6	43
DBP, mmHg	55.8 ± 17.1	43
HR, bpm	84.5 ± 29.1	43
Primary PCI	41 (95)	43
Time to reperfusion, min	197 [143 - 291]	41
Number of diseased vessels		
1	12 (29)	41
2	16 (39)	41
3	13 (32)	41
Left Main disease	10 (24)	41
LEVF, %	38.6 ± 13.0	43
Lactate (mmol/L) (On Admission)	9.2 ± 6.0	7
Hemoglobin (g/dL) (On Admission)	11.7 ± 2.5	43
Creatinine (mg/dL) (On Admission)	1.7 ± 0.7	43
CK-MB peak (ng/mL)	457.4 ± 444.6	43
cTnI peak (ng/mL)	212.2 ± 328.0	43
Complications		
Out-of-hospital cardiac arrest	15 (35)	43
Ventricular fibrillation	13 (30)	43
Complete cardiac block	12 (28)	43
Management		
Mechanical ventilation	22 (51)	43
Inotropic drugs	40 (93)	43
Intra-aortic balloon pump	24 (56)	43
Other mechanical circulatory support (Impella)	1 (2)	43
Death at 30 days	19 (44)	43

***Table 12**. Demographic and Clinical Characteristics of Studied Patients. CK-MB, creatine kinase-MB; cTnI, cardiac troponin I 99th percentile cutoff value for the upper reference limit: 0.5 ng/mL; DBP, diastolic blood pressure; HR, heart rate; LEVF, left ventricular ejection fraction; MI myocardial infarction; PCI, percutaneous coronary intervention; SBP, systolic blood pressure; STEMI, ST-segment elevation myocardial infarction.*

STEMI patients display a peak in miR-320a and miR-423-5p levels at 12h of CS complication

Analysis of the kinetics of the studied miRNAs revealed a significant increase in miR-320a and miR-423-5p at 12h compared to baseline ($p<0.001$). However, all studied miRNAs decreased significantly from 12 to 24h ($p<0.001$). MiR-21, miR-122a, and miR-320a levels decreased significantly to below baseline ($p=0.006$, $p=0.003$, and $p=0.000$, respectively), whereas miR-423-5p levels in the plasma returned to baseline ($p=0.09$; **Figure 21**).

Risk factors and clinical parameters do not contribute to all-cause of death at 30 days discrimination.

Using a multivariate analysis, 30-day decedents were found to be older (75.7±2.4 vs. 61.5±2.4; $p<0.001$) and to have lower LVEF; (32.6±2.8 vs. 43.3±2.4; $p=0.006$) in our cohort. We also analyzed the contribution of gender, various risk factors (including smoking, hypertension, DM, dyslipidemia, cerebrovascular disease, peripheral vascular disease, antecedents of HF, familial antecedents, antecedents of ischemic cardiomyopathy, antecedents of angina, Previous MI, and STEMI localization), and several clinical variables (including

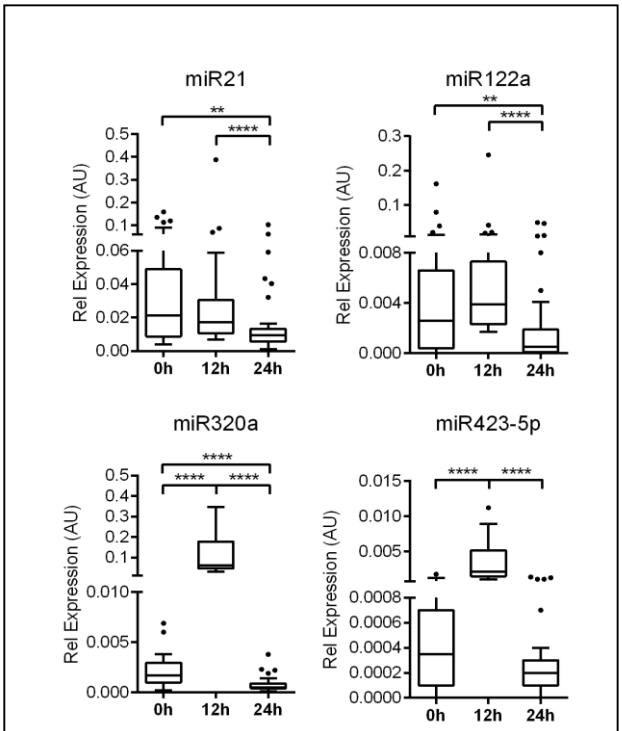

***Figure 21**. miRNA dynamics in cardiogenic shock. Data is presented as boxplots with the median depicted and outliers as separate dots. The data account for 43 different patients at 0 h, 12 h, and 24 h. **p<0.01 and ****p<0.001*

peak troponin I levels, Troponin T levels, heart rate, or blood pressure) to the primary end-point. No differences were found between survivors and decedents in any of the studied parameters (all $p > 0.1$).

miR-21, miR-122a, miR-320a and miR-423-5p do not correlate with 30-day mortality during the first 24h of CS

Neither univariate nor multivariate analysis revealed significant associations between the studied miRNAs at the three time-points (0h, 12h and 24h) and 30-day mortality (Data Not Shown). We also looked for potential correlations between miR-21, miR-122a, miR-320a, and miR-423-5p levels and the use of IABP at every time point (0h, 12h and 24h). No correlations were found to be statistically significant for any miRNA and the adoption of IABP at any time point. Moreover, following stratification of our cohort for the use of IABP, we did not exclude the possibility of correlations between all four miRNAs and the primary end-point (all-cause of death at 30 days) in every time point. No statistically significant correlations were found in this analysis either.

SUMMARY FIGURE

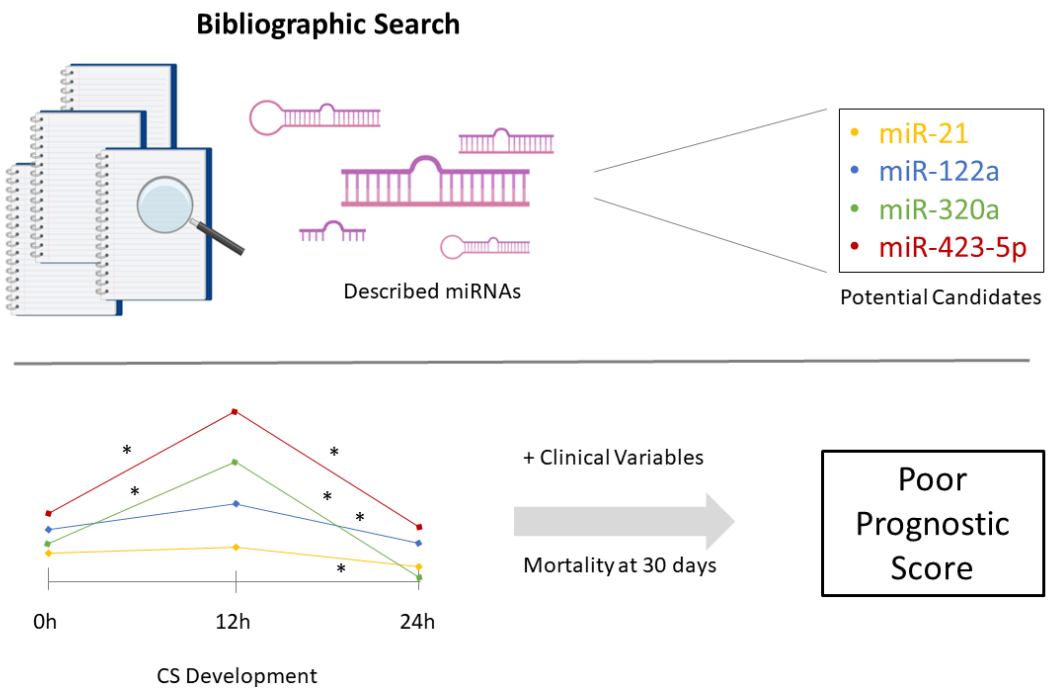

***Figure 22**. In this work, we investigated four miRNAs previously related to several CVDs, including miR-21, miR-122a, miR-320a and mir-423-5p. We wanted to assess their prognostic value for all-cause mortality at 30 days. Here, STEMI patients displayed a peak in miR-320a and miR-423-5p levels at 12h of CS complication of unknown origin. Interestingly, the levels of all miRNAs studied returned to baseline or below despite the persistence of CS. However, neither risk factors and clinical parameters nor any of the miRNAs did not contribute to or correlate with all-cause of death at 30 days discrimination during the first 24h of CS. miRNAs: microRNAs; CVDs: Cardiovascular diseases; STEMI: ST elevation myocardial infarction; CS: Cardiogenic shock.*

Unfortunately, attempts to demonstrate predictive value for these markers in CS beyond currently used variables have fallen short of statistical relevance (**Table 11**).

Proteomic biomarkers for CS

In this section, we will review the peptides used as biomarkers in cardiovascular diseases, renal dysfunction and systemic inflammation, proposed as potential biomarkers in CS, as well as the recently reported proteomic CS4P molecular score for CS prognosis (**Table 13**).

Value of current cardiac biomarkers: NT-proBNP, troponins, ST2

Troponins can assess minute changes in myocardial cell necrosis and can be measured within 3 to 4 hours after the onset of myocardial damage. The higher the level and the longer the level stays raised, larger is the area of myocardial damage and larger is its severity. Troponin I concentration is associated with outcome in several cardiac diseases, particularly in patients with HF and CS complicating myocardial infarction (214). Jolly SS *et al* studied if the extent of troponin elevation predicted mortality as well as in-hospital complications of several cardiac complications, including cardiogenic shock. They found that, for each 10-fold increase in the troponin ratio, there was an associated increase in cardiac arrest, sustained ventricular tachycardia or ventricular fibrillation and cardiogenic shock (215). A prospective study conducted on a group of 712 patients undergoing heart valve surgery identified that postoperative high-sensitivity Troponin T was valuable to predict postoperative cardiogenic shock requiring mechanical circulatory support (216). However, troponin levels are elevated in circumstances other than myocardial injury, and therefore this parameter should be interpreted cautiously

(217,218). Indeed, high-sensitivity cardiac troponin T elevation was found to be very common in patients hospitalized for non-cardiogenic shock (219).

B-type natriuretic peptide (BNP) and N-terminal pro-B-type natriuretic peptide (NT-proBNP) levels and are often elevated in intensive care patients regardless of the reason for their admission, and elevated levels of these biomarkers are independent predictors of mortality (220). In patients with CS, elevated BNP or NT-proBNP level may be related to both left and right ventricular dysfunction and may predict outcomes (221,222). Remarkably, low NT-proBNP values (<1,200 pg/ml) consistently display a negative prognostic value for CS (223). In patients with severe refractory cardiogenic shock elevated levels of BNP, hsCRP, sTNFR1, endothelin-1, and PIIINP were identified. Ventricular unloading with ventricular assist device support was associated with reductions in serum BNP, sFas, and endothelin-1 levels and increases in serum sFasL and PIIINP levels (224). Patients undergoing percutaneous coronary intervention for acute myocardial infarction with cardiogenic shock who received intra-aortic balloon pump counterpulsation also showed significantly lower BNP levels (225).

Soluble ST2, or IL-1 receptor-like-1 (IL1RL1), is a decoy receptor for IL-33. It is currently approved for prognosis in HF, and it is already incorporated into AHA/ACC HF guidelines (226). The ST2 cut-point values differ, being 35 ng/mL in HF and 500 ng/mL in CS. Such high levels of ST2 in patients with CS seem to be related to stimulation by IL-1β, IL-6, or TNF-α. Parenica *et al.* found that ST2 levels were elevated in shock, much more so in septic shock than in CS. ST2 levels were related to natriuretic peptides, but did not provide independent prognostic value at 90 days relative to CS mortality risk (227). In contrast, in a biomarker sub-analysis of the CardShock registry including only patients with CS caused by acute coronary syndrome, Tolppanen *et al.* found that the combination of ST2 and NT-proBNP showed good discrimination for 30-day mortality

(AUC = 0.77 at 12 h after CS onset). The addition of ST2 and NT-proBNP to the CardShock risk score improved the C-statistics (AUC = 0.81 vs 0.78; p = 0.046). The addition of ST2 or NT-proBNP alone to the Card-Shock risk score did not reach statistical significance (228).

Luyt *et al.* explored the usefulness of cardiac biomarkers to predict cardiac recovery in patients on extracorporeal membrane oxygenation support (ECMO) for refractory cardiogenic shock. NT-proBNP, troponin I, mid-regional pro-atrial natriuretic peptide (MR-proANP), pro-adrenomedullin (proADM), and copeptin levels were high in patients with refractory CS requiring ECMO support. Neither their crude blood levels nor their kinetics during the first week of ECMO support were predictive of cardiac recovery (229). The reasons expressed by the authors to explain these findings were multifaceted, including multi-organ failure with cardiac involvement.

Non-cardiac biomarkers

In CS, renal dysfunction is an important parameter of inadequate end-organ perfusion and an independent predictor of adverse outcome. The two contemporary risk scores available each incorporate a measure of renal dysfunction: the CardShock risk score $eGFR_{CKD\text{-}epi}$ <30 ml/min with 2 points (230), and the IABP-Shock risk score creatinine >132.6 µmol/L (1.5mg/dL) with 1 point (190). In a biomarker sub-study of the IABP-Shock Trial, Fuernau *et al.* examined the value of novel renal function biomarkers in CS (196). Neutrophil gelatinase-associated lipocalin (NGAL), kidney injury molecule 1 (KIM1), cystatin C (CysC), or calculation of glomerular filtration rate provided no additional prognostic information in patients with CS in comparison to creatinine. Therefore, creatinine may be considered the standard parameter to monitor kidney function in CS.

An increasing number of novel biomarkers of systemic inflammation have been reported in patients with CS, including interferon-γ (INF-γ), TNF-α, macrophage inflammatory protein-1β (MIP-1β), granulocyte colony stimulating factor (G-CSF), monocyte chemoattractant protein-1β (MCP-1β), angiopoietin-1 and -2 (Ang-1 and Ang-2), and the Th17/Treg ratio (231–233). Growth factors, such as fibroblast growth factor 23 (FGF-23) (234), osteoprotegerin (OPG), and growth-differentiation factor 15 (GDF-15) (235) have also been examined in CS. High levels of FGF-23 were independently related to a poor clinical outcome only in patients with impaired renal function.

Patient Status	*B2M, µg/mL*	*L-FABP, ng/mL*	*ALDOB, ng/mL*	*IC1, µg/mL*
Survivors	485.9	642.2	199.3	209.3
Non-Survivors	732.0	954.8	291.7	191.7

***Table 13**. Mean concentrations of CS4P proteins observed in patients as measured by ELISA assays.*

Finally, an increased number of extracellular vesicles derived from proinflammatory and prothrombotic cells were found in CS (236). Further studies are needed to better understand its potential clinical relevance. However, none of these biomarkers have been rigorously tested against current CS risk scores.

In sum, the biomarkers studied to date were pre-selected by investigators and biased by their origin or function, and their overall performance seems suboptimal in CS.

Novel proteomic-derived biomarkers: The CS4P Score

Very recently, our group performed a comprehensive proteomic analysis in which over 2600 proteins were identified in a derivation cohort (the Barcelona cohort). Combined with targeted proteomics in a validation cohort (the CardShock cohort) (204) we were

able to derive four proteins with predictive power for short-term risk assessment, and therefore a proteomic risk score was developed, the CS4P. CS4P comprises the abundances of liver fatty acid-binding protein (L-FABP), beta-2-microglobulin (B2M), fructose-bisphosphate aldolase B (ALDOB), and SerpinG1 (IC1) (Table 13).

The CS4P model had an AUC of 0.83, and showed a marked benefit in patient reclassification, with an NRI of 0.49 (P=0.020) compared to CardShock risk score and an NRI of 0.57 (P=0.032) compared with IABP-SHOCK II risk score. Overall, CS4P performance metrics were better than clinical and conventional biomarkers in CS. Indeed, none of the previously described protein biomarkers included in this analysis provided significant predictive value on top of CS4P. Furthermore, the value of these proteins obtained by proteomics technologies was validated using bedside ELISA. Of note, none of the 4 proteins of the CS4P are found in the heart, but they reflect multi-organ dysfunction, as well as systemic inflammation and immune activation.

We will devote the next section to better understand the significance of these proteins in terms of biology, synthesis, degradation, half-life, and pathophysiology (Table 14).

Protein	*Family*	*Biological fluid*	*Half-life*	*Subcellular localization*	*Tissue expression*	*Pathology*
B2M	Immunoglobulin	Blood & Urine	2.5h	Cell surface (nucleated cells)	Hematopoietic cell lines, lungs, spleen, peritoneum	Amyloidosis, retinitis pigmentosa, immunodeficiency 43, multiple sclerosis, thrombocytopenia
ALDOB	Class I Aldolase	Blood	24-48h	Cytoskeleton, Cytoplasm	Kidney cortex, liver, stomach, intestine	Hereditary fructose intolerance, obesity, liver inflammation, hepatic fibrosis
L-FABP	Fatty-acid binding proteins (FABP)	Blood & Urine	72h	Cytoplasm and Nucleus	Liver, kidney, intestine	Obesity, liver injury, acute kidney tubular necrosis, chronic kidney failure, lipoidosis
IC1	Serine proteinase inhibitors (Serpins)	Blood & Urine	28h	Extracellular	Vasculature, breast, adipose tissue, liver	Hereditary angioedema

***Table 14**. Summary of biologically relevant properties of a proteome-derived biomarker panel to stratify CS patients according to mortality at 90 days. Beta-2-microglobulin (B2M) participates in antigen presentation; aldolase B (ALDOB) is mainly involved in the glycolysis/gluconeogenesis pathways; liver fatty acid-binding protein (L-FABP) plays a role in lipoprotein-mediated cholesterol uptake in hepatocytes; and plasma protease C1 inhibitor (IC1) mainly participates in the coagulation, complement and contact cascades.*

Beta-2-microglobulin (B2M, P61769)

B2M, as a single protein, had the highest AUC score (204). B2M is a member of the immunoglobulin gene superfamily and associated with the surface of nearly all nucleated cells. It can be measured in its free form in most biological fluids, including serum and urine (237,238). B2M contains a C1-set domain, a classical Ig-like domain resembling the antibody constant region, found almost exclusively in molecules involved in the immune system, such as in immunoglobulin light and heavy chains, in the major histocompatibility complex (MHC) class I and II molecules (239,240). B2M association with MHC I is fundamental for functional expression of the protein complex, which plays an important role in the presentation of nine amino acid peptides to the T-cell receptor of

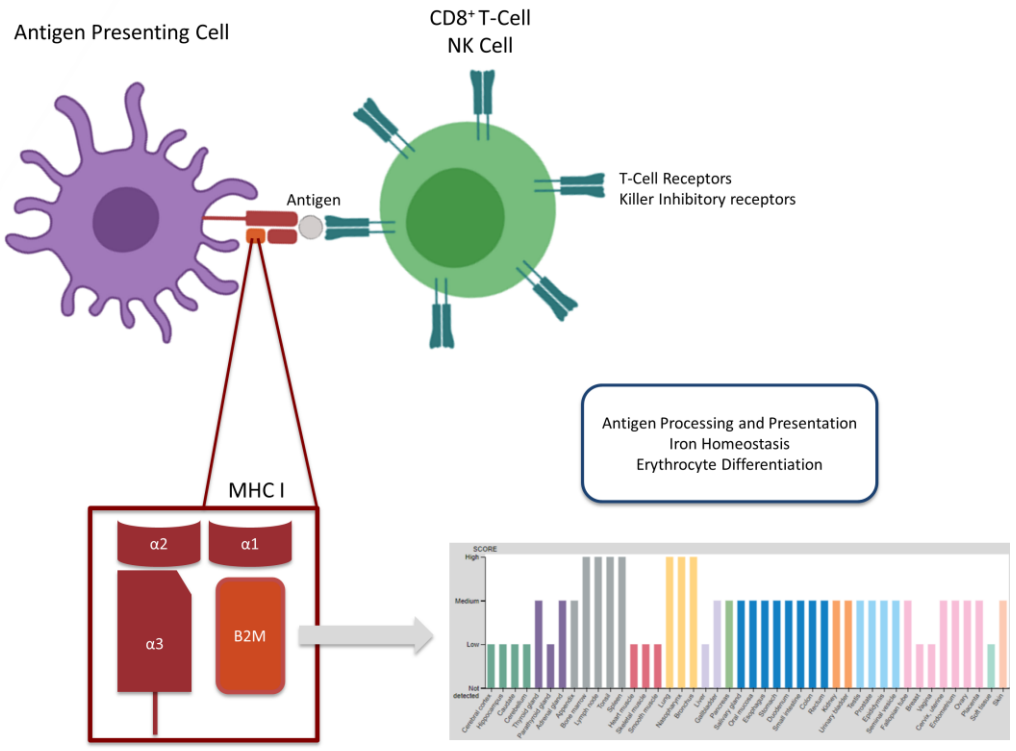

Figure 23. B2M is present on the surface of almost all nucleated cells, mainly participating in antigen presentation via MHC I to CD8+ T-cells and NK cells. B2M can be measured in blood and urine. B2M: beta-2-microglobulin; MHC I: major histocompatibility complex.

CD8+ T lymphocytes and killer inhibitory receptors on natural killer cells (241) (**Figure 23**).

Additionally, B2M also participates in iron homeostasis and erythrocyte differentiation regulation (242,243).

The synthesis rate of B2M ranges from 2-4 mg/kg/day, with a half-life of 2.5 hours. Plasma concentrations of B2M vary from 1-3µg/mL and is eliminated via glomerular filtration and reabsorbed by the proximal tubules. In tissue, it is mainly expressed in common hematopoietic cell lines, lungs, spleen, and peritoneum according to the Human Protein Atlas database (244).

Currently, B2M serum and plasma levels are used in the clinic to determine immune system activation and as biomarker for certain hematologic malignancies. Moreover, urine values can be indicative of renal filtration disorders (245). In the cardiovascular field, high levels of serum B2M were found to predict severity of coronary artery disease and sudden cardiac death. Finally, abnormal forms of B2M are involved in amyloidosis, retinitis pigmentosa, immunodeficiency 43, multiple sclerosis, and thrombocytopenia.

Fructose-bisphosphate aldolase B (ALDOB, P05062)

In vertebrates, 3 isoforms of the aldolase enzyme are found: aldolase A, aldolase B and aldolase C. These isoforms have homologous function within each tissue but are distinguished by their electrophoretic and catalytic properties: aldolases A and C are mainly involved in glycolysis, while aldolase B is involved in both glycolysis and gluconeogenesis (246). The developing embryo only produces aldolase A, but in adults its expression is limited to muscle, where it can be as much as 5% of total cellular protein. In adults, ALDOB is produced in the liver, kidney, stomach, and intestine, while aldolase C is produced in the brain.

ALDOB is a tetrameric glycolytic enzyme mainly involved in synthesizing D-glyceraldehyde 3-phosphate and glycerone phosphate from D-glucose as part of the glycolysis and carbohydrate degradation pathways (**Figure 24**). However, it also plays an important role in the biosynthesis of amino acids. ALDOB is found in the cytoplasm, cytoskeleton, and plasma membrane (247). The degradation mechanism of ALDOB in circulation is not clear, but detectable protein levels can be found in serum and plasma with an estimated half-life of 1-2 days (248). Protein levels of ALDOB in urine have not been found. In tissue, it is mainly expressed in the cortex of kidneys, liver, and small intestine Peyer's patch.

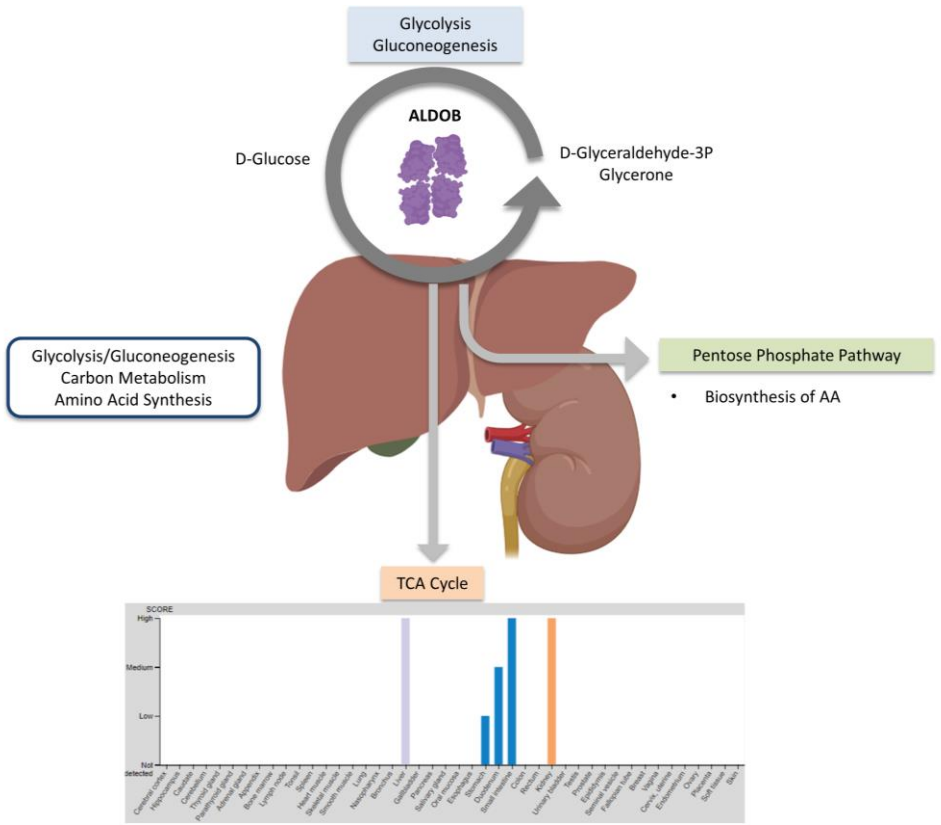

Figure 24*. ALDOB is a tetrameric enzyme involved in synthesizing D-glyceraldehyde 3-phosphate and glycerone phosphate from D-glucose as part of the glycolysis pathway. It also participates in the biosynthesis of amino acids and the TCA cycle. ALDOB can only be measured in the blood. ALDOB: fructose-bisphosphate aldolase B; TCA: tricarboxylic acid cycle.*

At present, ALDOB has been described as a putative prognostic biomarker for various cancers (249,250) but no current applications have been proposed in cardiology.

ALDOB has been related to obesity, liver inflammation, hypertransaminasemia and hepatic fibrosis, and defects in its production are causative of hereditary fructose intolerance.

Fatty acid-binding protein, liver (L-FABP or FABP1 P07148)

L-FABP belongs to a family of small and highly conserved proteins and it plays a role in lipoprotein-mediated cholesterol uptake in hepatocytes, binding cholesterol, free fatty acids and their coenzyme A derivatives, bilirubin, and some other small molecules in the

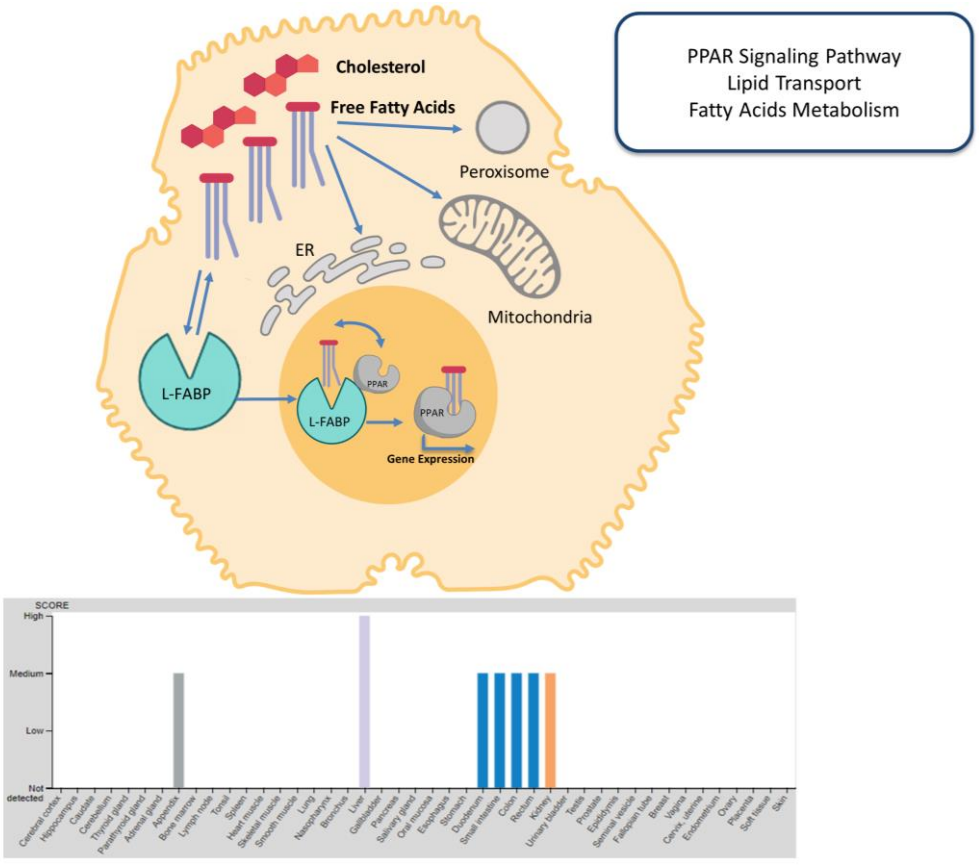

Figure 25*. L-FABP plays a role in lipoprotein-mediated cholesterol uptake, binding cholesterol and free fatty acids in the cytoplasm of hepatocytes. L-FABP can be measured in blood and urine. L-FABP: liver fatty acid-binding protein.*

cytoplasm (**Figure 25**) (251,252). L-FABP has a turnover of 3.1 days in the liver, closely resembling the half-life of the whole cytosol protein (253). At the tissue level, it is mainly expressed in the liver, but also in the cortex of kidneys, transverse colon, and small intestine Peyer's patch. It can be measured in serum, plasma, and urine (254).

Increased levels of urinary and serum L-FABP have proven to be effective markers in the detection of intestinal ischemia, progressive end-stage renal failure, and ischemic damage caused by renal transplantation or cardiac bypass surgery (255–257). Moreover, a relationship between serum L-FABP levels and lipid profile has been described, with increased BMI and insulin resistance in subjects with higher serum L-FABP (258). Studies have shown elevated serum levels of L-FABP associated with poorer prognosis in hypertensive patients and renal dysfunction in patients with HF, especially during acute phases (259). L-FABP is also involved in obesity, liver injury, acute kidney tubular necrosis, chronic kidney failure, and lipoidosis.

Plasma protease C1 inhibitor (IC1, P05155)

IC1, the protein encoded by the serpinG1 gene, belongs to the superfamily of serine proteinase inhibitors (serpins), and exhibits important anti-inflammatory properties, with various inhibitory and non-inhibitory biological functions (260). It is a highly glycosylated plasma protein, mainly known for its regulation of the complement cascade. However, it also plays a key role in blood coagulation (it is a very efficient inhibitor of FXIIa), fibrinolysis, and the contact amplification cascade (Kallikrein-kinin) (261). In healthy subjects, normal concentrations of IC1 are ~240 µg/mL (~3 µM) and display a ~28 h half-life, but its levels may double during inflammation (262,263). Low plasma content or dysfunctions with IC1 result in the activation of both complement and contact plasma cascades (**Figure 26**). Moreover, decrease in IC1 plasma content below 55 µg/mL

has been shown to induce spontaneous activation of C1 (264). Synthesis and secretion of IC1 primarily relies on hepatocytes, but is also produced by monocytes, fibroblasts, macrophages, microglial cells, endothelial cells and some other cells (265–267). Additionally, IC1 synthesis can be stimulated by several cytokines, particularly by interferon-γ (268). It is mainly expressed in the vasculature and the liver, but has also been found in lungs, subcutaneous adipose tissue, and breast.

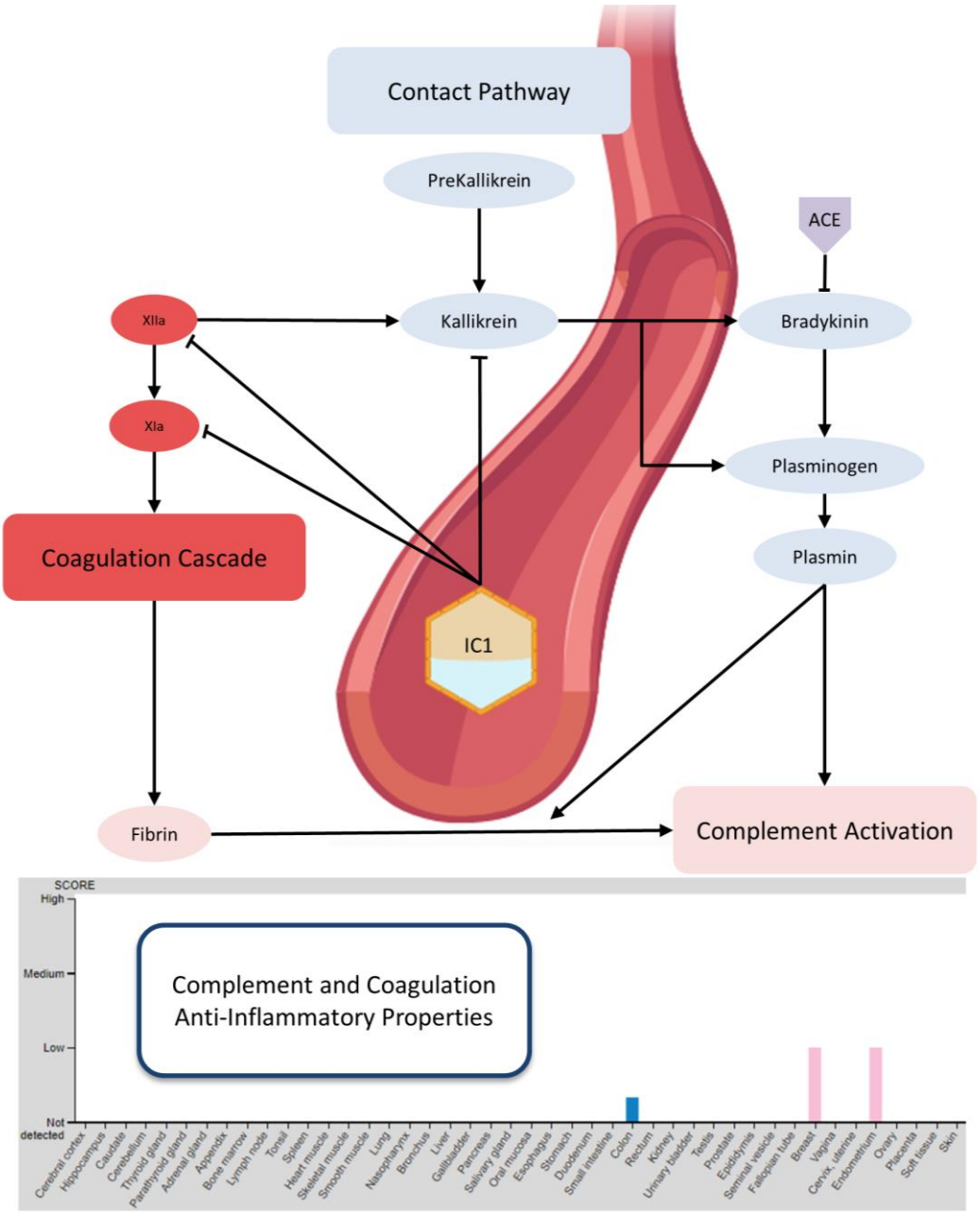

Figure 26. *IC1 is a plasma protein that participates in regulation of the complement cascade, blood coagulation and fibrinolysis, and the contact pathway. IC1: plasma protease C1 inhibitor; ACE: angiotensin converter enzyme; XIIa: coagulation factor XII, also known as Hageman factor; XIa: factor XI or plasma thromboplastin antecedent.*

SUMMARY FIGURE

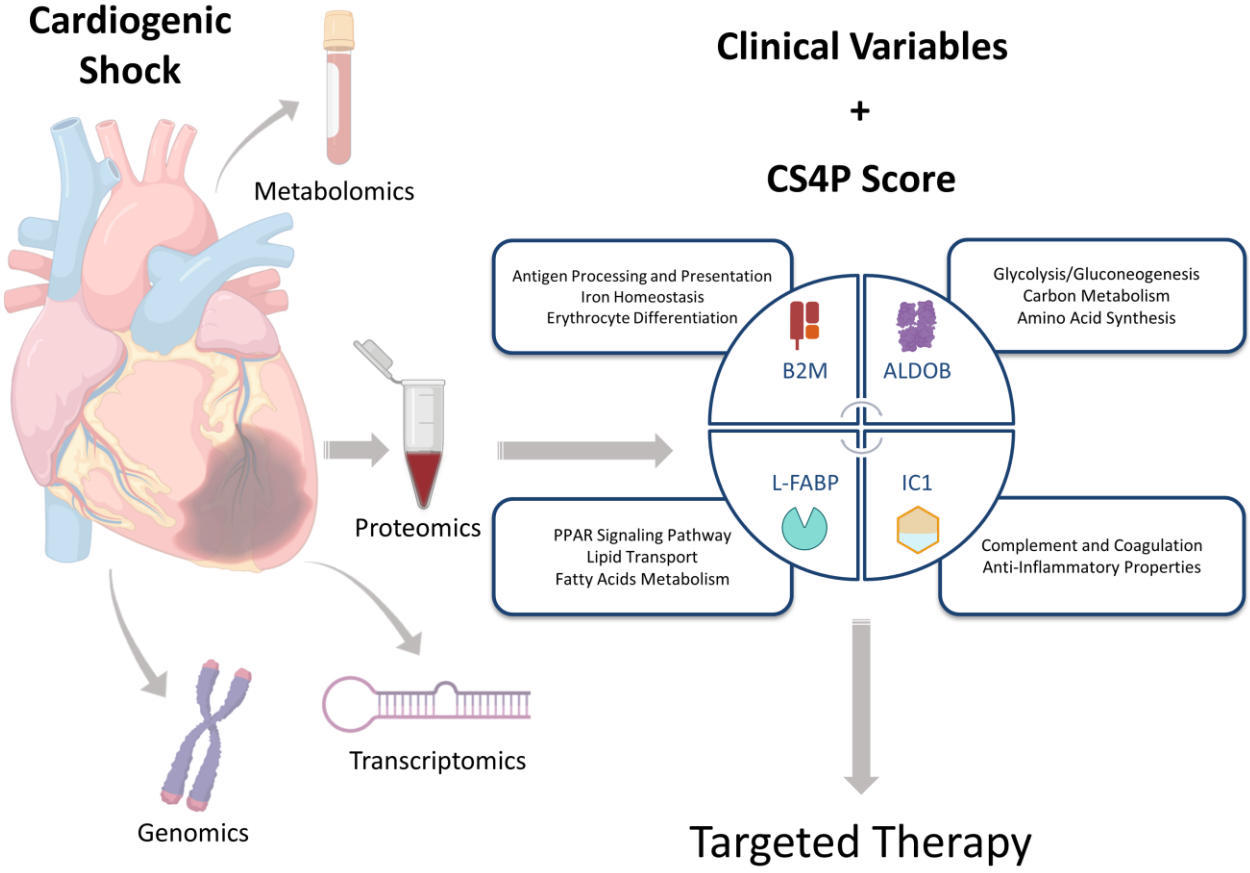

***Figure 27**. In this work, we have studied the current landscape of biomarker utilization in CS. We have investigated the -omics research fields to assess the current use and future possibilities of each discipline in CS and summarized the latest advances in targeted diagnosis/prognosis. Here, we have deepened in the knowledge of four new biomarkers (the CS4P) recently described to strongly predict CS mortality at 90 days. CS: cardiogenic shock; B2M: beta-2-microglobulin; ALDOB: fructose-bisphosphate aldolase B; L-FABP: liver fatty acid-binding protein. IC1: plasma protease C1 inhibitor.*

DISCUSSION

HF constitutes a severe pandemic that afflict millions of people every year. Although the etiology of the disease is highly heterogenic, many patients develop HF after an acute event that threatens their life, or experience a worsening of the condition during the recurrent hospitalizations. Thus, it becomes evident that what might seem an isolated occurrence is in fact not a static experience but rather an evolution towards a chronic condition.

In this thesis, we aimed to assess HF considering the whole spectrum of the disease progression. First, elucidating the MoAs of the most novel and promising pharmaceutical therapies that physicians have at their disposal to treat these advanced patients.

Here, growing evidence supports the idea that specific biological processes are likely influenced by their biological context—for example, a specific tissue or a certain disease. This approach constantly generates vast amounts of data, such that putting together, analyzing, and interpreting this information constitutes an overwhelming task.

Consequently, we harnessed artificial intelligence techniques to combine molecular data with clinical responses observed in patients, thus generating a mathematical model capable of both reproducing existing knowledge and discern MoAs hidden under thousands of molecular interactions, otherwise inaccessible.

We analyzed the two drugs that are revolutionizing HF management: sacubitril/valsartan, which showed a reduction in the number of deaths and admissions by 22% in recent clinical trials, and empagliflozin (a SGLT2 inhibitor indicated for type2 DM patients) that showed an unexpected 32% slash in development of new HF cases in the EMPAREG trial.

First, we intended to assess the MoA of sacubitril/valsartan, a new revolutionary drug in the management of chronic HF, which has been shown to reduce cardiovascular mortality and hospitalizations.

By doing so, we could predict the signaling cascade following the addition of the 1:1 salt that explained the improvement upon adverse cardiac remodeling.

Since its development and commercialization, many studies have assessed its pathophysiological effects, as well as pharmacokinetics and pharmacodynamics. However, relatively few studies have attempted to decipher the underlying signaling pathways responsible for its beneficial effects. Using a systems biology approach, we identified the main pathways regulated by sacubitril/valsartan implicated in reverse cardiac remodeling (Figure 28).

In this study, we analyzed the MoA of sacubitril and valsartan independently, as well as in combination as the salt complex. In this case, Figure 8 represents the MoA that more solutions comply with, and displays the molecular mechanisms most likely to underpin the synergistic action of the combination drug. The schematic shows the 8 protein nodes most highly implicated in its synergistic action, with an additional 6 nodes (Supplementary Table 7) that, although not constituting primary hits, may also play an important role.

Our analyses found that sacubitril/valsartan modulates cardiac remodeling, acting upon hypertrophic processes, via valsartan, and limiting myocardial cell death, via sacubitril. Indeed, it has recently been reported that sacubitril/valsartan has the potential to lower high-sensitivity troponin T (hs-TnT) levels, a biomarker for myocyte injury and myocardial cell death, in HF patients (269,270). Considering this, our analyses now provide a new perspective on relevant, though previously unknown, MoA.

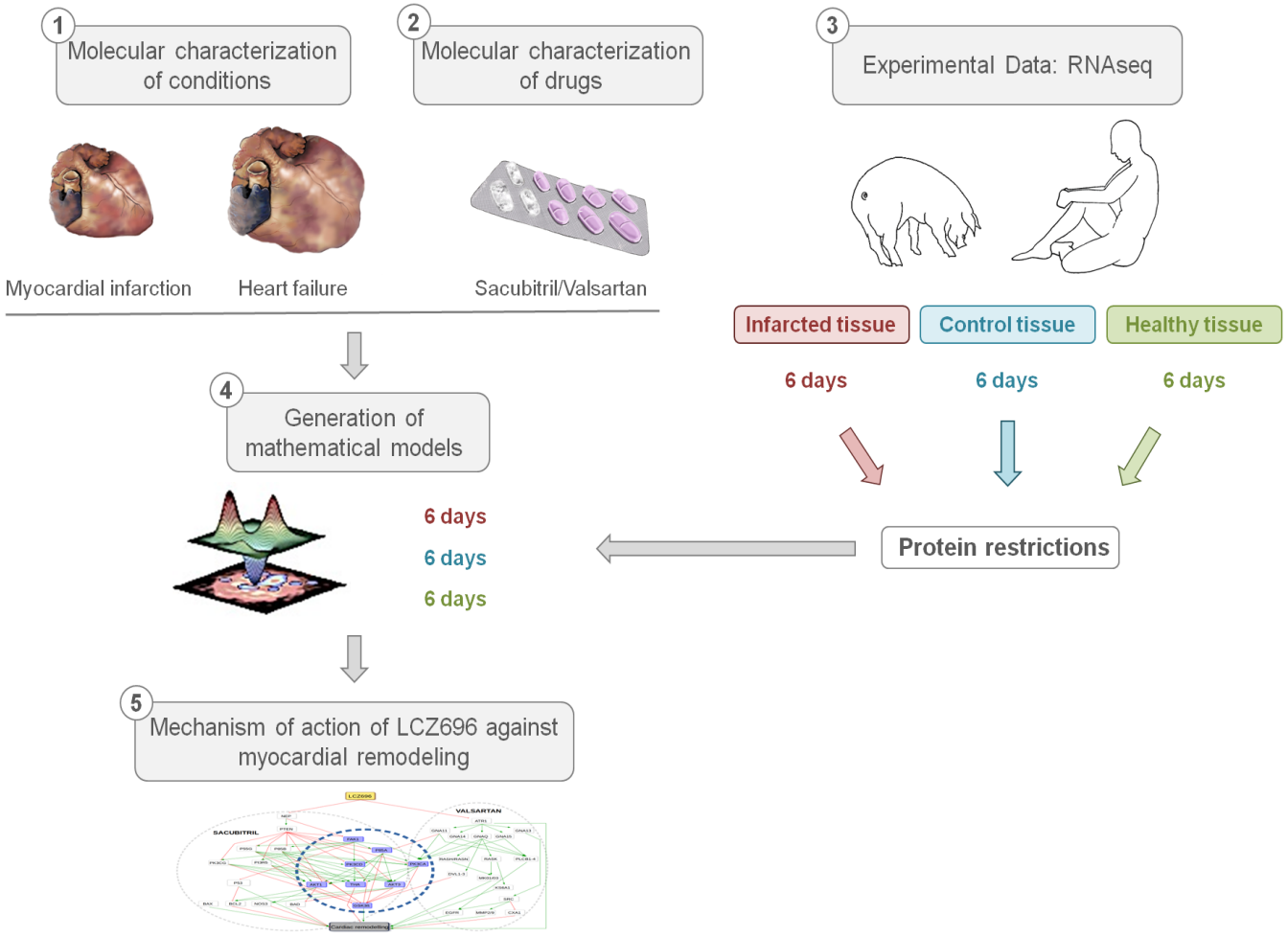

Figure 28. Depiction of the systems biology approach used to identify the mechanism of action of Sacubitril/Valsartan. At the top left corner, number 1 and number 2 depict the molecular characterization of both pathologies, MI and HF, and the drug under study, Sacubitril/Valsartan. Obtained from data mining, will serve to generate a truth table that every mathematical model must satisfy. At the top right corner, number 3 show the recollection of experimental data to generate a pathology signature for MI and HF (original pool of proteins). After analyzing all of them, only those previously related to cardiac remodeling and present in both sets of proteins (MI and HF) were used for the study (136 unique proteins), serving as protein restrictions. Number 4 depicts the generation of mathematical models using all the data collected in previous steps 1-3. Finally, number 5 displays the graphical representation of the Mechanism of Action (MoA) found by the mathematical models. All these steps, excluding the experimental data generation, explain how TPMS technology works. LCZ696 denotes Sacubitril/Valsartan.

Moreover, the data presented reveal that, when combined, Sacubitril/Valsartan act synergistically by reducing left ventricular ECM remodeling (LVECMR). This potential relationship had been suggested before, but without a supporting molecular mechanism (271). HF patients are prone to suffer sudden cardiac death, more so in ischemic cardiomyopathy due to large myocardial scarring (272). It is well known that ECM remodeling and fibrosis promote lethal arrhythmias (273). Remarkably, patients treated with Sacubitril/Valsartan experienced a reduced risk of this condition (271,274). Our *in-silico* data allow us to speculate that this beneficial effect may, at least in part, be due to the drug combination acting to reduce LVECMR.

The analysis displays the mechanism most likely to be affected according to our methods, which in this case turned out to be intracellular signaling. This was found to be the most robust pathway affected, but surely it can be that this is not the only one. The pharmacological effect of Sacubitril/Valsartan on cardiac remodeling could encompass, and most certainly be affecting, cell to cell communications as well as a wide variety of physiological cardiac phenotypes, such as the decrease in blood pressure, changes in heart rate, mechanical stress, valvular disorder, etc. However, our models take into account all of the proteins involved in cardiac remodeling present in our cohorts (regarding many different pathways, including those outlined above), and all the possible relationships between them (according to the current literature). Doing so, we can ensure that the models are representative and not biased towards a specific pathway.

We would like to emphasize that this MoA is not the complete mechanism by which the drug combination could reduce myocardial remodeling after a MI, or reverse myocardial remodeling after HF, but instead highlights the synergy achieved by the combination therapy.

The MoA provided by the model is validated in a two-step process. First, we checked that each link was accurate, e.g., was already described in the literature. Second, we checked that the MoA made sense overall, featuring pathways coherent with the living system, the combinations of drugs assessed (valsartan and sacubitril) and the known pathophysiology of cardiac remodeling.

Next, we investigated the MoA of the second drug under study, empagliflozin.

The EMPA-REG OUTCOME trial reported that empagliflozin exerted cardiovascular benefits, which did not depend on its effects on blood glucose. This observation led to the hypothesis that empagliflozin exerted an effect on the myocardium independent of its inhibition of SGLT2 in the kidneys, thereby benefiting HF patients (180). The exact mechanism remains unknown, but it was postulated to be a direct action on the heart. Our study used artificial intelligence and machine learning, further validated in an *in vivo* animal model, to investigate whether empagliflozin could exert direct effects on the heart and whether these effects were the same for patients with and without DM.

This study has two main findings. First, these results validate that empagliflozin interacts with the cardiac Na^+/H^+ exchanger NHE1 directly, and identifies a mechanistic pathway acting primarily by reducing cardiomyocyte cell death, the main effector of its cardioprotective effects. Indeed, the activity of cardiac NHE1 seems to be increased in HFrEF patients, and previous data in experimental models showed that NHE1 inhibition attenuates cardiomyocyte injury, remodeling, systolic dysfunction and ultimately HF (275–279).

Second, our data suggest that the cardiac effects of empagliflozin are independent of the presence of DM.

Uthman *et al*. reported that SGLT2i reduces cardiac cytosolic Na^+ and cytosolic Ca^{2+} concentrations by inhibiting NHE1 in mouse cardiomyocytes. Cardiac NHE1 activity and cytosolic Na^+ were measured in the presence of clinically relevant concentrations of empagliflozin (1 µmol/L), dapagliflozin (1 µmol/L) and canaglifozin (3 µmol/L). All three SGLT2is bound with high affinity to the extracellular Na+-binding site of NHE1 (280). Recently, Baartscheer *et al*. proposed a possible relationship between empagliflozin and NHE1 inhibition in rats and rabbits (281). In their study, an increase in extracellular glucose produced an increase in cytosolic Na^+ and Ca^{2+} levels, an effect that was inhibited by empagliflozin. The effects of empagliflozin were strongly reduced after cells were pre-treated with the NHE1 inhibitor cariporide. In addition, empagliflozin affected cytosolic Na^+ and NHE1 flux in the absence of extracellular glucose, which demonstrated its putative effects in normoglycemic conditions.

These mechanistic studies have the power to address specific mechanisms in detail, but the unravelling of the global molecular effects of empagliflozin in HFrEF with or without DM require the integration of complex big data, best handled by artificial intelligence and deep learning analyses. Considering all possible empagliflozin-derived cardiac mechanisms, our analysis pinpointed NHE1 modulation to be the most likely effector of the beneficial effects. Moreover, amelioration of cardiomyocyte cell death was found to be the most important effect of empagliflozin in HF.

Most importantly, our algorithm predicted a modulation of AKTs resulting in an inability of BIRC2 to degrade the anti-apoptotic factors XIAP and BIRC5. XIAP was found decreased in failing human hearts, suggesting that this potent inhibitor of apoptosis may play a key role protecting the heart from cell damage (282,283). Using an adeno-associated viral vector, Piacentino *et al*. increased XIAP expression in neonatal rat cardiomyocytes, which inhibited caspase-3/7 activity, showing a reduction of myocardial

injury. Relative to BIRC5, Lee *et al.* found that overexpression of this pathway may attenuate the progression of LV systolic dysfunction in doxorubicin-induced cardiomyopathy (284). Further, Levkau *et al.* showed that cardiac-specific deletion of BIRC5 pathway resulted in premature cardiac death caused by a dramatic reduction in total cardiomyocyte numbers. Again, using adenoviral vectors to restore this pathway (via restoration of survivin) expression in cardiomyocytes inhibited doxorubicin-induced apoptosis, induced DNA synthesis, and promoted cell cycle progression (285). Following this rationale and to further confirm our *in silico* data, mRNA levels of both XIAP and BIRC5 were measured in an *in vivo* MI-HF rat model. In agreement with existing literature, both XIAP and BIRC5 expression was substantially lower in vehicle-treated animals with dysfunctional myocardium. Remarkably, in the empagliflozin-treated groups, expression of both XIAP and BIRC5 returned to normal, thus being able to exert their anti-apoptotic effects.

Our study was designed to investigate whether the MoA of empagliflozin in HF was different in patients with or without DM. To our surprise, the most robust MoA identified here was identical in both groups, suggesting that empagliflozin may have value in HFrEF irrespective of the glycemic status, acting to ameliorate adverse cardiac remodeling. In other words, empagliflozin, currently only indicated to treat DM, may eventually be repurposed to treat patients with HFrEF. Several ongoing randomized clinical trials are testing the value of SGLTi in HF patients (both with HFrEF and HFpEF) with and without DM.

The mathematical models reported here were robust, and each link described is validated in the existing literature. However, there is an ongoing discussion about the mathematical algorithms used in artificial intelligence, often termed as “black boxes”, since sometimes it may not be easy to follow the determination of the output, no matter

how good or reliable this may be. Our analysis took the massive amount of information collected and looked for hidden patterns in the data that would be otherwise inaccessible to human stand-alone analyses, to understand how the drug can lead to a specific clinical outcome. These algorithms are widely used in other fields, and the techniques are among the best understood and developed, with time-tested characteristics which ensures an accurate application. A key differentiating feature of deep learning compared with other subtypes of artificial intelligence is their ability to operate without external guidance to draw conclusions; the neural network is not designed by humans, but rather the number of layers is determined by the data itself. Deep ANNs have primarily used supervised learning, with training from known patterns and labelled input data (truth table) to prospect reliable insights in large datasets. At the same time, all the outputs from the algorithm are restricted by the current scientific and medical standards. Taken together, all this limits the human bias, and the algorithm can act as a hypothesis-free, independent data-driven analysis (286).

However, both of these works do have limitations. The same premise that makes the models robust also serves as a potential downside. Specifically, the information considered here has already been described or validated in public repositories, but in turn limits the capacity of the analyses to incorporate data that has not been yet collected. In the case of the empagliflozin analysis, the data reported here is valid for HFrEF and cannot be extrapolated to HFpEF. Further research is required to better understand the MoA of empagliflozin in HFpEF.

Following these studies, it became apparent the key role of ventricular remodeling in explaining the beneficial effects of both drugs.

Thus, we investigated their common pathways involving adverse cardiac remodeling at the molecular level.

As mentioned previously, the ischemic injury caused by MI, albeit it seems a one-time event, it is not stationary but rather might be the beginning of a chronic illness.

Both, acute and chronic HF are highly intricate diseases, with multifactorial causes and even more heterogeneous clinical symptoms. Not surprisingly, biomedical research has invested a lot of efforts in understanding and unraveling the secrets of these conditions. Nevertheless, these studies have produced massive amounts of individual data points, which although have unequivocally helped improve clinical management greatly, remain disconnected from one another. Here, we aimed to gather all the molecular information publicly available on MI and HF, to fit in a mathematical model of artificial intelligence, which ideally could delineate the progression from the first to the latter.

In the present study, we used transcriptomic data obtained from *in vivo* experiments in swine, combined with the latest advances in artificial intelligence. Our results demonstrate the ability to analyze massive datasets and search for patterns, which can help explain the evolution of MI at the molecular level.

The models used in our present analyses work from a systems biology perspective. Therefore, the mechanisms are not identified based on a one-by-one gene analysis, but rather by considering the global changes in all the genes/proteins within the appropriate context.

Our first goal was to assess the data structure of the transcriptomic information obtained *in vivo.* We integrated this highly dimensional data and analyzed its composition, revealing that MI progression was accompanied by marked regulation of adipogenesis, fatty acid metabolism, and epithelial mesenchymal transition processes. Moreover, this

analysis uncovered robust segregation between the infarct core samples versus the remote myocardium and controls, indicating major differences between these areas at the regulatory level. We specifically investigated the biological significance underlying these structural variations, and found that the infarct core region of the heart was enriched in affected processes relating to muscle contraction and membrane depolarization. In contrast, the remote myocardium was heavily affected by respiratory metabolism deficiencies. These results helped contextualize the MI.

Adverse ventricular remodeling is a hallmark of MI evolution and progression towards HF (287–289); therefore, we next investigated which of the identified mechanisms were related to adverse cardiac remodeling. Using machine learning techniques to analyze all tissues and time-points, we pinpointed 105 altered proteins that were most likely related to cardiac remodeling in MI. This provided a list of potential biomarkers that might indicate the pathological evolution according to each time-point. Further analysis revealed two distinct combinations of proteins from the infarct core data at each time-point, which showed generalization capabilities and accuracies of 100%, suggesting that these proteins are of great importance for describing the whole progression.

With this information, we performed enrichment analysis to examine the MoA of cardiac remodeling in the infarct core at each time-point. A total of 355 processes were altered in the infarct core during at least one time-point, and 101 were altered at all time-points (6, 30, and 45 days after infarction). The high number of upregulated ECM-related processes was consistent with previous reports that glycosaminoglycan mediates cardiac remodeling by facilitating the inflammatory response (290). Aside from its role in remodeling, the ECM also plays an important role in cell communication (291), and contributes to helping damaged cardiac tissue. To avoid ischemic conditions, the organism will attempt to revascularize and repair the affected area, promoting

angiogenesis. Accordingly, angiogenesis was among the first morphogenic responses that we detected as sustained in time. We also detected the apparent upregulation of other processes related to morphogenesis of different organs, suggesting that the post-ischemic cells present in the heart could be trying to recapitulate embryogenic processes and bolster regeneration.

Upon identification of the altered processes, we performed a protein triggering analysis to establish the key proteins mediating the adverse remodeling response. We then model the behaviors of these proteins, generating the first description of an integrative MoA for MI progression. This mechanistic analysis was found to overlap between the different time-points, and the pathways that were common between the protein sources and cardiac remodeling involved IGF1R, RAF1, KPCA, JUN, and PTN11 as source modulators. The downstream signaling of these proteins produces a MoA potentially involving 18 proteins, 15 of which were identified as differentially expressed in at least one cohort.

Our present study is pioneer in performing an in-depth analysis of the molecular changes that characterize the progression of MI as a whole. Our results contain a large amount of intricate information. As expected, MI evolution encompasses a myriad of altered processes and specific proteins, which regulate the time-dependent stages and determine the final extent of the pathology.

Specifically, our objective was to integrate dynamic transcriptomic regulations, along with all presently information available on MI and cardiac remodeling, to delineate a structured, clear, and simplified picture of the complete post-MI remodeling process. In doing so, we have generated a framework into which new data can be fitted, improving our understanding of the context of future discoveries. Furthermore, due to the intrinsic characteristics of this work, our study also elucidates new potential targets and therapeutic

windows for the treatment of MI complications, and novel avenues for MI research with the ultimate goal of fully unravelling the whole pathology.

In the last few years, high-throughput technologies have generated an incredibly large amount of data across all omics' fields. Combined with the rapid growth of bioinformatics, these resources provide the scientific community with the opportunity to analyze and test hypothesis with a wider angle of view. In this regard, where researchers cannot focus and study every single possibility, due to their extensiveness, model-based approaches and network analyses stand as potent and helpful tools. Moreover, as they integrate so much data, usually are able to provide insights and find relationships that could go easily overlooked with other approaches. As demonstrated in our studies, these models are able to generate new data-driven predictions, which then researchers can put to validation and thus expand our capability to tackle complex biological frames that are otherwise inaccessible.

Chronic HF is the leading cause of inter-hospital mortality worldwide, which constitutes an authentic pandemic. However, many of these patients either develop HF derived from an acute event or experience a drastic worsening of the condition during the recurrent hospitalizations.

All within itself, acute HF already poses a big burden for the healthcare system, as these patients require highly experienced technical care and demand substantial resources to manage them properly. Here, CS is the most aggressive and difficult to manage condition. Even with complete dedication, mortality rates are still unacceptably high. Hence, in a condition in which time is of the utmost importance, an efficient strategy involves improving the diagnostic and prognostic capabilities to guide clinicians in assessing the best treatment as rapid as possible. Strikingly, when we investigated the literature to know what has been done to date, we baffled upon the scarce research surrounding this topic.

In cardiovascular research, the use of biomarkers is widely accepted to guide further treatments, and already exist many molecules capable of helping clinicians in this decision-making process, from metabolic signatures to genomic, transcriptomic and proteomic approaches. However, in the setting of CS, little advances have been made towards the implementation of such practices.

Consequently, in the second part of this thesis we aimed to review the current situation of the biomarker-related research in CS, and build upon it to develop new transcriptomic and/or proteomic scores to aid CS prognosis.

For this purpose, we thoroughly characterized a cohort of patients diagnosed with CS (n=48), as well as joined the European CARDSHOCK Consortium, with access to the largest cohort of CS patients in the world (n=97). By doing so, we could use one cohort to discover potential candidates and the other one to validate the results, strengthening the prognostic value of any newly found marker.

First, we discuss the research of transcriptomic analysis in CS, and describe the molecular dynamics of 4 of the most promising miRNAs investigated in cardiovascular research, which we thought could be of interest in acute settings of the disease. These included miR-21, miR-122a, miR-320a, and miR-423-5p, which we explored during the first 24h in patients with ST elevation MI and CS, as well as their prognostic value at 30 days.

Unfortunately, the evaluation of these miRNAs did not provide an increase in current prognostic scores, which could be due to the fact that the information captured in these circulating miRNAs is already reflected in contemporary clinical and biomarker data. We also wanted to further dissect our cohorts, but any of the clinical variables collected for these patients seemed to be associated with mortality at 30 days either.

Nonetheless, we could learn a great deal of their dynamics during the first 24h after clinical presentation. Here, our results show a significant increase in circulating miRNA during the first 12h of the disease evolution. In the presence of the multi-organ damage that characterizes CS, the origin of this boost is uncertain, but would be interesting to deep in in future studies. Remarkably, the 4-studied miRNAs returned to baseline (or lower) after 24h despite the persistence of CS, which could be indicating a hidden biological mechanism further down the line.

Now, a recent report of acute and chronic HF with large cohorts (i.e. hundreds of patients) have shown a statistically significant yet modest prognostic value for several studied miRNAs (292).

These results do not indicate that transcriptomic analyses in CS are not useful. Certainly, miRNAs remain a strong contender in the field of acute HF, especially when considering their technical advantages over other approaches. Moreover, it is estimated that ≈ 2300 true human miRNAs exist, but only 50% of them are annotated and few of them are characterized and experimentally validated (293).

However, we wanted to efficiently seize the full scope of biological nuances present in CS, and turned to advanced proteomics to unfold the potential in biomarker strategy for this complex condition.

Although it is not explicitly explained in this thesis, we used mass spectrometry analysis to screen our cohort of CS patients, in which we identified 2654 proteins that were further investigated in the independent CARDSHOCK cohort by targeted proteomics analyses (n=51 proteins included in the final candidate list). Here, we found that the combination of 4 circulating proteins (Cardiogenic Shock 4 proteins—CS4P), discriminated patients with low and high 90-day risk of mortality.

In this thesis, we have presented a review in which we elaborate on the current landscape of biomarker research in CS, and discus how the addition of the CS4P score, the first proteomic score of its kind, could change the clinical practice and shape the evolution of this field.

In short, we looked at the metabolic markers included in every clinical guideline since 60 years ago, glucose and lactate. Their use has been extensively implemented in almost all CVDs, but the results surrounding their clinical relevance in CS lack robust testing and specificity. We also investigated the status on genomic and transcriptomic research and found promising candidates, some of which have been used to develop new drug therapies. However, in the prognostic department, the results obtained in these disciplines remains remarkably poor. Finally, we discuss the gold standard of cardiovascular prognosis, which include cardiac-specific troponins, NT-ProBNP and ST2. All of them carry incredible successes in the diagnostic and prognostic of many CVDs, and thus have been extensively investigated in the acute HF setting as well. Indeed, some studies demonstrate their association with increased mortality risk, but cannot escape the looming controversy generated by their physiological increase in situations far from being dangerous to the patient, including after mild aerobic exercise, or in other clinical settings with little cardiac involvement, such as septic shock.

Thereafter, we put the focus on our novel CS4P score, which comprises the abundances of liver-type fatty acid-binding protein, beta-2-microglobulin, fructose-bisphosphate aldo- lase B, and SerpinG1. Within the CardShock cohort used for internal validation, the C-statistic was 0.78 for the CardShock risk score, 0.83 for the CS4P model, and 0.84 for the combination of CardShock risk score with the CS4P model. Most importantly, the CardShock risk score with the CS4P model showed a marked benefit in patient reclassification, with a net reclassification improvement of 0.49 compared with the

CardShock risk score or the IABP-SHOCK II alone. The CS4P patient classification power was confirmed by ELISA.

Thus, the combination of the CS4P model to existing risk scores improved their overall performance predictive metrics, which may help clinicians in the early identification of high-risk CS patients for prompt invasive procedures, such as mechanical circulatory support.

In general, systemic failure and the inflammatory cascade have been hypothesized to be important mechanisms of acute post-ischemic myocardial injury. Although the proteins contained in the CS4P are not well explored in the cardiovascular field, they reflect renal, hepatic and hemodynamic affliction, consistent with the clinical assessment on the bedside. Indeed, high levels of serum B2M have already been associated with increased severity in acute CAD. Moreover, several studies have shown that IC1 is effective in post-ischemic myocardial protection (294). Additionally, Thielmann *et al*. demonstrated that therapeutic administration of IC1 is safe and effective to inhibit complement activation, and thus may reduce inflammation and myocardial damage (295). This is consistent with our findings of increased IC1 levels in patients that survive CS. However, the clinical applications involving IC1 are currently focused on hereditary angioedema, the main pathology associated with IC1 deficiency.

The finding that 4 unique proteins of non-cardiac origin were identified in the circulating proteome in CS fits with the current changing paradigm from a focus on an "hemodynamic model" as the mechanism of systemic malperfusion, towards a "mechanistic disease-modifying model", in which an initial reduction in cardiac output takes place, but rapidly morphs into distinct molecular pathways (296). Indeed, recent clinical trials have suggested that increasing cardiac output may not translate into an

improvement in clinical outcomes, in patients with CS, despite observed improvements in hemodynamics (297).

Of note, this thesis has elaborated on the two most groundbreaking pharmacological therapies for HF of the last decades, describing for the first time their mechanistic role *in silico*, *in vitro* and *in vivo*. This can help us understand how to slow HF progression. Moreover, these mechanisms display a common pathway involving adverse ventricular remodeling as the leading process, the modulation of which exerts the observed beneficial effects of the drugs. By investigating the molecular transition of this remodeling from MI to HF, we could describe the time-dependent dynamics of this complex process and pinpoint new potential targets and pathways to slow the advancement of MI towards HF in the first place.

As mentioned previously, the ischemic injury caused by MI, albeit it seems a one-time event, it is not stationary but rather a convoluted progression. As such, acute HF also poses a big burden for the healthcare system, as these patients require highly experienced technical care and demand substantial resources to manage them properly.

Thus, here we assessed the current situation of the biomarker research field in CS and built upon it to develop new molecular scores to help aid CS prognosis. We used the latest advances in targeted proteomics and analyzed large, validated and independent cohorts, with the aim of finding molecular data that would be useful, simple to use and rapidly transferrable to the clinical setting. Here, we discovered that measuring a panel of just 4 proteins, we can confidently predict the outcome of a patient entering the emergency room suffering from CS.

These results assist present poor resource allocation (CS accounts for ~54B$ annually), treatment optimization, opens up the possibility to correctly conduct clinical trials in CS and help patients, and their families, cope with the disease evolution.

CONCLUSIONS

1. Monitoring of miR-21, miR-122a, miR-320a, and miR-423-5p in STEMI patients with CS revealed dynamic behavior during the first 24h, with a peak at 12h, without any prognostic value for 30-day all-cause mortality. Though these miRNAs seem to be crucial for disease progression, they are unlikely to be clinical biomarkers.
2. The newly described CS4P score has the chance to emerge as a breakthrough in CS management, where none of the recently generated genomic, transcriptomic or proteomic data have really entered the clinical realm.
3. By using machine learning techniques to analyze all tissues and time-points, we have delineated a structured, clear, and simplified picture of the complete post-MI remodeling process.
4. Sacubitril attenuates cardiomyocyte cell death, hypertrophy, and impaired myocyte contractility by inhibiting PTEN and valsartan improves cardiac remodeling by inhibiting the guanine nucleotide-binding protein family.

Moreover, the combination of sacubitril and valsartan acts synergistically against LVECMR and cardiomyocyte cell death.

5. Deep learning *in silico* analyses suggest that empagliflozin interacts and blocks the NHE1 co-transporter at the cardiomyocyte level, triggering a signaling cascade that halts detrimental cell death by restoring XIAP and BIRC5 anti-apoptotic activity, which has been demonstrated in both DM and MI rat models.

FUTURE RESEARCH

This thesis presented several lines of research to the reader, raising interesting questions about future ongoings to further improve cardiovascular diseases comprehension. To start, by reviewing the current landscape of biomarker research in CS, we identified a niche which still lacks empirical efforts to drive this field of research. Indeed, the newly described CS4P score has the chance to emerge as a game changer. Nevertheless, first, it will have to be developed as a multimarker assay apt for clinical use. Second, it will have to demonstrate that it is valuable for a more personalized approach in CS. Here, a prospective study randomizing patients to mechanical circulatory support if the CS4P is elevated or conventional inotrope-vasodilator management if CS4P is low could be of great interest.

Additionally, the mathematical models used in several works presented here exhibit great potential to be applied in unravelling the MoAs of novel drugs and therapies. More specifically, the results obtained by modelling sacubitril/valsartan effects should be validated in an *in vivo* model, possibly in rat and swine, as the *in vitro* characterization proved insufficient. Not only that, but both studies assessing sacubitril/valsartan and

empagliflozin effects have pinpointed new molecular targets that could be interesting to develop therapies around their modulation. However, not all lines of research have presented the opportunity to be expanded. Although circulating miRNAs have generated great expectations as emerging genetic prognosticators, the miRNAs studied in CS do not seem to hold prognostic value. However, technologies are rapidly improving, and more general use of novel techniques like next-generation sequencing may also change the standard measurement of circulating RNA molecules and thereby improve signal to noise ratios. Thus, we cannot rule out that some miRNA biomarkers for CS prediction are yet to be identified, but we sincerely believe that there are better avenues to pursue this important goal.

BIBLIOGRAPHY

1. Allam AH, Thompson RC, Wann LS, Miyamoto MI, Thomas GS. Computed Tomographic Assessment of Atherosclerosis in Ancient Egyptian Mummies. JAMA [Internet]. 2009 Nov 18 [cited 2019 Jul 25];302(19):2091. Available from: http://jama.jamanetwork.com/article.aspx?doi=10.1001/jama.2009.1641

2. Allam AH, Thompson RC, Wann LS, Miyamoto MI, Nur el-Din A el-H, el-Maksoud GA, et al. Atherosclerosis in Ancient Egyptian Mummies. JACC Cardiovasc Imaging [Internet]. 2011 Apr 1 [cited 2019 Jul 25];4(4):315–27. Available from: https://linkinghub.elsevier.com/retrieve/pii/S1936878X11000660

3. Ebbell B. The Papyrus Ebers : the greatest Egyptian medical document [Internet]. Copenhagen: Levin & Munksgaard; 1937 [cited 2019 Jul 31]. Available from: https://www.worldcat.org/title/papyrus-ebers-the-greatest-egyptian-medical-document/oclc/5435947

4. Boisaubin E V. Cardiology in ancient Egypt. Texas Hear Inst J [Internet]. 1988 [cited 2019 Jul 31];15(2):80–5. Available from: http://www.ncbi.nlm.nih.gov/pubmed/15227256

5. Persaud TVN. A history of anatomy : the post-Vesalian era [Internet]. Charles C Thomas Publisher; 1997 [cited 2019 Jul 31]. 357 p. Available from: https://books.google.es/books/about/A_history_of_anatomy.html?id=XGlsAAAAMAAJ&redir_esc=y

6. Persaud TVN, Loukas M, Tubbs RS. A history of human anatomy [Internet]. [cited 2019 Jul 31]. Available from: https://books.google.es/books/about/A_History_of_Human_Anatomy.html?id=vbfSoAEACAAJ&redir_esc=y

7. ATKINSON MH. MAN'S CHANGING CONCEPTS OF THE HEART AND CIRCULATION. Can Med Assoc J [Internet]. 1964 Sep 12 [cited 2019 Jul 31];91(11):596–601. Available from: http://www.ncbi.nlm.nih.gov/pubmed/14175877

8. Harris CRS (Charles RS. The heart and the vascular system in ancient Greek medicine; from Alcmaeon to Galen. [Internet]. Clarendon Press; 1973 [cited 2019 Jul 31]. 474 p. Available from: https://catalogue.nla.gov.au/Record/1917401

9. Jones WHS. Hippocrates Collected Works I [Internet]. Cambrodge: Harvard University Press; 1868 [cited 2019 Jul 31]. Available from: http://daedalus.umkc.edu/hippocrates/HippocratesLoeb1/page.ix.php

10. Garrison FH. History of Medicine. Philadelphia: W.B. Saunders Company; 1966.

11. Hippocrates, Adams F. The genuine works of Hippocrates: translated from the Greek with a preliminary discourse and annotations. [Internet]. New York: W. Wood; 1886 [cited 2019 Jul 31]. Available from: https://catalog.hathitrust.org/Record/009358009/Cite

12. Hippocrates. On the Heart. Hippocrates' Collected Writings. Athens: Kaktos; 1992. Vol.4.

13. Lonie IM. The paradoxical test "On the Heart". I. Med Hist [Internet]. 1973 Jan [cited 2019 Jul 31];17(1):1-15 contd. Available from: http://www.ncbi.nlm.nih.gov/pubmed/4595530

14. WILSON LG. Erasistratus, Galen, and the pneuma. Bull Hist Med [Internet]. [cited 2019 Jul 31];33:293–314. Available from: http://www.ncbi.nlm.nih.gov/pubmed/13845095

15. Hajar R. The greco - islamic pulse [Internet]. Vol. 1, Heart Views. Medknow Publications; 2000 [cited 2019 Jul 31]. 136 p. Available from: http://www.heartviews.org/article.asp?issn=1995-705X;year=1999;volume=1;issue=4;spage=136;epage=140;aulast=Hajar;type=0

16. Dalfardi B, Mahmoudi Nezhad GS, Mehdizadeh A. How did Haly Abbas look at the cardiovascular system? Int J Cardiol [Internet]. 2014 Mar [cited 2019 Jul 31];172(1):36–9. Available from: https://linkinghub.elsevier.com/retrieve/pii/S016752731400031X

17. Sterpetti A V. Cardiovascular Research by Leonardo da Vinci (1452-1519). Circ Res [Internet]. 2019 Jan 18 [cited 2019 Jul 31];124(2):189–91. Available from: https://www.ahajournals.org/doi/10.1161/CIRCRESAHA.118.314253

18. Ghiselin MT. William Harvey's methodology in De motu cordis from the standpoint of comparative anatomy. Bull Hist Med [Internet]. [cited 2019 Jul 31];40(4):314–27. Available from: http://www.ncbi.nlm.nih.gov/pubmed/5329578

19. Tubbs RS, Gianaris N, Shoja MM, Loukas M, Cohen Gadol AA. ?The heart is simply a muscle? and first description of the tetralogy of ?Fallot?. Early contributions to cardiac anatomy and pathology by bishop and anatomist Niels Stensen (1638?1686). Int J Cardiol [Internet]. 2012 Feb [cited 2019 Jul 31];154(3):312–5. Available from: https://linkinghub.elsevier.com/retrieve/pii/S0167527310007709

20. Vieussens R. Traité nouveau de la structure et des causes du mouvement naturel du coeur [Internet]. 1st ed. Jean Guillemette, editor. Toulousse; 1715 [cited 2019 Jul 31]. Available from: https://catalog.hathitrust.org/Record/009296018

21. Thebesius A. De circulosanguinis in corde. Leiden: Lugduni Batavorum; 1708.

22. Ellis H. A History of Surgery. London: Greenwich Medical Media; 2001.

23. Tawara S, Aschoff L. The Conduction System of the Mammalian Heart [Internet]. PUBLISHED BY IMPERIAL COLLEGE PRESS AND DISTRIBUTED BY WORLD SCIENTIFIC PUBLISHING CO.; 2000 [cited 2019 Jul 31]. (Cardiopulmonary Medicine from Imperial College Press; vol. 0). Available from: https://www.worldscientific.com/worldscibooks/10.1142/p099

24. Nicholls M, Anderson R. Pioneer: Robert Anderson, MD, PhD, FRCPath. Circ , 121 F133-F135 [Internet]. 2010 Jun 15 [cited 2019 Jul 31]; Available from: http://discovery.ucl.ac.uk/1338891/

25. Bendiner E. William Heberden: Father of Clinical Observation. Hosp Pract [Internet]. 1991 Jul 15 [cited 2019 Aug 1];26(7):103–34. Available from: http://www.tandfonline.com/doi/full/10.1080/21548331.1991.11704210

26. Golden RL. Sir William Osler's angina pectoris and other disorders. Am J Cardiol [Internet]. 1987 Jul 1 [cited 2019 Aug 1];60(1):175–8. Available from: http://www.ncbi.nlm.nih.gov/pubmed/3300246

27. Herrick JB. Landmark article (JAMA 1912). Clinical features of sudden obstruction of the coronary arteries. By James B. Herrick. JAMA [Internet]. 1983 Oct 7 [cited 2019 Aug 1];250(13):1757–65. Available from: http://www.ncbi.nlm.nih.gov/pubmed/6350634

28. Forssmann-Falck R. Werner Forssmann: A Pioneer of Cardiology. Am J Cardiol [Internet]. 1997 Mar 1 [cited 2019 Aug 1];79(5):651–60. Available from: https://www.sciencedirect.com/science/article/pii/S0002914996008338?via%3Dihub

29. Artico M, Spoletini M, Fumagalli L, Biagioni F, Ryskalin L, Fornai F, et al. Egas Moniz: 90 Years (1927-2017) from Cerebral Angiography. Front Neuroanat [Internet]. 2017 [cited 2019 Aug 1];11:81. Available from: http://www.ncbi.nlm.nih.gov/pubmed/28974927

30. Ryan TJ. The Coronary Angiogram and Its Seminal Contributions to Cardiovascular Medicine Over Five Decades. Circulation [Internet]. 2002 Aug 6 [cited 2019 Aug 1];106(6):752–6. Available from: https://www.ahajournals.org/doi/10.1161/01.CIR.0000024109.12658.D4

31. Cheng TO. First Selective Coronary Arteriogram. Circulation [Internet]. 2003 Feb 11 [cited 2019 Aug 1];107(5). Available from: https://www.ahajournals.org/doi/10.1161/01.CIR.0000053958.38681.81

32. SONES FM, SHIREY EK. Cine coronary arteriography. Mod Concepts Cardiovasc Dis [Internet]. 1962 Jul [cited 2019 Aug 1];31:735–8. Available from: http://www.ncbi.nlm.nih.gov/pubmed/13915182

33. Fye WB. A history of the origin, evolution, and impact of electrocardiography. Am J Cardiol [Internet]. 1994 May 15 [cited 2019 Aug 2];73(13):937–49. Available from: http://www.ncbi.nlm.nih.gov/pubmed/8184849

34. Burnett J. The origins of the electrocardiograph as a clinical instrument. Med Hist Suppl [Internet]. 1985 [cited 2019 Aug 2];(5):53–76. Available from: http://www.ncbi.nlm.nih.gov/pubmed/3915524

35. Mehta NJ, Khan IA. Cardiology's 10 Greatest Discoveries of the 20th Century. Texas Hear Inst J [Internet]. 2002 [cited 2019 Aug 2];29(3):164. Available from: https://www.ncbi.nlm.nih.gov/pmc/articles/PMC124754/

36. Edler I. Ultrasound cardiogram in mitral valve disease. Acta Chir Scand. 1956;111:230.

37. Edler I, Hertz CH. The Use of Ultrasonic Reflectoscope for the Continuous Recording of the Movements of Heart Walls. Clin Physiol Funct Imaging [Internet]. 2004 May [cited 2019 Aug 2];24(3):118–36. Available from: http://www.ncbi.nlm.nih.gov/pubmed/15165281

38. Rogers DE, Blendon RJ. The changing American health scene. Sometimes things get better. JAMA [Internet]. 1977 Apr 18 [cited 2019 Aug 2];237(16):1710–4. Available from: http://www.ncbi.nlm.nih.gov/pubmed/403305

39. NIH Fact Sheets - Heart Disease [Internet]. [cited 2019 Aug 2]. Available from: https://report.nih.gov/nihfactsheets/ViewFactSheet.aspx?csid=96

40. Dee R. Who assisted whom? Texas Hear Inst J [Internet]. 2003 [cited 2019 Aug 1];30(1):90. Available from: http://www.ncbi.nlm.nih.gov/pubmed/12638685

41. Haller JD, Olearchyk AS. Cardiology's 10 greatest discoveries. Texas Hear Inst J [Internet]. 2002 [cited 2019 Aug 1];29(4):342–4. Available from: http://www.ncbi.nlm.nih.gov/pubmed/12484626

42. DOTTER CT, JUDKINS MP. TRANSLUMINAL TREATMENT OF ARTERIOSCLEROTIC OBSTRUCTION. DESCRIPTION OF A NEW TECHNIC AND A PRELIMINARY REPORT OF ITS APPLICATION. Circulation [Internet]. 1964 Nov [cited 2019 Aug 1];30:654–70. Available from: http://www.ncbi.nlm.nih.gov/pubmed/14226164

43. Rösch J, Keller F, Kaufman J. The birth, early years, and future of interventional radiology. - PubMed - NCBI. J Vasc Interv Radiol [Internet]. 2003 [cited 2019 Aug 1];14(7):841–53. Available from: https://www.ncbi.nlm.nih.gov/pubmed/12847192

44. Tomberli B, Mattesini A, Baldereschi GI, Di Mario C. A Brief History of Coronary Artery Stents. Rev Española Cardiol (English Ed [Internet]. 2018 May 1 [cited 2019 Aug 12];71(5):312–9. Available from: https://linkinghub.elsevier.com/retrieve/pii/S1885585717305881

45. Neumann F-J, Sousa-Uva M, Ahlsson A, Alfonso F, Banning AP, Benedetto U, et al. 2018 ESC/EACTS Guidelines on myocardial revascularization. Eur Heart J [Internet]. 2019 Jan 7 [cited 2019 Aug 12];40(2):87–165. Available from: https://academic.oup.com/eurheartj/article/40/2/87/5079120

46. De Bruyne B, Pijls NHJ, Kalesan B, Barbato E, Tonino PAL, Piroth Z, et al. Fractional Flow Reserve–Guided PCI versus Medical Therapy in Stable Coronary Disease. N Engl J Med [Internet]. 2012 Sep 13 [cited 2019 Aug 12];367(11):991–1001. Available from: http://www.ncbi.nlm.nih.gov/pubmed/22924638

47. Fearon WF, Nishi T, De Bruyne B, Boothroyd DB, Barbato E, Tonino P, et al. Clinical Outcomes and Cost-Effectiveness of Fractional Flow Reserve–Guided Percutaneous Coronary Intervention in Patients With Stable Coronary Artery Disease. Circulation [Internet]. 2018 Jan 30 [cited 2019 Aug 12];137(5):480–7. Available from: http://www.ncbi.nlm.nih.gov/pubmed/29097450

48. Liu K, Daviglus ML, Loria CM, Colangelo LA, Spring B, Moller AC, et al. Healthy Lifestyle Through Young Adulthood and the Presence of Low Cardiovascular Disease Risk Profile in Middle Age. Circulation [Internet]. 2012 Feb 28 [cited 2019 Aug 12];125(8):996–1004. Available from: http://www.ncbi.nlm.nih.gov/pubmed/22291127

49. Overview | Cardiovascular disease prevention | Guidance | NICE. [cited 2019 Aug 12]; Available from: https://www.nice.org.uk/guidance/PH25

50. Piepoli MF, Hoes AW, Agewall S, Albus C, Brotons C, Catapano AL, et al. 2016 European Guidelines on cardiovascular disease prevention in clinical practice. Eur Heart J [Internet]. 2016 Aug 1 [cited 2019 Aug 12];37(29):2315–81. Available from: https://academic.oup.com/eurheartj/article-lookup/doi/10.1093/eurheartj/ehw106

51. Mahmood SS, Levy D, Vasan RS, Wang TJ. The Framingham Heart Study and the epidemiology of cardiovascular disease: a historical perspective. Lancet (London, England) [Internet]. 2014 Mar 15 [cited 2019 Aug 1];383(9921):999–1008. Available from: http://www.ncbi.nlm.nih.gov/pubmed/24084292

52. Szabo DT. Transcriptomic biomarkers in safety and risk assessment of chemicals. Biomarkers Toxicol [Internet]. 2014 Jan 1 [cited 2019 Aug 21];1033–8. Available from: https://www.sciencedirect.com/science/article/pii/B9780124046306000622

53. Xue M, Zhuo Y, Shan B. MicroRNAs, Long Noncoding RNAs, and Their Functions in Human Disease. In: Methods in molecular biology (Clifton, NJ) [Internet]. 2017 [cited 2019 Aug 21]. p. 1–25. Available from: http://www.ncbi.nlm.nih.gov/pubmed/28540673

54. Mitchell PS, Parkin RK, Kroh EM, Fritz BR, Wyman SK, Pogosova-Agadjanyan EL, et al. Circulating microRNAs as stable blood-based markers for cancer detection. Proc Natl Acad Sci [Internet]. 2008 Jul 29 [cited 2019 Aug 21];105(30):10513–8. Available from: http://www.ncbi.nlm.nih.gov/pubmed/18663219

55. Chiva C, Pastor O, Trilla-Fuertes L, Gámez-Pozo A, Fresno Vara JÁ, Sabidó E. Isotopologue Multipoint Calibration for Proteomics Biomarker Quantification in Clinical

Practice. Anal Chem [Internet]. 2019 Apr 16 [cited 2019 Aug 20];91(8):4934–8. Available from: http://pubs.acs.org/doi/10.1021/acs.analchem.8b05802

56. Aranda S, Alcaine-Colet A, Blanco E, Borràs E, Caillot C, Sabidó E, et al. Chromatin capture links the metabolic enzyme AHCY to stem cell proliferation. Sci Adv [Internet]. 2019 Mar 6 [cited 2019 Aug 20];5(3):eaav2448. Available from: http://advances.sciencemag.org/lookup/doi/10.1126/sciadv.aav2448

57. Cheng S, Vasan RS. Advances in the Epidemiology of Heart Failure and Left Ventricular Remodeling. Circulation [Internet]. 2011 Nov 15 [cited 2019 Aug 19];124(20):e516-9. Available from: http://www.ncbi.nlm.nih.gov/pubmed/22083151

58. Mann DL, Bristow MR. Mechanisms and Models in Heart Failure. Circulation [Internet]. 2005 May 31 [cited 2019 Aug 19];111(21):2837–49. Available from: http://www.ncbi.nlm.nih.gov/pubmed/15927992

59. Wang TJ, Evans JC, Benjamin EJ, Levy D, LeRoy EC, Vasan RS. Natural History of Asymptomatic Left Ventricular Systolic Dysfunction in the Community. Circulation [Internet]. 2003 Aug 26 [cited 2019 Aug 13];108(8):977–82. Available from: http://www.ncbi.nlm.nih.gov/pubmed/12912813

60. SOLVD Investigators, Yusuf S, Pitt B, Davis CE, Hood WB, Cohn JN. Effect of Enalapril on Mortality and the Development of Heart Failure in Asymptomatic Patients with Reduced Left Ventricular Ejection Fractions. N Engl J Med [Internet]. 1992 Sep 3 [cited 2019 Aug 13];327(10):685–91. Available from: http://www.ncbi.nlm.nih.gov/pubmed/1463530

61. Redfield MM, Jacobsen SJ, Burnett, Jr JC, Mahoney DW, Bailey KR, Rodeheffer RJ. Burden of Systolic and Diastolic Ventricular Dysfunction in the

Community. JAMA [Internet]. 2003 Jan 8 [cited 2019 Jul 25];289(2):194. Available from: http://www.ncbi.nlm.nih.gov/pubmed/12517230

62. Mosterd A, Hoes AW. Clinical epidemiology of heart failure. Heart [Internet]. 2007 Sep 1 [cited 2019 Jul 25];93(9):1137–46. Available from: http://www.ncbi.nlm.nih.gov/pubmed/17699180

63. Ceia F, Fonseca C, Mota T, Morais H, Matias F, de Sousa A, et al. Prevalence of chronic heart failure in Southwestern Europe: the EPICA study. Eur J Heart Fail [Internet]. 2002 Aug [cited 2019 Jul 25];4(4):531–9. Available from: http://www.ncbi.nlm.nih.gov/pubmed/12167394

64. Maggioni AP, Dahlström U, Filippatos G, Chioncel O, Leiro MC, Drozdz J, et al. EUR *Observational* Research Programme: regional differences and 1-year follow-up results of the Heart Failure Pilot Survey (ESC-HF Pilot). Eur J Heart Fail [Internet]. 2013 Jul [cited 2019 Aug 19];15(7):808–17. Available from: http://www.ncbi.nlm.nih.gov/pubmed/23537547

65. Pocock SJ, Ariti CA, McMurray JJV, Maggioni A, Køber L, Squire IB, et al. Predicting survival in heart failure: a risk score based on 39 372 patients from 30 studies. Eur Heart J [Internet]. 2013 May 14 [cited 2019 Aug 19];34(19):1404–13. Available from: http://www.ncbi.nlm.nih.gov/pubmed/23095984

66. Davie A. Assessing diagnosis in heart failure: which features are any use? QJM [Internet]. 1997 May 1 [cited 2019 Aug 19];90(5):335–9. Available from: https://academic.oup.com/qjmed/article-lookup/doi/10.1093/qjmed/90.5.335

67. Mant J, Doust J, Roalfe A, Barton P, Cowie M, Glasziou P, et al. Systematic review and individual patient data meta-analysis of diagnosis of heart failure, with modelling of implications of different diagnostic strategies in primary care. Health

Technol Assess (Rockv) [Internet]. 2009 Jul [cited 2019 Aug 19];13(32). Available from: https://www.journalslibrary.nihr.ac.uk/hta/hta13320/

68. Fonseca C. Diagnosis of heart failure in primary care. Heart Fail Rev [Internet]. 2006 Jun [cited 2019 Aug 19];11(2):95–107. Available from: http://www.ncbi.nlm.nih.gov/pubmed/16937029

69. Oudejans I, Mosterd A, Bloemen JA, Valk MJ, van Velzen E, Wielders JP, et al. Clinical evaluation of geriatric outpatients with suspected heart failure: value of symptoms, signs, and additional tests. Eur J Heart Fail [Internet]. 2011 May [cited 2019 Aug 19];13(5):518–27. Available from: http://doi.wiley.com/10.1093/eurjhf/hfr021

70. Kelder JC, Cramer MJ, van Wijngaarden J, van Tooren R, Mosterd A, Moons KGM, et al. The Diagnostic Value of Physical Examination and Additional Testing in Primary Care Patients With Suspected Heart Failure. Circulation [Internet]. 2011 Dec [cited 2019 Aug 19];124(25):2865–73. Available from: https://www.ahajournals.org/doi/10.1161/CIRCULATIONAHA.111.019216

71. van Riet EES, Hoes AW, Limburg A, Landman MAJ, van der Hoeven H, Rutten FH. Prevalence of unrecognized heart failure in older persons with shortness of breath on exertion. Eur J Heart Fail [Internet]. 2014 Jul [cited 2019 Aug 19];16(7):772–7. Available from: http://www.ncbi.nlm.nih.gov/pubmed/24863953

72. Boonman-de Winter LJM, Rutten FH, Cramer MJ, Landman MJ, Zuithoff NPA, Liem AH, et al. Efficiently screening heart failure in patients with type 2 diabetes. Eur J Heart Fail [Internet]. 2015 Feb [cited 2019 Aug 19];17(2):187–95. Available from: http://www.ncbi.nlm.nih.gov/pubmed/25557025

73. Rutten FH, Moons KGM, Cramer M-JM, Grobbee DE, Zuithoff NPA, Lammers an-WJ, et al. Recognising heart failure in elderly patients with stable chronic obstructive

pulmonary disease in primary care: cross sectional diagnostic study. BMJ [Internet]. 2005 Dec 10 [cited 2019 Aug 19];331(7529):1379. Available from: http://www.ncbi.nlm.nih.gov/pubmed/16321994

74. Hawkins NM, Petrie MC, Jhund PS, Chalmers GW, Dunn FG, McMurray JJV. Heart failure and chronic obstructive pulmonary disease: diagnostic pitfalls and epidemiology. Eur J Heart Fail [Internet]. 2009 Feb [cited 2019 Aug 19];11(2):130–9. Available from: http://www.ncbi.nlm.nih.gov/pubmed/19168510

75. Daniels LB, Clopton P, Bhalla V, Krishnaswamy P, Nowak RM, McCord J, et al. How obesity affects the cut-points for B-type natriuretic peptide in the diagnosis of acute heart failure. Am Heart J [Internet]. 2006 May [cited 2019 Aug 19];151(5):999–1005. Available from: https://linkinghub.elsevier.com/retrieve/pii/S0002870305009488

76. Rahimi K, Bennett D, Conrad N, Williams TM, Basu J, Dwight J, et al. Risk Prediction in Patients With Heart Failure. JACC Hear Fail [Internet]. 2014 Oct [cited 2019 Aug 19];2(5):440–6. Available from: http://www.ncbi.nlm.nih.gov/pubmed/25194291

77. Ouwerkerk W, Voors AA, Zwinderman AH. Factors Influencing the Predictive Power of Models for Predicting Mortality and/or Heart Failure Hospitalization in Patients With Heart Failure. JACC Hear Fail [Internet]. 2014 Oct [cited 2019 Aug 19];2(5):429–36. Available from: http://www.ncbi.nlm.nih.gov/pubmed/25194294

78. Lupón J, de Antonio M, Vila J, Peñafiel J, Galán A, Zamora E, et al. Development of a Novel Heart Failure Risk Tool: The Barcelona Bio-Heart Failure Risk Calculator (BCN Bio-HF Calculator). Abbate A, editor. PLoS One [Internet]. 2014 Jan 15 [cited 2019 Aug 19];9(1):e85466. Available from: http://www.ncbi.nlm.nih.gov/pubmed/24454874

79. Levy WC, Mozaffarian D, Linker DT, Sutradhar SC, Anker SD, Cropp AB, et al. The Seattle Heart Failure Model. Circulation [Internet]. 2006 Mar 21 [cited 2019 Aug 19];113(11):1424–33. Available from: http://www.ncbi.nlm.nih.gov/pubmed/16534009

80. Mozaffarian D, Anker SD, Anand I, Linker DT, Sullivan MD, Cleland JGF, et al. Prediction of Mode of Death in Heart Failure. Circulation [Internet]. 2007 Jul 24 [cited 2019 Aug 19];116(4):392–8. Available from: http://www.ncbi.nlm.nih.gov/pubmed/17620506

81. Maisel A, Mueller C, Adams K, Anker SD, Aspromonte N, Cleland JGF, et al. State of the art: Using natriuretic peptide levels in clinical practice. Eur J Heart Fail [Internet]. 2008 Sep [cited 2019 Aug 19];10(9):824–39. Available from: http://www.ncbi.nlm.nih.gov/pubmed/18760965

82. Davie AP, Francis CM, Love MP, Caruana L, Starkey IR, Shaw TRD, et al. Value of the electrocardiogram in identifying heart failure due to left ventricular systolic dysfunction. BMJ [Internet]. 1996 Jan 27 [cited 2019 Aug 19];312(7025):222–222. Available from: http://www.ncbi.nlm.nih.gov/pubmed/8563589

83. Thomas JT, Kelly RF, Thomas SJ, Stamos TD, Albasha K, Parrillo JE, et al. Utility of history, physical examination, electrocardiogram, and chest radiograph for differentiating normal from decreased systolic function in patients with heart failure. Am J Med [Internet]. 2002 Apr 15 [cited 2019 Aug 19];112(6):437–45. Available from: http://www.ncbi.nlm.nih.gov/pubmed/11959053

84. Paulus WJ, Tschöpe C, Sanderson JE, Rusconi C, Flachskampf FA, Rademakers FE, et al. How to diagnose diastolic heart failure: a consensus statement on the diagnosis of heart failure with normal left ventricular ejection fraction by the Heart Failure and Echocardiography Associations of the European Society of Cardiology. Eur Heart J

[Internet]. 2007 Oct [cited 2019 Aug 19];28(20):2539–50. Available from: http://www.ncbi.nlm.nih.gov/pubmed/17428822

85. Marwick TH, Raman S V., Carrió I, Bax JJ. Recent Developments in Heart Failure Imaging. JACC Cardiovasc Imaging [Internet]. 2010 Apr [cited 2019 Aug 19];3(4):429–39. Available from: http://www.ncbi.nlm.nih.gov/pubmed/20394905

86. Dokainish H, Nguyen JS, Bobek J, Goswami R, Lakkis NM. Assessment of the American Society of Echocardiography-European Association of Echocardiography guidelines for diastolic function in patients with depressed ejection fraction: an echocardiographic and invasive haemodynamic study. Eur J Echocardiogr [Internet]. 2011 Nov 1 [cited 2019 Aug 19];12(11):857–64. Available from: http://www.ncbi.nlm.nih.gov/pubmed/21890470

87. Kirkpatrick JN, Vannan MA, Narula J, Lang RM. Echocardiography in Heart Failure. J Am Coll Cardiol [Internet]. 2007 Jul 31 [cited 2019 Aug 19];50(5):381–96. Available from: http://www.ncbi.nlm.nih.gov/pubmed/17662389

88. Nagueh SF, Bhatt R, Vivo RP, Krim SR, Sarvari SI, Russell K, et al. Echocardiographic Evaluation of Hemodynamics in Patients With Decompensated Systolic Heart Failure. Circ Cardiovasc Imaging [Internet]. 2011 May [cited 2019 Aug 19];4(3):220–7. Available from: http://www.ncbi.nlm.nih.gov/pubmed/21398512

89. Caballero L, Kou S, Dulgheru R, Gonjilashvili N, Athanassopoulos GD, Barone D, et al. Echocardiographic reference ranges for normal cardiac Doppler data: results from the NORRE Study. Eur Hear J - Cardiovasc Imaging [Internet]. 2015 Apr 20 [cited 2019 Aug 19];16(9):1031–41. Available from: http://www.ncbi.nlm.nih.gov/pubmed/25896355

90. Garbi M, McDonagh T, Cosyns B, Bucciarelli-Ducci C, Edvardsen T, Kitsiou A, et al. Appropriateness criteria for cardiovascular imaging use in heart failure: report of literature review. Eur Hear J - Cardiovasc Imaging [Internet]. 2015 Feb 1 [cited 2019 Aug 19];16(2):147–53. Available from: http://www.ncbi.nlm.nih.gov/pubmed/25550363

91. Gimelli A, Lancellotti P, Badano LP, Lombardi M, Gerber B, Plein S, et al. Non-invasive cardiac imaging evaluation of patients with chronic systolic heart failure: a report from the European Association of Cardiovascular Imaging (EACVI). Eur Heart J [Internet]. 2014 Dec 2 [cited 2019 Aug 19];35(48):3417–25. Available from: http://www.ncbi.nlm.nih.gov/pubmed/25416326

92. Ponikowski P, Jankowska EA. Pathogenesis and Clinical Presentation of Acute Heart Failure. Rev Española Cardiol (English Ed [Internet]. 2015 Apr [cited 2019 Aug 19];68(4):331–7. Available from: http://www.ncbi.nlm.nih.gov/pubmed/25743769

93. Metra M, Felker GM, Zacà V, Bugatti S, Lombardi C, Bettari L, et al. Acute heart failure: Multiple clinical profiles and mechanisms require tailored therapy. Int J Cardiol [Internet]. 2010 Oct 8 [cited 2019 Aug 19];144(2):175–9. Available from: http://www.ncbi.nlm.nih.gov/pubmed/20537739

94. Alla F, Zannad F, Filippatos G. Epidemiology of acute heart failure syndromes. Heart Fail Rev [Internet]. 2007 Jun 12 [cited 2019 Aug 19];12(2):91–5. Available from: http://www.ncbi.nlm.nih.gov/pubmed/17450426

95. Filippatos G, Zannad F. An introduction to acute heart failure syndromes: definition and classification. Heart Fail Rev [Internet]. 2007 Jun 12 [cited 2019 Aug 19];12(2):87–90. Available from: http://www.ncbi.nlm.nih.gov/pubmed/17508282

96. Piotr Ponikowski* (Chairperson) (Poland), Adriaan A. Voors* (Co-Chairperson) (The Netherlands) SDA (Germany), He´ctor Bueno (Spain), John G. F.

Cleland (UK) AJSC (UK), Volkmar Falk (Germany), Jose´ Ramo´n Gonza´lez-Juanatey (Spain) V-PH, (Finland), Ewa A. Jankowska (Poland), Mariell Jessup (USA) CL (Sweden), Petros Nihoyannopoulos (UK), John T. Parissis (Greece) BP (Germany), et al. 2016 ESC Guidelines for the diagnosis and treatment of acute and chronic heart failure. [cited 2019 Jul 25]; Available from: http://www.escardio.org/guidelines.

97. Nohria A, Tsang SW, Fang JC, Lewis EF, Jarcho JA, Mudge GH, et al. Clinical assessment identifies hemodynamic profiles that predict outcomes in patients admitted with heart failure. J Am Coll Cardiol [Internet]. 2003 May 21 [cited 2019 Aug 19];41(10):1797–804. Available from: http://www.ncbi.nlm.nih.gov/pubmed/12767667

98. Stevenson LW. Design of therapy for advanced heart failure. Eur J Heart Fail [Internet]. 2005 Mar 16 [cited 2019 Aug 19];7(3):323–31. Available from: http://www.ncbi.nlm.nih.gov/pubmed/15718172

99. El-Menyar A, Zubaid M, AlMahmeed W, Sulaiman K, AlNabti A, Singh R, et al. Killip classification in patients with acute coronary syndrome: insight from a multicenter registry. Am J Emerg Med [Internet]. 2012 Jan [cited 2019 Aug 13];30(1):97–103. Available from: http://www.ncbi.nlm.nih.gov/pubmed/21159479

100. van Diepen S, Katz JN, Albert NM, Henry TD, Jacobs AK, Kapur NK, et al. Contemporary Management of Cardiogenic Shock: A Scientific Statement From the American Heart Association. Circulation [Internet]. 2017 Oct 17 [cited 2019 Aug 19];136(16):e232–68. Available from: http://www.ncbi.nlm.nih.gov/pubmed/28923988

101. Mandawat A, Rao S V. Percutaneous Mechanical Circulatory Support Devices in Cardiogenic Shock. Circ Cardiovasc Interv [Internet]. 2017 May [cited 2019 Aug 19];10(5). Available from: http://www.ncbi.nlm.nih.gov/pubmed/28500136

102. Chakko S, Woska D, Martinez H, de Marchena E, Futterman L, Kessler KM, et al. Clinical, radiographic, and hemodynamic correlations in chronic congestive heart failure: conflicting results may lead to inappropriate care. Am J Med [Internet]. 1991 Mar [cited 2019 Aug 19];90(3):353–9. Available from: https://linkinghub.elsevier.com/retrieve/pii/000293439180016F

103. Wang CS, FitzGerald JM, Schulzer M, Mak E, Ayas NT. Does This Dyspneic Patient in the Emergency Department Have Congestive Heart Failure? JAMA [Internet]. 2005 Oct 19 [cited 2019 Aug 19];294(15):1944. Available from: http://www.ncbi.nlm.nih.gov/pubmed/16234501

104. Rawles JM, Kenmure AC. Controlled trial of oxygen in uncomplicated myocardial infarction. BMJ [Internet]. 1976 May 8 [cited 2019 Aug 19];1(6018):1121–3. Available from: http://www.ncbi.nlm.nih.gov/pubmed/773507

105. Park JH, Balmain S, Berry C, Morton JJ, McMurray JJ V. Potentially detrimental cardiovascular effects of oxygen in patients with chronic left ventricular systolic dysfunction. Heart [Internet]. 2010 Apr 1 [cited 2019 Aug 19];96(7):533–8. Available from: http://www.ncbi.nlm.nih.gov/pubmed/20350990

106. Park M, Sangean MC, Volpe M de S, Feltrim MIZ, Nozawa E, Leite PF, et al. Randomized, prospective trial of oxygen, continuous positive airway pressure, and bilevel positive airway pressure by face mask in acute cardiogenic pulmonary edema. Crit Care Med [Internet]. 2004 Dec [cited 2019 Aug 19];32(12):2407–15. Available from: http://www.ncbi.nlm.nih.gov/pubmed/15599144

107. Gray A, Goodacre S, Newby DE, Masson M, Sampson F, Nicholl J, et al. Noninvasive Ventilation in Acute Cardiogenic Pulmonary Edema. N Engl J Med

[Internet]. 2008 Jul 10 [cited 2019 Aug 19];359(2):142–51. Available from: http://www.ncbi.nlm.nih.gov/pubmed/18614781

108. Weng C-L, Zhao Y-T, Liu Q-H, Fu C-J, Sun F, Ma Y-L, et al. Meta-analysis: Noninvasive Ventilation in Acute Cardiogenic Pulmonary Edema. Ann Intern Med [Internet]. 2010 May 4 [cited 2019 Aug 19];152(9):590. Available from: http://www.ncbi.nlm.nih.gov/pubmed/20439577

109. Vital FM, Ladeira MT, Atallah ÁN. Non-invasive positive pressure ventilation (CPAP or bilevel NPPV) for cardiogenic pulmonary oedema. Cochrane Database Syst Rev [Internet]. 2013 May 31 [cited 2019 Aug 19]; Available from: http://doi.wiley.com/10.1002/14651858.CD005351.pub3

110. Barbour DL. Precision medicine and the cursed dimensions. npj Digit Med [Internet]. 2019 Dec 4 [cited 2019 Aug 20];2(1):4. Available from: http://www.nature.com/articles/s41746-019-0081-5

111. Dance A. Medical histories. Nature [Internet]. 2016 Sep 7 [cited 2019 Jul 22];537(7619):S52–3. Available from: http://www.nature.com/articles/537S52a

112. Hodson R. Precision medicine. Nat 2016 5377619. 2016 Sep 7;

113. Langlotz CP, Allen B, Erickson BJ, Kalpathy-Cramer J, Bigelow K, Cook TS, et al. A Roadmap for Foundational Research on Artificial Intelligence in Medical Imaging: From the 2018 NIH/RSNA/ACR/The Academy Workshop. Radiology [Internet]. 2019 Jun 16 [cited 2019 Aug 20];291(3):781–91. Available from: http://pubs.rsna.org/doi/10.1148/radiol.2019190613

114. Saraf RP, Suresh P, Maheshwari S, Shah SS. Pediatric echocardiograms performed at primary centers: Diagnostic errors and missing links! Ann Pediatr Cardiol

[Internet]. 2015 [cited 2019 Aug 20];8(1):20–4. Available from: http://www.ncbi.nlm.nih.gov/pubmed/25684883

115. Elmore JG, Wells CK, Lee CH, Howard DH, Feinstein AR. Variability in Radiologists' Interpretations of Mammograms. N Engl J Med [Internet]. 1994 Dec 15 [cited 2019 Aug 20];331(22):1493–9. Available from: http://www.nejm.org/doi/abs/10.1056/NEJM199412013312206

116. Borgstede JP, Lewis RS, Bhargavan M, Sunshine JH. RADPEER quality assurance program: a multifacility study of interpretive disagreement rates. J Am Coll Radiol [Internet]. 2004 Jan 1 [cited 2019 Aug 20];1(1):59–65. Available from: https://www.sciencedirect.com/science/article/pii/S1546144003000024

117. Russakovsky O, Deng J, Su H, Krause J, Satheesh S, Ma S, et al. ImageNet Large Scale Visual Recognition Challenge. Int J Comput Vis [Internet]. 2015 Dec 11 [cited 2019 Aug 20];115(3):211–52. Available from: http://link.springer.com/10.1007/s11263-015-0816-y

118. Greco S, Fasanaro P, Castelvecchio S, D'Alessandra Y, Arcelli D, Di Donato M, et al. MicroRNA Dysregulation in Diabetic Ischemic Heart Failure Patients. Diabetes [Internet]. 2012 Jun 1 [cited 2019 Aug 22];61(6):1633–41. Available from: http://www.ncbi.nlm.nih.gov/pubmed/22427379

119. Liu Y, Morley M, Brandimarto J, Hannenhalli S, Hu Y, Ashley EA, et al. RNA-Seq identifies novel myocardial gene expression signatures of heart failure. Genomics [Internet]. 2015 Feb [cited 2019 Aug 22];105(2):83–9. Available from: http://www.ncbi.nlm.nih.gov/pubmed/25528681

120. Prat-Vidal C, Gálvez-Montón C, Nonell L, Puigdecanet E, Astier L, Solé F, et al. Identification of Temporal and Region-Specific Myocardial Gene Expression Patterns

in Response to Infarction in Swine. Grundmann S, editor. PLoS One [Internet]. 2013 Jan 25 [cited 2019 Aug 22];8(1):e54785. Available from: http://dx.plos.org/10.1371/journal.pone.0054785

121. Sonnhammer ELL, Östlund G. InParanoid 8: orthology analysis between 273 proteomes, mostly eukaryotic. Nucleic Acids Res [Internet]. 2015 Jan [cited 2019 Aug 21];43(Database issue):D234-9. Available from: http://www.ncbi.nlm.nih.gov/pubmed/25429972

122. Barrett T, Wilhite SE, Ledoux P, Evangelista C, Kim IF, Tomashevsky M, et al. NCBI GEO: archive for functional genomics data sets—update. Nucleic Acids Res [Internet]. 2012 Nov 26 [cited 2019 Aug 21];41(D1):D991–5. Available from: http://www.ncbi.nlm.nih.gov/pubmed/23193258

123. Shi W, Oshlack A, Smyth GK. Optimizing the noise versus bias trade-off for Illumina whole genome expression BeadChips. Nucleic Acids Res [Internet]. 2010 Dec 1 [cited 2019 Aug 21];38(22):e204–e204. Available from: http://www.ncbi.nlm.nih.gov/pubmed/20929874

124. Smyth GK. Linear Models and Empirical Bayes Methods for Assessing Differential Expression in Microarray Experiments. Stat Appl Genet Mol Biol [Internet]. 2004 Jan 12 [cited 2019 Aug 21];3(1):1–25. Available from: http://www.ncbi.nlm.nih.gov/pubmed/16646809

125. Smyth GK. limma: Linear Models for Microarray Data. In: Bioinformatics and Computational Biology Solutions Using R and Bioconductor [Internet]. New York: Springer-Verlag; 2005 [cited 2019 Aug 21]. p. 397–420. Available from: http://link.springer.com/10.1007/0-387-29362-0_23

126. Wright SP. Adjusted P-Values for Simultaneous Inference. Biometrics [Internet]. 1992 Dec [cited 2019 Aug 21];48(4):1005. Available from: https://www.jstor.org/stable/2532694?origin=crossref

127. Yoav Benjamini, Yosef Hochberg. Controlling the False Discovery Rate: A Practical and Powerful Approach to Multiple Testing on JSTOR. J R Stat Soc [Internet]. 1995 [cited 2019 Aug 21];57:289–300. Available from: https://www.jstor.org/stable/2346101?seq=1#metadata_info_tab_contents

128. Anellis IH. Peirce's Truth-functional Analysis and the Origin of the Truth Table. Hist Philos Log [Internet]. 2012 Feb [cited 2019 Aug 22];33(1):87–97. Available from: http://www.tandfonline.com/doi/abs/10.1080/01445340.2011.621702

129. Pujol A, Mosca R, Farrés J, Aloy P. Unveiling the role of network and systems biology in drug discovery. Trends Pharmacol Sci [Internet]. 2010 Mar [cited 2019 Aug 22];31(3):115–23. Available from: http://www.ncbi.nlm.nih.gov/pubmed/20117850

130. Herrando-Grabulosa M, Mulet R, Pujol A, Mas JM, Navarro X, Aloy P, et al. Novel Neuroprotective Multicomponent Therapy for Amyotrophic Lateral Sclerosis Designed by Networked Systems. Duce JA, editor. PLoS One [Internet]. 2016 Jan 25 [cited 2019 Aug 22];11(1):e0147626. Available from: http://dx.plos.org/10.1371/journal.pone.0147626

131. Cicero AFG, Colletti A, Bellentani S. Nutraceutical Approach to Non-Alcoholic Fatty Liver Disease (NAFLD): The Available Clinical Evidence. Nutrients [Internet]. 2018 Aug 23 [cited 2019 Aug 22];10(9). Available from: http://www.ncbi.nlm.nih.gov/pubmed/30142943

132. Gómez-Serrano M, Camafeita E, García-Santos E, López JA, Rubio MA, Sánchez-Pernaute A, et al. Proteome-wide alterations on adipose tissue from obese

patients as age-, diabetes- and gender-specific hallmarks. Sci Rep [Internet]. 2016 [cited 2019 Aug 22];6:25756. Available from: http://www.ncbi.nlm.nih.gov/pubmed/27160966

133. Russell SJ (Stuart J, Norvig P, Davis E. Artificial intelligence : a modern approach. 1132 p.

134. Kirkpatrick S, Gelatt CD, Vecchi MP. Optimization by simulated annealing. Science [Internet]. 1983 May 13 [cited 2019 Aug 22];220(4598):671–80. Available from: http://www.ncbi.nlm.nih.gov/pubmed/17813860

135. Goldberg DE (David E, E. D. Genetic algorithms in search, optimization, and machine learning [Internet]. Addison-Wesley Longman Publishing Co., Inc.; 1989 [cited 2019 Aug 22]. 412 p. Available from: https://dl.acm.org/citation.cfm?id=534133

136. Wishart DS, Knox C, Guo AC, Shrivastava S, Hassanali M, Stothard P, et al. DrugBank: a comprehensive resource for in silico drug discovery and exploration. Nucleic Acids Res [Internet]. 2006 Jan 1 [cited 2019 Aug 22];34(90001):D668–72. Available from: http://www.ncbi.nlm.nih.gov/pubmed/16381955

137. Kanehisa M, Goto S, Hattori M, Aoki-Kinoshita KF, Itoh M, Kawashima S, et al. From genomics to chemical genomics: new developments in KEGG. Nucleic Acids Res [Internet]. 2006 Jan 1 [cited 2019 Aug 22];34(90001):D354–7. Available from: http://www.ncbi.nlm.nih.gov/pubmed/16381885

138. Licata L, Briganti L, Peluso D, Perfetto L, Iannuccelli M, Galeota E, et al. MINT, the molecular interaction database: 2012 update. Nucleic Acids Res [Internet]. 2012 Jan [cited 2019 Aug 22];40(D1):D857–61. Available from: https://academic.oup.com/nar/article-lookup/doi/10.1093/nar/gkr930

139. Kerrien S, Aranda B, Breuza L, Bridge A, Broackes-Carter F, Chen C, et al. The IntAct molecular interaction database in 2012. Nucleic Acids Res [Internet]. 2012 Jan 1

[cited 2019 Aug 22];40(D1):D841–6. Available from: https://academic.oup.com/nar/article-lookup/doi/10.1093/nar/gkr1088

140. Croft D, Mundo AF, Haw R, Milacic M, Weiser J, Wu G, et al. The Reactome pathway knowledgebase. Nucleic Acids Res [Internet]. 2014 Jan [cited 2019 Aug 22];42(D1):D472–7. Available from: https://academic.oup.com/nar/article-lookup/doi/10.1093/nar/gkt1102

141. Oughtred R, Chatr-aryamontri A, Breitkreutz B-J, Chang CS, Rust JM, Theesfeld CL, et al. Use of the BioGRID Database for Analysis of Yeast Protein and Genetic Interactions. Cold Spring Harb Protoc [Internet]. 2016 [cited 2019 Aug 22];2016(1):pdb.prot088880. Available from: https://www.ncbi.nlm.nih.gov/pmc/articles/PMC5975959/

142. Bishop CM. Pattern recognition and machine learning. Springer; 2006. 738 p.

143. Subramanian A, Tamayo P, Mootha VK, Mukherjee S, Ebert BL, Gillette MA, et al. Gene set enrichment analysis: A knowledge-based approach for interpreting genome-wide expression profiles. Proc Natl Acad Sci [Internet]. 2005 Oct 25 [cited 2019 Aug 21];102(43):15545–50. Available from: https://www.pnas.org/content/102/43/15545

144. Mootha VK, Lindgren CM, Eriksson K-F, Subramanian A, Sihag S, Lehar J, et al. PGC-1α-responsive genes involved in oxidative phosphorylation are coordinately downregulated in human diabetes. Nat Genet [Internet]. 2003 Jul 15 [cited 2019 Aug 21];34(3):267–73. Available from: http://www.nature.com/articles/ng1180

145. Wishart DS, Jewison T, Guo AC, Wilson M, Knox C, Liu Y, et al. HMDB 3.0—The Human Metabolome Database in 2013. Nucleic Acids Res [Internet]. 2012 Nov 17

[cited 2019 Aug 22];41(D1):D801–7. Available from: http://www.ncbi.nlm.nih.gov/pubmed/23161693

146. Van Der Malsburg C. Frank Rosenblatt: Principles of Neurodynamics: Perceptrons and the Theory of Brain Mechanisms. In: Brain Theory [Internet]. Berlin, Heidelberg: Springer Berlin Heidelberg; 1986 [cited 2019 Aug 22]. p. 245–8. Available from: http://link.springer.com/10.1007/978-3-642-70911-1_20

147. Rumelhart DE, McClelland JL, University of California SDPRG. Parallel distributed processing : explorations in the microstructure of cognition [Internet]. MIT Press; 1986 [cited 2019 Aug 22]. Available from: https://dl.acm.org/citation.cfm?id=104279

148. Cybenko G. Approximation by superpositions of a sigmoidal function. Math Control Signals, Syst [Internet]. 1989 Dec [cited 2019 Aug 22];2(4):303–14. Available from: http://link.springer.com/10.1007/BF02551274

149. Tripathi S, Pohl MO, Zhou Y, Rodriguez-Frandsen A, Wang G, Stein DA, et al. Meta- and Orthogonal Integration of Influenza "OMICs" Data Defines a Role for UBR4 in Virus Budding. Cell Host Microbe [Internet]. 2015 Dec 9 [cited 2019 Aug 21];18(6):723–35. Available from: http://www.ncbi.nlm.nih.gov/pubmed/26651948

150. Tyanova S, Temu T, Sinitcyn P, Carlson A, Hein MY, Geiger T, et al. The Perseus computational platform for comprehensive analysis of (prote)omics data. Nat Methods [Internet]. 2016 Sep 27 [cited 2019 Aug 21];13(9):731–40. Available from: http://www.nature.com/articles/nmeth.3901

151. Szklarczyk D, Gable AL, Lyon D, Junge A, Wyder S, Huerta-Cepas J, et al. STRING v11: protein-protein association networks with increased coverage, supporting functional discovery in genome-wide experimental datasets. Nucleic Acids Res

[Internet]. 2019 Jan 8 [cited 2019 Aug 21];47(D1):D607–13. Available from: http://www.ncbi.nlm.nih.gov/pubmed/30476243

152. Yurista SR, Silljé HHW, Oberdorf-Maass SU, Schouten E, Pavez Giani MG, Hillebrands J, et al. Sodium–glucose co-transporter 2 inhibition with empagliflozin improves cardiac function in non-diabetic rats with left ventricular dysfunction after myocardial infarction. Eur J Heart Fail [Internet]. 2019 Apr 29 [cited 2019 Aug 22];21(7):ejhf.1473. Available from: http://www.ncbi.nlm.nih.gov/pubmed/31033127

153. Irizarry RA, Hobbs B, Collin F, Beazer-Barclay YD, Antonellis KJ, Scherf U, et al. Exploration, normalization, and summaries of high density oligonucleotide array probe level data. Biostatistics [Internet]. 2003 Apr 1 [cited 2019 Aug 21];4(2):249–64. Available from: http://www.ncbi.nlm.nih.gov/pubmed/12925520

154. Plieskatt JL, Feng Y, Rinaldi G, Mulvenna JP, Bethony JM, Brindley PJ. Circumventing qPCR inhibition to amplify miRNAs in plasma. Biomark Res [Internet]. 2014 [cited 2019 Aug 21];2(1):13. Available from: http://www.ncbi.nlm.nih.gov/pubmed/25075309

155. Galli A, Lombardi F. Postinfarct Left Ventricular Remodelling: A Prevailing Cause of Heart Failure. Cardiol Res Pract [Internet]. 2016 [cited 2019 Aug 22];2016:1–12. Available from: http://www.ncbi.nlm.nih.gov/pubmed/26989555

156. Deedwania PC, Carbajal E. Evidence-Based Therapy for Heart Failure. Med Clin North Am [Internet]. 2012 Sep [cited 2019 Aug 22];96(5):915–31. Available from: http://www.ncbi.nlm.nih.gov/pubmed/22980055

157. McMurray JJV, Packer M, Desai AS, Gong J, Lefkowitz MP, Rizkala AR, et al. Angiotensin–Neprilysin Inhibition versus Enalapril in Heart Failure. N Engl J Med

[Internet]. 2014 Sep 11 [cited 2019 Aug 22];371(11):993–1004. Available from: http://www.nejm.org/doi/10.1056/NEJMoa1409077

158. Zinman B, Wanner C, Lachin JM, Fitchett D, Bluhmki E, Hantel S, et al. Empagliflozin, Cardiovascular Outcomes, and Mortality in Type 2 Diabetes. N Engl J Med [Internet]. 2015 Nov 26 [cited 2019 Aug 22];373(22):2117–28. Available from: http://www.nejm.org/doi/10.1056/NEJMoa1504720

159. de la Fuente A. From 'differential expression' to 'differential networking' – identification of dysfunctional regulatory networks in diseases. Trends Genet [Internet]. 2010 Jul [cited 2019 Jul 22];26(7):326–33. Available from: http://www.ncbi.nlm.nih.gov/pubmed/20570387

160. WRITING COMMITTEE MEMBERS CW, Yancy CW, Jessup M, Bozkurt B, Butler J, Casey DE, et al. 2016 ACC/AHA/HFSA Focused Update on New Pharmacological Therapy for Heart Failure: An Update of the 2013 ACCF/AHA Guideline for the Management of Heart Failure: A Report of the American College of Cardiology/American Heart Association Task Force on Clinical Practice Guidelines and the Heart Failure Society of America. Circulation [Internet]. 2016 Sep 27 [cited 2019 Aug 22];134(13):e282-93. Available from: https://www.ahajournals.org/doi/10.1161/CIR.0000000000000435

161. Bayés-Genís A. Neprilysin in Heart Failure. JACC Hear Fail [Internet]. 2015 Aug [cited 2019 Aug 22];3(8):637–40. Available from: http://www.ncbi.nlm.nih.gov/pubmed/26251091

162. Bayes-Genis A, Barallat J, Richards AM. A Test in Context: Neprilysin. J Am Coll Cardiol [Internet]. 2016 Aug 9 [cited 2019 Aug 22];68(6):639–53. Available from: http://www.ncbi.nlm.nih.gov/pubmed/27491909

163. Song B, Zhang Z-Z, Zhong J-C, Yu X-Y, Oudit GY, Jin H-Y, et al. Loss of angiotensin-converting enzyme 2 exacerbates myocardial injury via activation of the CTGF-fractalkine signaling pathway. Circ J [Internet]. 2013 [cited 2019 Aug 22];77(12):2997–3006. Available from: http://www.ncbi.nlm.nih.gov/pubmed/24161906

164. Altin SE, Schulze PC. Fractalkine: a novel cardiac chemokine? Cardiovasc Res [Internet]. 2011 Dec 1 [cited 2019 Aug 22];92(3):361–2. Available from: http://www.ncbi.nlm.nih.gov/pubmed/22012953

165. Ma Y, Yabluchanskiy A, Lindsey ML. Neutrophil roles in left ventricular remodeling following myocardial infarction. Fibrogenesis Tissue Repair [Internet]. 2013 Dec 3 [cited 2019 Aug 22];6(1):11. Available from: http://www.ncbi.nlm.nih.gov/pubmed/23731794

166. Ito H, Takemori K, Suzuki T. Role of angiotensin II type 1 receptor in the leucocytes and endothelial cells of brain microvessels in the pathogenesis of hypertensive cerebral injury. J Hypertens [Internet]. 2001 Mar [cited 2019 Aug 22];19(3 Pt 2):591–7. Available from: http://www.ncbi.nlm.nih.gov/pubmed/11327634

167. Marino F, Guasti L, Cosentino M, Ferrari M, Rasini E, Maio RC, et al. Angiotensin II Type 1 Receptor Expression in Polymorphonuclear Leukocytes From High-Risk Subjects: Changes After Treatment With Simvastatin. J Cardiovasc Pharmacol [Internet]. 2007 May [cited 2019 Aug 22];49(5):299–305. Available from: http://www.ncbi.nlm.nih.gov/pubmed/17513949

168. Naccache PH. Signalling in Neutrophils: A Retro Look. ISRN Physiol [Internet]. 2013 Nov 7 [cited 2019 Aug 22];2013:1–13. Available from: https://www.hindawi.com/archive/2013/986320/

169. Fejes-Tóth G, Náray-Fejes-Tóth A. Early Aldosterone-Regulated Genes in Cardiomyocytes: Clues to Cardiac Remodeling? Endocrinology [Internet]. 2007 Apr [cited 2019 Aug 22];148(4):1502–10. Available from: http://www.ncbi.nlm.nih.gov/pubmed/17234708

170. Yoon SY, Lee YJ, Seo JH, Sung HJ, Park KH, Choi IK, et al. uPAR expression under hypoxic conditions depends on iNOS modulated ERK phosphorylation in the MDA-MB-231 breast carcinoma cell line. Cell Res [Internet]. 2006 Jan 16 [cited 2019 Aug 22];16(1):75–81. Available from: http://www.ncbi.nlm.nih.gov/pubmed/16467878

171. Bessard A, Frémin C, Ezan F, Coutant A, Baffet G. MEK/ERK-dependent uPAR expression is required for motility via phosphorylation of P70S6K in human hepatocarcinoma cells. J Cell Physiol [Internet]. 2007 Aug [cited 2019 Aug 22];212(2):526–36. Available from: http://www.ncbi.nlm.nih.gov/pubmed/17427199

172. Kiyan J, Smith G, Haller H, Dumler I. Urokinase-receptor-mediated phenotypic changes in vascular smooth muscle cells require the involvement of membrane rafts. Biochem J [Internet]. 2009 Nov 1 [cited 2019 Aug 22];423(3):343–51. Available from: http://www.ncbi.nlm.nih.gov/pubmed/19691446

173. Ling Q, Chen TH, Guo ZG. Inhibition of beta-myosin heavy chain gene expression in pressure overload rat heart by losartan and captopril. Zhongguo Yao Li Xue Bao [Internet]. 1997 Jan [cited 2019 Aug 22];18(1):63–6. Available from: http://www.ncbi.nlm.nih.gov/pubmed/10072897

174. Liu X, Sentex E, Golfman L, Takeda S, Osada M, Dhalla NS. Modification of Cardiac Subcellular Remodeling Due to Pressure Overload by Captopril and Losartan. Clin Exp Hypertens [Internet]. 1999 Jan 3 [cited 2019 Aug 22];21(1–2):145–56. Available from: http://www.ncbi.nlm.nih.gov/pubmed/10052650

175. Horckmans M, Robaye B, Léon-Gómez E, Lantz N, Unger P, Dol-Gleizes F, et al. P2Y4 nucleotide receptor: a novel actor in post-natal cardiac development. Angiogenesis [Internet]. 2012 Sep 22 [cited 2019 Aug 22];15(3):349–60. Available from: http://link.springer.com/10.1007/s10456-012-9265-1

176. Di Angelantonio E, Kaptoge S, Wormser D, Willeit P, Butterworth AS, Bansal N, et al. Association of Cardiometabolic Multimorbidity With Mortality. JAMA [Internet]. 2015 Jul 7 [cited 2019 Aug 22];314(1):52. Available from: http://www.ncbi.nlm.nih.gov/pubmed/26151266

177. ORIGIN Trial Investigators, Gerstein HC, Bosch J, Dagenais GR, Díaz R, Jung H, et al. Basal Insulin and Cardiovascular and Other Outcomes in Dysglycemia. N Engl J Med [Internet]. 2012 Jul 26 [cited 2019 Aug 22];367(4):319–28. Available from: http://www.ncbi.nlm.nih.gov/pubmed/22686416

178. Wiviott SD, Raz I, Bonaca MP, Mosenzon O, Kato ET, Cahn A, et al. Dapagliflozin and Cardiovascular Outcomes in Type 2 Diabetes. N Engl J Med [Internet]. 2019 Jan 24 [cited 2019 Aug 22];380(4):347–57. Available from: http://www.ncbi.nlm.nih.gov/pubmed/30415602

179. Cavender MA, Norhammar A, Birkeland KI, Jørgensen ME, Wilding JP, Khunti K, et al. SGLT-2 Inhibitors and Cardiovascular Risk. J Am Coll Cardiol [Internet]. 2018 Jun 5 [cited 2019 Aug 22];71(22):2497–506. Available from: http://www.ncbi.nlm.nih.gov/pubmed/29852973

180. Zelniker TA, Braunwald E. Cardiac and Renal Effects of Sodium-Glucose Co-Transporter 2 Inhibitors in Diabetes. J Am Coll Cardiol [Internet]. 2018 Oct 9 [cited 2019 Aug 22];72(15):1845–55. Available from: http://www.ncbi.nlm.nih.gov/pubmed/30075873

181. Flores E, Santos-Gallego CG, Diaz-Mejía N, Badimon JJ. Do the SGLT-2 Inhibitors Offer More than Hypoglycemic Activity? Cardiovasc Drugs Ther [Internet]. 2018 Apr 20 [cited 2019 Aug 22];32(2):213–22. Available from: http://www.ncbi.nlm.nih.gov/pubmed/29679303

182. Packer M, Anker SD, Butler J, Filippatos G, Zannad F. Effects of Sodium-Glucose Cotransporter 2 Inhibitors for the Treatment of Patients With Heart Failure. JAMA Cardiol [Internet]. 2017 Sep 1 [cited 2019 Aug 22];2(9):1025. Available from: http://www.ncbi.nlm.nih.gov/pubmed/28768320

183. Pfeffer MA, Braunwald E. Ventricular remodeling after myocardial infarction. Experimental observations and clinical implications. Circulation [Internet]. 1990 Apr [cited 2019 Jul 22];81(4):1161–72. Available from: http://www.ncbi.nlm.nih.gov/pubmed/2138525

184. Sutton MGSJ, Sharpe N. Left Ventricular Remodeling After Myocardial Infarction. Circulation [Internet]. 2000 Jun 27 [cited 2019 Jul 22];101(25):2981–8. Available from: https://www.ahajournals.org/doi/10.1161/01.CIR.101.25.2981

185. Mudd JO, Kass DA. Tackling heart failure in the twenty-first century. Nature [Internet]. 2008 Feb 20 [cited 2019 Jul 22];451(7181):919–28. Available from: http://www.ncbi.nlm.nih.gov/pubmed/18288181

186. Stanton LW, Garrard LJ, Damm D, Garrick BL, Lam A, Kapoun AM, et al. Altered patterns of gene expression in response to myocardial infarction. Circ Res [Internet]. 2000 May 12 [cited 2019 Jul 22];86(9):939–45. Available from: http://www.ncbi.nlm.nih.gov/pubmed/10807865

187. Harpster MH, Bandyopadhyay S, Thomas DP, Ivanov PS, Keele JA, Pineguina N, et al. Earliest changes in the left ventricular transcriptome post-myocardial infarction.

Mamm Genome [Internet]. 2006 Jul 14 [cited 2019 Jul 22];17(7):701–15. Available from: http://www.ncbi.nlm.nih.gov/pubmed/16845475

188. Witt H, Schubert C, Jaekel J, Fliegner D, Penkalla A, Tiemann K, et al. Sex-specific pathways in early cardiac response to pressure overload in mice. J Mol Med (Berl) [Internet]. 2008 Sep [cited 2019 Jul 22];86(9):1013. Available from: http://www.ncbi.nlm.nih.gov/pubmed/18665344

189. Romeo-Guitart D, Forés J, Herrando-Grabulosa M, Valls R, Leiva-Rodríguez T, Galea E, et al. Neuroprotective Drug for Nerve Trauma Revealed Using Artificial Intelligence. Sci Rep [Internet]. 2018 Dec 30 [cited 2019 Aug 22];8(1):1879. Available from: http://www.nature.com/articles/s41598-018-19767-3

190. Pöss J, Köster J, Fuernau G, Eitel I, de Waha S, Ouarrak T, et al. Risk Stratification for Patients in Cardiogenic Shock After Acute Myocardial Infarction. J Am Coll Cardiol [Internet]. 2017 Apr 18 [cited 2019 Aug 19];69(15):1913–20. Available from: http://www.ncbi.nlm.nih.gov/pubmed/28408020

191. Bernard C. Leçons sur le Diabète et la Glycogenase Animale. Baillere, editor. Paris; 1877.

192. Deane AM, Horowitz M. Dysglycaemia in the critically ill - significance and management. Diabetes, Obes Metab [Internet]. 2013 Sep [cited 2019 Aug 19];15(9):792–801. Available from: http://www.ncbi.nlm.nih.gov/pubmed/23368662

193. Mehta VK, Hao W, Brooks-Worrell BM, Palmer JP. Low-dose interleukin 1 and tumor necrosis factor individually stimulate insulin release but in combination cause suppression. Eur J Endocrinol [Internet]. 1994 Feb 1 [cited 2019 Aug 19];130(2):208–14. Available from: https://eje.bioscientifica.com/view/journals/eje/130/2/eje_130_2_016.xml

194. Zeller M, Cottin Y, Brindisi M-C, Dentan G, Laurent Y, Janin-Manificat L, et al. ?Impaired fasting glucose and cardiogenic shock in patients with acute myocardial infarction. Eur Heart J [Internet]. 2004 Feb [cited 2019 Aug 22];25(4):308–12. Available from: http://www.ncbi.nlm.nih.gov/pubmed/14984919

195. Kataja A, Tarvasmäki T, Lassus J, Cardoso J, Mebazaa A, Køber L, et al. The association of admission blood glucose level with the clinical picture and prognosis in cardiogenic shock – Results from the CardShock Study. Int J Cardiol [Internet]. 2017 Jan 1 [cited 2019 Aug 19];226:48–52. Available from: http://www.ncbi.nlm.nih.gov/pubmed/27788389

196. Abdin A, Pöss J, Fuernau G, Ouarrak T, Desch S, Eitel I, et al. Correction to: Prognostic impact of baseline glucose levels in acute myocardial infarction complicated by cardiogenic shock—a substudy of the IABP-SHOCK II-trial. Clin Res Cardiol [Internet]. 2018 Jun 28 [cited 2019 Aug 19];107(6):531–531. Available from: http://www.ncbi.nlm.nih.gov/pubmed/29492702

197. Yang J, Song P, Song Y, Hahn J-Y, Choi S-H, Choi J-H, et al. Prognostic value of admission blood glucose level in patients with and without diabetes mellitus who sustain ST segment elevation myocardial infarction complicated by cardiogenic shock. Crit Care [Internet]. 2013 Oct 3 [cited 2019 Aug 19];17(5):R218. Available from: http://www.ncbi.nlm.nih.gov/pubmed/24090250

198. Kompanje EJO, Jansen TC, van der Hoven B, Bakker J. The first demonstration of lactic acid in human blood in shock by Johann Joseph Scherer (1814-1869) in January 1843. Intensive Care Med [Internet]. 2007 Nov [cited 2019 Aug 19];33(11):1967–71. Available from: http://www.ncbi.nlm.nih.gov/pubmed/17661014

199. Kubiak GM, Tomasik AR, Bartus K, Olszanecki R, Ceranowicz P. Lactate in cardiogenic shock - current understanding and clinical implications. J Physiol Pharmacol [Internet]. 2018 Feb [cited 2019 Aug 19];69(1):15–21. Available from: http://www.ncbi.nlm.nih.gov/pubmed/29769417

200. Schmiechen NJ, Han C, Milzman DP. ED use of rapid lactate to evaluate patients with acute chest pain. Ann Emerg Med [Internet]. 1997 Nov [cited 2019 Aug 19];30(5):571–7. Available from: http://www.ncbi.nlm.nih.gov/pubmed/9360564

201. Mavrić Z, Zaputović L, Zagar D, Matana A, Smokvina D. Usefulness of blood lactate as a predictor of shock development in acute myocardial infarction. Am J Cardiol [Internet]. 1991 Mar 15 [cited 2019 Aug 19];67(7):565–8. Available from: http://www.ncbi.nlm.nih.gov/pubmed/2000787

202. Vermeulen RP, Hoekstra M, Nijsten MW, van der Horst IC, van Pelt LJ, Jessurun GA, et al. Clinical correlates of arterial lactate levels in patients with ST-segment elevation myocardial infarction at admission: a descriptive study. Crit Care [Internet]. 2010 [cited 2019 Aug 19];14(5):R164. Available from: http://ccforum.biomedcentral.com/articles/10.1186/cc9253

203. Thiele H, Jobs A, Ouweneel DM, Henriques JPS, Seyfarth M, Desch S, et al. Percutaneous short-term active mechanical support devices in cardiogenic shock: a systematic review and collaborative meta-analysis of randomized trials. Eur Heart J [Internet]. 2017 Dec 14 [cited 2019 Aug 19];38(47):3523–31. Available from: http://www.ncbi.nlm.nih.gov/pubmed/29020341

204. Rueda F, Borràs E, García-García C, Iborra-Egea O, Revuelta-López E, Harjola V-P, et al. Protein-based cardiogenic shock patient classifier. Eur Heart J [Internet]. 2019 Jun 17 [cited 2019 Aug 19]; Available from:

https://academic.oup.com/eurheartj/advance-article/doi/10.1093/eurheartj/ehz294/5519422

205. J L, J P, K D, K H, J T, L K, et al. Association of circulating levels of RANTES and -403G/A promoter polymorphism to acute heart failure after STEMI and to cardiogenic shock. Clin Exp Med. 2015;15:405–14.

206. Appoloni O, Dupont E, Vandercruys M, Andrien M, Duchateau J, Vincent J-L. Association Between the TNF-2 Allele and a Better Survival in Cardiogenic Shock. Chest [Internet]. 2004 Jun [cited 2019 Aug 22];125(6):2232–7. Available from: http://www.ncbi.nlm.nih.gov/pubmed/15189946

207. Charniot JC, Sutton A, Bonnefont-Rousselot D, Cosson C, Khani-Bittar R, Giral P, et al. Manganese superoxide dismutase dimorphism relationship with severity and prognosis in cardiogenic shock due to dilated cardiomyopathy. Free Radic Res [Internet]. 2011 Apr 10 [cited 2019 Aug 22];45(4):379–88. Available from: http://www.ncbi.nlm.nih.gov/pubmed/21062213

208. Bartel DP. MicroRNAs: genomics, biogenesis, mechanism, and function. Cell [Internet]. 2004 Jan 23 [cited 2019 Aug 21];116(2):281–97. Available from: http://www.ncbi.nlm.nih.gov/pubmed/14744438

209. Goldbergova MP, ipkova J, Fedorko J, Sevcikova J, Parenica J, Spinar J, et al. MicroRNAs in pathophysiology of acute myocardial infarction and cardiogenic shock. Bratislava Med J [Internet]. 2018 [cited 2019 Aug 22];119(06):341–7. Available from: http://www.ncbi.nlm.nih.gov/pubmed/29947233

210. Romaine SPR, Tomaszewski M, Condorelli G, Samani NJ. MicroRNAs in cardiovascular disease: an introduction for clinicians. Heart [Internet]. 2015 Jun 15 [cited

2019 Aug 21];101(12):921–8. Available from: http://www.ncbi.nlm.nih.gov/pubmed/25814653

211. da Costa Martins PA, De Windt LJ. miR-21: a miRaculous Socratic paradox. Cardiovasc Res [Internet]. 2010 Aug 1 [cited 2019 Aug 21];87(3):397–400. Available from: https://academic.oup.com/cardiovascres/article-lookup/doi/10.1093/cvr/cvq196

212. Vegter EL, van der Meer P, de Windt LJ, Pinto YM, Voors AA. MicroRNAs in heart failure: from biomarker to target for therapy. Eur J Heart Fail [Internet]. 2016 May [cited 2019 Aug 21];18(5):457–68. Available from: http://www.ncbi.nlm.nih.gov/pubmed/26869172

213. Cheng Y, Zhang C. MicroRNA-21 in Cardiovascular Disease. J Cardiovasc Transl Res [Internet]. 2010 Jun 1 [cited 2019 Aug 21];3(3):251–5. Available from: http://link.springer.com/10.1007/s12265-010-9169-7

214. Kociol RD, Pang PS, Gheorghiade M, Fonarow GC, O'Connor CM, Felker GM. Troponin Elevation in Heart Failure. J Am Coll Cardiol [Internet]. 2010 Sep 28 [cited 2019 Aug 22];56(14):1071–8. Available from: http://www.ncbi.nlm.nih.gov/pubmed/20863950

215. Jolly SS, Shenkman H, Brieger D, Fox KA, Yan AT, Eagle KA, et al. Quantitative troponin and death, cardiogenic shock, cardiac arrest and new heart failure in patients with non-ST-segment elevation acute coronary syndromes (NSTE ACS): insights from the Global Registry of Acute Coronary Events. Heart [Internet]. 2011 Feb 1 [cited 2019 Aug 19];97(3):197–202. Available from: http://heart.bmj.com/cgi/doi/10.1136/hrt.2010.195511

216. Duchnowski P, Hryniewiecki T, Kuśmierczyk M, Szymański P. High-Sensitivity Troponin T Predicts Postoperative Cardiogenic Shock Requiring Mechanical

Circulatory Support in Patients with Valve Disease. SHOCK [Internet]. 2019 Apr 20 [cited 2019 Aug 22];1. Available from: http://www.ncbi.nlm.nih.gov/pubmed/31162290

217. Wright RS, Williams BA, Cramner H, Gallahue F, Willmore T, Lewis L, et al. Elevations of cardiac troponin I are associated with increased short-term mortality in noncardiac critically ill emergency department patients. Am J Cardiol [Internet]. 2002 Sep 15 [cited 2019 Aug 19];90(6):634–6. Available from: http://www.ncbi.nlm.nih.gov/pubmed/12231092

218. Zellweger MJ, Schaer BA, Cron TA, Pfisterer ME, Osswald S. Elevated troponin levels in absence of coronary artery disease after supraventricular tachycardia. Swiss Med Wkly [Internet]. 2003 Aug 9 [cited 2019 Aug 19];133(31–32):439–41. Available from: http://www.ncbi.nlm.nih.gov/pubmed/14562187

219. Caujolle M, Allyn J, Brulliard C, Valance D, Vandroux D, Martinet O, et al. Determinants and prognosis of high-sensitivity cardiac troponin T peak plasma concentration in patients hospitalized for non-cardiogenic shock. SAGE Open Med [Internet]. 2018 Jan 3 [cited 2019 Aug 19];6:205031211877171. Available from: http://www.ncbi.nlm.nih.gov/pubmed/29770219

220. Salah K, Stienen S, Pinto YM, Eurlings LW, Metra M, Bayes-Genis A, et al. Prognosis and NT-proBNP in heart failure patients with preserved versus reduced ejection fraction. Heart [Internet]. 2019 Apr 8 [cited 2019 Aug 19];105(15):heartjnl-2018-314173. Available from: http://www.ncbi.nlm.nih.gov/pubmed/30962192

221. Bal L, Thierry S, Brocas E, Van de Louw A, Pottecher J, Hours S, et al. B-type natriuretic peptide (BNP) and N-terminal-proBNP for heart failure diagnosis in shock or acute respiratory distress. Acta Anaesthesiol Scand [Internet]. 2006 Mar [cited 2019 Aug 19];50(3):340–7. Available from: http://www.ncbi.nlm.nih.gov/pubmed/16480468

222. Pruszczyk P. N-terminal pro-brain natriuretic peptide as an indicator of right ventricular dysfunction. J Card Fail [Internet]. 2005 Jun [cited 2019 Aug 19];11(5 Suppl):S65-9. Available from: http://www.ncbi.nlm.nih.gov/pubmed/15948104

223. Januzzi J, Morss A, Tung R, Pino R, Fifer M, Thompson BT, et al. Natriuretic peptide testing for the evaluation of critically ill patients with shock in the intensive care unit: a prospective cohort study. Crit Care [Internet]. 2006 Feb [cited 2019 Aug 22];10(1):R37. Available from: http://www.ncbi.nlm.nih.gov/pubmed/16507171

224. Shah NR, Bieniarz MC, Basra SS, Paisley RD, Loyalka P, Gregoric ID, et al. Serum Biomarkers in Severe Refractory Cardiogenic Shock. JACC Hear Fail [Internet]. 2013 Jun [cited 2019 Aug 22];1(3):200–6. Available from: http://www.ncbi.nlm.nih.gov/pubmed/24621870

225. Prondzinsky R, Lemm H, Swyter M, Wegener N, Unverzagt S, Carter JM, et al. Intra-aortic balloon counterpulsation in patients with acute myocardial infarction complicated by cardiogenic shock: The prospective, randomized IABP SHOCK Trial for attenuation of multiorgan dysfunction syndrome*. Crit Care Med [Internet]. 2010 Jan [cited 2019 Aug 22];38(1):152–60. Available from: http://www.ncbi.nlm.nih.gov/pubmed/19770739

226. Bayés-Genís A, Núñez J, Lupón J. Soluble ST2 for Prognosis and Monitoring in Heart Failure. J Am Coll Cardiol [Internet]. 2017 Nov 7 [cited 2019 Aug 19];70(19):2389–92. Available from: http://www.ncbi.nlm.nih.gov/pubmed/29096810

227. Parenica J, Malaska J, Jarkovsky J, Lipkova J, Dastych M, Helanova K, et al. Soluble ST2 levels in patients with cardiogenic and septic shock are not predictors of mortality. Exp Clin Cardiol [Internet]. 2012 [cited 2019 Aug 19];17(4):205–9. Available from: http://www.ncbi.nlm.nih.gov/pubmed/23592937

228. Tolppanen H, Rivas-Lasarte M, Lassus J, Sadoune M, Gayat E, Pulkki K, et al. Combined Measurement of Soluble ST2 and Amino-Terminal Pro-B-Type Natriuretic Peptide Provides Early Assessment of Severity in Cardiogenic Shock Complicating Acute Coronary Syndrome. Crit Care Med [Internet]. 2017 Jul [cited 2019 Aug 22];45(7):e666–73. Available from: http://www.ncbi.nlm.nih.gov/pubmed/28403119

229. Luyt C-E, Landivier A, Leprince P, Bernard M, Pavie A, Chastre J, et al. Usefulness of cardiac biomarkers to predict cardiac recovery in patients on extracorporeal membrane oxygenation support for refractory cardiogenic shock. J Crit Care [Internet]. 2012 Oct [cited 2019 Aug 22];27(5):524.e7-524.e14. Available from: http://www.ncbi.nlm.nih.gov/pubmed/22386227

230. Harjola V-P, Lassus J, Sionis A, Køber L, Tarvasmäki T, Spinar J, et al. Clinical picture and risk prediction of short-term mortality in cardiogenic shock. Eur J Heart Fail [Internet]. 2015 May [cited 2019 Aug 19];17(5):501–9. Available from: http://www.ncbi.nlm.nih.gov/pubmed/25820680

231. Prondzinsky R, Unverzagt S, Lemm H, Wegener N, Heinroth K, Buerke U, et al. Acute myocardial infarction and cardiogenic shock. Medizinische Klin - Intensivmed und Notfallmedizin [Internet]. 2012 Sep 20 [cited 2019 Aug 19];107(6):476–84. Available from: http://www.ncbi.nlm.nih.gov/pubmed/22810435

232. Link A, Pöss J, Rbah R, Barth C, Feth L, Selejan S, et al. Circulating angiopoietins and cardiovascular mortality in cardiogenic shock. Eur Heart J [Internet]. 2013 Jun 7 [cited 2019 Aug 19];34(22):1651–62. Available from: http://www.ncbi.nlm.nih.gov/pubmed/23349297

233. del Rosario Espinoza Mora M, Böhm M, Link A. The Th17/Treg imbalance in patients with cardiogenic shock. Clin Res Cardiol [Internet]. 2014 Apr 28 [cited 2019

Aug 19];103(4):301–13. Available from: http://www.ncbi.nlm.nih.gov/pubmed/24374759

234. Fuernau G, Pöss J, Denks D, Desch S, Heine GH, Eitel I, et al. Fibroblast growth factor 23 in acute myocardial infarction complicated by cardiogenic shock: a biomarker substudy of the Intraaortic Balloon Pump in Cardiogenic Shock II (IABP-SHOCK II) trial. Crit Care [Internet]. 2014 Dec 21 [cited 2019 Aug 19];18(6):713. Available from: http://www.ncbi.nlm.nih.gov/pubmed/25528363

235. Fuernau G, Poenisch C, Eitel I, de Waha S, Desch S, Schuler G, et al. Growth-differentiation factor 15 and osteoprotegerin in acute myocardial infarction complicated by cardiogenic shock: a biomarker substudy of the IABP-SHOCK II-trial. Eur J Heart Fail [Internet]. 2014 Aug [cited 2019 Aug 19];16(8):880–7. Available from: http://www.ncbi.nlm.nih.gov/pubmed/24903195

236. Sionis A, Suades R, Sans-Roselló J, Sánchez-Martínez M, Crespo J, Padró T, et al. Circulating microparticles are associated with clinical severity of persistent ST-segment elevation myocardial infarction complicated with cardiogenic shock. Int J Cardiol [Internet]. 2018 May 1 [cited 2019 Aug 19];258:249–56. Available from: http://www.ncbi.nlm.nih.gov/pubmed/29544939

237. Vincent C, Revillard JP. Beta-2-microglobulin and HLA-related glycoproteins in human urine and serum. Contrib Nephrol [Internet]. 1981 [cited 2019 Aug 23];26:66–88. Available from: http://www.ncbi.nlm.nih.gov/pubmed/6169488

238. Güssow D, Rein R, Ginjaar I, Hochstenbach F, Seemann G, Kottman A, et al. The human beta 2-microglobulin gene. Primary structure and definition of the transcriptional unit. J Immunol [Internet]. 1987 Nov 1 [cited 2019 Aug 23];139(9):3132–8. Available from: http://www.ncbi.nlm.nih.gov/pubmed/3312414

239. Pamer E, Cresswell P. MECHANISMS OF MHC CLASS I–RESTRICTED ANTIGEN PROCESSING. Annu Rev Immunol [Internet]. 1998 Apr [cited 2019 Aug 23];16(1):323–58. Available from: http://www.ncbi.nlm.nih.gov/pubmed/9597133

240. Radosevich M, Ono SJ. Novel Mechanisms of Class II Major Histocompatibility Complex Gene Regulation. Immunol Res [Internet]. 2003 [cited 2019 Aug 23];27(1):85–106. Available from: http://www.ncbi.nlm.nih.gov/pubmed/12637770

241. Dam J, Guan R, Natarajan K, Dimasi N, Chlewicki LK, Kranz DM, et al. Variable MHC class I engagement by Ly49 natural killer cell receptors demonstrated by the crystal structure of Ly49C bound to H-2Kb. Nat Immunol [Internet]. 2003 Dec 2 [cited 2019 Aug 23];4(12):1213–22. Available from: http://www.ncbi.nlm.nih.gov/pubmed/14595439

242. Christianson SW, Greiner DL, Hesselton RA, Leif JH, Wagar EJ, Schweitzer IB, et al. Enhanced human CD4+ T cell engraftment in beta2-microglobulin-deficient NOD-scid mice. J Immunol [Internet]. 1997 Apr 15 [cited 2019 Aug 23];158(8):3578–86. Available from: http://www.ncbi.nlm.nih.gov/pubmed/9103418

243. Ebert BL, Galili N, Tamayo P, Bosco J, Mak R, Pretz J, et al. An Erythroid Differentiation Signature Predicts Response to Lenalidomide in Myelodysplastic Syndrome. Appelbaum FR, editor. PLoS Med [Internet]. 2008 Feb 12 [cited 2019 Aug 23];5(2):e35. Available from: http://www.ncbi.nlm.nih.gov/pubmed/18271621

244. Uhlen M, Zhang C, Lee S, Sjöstedt E, Fagerberg L, Bidkhori G, et al. A pathology atlas of the human cancer transcriptome. Science (80-) [Internet]. 2017 Aug 18 [cited 2019 Aug 23];357(6352):eaan2507. Available from: http://www.ncbi.nlm.nih.gov/pubmed/28818916

245. Bethea M, Forman DT. Beta 2-microglobulin: its significance and clinical usefulness. Ann Clin Lab Sci [Internet]. [cited 2019 Aug 23];20(3):163–8. Available from: http://www.ncbi.nlm.nih.gov/pubmed/2188562

246. Dalby AR, Tolan DR, Littlechild JA. The structure of human liver fructose-1,6-bisphosphate aldolase. Acta Crystallogr D Biol Crystallogr [Internet]. 2001 Nov [cited 2019 Aug 23];57(Pt 11):1526–33. Available from: http://www.ncbi.nlm.nih.gov/pubmed/11679716

247. Oeffner F, Moch C, Neundorf A, Hofmann J, Koch M, Grzeschik KH. Novel interaction partners of Bardet-Biedl syndrome proteins. Cell Motil Cytoskeleton [Internet]. 2008 Feb [cited 2019 Aug 23];65(2):143–55. Available from: http://www.ncbi.nlm.nih.gov/pubmed/18000879

248. Kazmierczak SC, Azzazy HME, Preceded by (work): Lott JA (John A. Diagnostic enzymology [Internet]. 2014 [cited 2019 Aug 23]. 197 p. Available from: https://www.worldcat.org/title/diagnostic-enzymology/oclc/863383000

249. Tao Q, Yuan S, Yang F, Yang S, Yang Y, Yuan J, et al. Aldolase B inhibits metastasis through Ten–Eleven Translocation 1 and serves as a prognostic biomarker in hepatocellular carcinoma. Mol Cancer [Internet]. 2015 Dec 17 [cited 2019 Aug 23];14(1):170. Available from: http://www.ncbi.nlm.nih.gov/pubmed/26376879

250. Li Q, Li Y, Xu J, Wang S, Xu Y, Li X, et al. Aldolase B Overexpression is Associated with Poor Prognosis and Promotes Tumor Progression by Epithelial-Mesenchymal Transition in Colorectal Adenocarcinoma. Cell Physiol Biochem [Internet]. 2017 [cited 2019 Aug 23];42(1):397–406. Available from: http://www.ncbi.nlm.nih.gov/pubmed/28558381

251. Huang H, McIntosh AL, Landrock KK, Landrock D, Storey SM, Martin GG, et al. Human FABP1 T94A variant enhances cholesterol uptake. Biochim Biophys Acta - Mol Cell Biol Lipids [Internet]. 2015 Jul [cited 2019 Aug 23];1851(7):946–55. Available from: http://www.ncbi.nlm.nih.gov/pubmed/25732850

252. Pelsers MMAL, Glatz JFC. Detection of brain injury by fatty acid-binding proteins. Clin Chem Lab Med [Internet]. 2005 Jan 1 [cited 2019 Aug 23];43(8):802–9. Available from: http://www.ncbi.nlm.nih.gov/pubmed/16201888

253. Bass NM, Manning JA, Ockner RK. Turnover and short-term regulation of fatty acid binding protein in liver. J Biol Chem [Internet]. 1985 Aug 15 [cited 2019 Aug 23];260(17):9603–7. Available from: http://www.ncbi.nlm.nih.gov/pubmed/4040517

254. Khatir DS, Bendtsen MD, Birn H, Nørregaard R, Ivarsen P, Jespersen B, et al. Urine liver fatty acid binding protein and chronic kidney disease progression. Scand J Clin Lab Invest [Internet]. 2017 Oct 3 [cited 2019 Aug 23];77(7):549–54. Available from: http://www.ncbi.nlm.nih.gov/pubmed/28745927

255. Thuijls G, Wijck K van, Grootjans J, Derikx JPM, van Bijnen AA, Heineman E, et al. Early Diagnosis of Intestinal Ischemia Using Urinary and Plasma Fatty Acid Binding Proteins. Ann Surg [Internet]. 2011 Feb [cited 2019 Aug 23];253(2):303–8. Available from: http://insights.ovid.com/crossref?an=00000658-201102000-00015

256. Obata Y, Kamijo-Ikemori A, Ichikawa D, Sugaya T, Kimura K, Shibagaki Y, et al. Clinical usefulness of urinary liver-type fatty-acid-binding protein as a perioperative marker of acute kidney injury in patients undergoing endovascular or open-abdominal aortic aneurysm repair. J Anesth [Internet]. 2016 Feb 19 [cited 2019 Aug 23];30(1):89–99. Available from: http://www.ncbi.nlm.nih.gov/pubmed/26585768

257. Kamijo A, Sugaya T, Hikawa A, Kimura K. [Urinary fatty acid binding protein as a new clinical marker for the progression of chronic renal disease]. Rinsho Byori [Internet]. 2003 Mar [cited 2019 Aug 23];51(3):219–24. Available from: http://www.ncbi.nlm.nih.gov/pubmed/12707994

258. Shi J, Zhang Y, Gu W, Cui B, Xu M, Yan Q, et al. Serum Liver Fatty Acid Binding Protein Levels Correlate Positively with Obesity and Insulin Resistance in Chinese Young Adults. Xu H, editor. PLoS One [Internet]. 2012 Nov 7 [cited 2019 Aug 23];7(11):e48777. Available from: http://www.ncbi.nlm.nih.gov/pubmed/23144966

259. Karvellas CJ, Speiser JL, Tremblay M, Lee WM, Rose CF, US Acute Liver Failure Study Group. Elevated FABP1 serum levels are associated with poorer survival in acetaminophen-induced acute liver failure. Hepatology [Internet]. 2017 Mar [cited 2019 Aug 23];65(3):938–49. Available from: http://www.ncbi.nlm.nih.gov/pubmed/27859489

260. Karnaukhova E. Therapeutic Applications. J Hematol Thromb Dis [Internet]. 2013 [cited 2019 Aug 23];1(3):113. Available from: https://www.longdom.org/open-access/c1-esterase-inhibitor-biological-activities-and-therapeutic-applications-2329-8790.1000113.pdf

261. Aulak KS, Davis AE, Donaldson VH, Harrison RA. Chymotrypsin inhibitory activity of normal C1-inhibitor and a P1 Arg to His mutant: Evidence for the presence of overlapping reactive centers. Protein Sci [Internet]. 1993 May [cited 2019 Aug 23];2(5):727–32. Available from: http://www.ncbi.nlm.nih.gov/pubmed/8495195

262. Kalter ES, Daha MR, ten Cate JW, Verhoef J, Bouma BN. Activation and Inhibition of Hageman Factor-Dependent Pathways and the Complement System in Uncomplicated Bacteremia or Bacterial Shock. J Infect Dis [Internet]. 1985 Jun 1 [cited

2019 Aug 23];151(6):1019–27. Available from: http://www.ncbi.nlm.nih.gov/pubmed/2582065

263. Woo P, Lachmann PJ, Harrison RA, Amos N, Cooper C, Rosen FS. Simultaneous turnover of normal and dysfunctional C1 inhibitor as a probe of in vivo activation of C1 and contact activatable proteases. Clin Exp Immunol [Internet]. 1985 Jul [cited 2019 Aug 23];61(1):1–8. Available from: http://www.ncbi.nlm.nih.gov/pubmed/4042415

264. WINDFUHR J, ALSENZ J, LOOS M. The critical concentration of C1-esterase inhibitor (C1-INH) in human serum preventing auto-activation of the first component of complement (C1). Mol Immunol [Internet]. 2005 Apr [cited 2019 Aug 23];42(6):657–63. Available from: http://www.ncbi.nlm.nih.gov/pubmed/15781109

265. Katz Y, Strunk RC. Synthesis and regulation of C1 inhibitor in human skin fibroblasts. J Immunol [Internet]. 1989 Mar 15 [cited 2019 Aug 23];142(6):2041–5. Available from: http://www.ncbi.nlm.nih.gov/pubmed/2537870

266. Yeung Laiwah AC, Jones L, Hamilton AO, Whaley K. Complement-subcomponent-C1-inhibitor synthesis by human monocytes. Biochem J [Internet]. 1985 Feb 15 [cited 2019 Aug 23];226(1):199–205. Available from: http://www.ncbi.nlm.nih.gov/pubmed/3977865

267. Walker DG, Yasuhara O, Patston PA, McGeer EG, McGeer PL. Complement C1 inhibitor is produced by brain tissue and is cleaved in Alzheimer disease. Brain Res [Internet]. 1995 Mar 27 [cited 2019 Aug 23];675(1–2):75–82. Available from: http://www.ncbi.nlm.nih.gov/pubmed/7796155

268. Lotz M, Zuraw BL. Interferon-gamma is a major regulator of C1-inhibitor synthesis by human blood monocytes. J Immunol [Internet]. 1987 Nov 15 [cited 2019

Aug 23];139(10):3382–7. Available from: http://www.ncbi.nlm.nih.gov/pubmed/3119706

269. von Lueder TG, Krum H. New medical therapies for heart failure. Nat Rev Cardiol [Internet]. 2015 Dec 29 [cited 2019 Aug 22];12(12):730–40. Available from: http://www.nature.com/articles/nrcardio.2015.137

270. Packer M, McMurray JJV, Desai AS, Gong J, Lefkowitz MP, Rizkala AR, et al. Angiotensin Receptor Neprilysin Inhibition Compared With Enalapril on the Risk of Clinical Progression in Surviving Patients With Heart Failure. Circulation [Internet]. 2015 Jan 6 [cited 2019 Aug 22];131(1):54–61. Available from: https://www.ahajournals.org/doi/10.1161/CIRCULATIONAHA.114.013748

271. von Lueder TG, Wang BH, Kompa AR, Huang L, Webb R, Jordaan P, et al. Angiotensin Receptor Neprilysin Inhibitor LCZ696 Attenuates Cardiac Remodeling and Dysfunction After Myocardial Infarction by Reducing Cardiac Fibrosis and Hypertrophy. Circ Hear Fail [Internet]. 2015 Jan [cited 2019 Aug 22];8(1):71–8. Available from: http://www.ncbi.nlm.nih.gov/pubmed/25362207

272. Desai AS, McMurray JJV, Packer M, Swedberg K, Rouleau JL, Chen F, et al. Effect of the angiotensin-receptor-neprilysin inhibitor LCZ696 compared with enalapril on mode of death in heart failure patients. Eur Heart J [Internet]. 2015 Aug 7 [cited 2019 Aug 22];36(30):1990–7. Available from: http://www.ncbi.nlm.nih.gov/pubmed/26022006

273. Piek A, de Boer RA, Silljé HHW. The fibrosis-cell death axis in heart failure. Heart Fail Rev [Internet]. 2016 Mar 16 [cited 2019 Aug 22];21(2):199–211. Available from: http://www.ncbi.nlm.nih.gov/pubmed/26883434

274. Suematsu Y, Miura S, Goto M, Matsuo Y, Arimura T, Kuwano T, et al. LCZ696, an angiotensin receptor-neprilysin inhibitor, improves cardiac function with the attenuation of fibrosis in heart failure with reduced ejection fraction in streptozotocin-induced diabetic mice. Eur J Heart Fail [Internet]. 2016 Apr [cited 2019 Aug 22];18(4):386–93. Available from: http://www.ncbi.nlm.nih.gov/pubmed/26749570

275. Kilić A, Huang CX, Rajapurohitam V, Madwed JB, Karmazyn M. Early and Transient Sodium-Hydrogen Exchanger Isoform 1 Inhibition Attenuates Subsequent Cardiac Hypertrophy and Heart Failure Following Coronary Artery Ligation. J Pharmacol Exp Ther [Internet]. 2014 Dec [cited 2019 Aug 22];351(3):492–9. Available from: http://jpet.aspetjournals.org/lookup/doi/10.1124/jpet.114.217091

276. AKER S, Snabaitis AK, Konietzka I, Van De Sand A, Böngler K, Avkiran M, et al. Inhibition of the Na+/H+ exchanger attenuates the deterioration of ventricular function during pacing-induced heart failure in rabbits. Cardiovasc Res [Internet]. 2004 Aug 1 [cited 2019 Aug 22];63(2):273–82. Available from: http://www.ncbi.nlm.nih.gov/pubmed/15249185

277. BAARTSCHEER A, SCHUMACHER C, VANBORREN M, BELTERMAN C, CORONEL R, OPTHOF T, et al. Chronic inhibition of Na/H-exchanger attenuates cardiac hypertrophy and prevents cellular remodeling in heart failure. Cardiovasc Res [Internet]. 2005 Jan 1 [cited 2019 Aug 22];65(1):83–92. Available from: http://www.ncbi.nlm.nih.gov/pubmed/15621036

278. Engelhardt S, Hein L, Keller U, Klämbt K, Lohse MJ. Inhibition of Na(+)-H(+) exchange prevents hypertrophy, fibrosis, and heart failure in beta(1)-adrenergic receptor transgenic mice. Circ Res [Internet]. 2002 Apr 19 [cited 2019 Aug 22];90(7):814–9. Available from: http://www.ncbi.nlm.nih.gov/pubmed/11964375

279. Kusumoto K, Haist J V., Karmazyn M. Na $^{+}$ /H $^{+}$ exchange inhibition reduces hypertrophy and heart failure after myocardial infarction in rats. Am J Physiol Circ Physiol [Internet]. 2001 Feb [cited 2019 Aug 22];280(2):H738–45. Available from: http://www.ncbi.nlm.nih.gov/pubmed/11158973

280. Uthman L, Baartscheer A, Bleijlevens B, Schumacher CA, Fiolet JWT, Koeman A, et al. Class effects of SGLT2 inhibitors in mouse cardiomyocytes and hearts: inhibition of Na+/H+ exchanger, lowering of cytosolic Na+ and vasodilation. Diabetologia [Internet]. 2018 Mar 2 [cited 2019 Aug 22];61(3):722–6. Available from: http://www.ncbi.nlm.nih.gov/pubmed/29197997

281. Baartscheer A, Schumacher CA, Wüst RCI, Fiolet JWT, Stienen GJM, Coronel R, et al. Empagliflozin decreases myocardial cytoplasmic Na+ through inhibition of the cardiac Na+/H+ exchanger in rats and rabbits. Diabetologia [Internet]. 2017 Mar 17 [cited 2019 Aug 22];60(3):568–73. Available from: http://www.ncbi.nlm.nih.gov/pubmed/27752710

282. Piacentino V, Milano CA, Bolanos M, Schroder J, Messina E, Cockrell AS, et al. X-linked inhibitor of apoptosis protein-mediated attenuation of apoptosis, using a novel cardiac-enhanced adeno-associated viral vector. Hum Gene Ther [Internet]. 2012 Jun [cited 2019 Aug 22];23(6):635–46. Available from: http://www.ncbi.nlm.nih.gov/pubmed/22339372

283. Haider N, Arbustini E, Gupta S, Liu H, Narula N, Hajjar R, et al. Concurrent upregulation of endogenous proapoptotic and antiapoptotic factors in failing human hearts. Nat Rev Cardiol [Internet]. 2009 Mar [cited 2019 Aug 22];6(3):250–61. Available from: http://www.ncbi.nlm.nih.gov/pubmed/19234503

284. Lee PJH, Rudenko D, Kuliszewski MA, Liao C, Kabir MG, Connelly KA, et al. Survivin gene therapy attenuates left ventricular systolic dysfunction in doxorubicin cardiomyopathy by reducing apoptosis and fibrosis. Cardiovasc Res [Internet]. 2014 Mar 1 [cited 2019 Aug 22];101(3):423–33. Available from: http://www.ncbi.nlm.nih.gov/pubmed/24403316

285. Levkau B, Schäfers M, Wohlschlaeger J, von Wnuck Lipinski K, Keul P, Hermann S, et al. Survivin Determines Cardiac Function by Controlling Total Cardiomyocyte Number. Circulation [Internet]. 2008 Mar 25 [cited 2019 Aug 22];117(12):1583–93. Available from: http://www.ncbi.nlm.nih.gov/pubmed/18332262

286. Topol EJ. High-performance medicine: the convergence of human and artificial intelligence. Nat Med [Internet]. 2019 Jan 7 [cited 2019 Aug 22];25(1):44–56. Available from: http://www.ncbi.nlm.nih.gov/pubmed/30617339

287. de Kleijn DP V, Chong SY, Wang X, Yatim SMJM, Fairhurst A-M, Vernooij F, et al. Toll-like receptor 7 deficiency promotes survival and reduces adverse left ventricular remodelling after myocardial infarction. Cardiovasc Res [Internet]. 2019 Mar 4 [cited 2019 Aug 22]; Available from: http://www.ncbi.nlm.nih.gov/pubmed/30830156

288. Frangogiannis NG. The inflammatory response in myocardial injury, repair, and remodelling. Nat Rev Cardiol [Internet]. 2014 May 25 [cited 2019 Aug 22];11(5):255–65. Available from: http://www.ncbi.nlm.nih.gov/pubmed/24663091

289. French BA, Kramer CM. Mechanisms of postinfarct left ventricular remodeling. Drug Discov Today Dis Mech [Internet]. 2007 Sep [cited 2019 Aug 22];4(3):185–96. Available from: http://www.ncbi.nlm.nih.gov/pubmed/18690295

290. Cavalera M, Frangogiannis NG. Targeting the chemokines in cardiac repair. Curr Pharm Des [Internet]. 2014 [cited 2019 Aug 22];20(12):1971–9. Available from: http://www.ncbi.nlm.nih.gov/pubmed/23844733

291. Madhusoodanan J. Matrix mimics shape cell studies. Nature [Internet]. 2019 Feb 26 [cited 2019 Aug 22];566(7745):563–5. Available from: http://www.ncbi.nlm.nih.gov/pubmed/30809069

292. Bayés-Genis A, Lanfear DE, de Ronde MWJ, Lupón J, Leenders JJ, Liu Z, et al. Prognostic value of circulating microRNAs on heart failure-related morbidity and mortality in two large diverse cohorts of general heart failure patients. Eur J Heart Fail [Internet]. 2018 Jan [cited 2019 Aug 21];20(1):67–75. Available from: http://www.ncbi.nlm.nih.gov/pubmed/28949058

293. Alles J, Fehlmann T, Fischer U, Backes C, Galata V, Minet M, et al. An estimate of the total number of true human miRNAs. Nucleic Acids Res [Internet]. 2019 Apr 23 [cited 2019 Aug 28];47(7):3353–64. Available from: https://academic.oup.com/nar/article/47/7/3353/5366472

294. Fattouch K, Bianco G, Speziale G, Sampognaro R, Lavalle C, Guccione F, et al. Beneficial effects of C1 esterase inhibitor in ST-elevation myocardial infarction in patients who underwent surgical reperfusion: a randomised double-blind study. Eur J Cardio-Thoracic Surg [Internet]. 2007 Aug [cited 2019 Aug 23];32(2):326–32. Available from: http://www.ncbi.nlm.nih.gov/pubmed/17576071

295. THIELMANN M, MARGGRAF G, NEUHAUSER M, FORKEL J, HEROLD U, KAMLER M, et al. Administration of C1-esterase inhibitor during emergency coronary artery bypass surgery in acute ST-elevation myocardial infarction☆. Eur J

Cardio-Thoracic Surg [Internet]. 2006 Aug [cited 2019 Aug 23];30(2):285–93. Available from: http://www.ncbi.nlm.nih.gov/pubmed/16829095

296. Lawler PR, Mehra MR. Advancing from a “hemodynamic model” to a “mechanistic disease-modifying model” of cardiogenic shock. J Hear Lung Transplant [Internet]. 2018 Nov [cited 2019 Aug 23];37(11):1285–8. Available from: http://www.ncbi.nlm.nih.gov/pubmed/30197209

297. Cheng JM, den Uil CA, Hoeks SE, van der Ent M, Jewbali LSD, van Domburg RT, et al. Percutaneous left ventricular assist devices vs. intra-aortic balloon pump counterpulsation for treatment of cardiogenic shock: a meta-analysis of controlled trials. Eur Heart J [Internet]. 2009 Sep 1 [cited 2019 Aug 23];30(17):2102–8. Available from: http://www.ncbi.nlm.nih.gov/pubmed/19617601

ANNEXES

Supplementary Figures

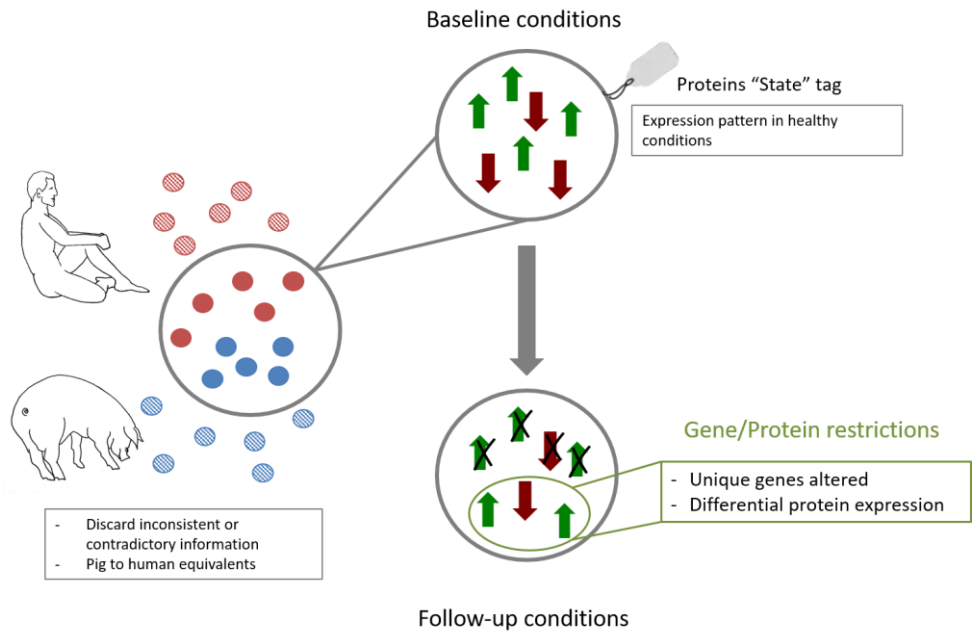

Supplementary Figure 1. Gene/Protein restriction selection. First, those proteins in the microarray data that fulfilled and passed the filters after translating the pig proteome were used to further analysis. Then, the proteins are tagged accordingly to their state, activated or inhibited, in healthy conditions. Using this information as baseline, we restrict the models to account only for those proteins that vary from these values on the follow-up. Red circles refer to human data obtained. Blue circles refer to pig data obtained. Grated circles depict

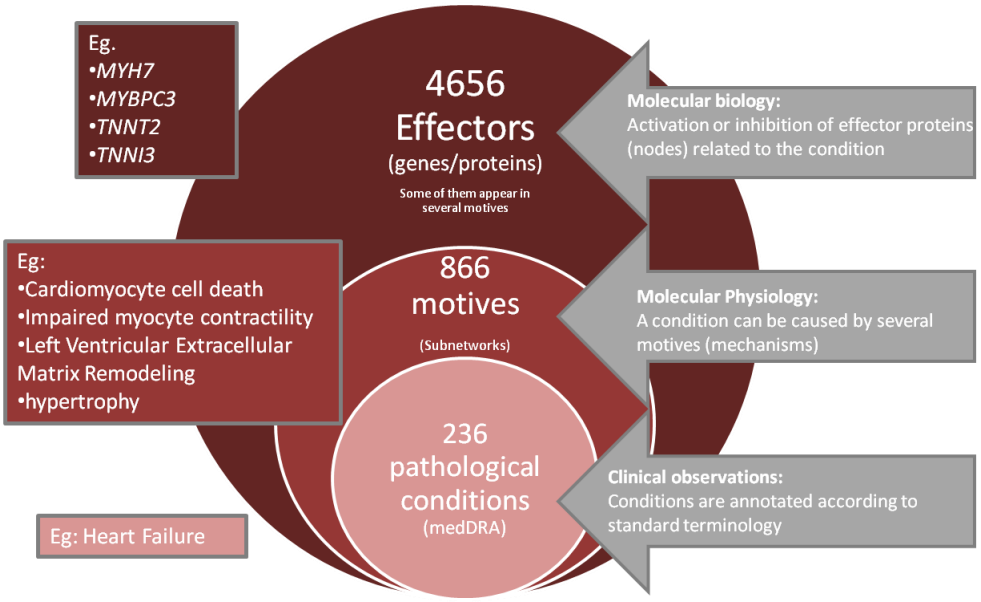

Supplementary Figure 2. Biological Effectors Database. (BED) representation. BED is a database property of Anaxomics Biotech SL. It includes several conditions (in our case we focused on MI and HF), the motives that cause them and the effector proteins/genes related to those conditions.

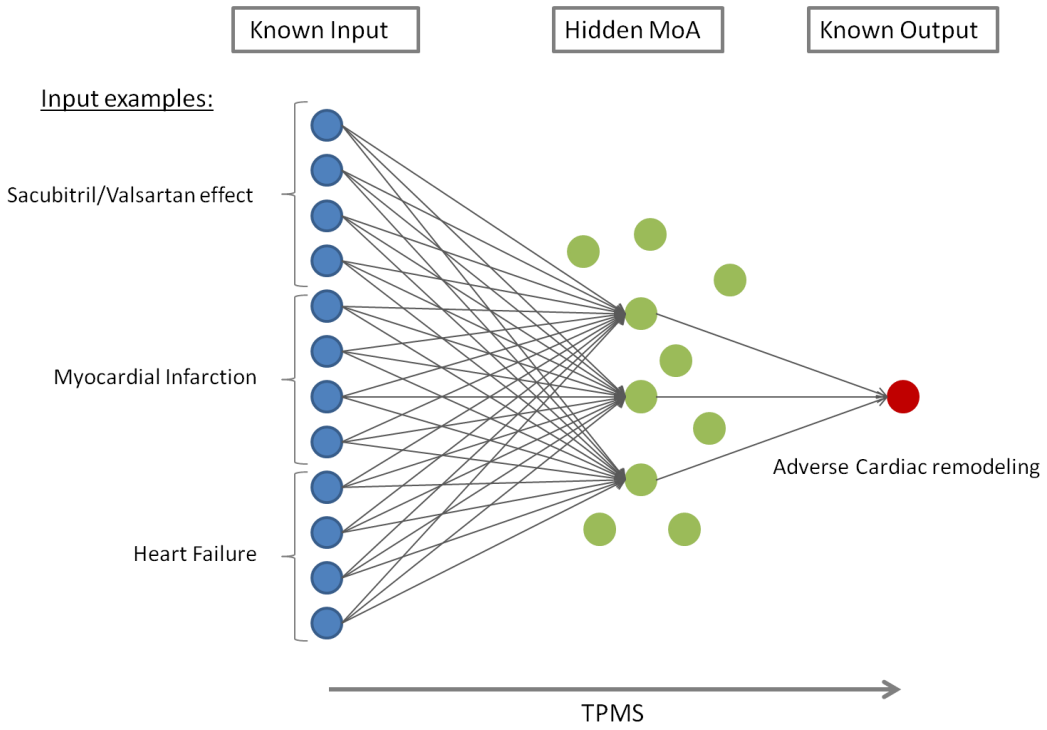

Supplementary Figure 3. Artificial neural network depiction. The learning methodology used consisted in a mixture of neural networks as a model, trained with a gradient descent algorithm to approximate the values of the given truth-table. Known input (Blue circles) refers to any element that affects gene/protein expression level or activity in the network. Every link has been previously described in the literature. TPMS technology collect these stimulus, relates them with the known output (in this case adverse cardiac remodeling; red circle) and traces back the pathway most likely to be responsible for the observed outcome (Green circles refers to our pool of proteins/genes).

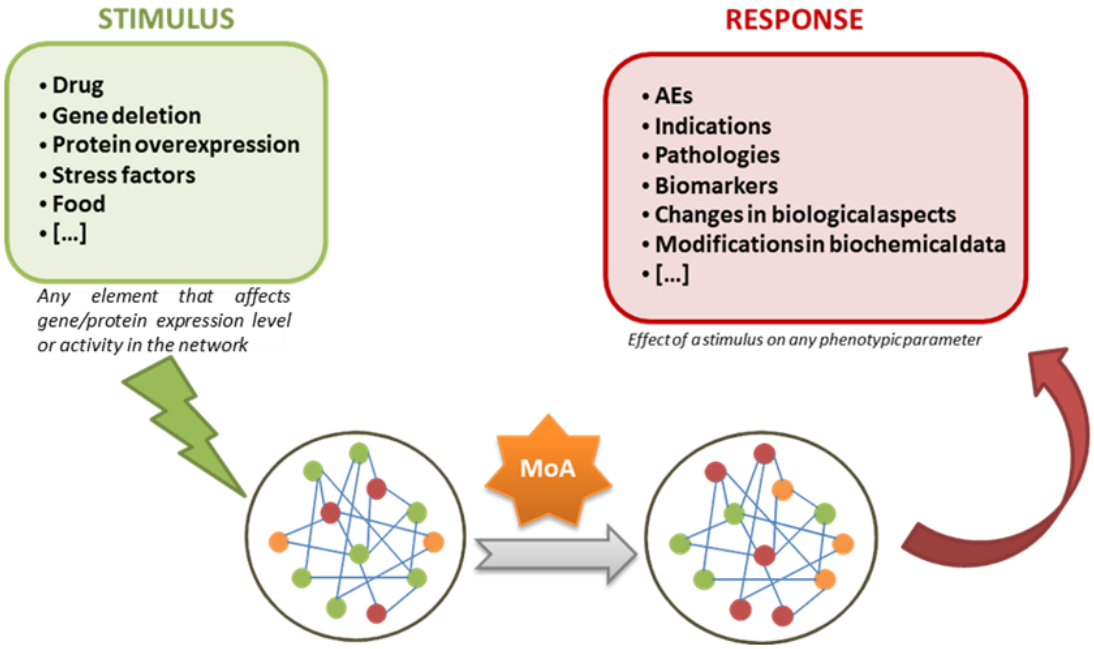

Supplementary Figure 4. TPMS technology illustration. TPMS Technology takes into account all known stimulus (inputs) that may affect our group of proteins (136 proteins in this case) under the pathology of study. Then, allows us to trace back the molecular pathway most likely to cause the known response (output) (in this case adverse cardiac remodeling). Colored nodes on the left circle represent different proteins on basal condition that are affected by different stimulus. Colored nodes on the right circle represent the same proteins responding to the stimulus; hence the change of color on some examples. MoA= Mechanism of Action; AEs= drugs Adverse Effects.

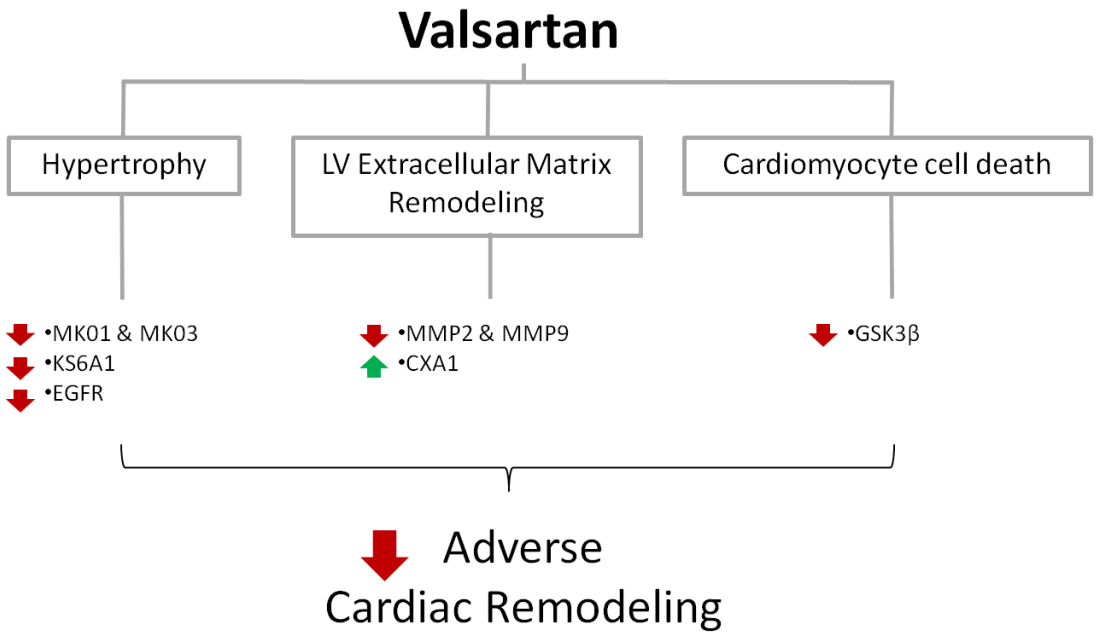

Supplementary Figure 5. Valsartan's effect on cardiac remodeling. Highlights extracted from the MoA (Figure 20) that explain which proteins affected by Valsartan are ultimately involved in reducing adverse cardiac remodeling via specific motives (e.g. Hypertrophy), according to the mathematical models.

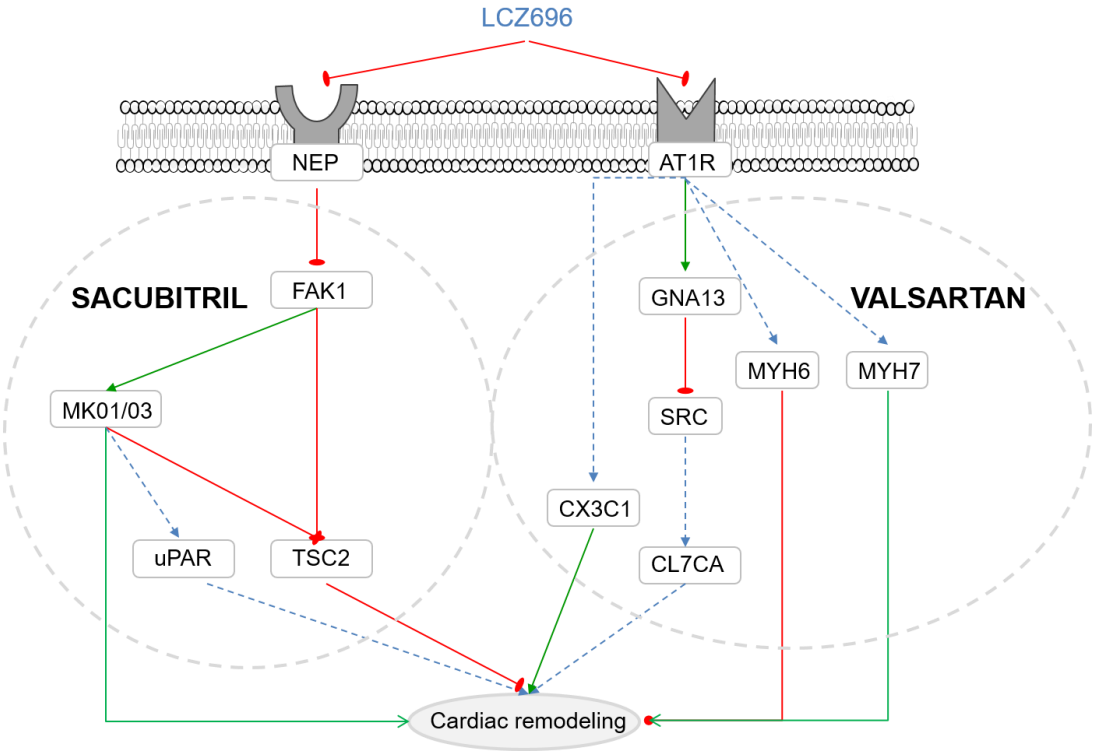

Supplementary Figure 6. ***Representation of the mechanistic roles of an alternative synergistic pathway.*** *The model indicates a second potential synergistic pathway for Sacubitril/Valsartan's effects on cardiac remodeling. Red lines indicate inhibition, green lines indicate activation, and dashed blue lines indicate an indirect relationship. Grey dotted-line circles encompass the proteins affected either by Sacubitril or Valsartan.*

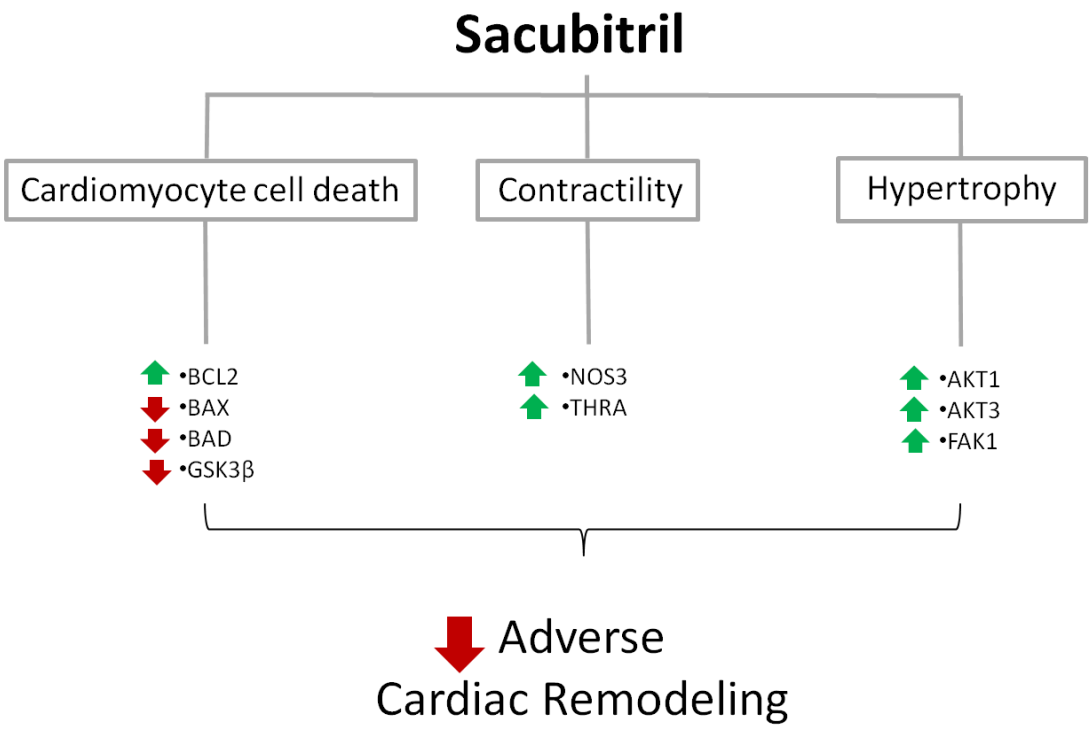

Supplementary Figure 7. ***Sacubitril's effects on cardiac remodeling.*** *Highlights extracted from the MoA (Figure 20) that explain which proteins affected by Sacubitril are ultimately involved in reducing adverse cardiac remodeling via specific motives (e.g. Hypertrophy), according to the mathematical models.*

Supplementary Tables

Localization	*C6*	*C30*	*C45*	*R6*	*R30*	*R45*
Initial entries	6047	6030	5251	127	125	21
Non- contradictory entries	5656	5697	4979	127	125	21
Single entries (no gene duplicates)	4747	4740	4212	121	116	20
Entries with a human UniProt correspondence	4737	4730	4203	121	116	20

Supplementary Table 1.Initial protein filtering process to generate the truth table. After discarding contradictory and duplicated entries, and translating to human proteome, the number of proteins shown in row entries with a human uniprot correspondence for each cohort has been used as restrictions for the model.

Protein information		*Identification method*	*Identified as classifier*						*Differential in experimental data*				
UniProt	Protein name		C6	C30	C45	R6	R30	R45	C30	C45	R6	R30	R45
P27487	DPP4	Models, Models/HT	1	1	1	-	1	1	-3,016	-2,022	-	-	-
Q6R327	RICTR	Models	1	1	1	-	-	1	-	-	-	-	-
Q15759	MK11	Models	1	1	1	-	-	-	-	-	-	-	-
P53778	MK12	Models, Models/HT, HT/Models	1	-	1	1	1	-	-2,185	-1,191	-	-	-
Q9Y243	AKT3	Models, Models/HT	1	-	1	-	-	-	1,417	0,959	-	-	-
P19838	NFKB1	Models/HT	1	-	1	-	-	-	-	-	-	-	-
P28482	MK01	Models/HT	1	-	1	-	-	-	-	-0,782	-	-	-
P45984	MK09	Models/HT	1	-	1	-	-	-	1,359	-	-	-	-
Q06187	BTK	Models, Models/HT	1	-	-	1	-	-	-	-	-	-	-
P01100	FOS	Models/HT	1	-	-	-	1	-	3,655	-	-	-	-
O14641	DVL2	Models, Models/HT, HT/Models	1	-	-	-	1	-	-	-	-	-	-
O75626	PRDM1	Models/HT	1	-	-	-	-	1	-	-	-	-	-
P19438	TNR1A	Models	1	-	-	-	-	-	0,86	0,674	-	-	-
Q15628	TRADD	Models	1	-	-	-	-	-	-	-	-	-	-
P19105	ML12A	Models	1	-	-	-	-	-	-	-	-	-	-
Q16539	MK14	Models	1	-	-	-	-	-	-	-	-	-	-
P61981	1433G	Models/HT	1	-	-	-	-	-	-	-	-	-	-
P02775	CXCL7	Models/HT	1	-	-	-	-	-	-	-	-	-	-
Q9UNS2	CSN3	HT	1	-	-	-	-	-	-0,506	-	-	-	-
Q9BRJ6	CG050	HT	1	-	-	-	-	-	-	-	-	-	-
P07585	PGS2	Models	-	1	1	1	-	1	2,005	1,786	-	-	-
O75676	KS6A4	Models	-	1	1	1	-	-	-	-	-	-	-
Q04724	TLE1	Models, Models/HT, HT/Models	-	1	1	-	1	-	1,968	1,691	-	-	-
P62942	FKB1A	Models, Models/HT, HT/Models	-	1	1	-	-	1	-	-	-	-	-
Q6ZSZ5	ARHGI	Models	-	1	1	-	-	1	0,568	0,454	-	-	-
O75330	HMMR	Models, Models/HT	-	1	1	-	-	1	-	-	-	-	-
Q16082	HSPB2	Models, Models/HT	-	1	-	1	1	-	-	-	-	-	-
P13797	PLST	HT	-	1	-	1	-	-	1,256	0,803	-	-	-

ANNEXES

Protein information		*Identification method*	*Identified as classifier*						*Differential in experimental data*				
UniProt	Protein name		C6	C30	C45	R6	R30	R45	C30	C45	R6	R30	R45
O43541	SMAD6	Models, Models/HT	-	1	-	-	1	-	0,86	-	-	-	-
Q9NWZ3	IRAK4	Models	-	1	-	-	-	-	-	-	-	-	-
Q12778	FOXO1	Models	-	1	-	-	-	-	1,117	1,33	-	-	-
P98177	FOXO4	Models	-	1	-	-	-	-	-	-	-	-	-
P63096	GNAI1	Models	-	1	-	-	-	-	-0,683	-1,281	-	-	-
O00206	TLR4	Models	-	1	-	-	-	-	-	-	-	-	-
Q15796	SMAD2	Models	-	1	-	-	-	-	1,321	1,015	-	-	-
O60341	KDM1A	Models	-	1	-	-	-	-	-0,55	-0,505	-	-	-
Q96S42	NODAL	Models	-	1	-	-	-	-	-	-	-	-	-
Q92843	B2CL2	Models	-	1	-	-	-	-	-	-	-	-	-
Q14790	CASP8	Models/HT	-	1	-	-	-	-	-	-	-	-	-
P30559	OXYR	Models/HT	-	1	-	-	-	-	-	-	-	-	-
P06400	RB	Models/HT	-	1	-	-	-	-	-0,809	-0,521	-	-	-
P54646	AAPK2	Models/HT	-	1	-	-	-	-	-2,548	-1,092	-	-	-
Q9Y592	CEP83	HT	-	1	-	-	-	-	2,442	1,74	-	-	-
Q9UKL0	RCOR1	Models	-	-	1	1	1	-	-	-	-	-	-
Q16644	MAPK3	Models, Models/HT, HT/Models	-	-	1	1	-	1	-0,906	-0,544	-	-	-
P19525	E2AK2	Models, Models/HT	-	-	1	1	-	-	2,145	1,426	-	-	-
O15287	FANCG	Models	-	-	1	-	1	1	-	-	-	-	-
P07203	GPX1	Models, Models/HT	-	-	1	-	1	-	-	-	-	-	-
P48643	TCPE	Models, Models/HT	-	-	1	-	1	-	-	-	-	-	-
O60906	NSMA	Models/HT	-	-	1	-	1	-	-	-	-	-	-
P03952	KLKB1	Models/HT	-	-	1	-	1	-	-	-	-	-	-
P29034	S10A2	Models	-	-	1	-	-	1	-	-	-	-	-
P46013	KI67	Models	-	-	1	-	-	1	-	-	-	-	-
P21980	TGM2	Models, Models/HT	-	-	1	-	-	1	-	-	-	-	-
Q92990	GLMN	Models/HT	-	-	1	-	-	1	-	-	-	-	-
Q92974	ARHG2	Models/HT	-	-	1	-	-	1	-	-	-	-	-
Q99466	NOTC4	HT	-	-	1	-	-	1	-	-	-	-	-

Protein information		*Identification method*	*Identified as classifier*						*Differential in experimental data*				
UniProt	Protein name		C6	C30	C45	R6	R30	R45	C30	C45	R6	R30	R45
Q8N1Q8	THEM5	HT	-	-	1	-	-	1	-	-	-	-	-
Q86Y07	VRK2	Models	-	-	1	-	-	-	-	-	-	-	-
P15923	TFE2	Models	-	-	1	-	-	-	-	-	-	-	-
O15264	MK13	Models	-	-	1	-	-	-	-	-	-	-	-
Q9BPZ7	SIN1	Models	-	-	1	-	-	-	-	-0,734	-	-	-
Q16099	GRIK4	Models	-	-	1	-	-	-	-	-	-	-	-
P18074	ERCC2	Models	-	-	1	-	-	-	-	-	-	-	-
P00749	UROK	Models/HT	-	-	1	-	-	-	1,384	0,871	-	-	-
Q04206	TF65	Models/HT	-	-	1	-	-	-	0,396	-	-	-	-
P31645	SC6A4	Models/HT	-	-	1	-	-	-	-	-	-	-	-
Q15797	SMAD1	Models/HT	-	-	1	-	-	-	0,657	0,552	-	-	-
P13501	CCL5	Models/HT	-	-	1	-	-	-	-	-	-	-	-
O00253	AGRP	Models/HT	-	-	1	-	-	-	-	-	-	-	-
Q9Y2C9	TLR6	Models/HT	-	-	1	-	-	-	-	-	-	-	-
P35052	GPC1	Models	-	-	-	1	1	-	-	-	-	-	-
P10966	CD8B	Models, Models/HT	-	-	-	1	-	1	-	-	-	-	-
P78347	GTF2I	Models	-	-	-	1	-	-	-0,379	-	-	-	-
P01906	DQA2	Models	-	-	-	1	-	-	-	-	-	-	-
O60239	3BP5	Models	-	-	-	1	-	-	0,702	0,852	-	-	-
O95970	LGI1	Models	-	-	-	1	-	-	-	-	-	-	-
Q13002	GRIK2	Models	-	-	-	1	-	-	-	0,664	-	-	-
P15407	FOSL1	Models	-	-	-	1	-	-	-	-	-	-	-
P17275	JUNB	Models	-	-	-	1	-	-	-	-	-	-	-
P15735	PHKG2	Models/HT	-	-	-	1	-	-	-	-	-	-	-
P01024	CO3	Models/HT	-	-	-	1	-	-	-	-	-	-	-
O00254	PAR3	Models/HT	-	-	-	1	-	-	2,55	2,161	-	-	-
P19419	ELK1	Models/HT	-	-	-	1	-	-	-	-	-	-	-
P63279	UBC9	Models/HT	-	-	-	1	-	-	0,512	-	-	-	-
Q92556	ELMO1	HT	-	-	-	1	-	-	0,936	0,669	-	-	-

Protein information		*Identification method*	*Identified as classifier*						*Differential in experimental data*				
UniProt	Protein name		C6	C30	C45	R6	R30	R45	C30	C45	R6	R30	R45
P46940	IQGA1	Models	-	-	-	-	1	-	-	-	-	-	-
Q9BVC4	LST8	Models	-	-	-	-	1	-	-	-	-	-	-
Q9NY61	AATF	Models	-	-	-	-	1	-	-	-	-	-	-
P20339	RAB5A	Models	-	-	-	-	1	-	-	-	-	-	-
P16581	LYAM2	Models/HT	-	-	-	-	1	-	-	-	-	-	-
Q86XR7	TCAM2	Models/HT	-	-	-	-	1	-	-	-	-	-	-
P11498	PYC	Models/HT	-	-	-	-	1	-	-	-	-	-	-
Q96KB5	TOPK	Models/HT	-	-	-	-	1	-	1,238	2,053	-	-	-
Q9H1U4	MEGF9	HT	-	-	-	-	1	-	1,248	1,56	-	-	-
Q00535	CDK5	HT	-	-	-	-	1	-	-0,587	-0,417	-	-	-
Q96ST8	CEP89	Models	-	-	-	-	-	1	-	-	-	-	-
Q96NL6	SCLT1	Models	-	-	-	-	-	1	-	-	-	-	-
Q9UKV3	ACINU	Models	-	-	-	-	-	1	-	-	-	-	-
Q12913	PTPRJ	Models	-	-	-	-	-	1	2,165	1,042	-	-	-
P28222	5HT1B	Models/HT	-	-	-	-	-	1	-	-	-	-	-
P48443	RXRG	Models/HT	-	-	-	-	-	1	-2,88	-2,191	-	-	-

Supplementary Table 2. List of potential biomarkers to describe MI progression. This table depicts the time point each protein has been detected and the log Ratio of each measurement in the microarray. Models refer to the combinations of proteins that had better classify the solutions of the models to their corresponding cohort. HT refers to the combinations of proteins that had better classify the microarray experiments to their corresponding cohort without using the information from the disease models. Models/HT refers to the combinations of proteins that had better classify the solutions of the models to their corresponding cohort, but filtering them by the proteins acting in accordance to the highthroughput (HT) data. HT/Models refers to the combinations of proteins that had better classify the microarray experiments to their corresponding cohort, filtering them by the proteins relevant in the models. 1: detected; -: Not detected.

MOTIVE ID	*Uniprot*	*Displayed Name*	*Protein name*
1	O00165	HAX-1	HCLS1-associated protein X-1
1	P30405	CyP-D	Peptidyl-prolyl cis-trans isomerase F, mitochondrial; Cyclophilin D
1	P21796	VDAC1	Voltage-dependent anion-selective channel protein 1
1	P45880	VDAC2	Voltage-dependent anion-selective channel protein 2
1	Q9Y277	VDAC3	Voltage-dependent anion-selective channel protein 3
1	P12235	ANT1	ADP/ATP translocase 1
1	P05141	ANT2	ADP/ATP translocase 2
1	P12236	ANT3	ADP/ATP translocase 3
1	Q9H0C2	ANT4	ADP/ATP translocase 4
1	P49841	GSK3B	Glycogen synthase kinase-3 beta
1	P25445	FAS	Tumor necrosis factor receptor superfamily member 6
1	P48023	FASLG	Tumor necrosis factor ligand superfamily member 6
1	P01375	TNFA	Tumor necrosis factor
1	P50591	TRAIL	Tumor necrosis factor ligand superfamily member 10
1	Q13158	FADD	FAS-associated death domain protein
1	Q15628	TRADD	Tumor necrosis factor receptor type 1-associated DEATH domain protein

1	Q14790	CASP8	Caspase-8
1	P42574	CASP3	Caspase-3
1	P10415	BCL2	Apoptosis regulator Bcl-2
1	Q07812	Bax	Apoptosis regulator BAX
1	Q99683	MAP3K5 / ASK-1	Mitogen-activated protein kinase kinase kinase 5
1	P31152	MAPK4	Mitogen-activated protein kinase 4
1	Q16659	MAPK6	Mitogen-activated protein kinase 6
1	P55957	BID	BH3-interacting domain death agonist
1	P98170	XIAP	E3 ubiquitin-protein ligase XIAP
1	Q13490	C-IAP1	Baculoviral IAP repeat-containing protein 2
1	O15392	BIRC5	Baculoviral IAP repeat-containing protein 5 / survivin
1	Q9NR28	DIABLO / SMAC	Diablo homolog, mitochondrial
1	O43464	Omi/HtrA2	Serine protease HTRA2, mitochondrial
1	Q811U4	Mfn1	Mitofusin-1
1	Q07820	MCL1	Induced myeloid leukemia cell differentiation protein Mcl-1
1	Q92934	BAD	Bcl2-associated agonist of cell death
1	P04637	p53	Cellular tumor antigen p53
1	P19634	NHE1	Sodium/hydrogen exchanger 1
1	P29466	CASP1	Caspase-1
1	P13473	LAMP2	Lysosome-associated membrane glycoprotein 2
1	Q9H1Y0	ATG5	Autophagy protein 5

1	O75385	ULK1	Serine/threonine-protein kinase ULK1
1	P42345	mTORC1	Serine/threonine-protein kinase mTOR
1	P49815	TSC2	Tuberin
1	Q8N122	Raptor	Regulatory-associated protein of mTOR
1	Q14457	BECN1	Beclin-1
1	Q12983	BNIP3	BCL2/adenovirus E1B 19 kDa protein-interacting protein 3
1	O00429	Drp1	Dynamin-1-like protein
1	P12644	BMP4	Bone morphogenetic protein 4
1	O95140	Mfn2	Mitofusin-2
2	P63098	PPP3R1	Calcineurin subunit B type 1
2	Q96LZ3	PPP3R2	Calcineurin subunit B type 2
2	P17612	PKACA	cAMP-dependent protein kinase catalytic subunit alpha
2	P22694	PKACB	cAMP-dependent protein kinase catalytic subunit beta
2	P22612	PKACC	cAMP-dependent protein kinase catalytic subunit gamma
2	Q13237	cGK2	cGMP-dependent protein kinase 2
2	Q13976	cGK1	cGMP-dependent protein kinase 1
2	P78423	CX3CL1	Fractalkine
2	P33402	GCSA2	Guanylate cyclase soluble subunit alpha-2
2	Q02108	GCSA3	Guanylate cyclase soluble subunit alpha-3
2	Q02153	GCSB1	Guanylate cyclase soluble subunit beta-1

2	O75343	GCSB2	Guanylate cyclase soluble subunit beta-2
2	Q9UQL6	HDAC5	Histone deacetylase 5
2	Q9UKV0	HDAC9	Histone deacetylase 9
2	Q02078	MEF2A	Myocyte-specific enhancer factor 2A
2	Q02080	MEF2B	Myocyte-specific enhancer factor 2B
2	Q06413	MEF2C	Myocyte-specific enhancer factor 2C
2	Q14814	MEF2D	Myocyte-specific enhancer factor 2D
2	P13533	MYH7 / aMHC	Myosin-6 (alternative name: a–myosin heavy chain)
2	P12883	MYH6 / bMHC	Myosin-7 (alternative name: b-myosin heavy chain)
2	P29474	NOS3	Nitric oxide synthase, endothelial
2	O95644	NFATc1	Nuclear factor of activated T-cells 1
2	Q13469	NFATc2	Nuclear factor of activated T-cells 2
2	Q12968	NFATc3	Nuclear factor of activated T-cells 3
2	Q14934	NFATc4	Nuclear factor of activated T-cells 4
2	P26678	PPLA	phospholamban
2	O14983	SERCA1	Sarcoplasmic/endoplasmic reticulum calcium ATPase 1
2	P16615	SERCA2	Sarcoplasmic/endoplasmic reticulum calcium ATPase 2
2	Q93084	SERCA3	Sarcoplasmic/endoplasmic reticulum calcium ATPase 3
2	Q08209	PPP3CA	Serine/threonine-protein phosphatase 2B catalytic subunit alpha isoform

2	P16298	PPP3CB	Serine/threonine-protein phosphatase 2B catalytic subunit beta isoform
2	P48454	PPP3CC	Serine/threonine-protein phosphatase 2B catalytic subunit gamma isoform
2	P10827	THRA	Thyroid hormone receptor alpha
2	P10828	THRB	Thyroid hormone receptor beta
2	Q8WZ42	TTN	Titin
3	P01583	IL1A	Interleukin-1
3	P08254	MMP-3	Stromelysin-1
3	P14780	MMP-9	Matrix metalloproteinase-9
3	P03956	MMP-1	Interstitial collagenase
3	P16035	TIMP2	Metalloproteinase inhibitor 2
3	P01137	TGFB1	Transforming growth factor beta-1
3	A8TX70	COL6A5	Collagen alpha-5(VI) chain
3	P12109	COL6A1	Collagen alpha-1(VI) chain
3	P12110	COL6A2	Collagen alpha-2(VI) chain
3	P12111	COL6A3	Collagen alpha-3(VI) chain
3	P25391	LAMA1	Laminin subunit alpha-1
3	P24043	LAMA2	Laminin subunit alpha-2
3	Q16787	LAMA3	Laminin subunit alpha-3
3	Q16363	LAMA4	Laminin subunit alpha-4
3	O15230	LAMA5	Laminin subunit alpha-5
3	P07942	LAMB1	Laminin subunit beta-1

3	P55268	LAMB2	Laminin subunit beta-2
3	Q13751	LAMB3	Laminin subunit beta-3
3	A4D0S4	LAMB4	Laminin subunit beta-4
3	P11047	LAMC1	Laminin subunit gamma-1
3	Q13753	LAMC2	Laminin subunit gamma-2
3	Q9Y6N6	LAMC3	Laminin subunit gamma-3
3	P01019	AGT	Angiotensinogen
3	P35625	TIMP3	Metalloproteinase inhibitor 3
3	P16035	TIMP4	Metalloproteinase inhibitor 4
3	P02751	FN1	Fibronectin
3	P09486	SPARC / ON	Secreted protein acidic and rich in cysteine / Osteonectin
3	P00488	F13A1 F13	Transglutaminase A chain
3	P01033	TIMP1	Metalloproteinase inhibitor 1
3	P09237	MMP-7	Matrix metalloproteinase-7
3	P17302	GJA1	Gap junction alpha-1 protein / Connexin-43
3	P12821	ACE	Angiotensin-converting enzyme
3	P05305	EDN1	Endothelin-1
3	P24821	TN-C	Tenascin-C
3	P10451	OPN	Osteopontin
3	P08253	MMP-2	Matrix metalloproteinase-2
3	P50281	MMP-14	Matrix metalloproteinase-14

4	Q9UBK2	PPARGC1A // PGC1	Peroxisome proliferator-activated receptor gamma coactivator 1-alpha
4	P06396	GSN	Gelsolin
4	P49238	CX3CR1	CX3C chemokine receptor 1
4	P78423	CX3CL1	Fractalkine
4	P49116	NR2C2 TAK1	Nuclear receptor subfamily 2 group C member 2
4	P12644	BMP4	Bone morphogenetic protein 4
4	P63098	PPP3R1	Calcineurin subunit B type 1
4	Q96LZ3	PPP3R2	Calcineurin subunit B type 2
4	P00533	EGFR	epidermal growth factor receptor
4	P09038	FGF-2 / bFGF	Fibroblast growth factor 2 / Basic fibroblast growth factor
4	Q14571	IP3R2	Inositol 1,4,5-trisphosphate receptor type 2
4	P03956	MMP1	Matrix metalloproteinase-1
4	P08235	MR	Mineralocorticoid receptor
4	P28482	ERK2	Mitogen-activated protein kinase 1
4	P27361	ERK1	Mitogen-activated protein kinase 3
4	Q99836	MyD88	Myeloid differentiation primary response protein MyD88
4	P29474	NOS3	Nitric oxide synthase, endothelial
4	O95644	NFATc1	Nuclear factor of activated T-cells 1
4	Q13469	NFATc2	Nuclear factor of activated T-cells 2
4	Q12968	NFATc3	Nuclear factor of activated T-cells 3
4	Q14934	NFATc4	Nuclear factor of activated T-cells 4

4	P61296	HAND2	Heart- and neural crest derivatives-expressed protein 2
4	P05121	PAI	Plasminogen activator inhibitor 1
4	Q15418	S6KA1	Ribosomal protein S6 kinase alpha-1
4	Q15349	S6KA2	Ribosomal protein S6 kinase alpha-2
4	P51812	S6KA3	Ribosomal protein S6 kinase alpha-3
4	Q08209	PPP3CA	Serine/threonine-protein phosphatase 2B catalytic subunit alpha isoform
4	P16298	PPP3CB	Serine/threonine-protein phosphatase 2B catalytic subunit beta isoform
4	P48454	PPP3CC	Serine/threonine-protein phosphatase 2B catalytic subunit gamma isoform
4	Q9UBN4	TRPC4	Short transient receptor potential channel 4
4	P32418	NCX	Sodium/calcium exchanger 1
4	P19634	NHE1	sodium-hydrogen antiporter1
4	P30556	AT1	Type-1 angiotensin II receptor

Supplementary Table 3.List of proteins for cardiac remodeling used to focus our analyses on the pathological condition of interest. Motive ID refers to the remodeling condition that the protein is associated with; 1: Cardiomyocyte cell death; 2: Impaired myocyte contractility; 3: Left ventricle extracellular matrix remodeling (including necrosis and apoptosis); 4: Hypertrophy.

PMID: 26564789	*PMID: 24080184*	*PMID: 19797822*
PMID: 26562414	PMID: 24072174	PMID: 19679836
PMID: 26553996	PMID: 23909633	PMID: 19593942
PMID: 26356605	PMID: 23806284	PMID: 19246681
PMID: 25977452	PMID: 23704873	PMID: 19179805
PMID: 25752645	PMID: 23506867	PMID: 19144865
PMID: 25663976	PMID: 23429007	PMID: 18981739
PMID: 25595790	PMID: 23316962	PMID: 18585734
PMID: 25520329	PMID: 23316291	PMID: 18535174
PMID: 25047165	PMID: 23176689	PMID: 18276618
PMID: 24905188	PMID: 22803959	PMID: 17928585
PMID: 24859226	PMID: 22535253	PMID: 17657164
PMID: 24827991	PMID: 21799152	PMID: 17490677
PMID: 24736806	PMID: 21784127	PMID: 17379774
PMID: 24615014	PMID: 21671800	PMID: 16847152
PMID: 24530674	PMID: 20888832	PMID: 15526239
PMID: 24505034	PMID: 20564207	PMID: 15364610
PMID: 24415751	PMID: 20125030	PMID: 14998631
PMID: 24161931	PMID: 19919994	PMID: 14962485
PMID: 24126173	PMID: 19893013	PMID: 11120693

Supplementary Table 4. Manual curation of the literature. List of articles used for molecular characterization of the pathologies under study, and Sacubitril/Valsartan.

DATA SOURCES	*# ENTRIES*
Considered Interactions	312445
Considered Proteins	15555
Characterized Drugs	6605
Drug Targets	11265
Characterized Clinical Conditions	222
Clinical Conditions Key Proteins Characterized	3712

Supplementary Table 5. Data sources for generation and training of the mathematical models. List of the different types of information used to generate and train the mathematical models, as well as their quantity.

MAIN MODEL CONSTRUCTION RESTRICTIONS	*DIRECT RESTRICTIONS*	
CLINICAL CONDITION PREDICTIVE MODELS - ANNs		
Curated drug indication/ADRs database	2500830	
SAMPLING METHODS		
Curated drug indication/ADRs database	2500830	
Drug indication/ADRs protein correlations	3970	
SPECIFIC POPULATION RESTRICTIONS (High Throughput Differential Expression Restrictions)	Myocardial infarction	Heart failure
	4738	6074

Supplementary Table 6. Molecular restrictions used for generation and training of the mathematical models. Type and quantity of restrictions used to generate the mathematical models. ADR= Adverse Drug Reactions.

Uniprot	*Displayed Name*	*Protein name*	*Remodeling effector*
P31749	AKT1	RAC-alpha serine/threonine-protein kinase	Cardiomyocyte cell death, Impaired myocyte contractility
Q9Y243	AKT3	RAC-gamma serine/threonine-protein kinase	Cardiomyocyte cell death, Impaired myocyte contractility
Q05397	FAK1	Focal adhesion kinase 1	Cardiomyocyte cell death, Hypertrophy,
P49841	GSK3B	Glycogen synthase kinase-3 beta	Cardiomyocyte cell death
P27986	P85A	Phosphatidylinositol 3-kinase regulatory subunit alpha	Cardiomyocyte cell death, Impaired myocyte contractility
P42336	PK3CA	Phosphatidylinositol 4,5-bisphosphate 3-kinase catalytic subunit alpha isoform	Cardiomyocyte cell death, Impaired myocyte contractility
O00329	PK3CD	Phosphatidylinositol 4,5-bisphosphate 3-kinase catalytic subunit delta isoform	Cardiomyocyte cell death, Impaired myocyte contractility
P10827	THRA	Thyroid hormone receptor alpha	Impaired myocyte contractility
Q13490	BIRC2	Baculoviral IAP repeat-containing protein 2	Cardiomyocyte cell death
P09038	FGF2	Fibroblast growth factor 2	Hypertrophy
P02751	FINC	Fibronectin	Left ventricle extracellular matrix remodeling
P14780	MMP9	Matrix metalloproteinase-9	Left ventricle extracellular matrix remodeling
P42345	MTOR	Serine/threonine-protein kinase mTOR	Cardiomyocyte cell death
P01137	TGFB1	Transforming growth factor beta-1	Left ventricle extracellular matrix remodeling

Supplementary Table 7.Potential synergistic nodes involved in the downstream effects of sacubitril/valsartan. The first eight proteins of the list scored the best likelihood of occupying synergistic nodes, and so are included in the MoA representation (Fig 2). However, the models predicted 6 additional proteins that could potentially act synergistically, so are included in this table as the six last proteins on the list.

Uniprot	*Displayed Name*
P49238	CX3C1 (Fractalkine)
Q9BXN2	CLEC7A (Dectin-1)
P13533	MYH6
P12883	MYH7

Supplementary Table 8. Specific proteins identified as only associated with the model simulating the efficacy of LCZ696 on MI patients.

MOTIVE NAME	Uniprot	Displayed Name	Protein name
Retention of sodium (hypertension)	P37088	SCNNA	Amiloride-sensitive sodium channel subunit alpha
Retention of sodium (hypertension)	P51168	SCNNB	Amiloride-sensitive sodium channel subunit beta
Retention of sodium (hypertension)	P51172	SCNND	Amiloride-sensitive sodium channel subunit delta
Retention of sodium (hypertension)	P51170	SCNNG	Amiloride-sensitive sodium channel subunit gamma
Retention of sodium (hypertension)	P08235	MCR	Mineralocorticoid receptor
Retention of sodium (hypertension)	P28845	DHI1	Corticosteroid 11-beta-dehydrogenase isozyme 1
Retention of sodium (hypertension)	P80365	DHI2	Corticosteroid 11-beta-dehydrogenase isozyme 2
Retention of sodium (hypertension)	P00797	RENI	Renin
Retention of sodium (hypertension)	P12821	ACE	Angiotensin-converting enzyme
Retention of sodium (hypertension)	P19099	C11B2	Cytochrome P450 11B2, mitochondrial
Retention of sodium (hypertension)	P01160	ANF	Atrial natriuretic factor
Retention of sodium (hypertension)	P25101	EDNRA	Endothelin-1 receptor
Retention of sodium (hypertension)	P05305	EDN1	Endothelin-1
Retention of sodium (hypertension)	P24530	EDNRB	Endothelin B receptor
Retention of sodium (hypertension)	P54710	ATNG	Sodium/potassium-transporting ATPase subunit gamma
Retention of sodium (hypertension)	P05026	AT1B1	Sodium/potassium-transporting ATPase subunit beta-1
Retention of sodium (hypertension)	P50993	AT1A2	Sodium/potassium-transporting ATPase subunit alpha-2
Retention of sodium (hypertension)	P14415	AT1B2	Sodium/potassium-transporting ATPase subunit beta-2
Retention of sodium (hypertension)	P51800	CLCKA	Chloride channel protein ClC-Ka
Retention of sodium (hypertension)	P51801	CLCKB	Chloride channel protein ClC-Kb
Retention of sodium (hypertension)	P55017	S12A3	Solute carrier family 12 member 3
Retention of sodium (hypertension)	Q8WZ55	BSND	Barttin
Retention of sodium (hypertension)	Q9H4A3	WNK1	Serine/threonine-protein kinase WNK1
Retention of sodium (hypertension)	Q96J92	WNK4	Serine/threonine-protein kinase WNK4
Retention of sodium (hypertension)	Q13621	S12A1	Solute carrier family 12 member 1
Retention of sodium (hypertension)	P05019	IGF1	Insulin-like growth factor I
Retention of sodium (hypertension)	P46934	NEDD4	E3 ubiquitin-protein ligase NEDD4

Retention of sodium (hypertension)	O00141	SGK1	Serine/threonine-protein kinase Sgk1
Retention of sodium (hypertension)	Q9HBY8	SGK2	Serine/threonine-protein kinase Sgk2
Retention of sodium (hypertension)	Q96BR1	SGK3	Serine/threonine-protein kinase Sgk3
Retention of sodium (hypertension)	P21728	DRD1	D(1A) dopamine receptor
Retention of sodium (hypertension)	P21918	DRD5	D(1B) dopamine receptor
Retention of sodium (hypertension)	P35462	DRD3	D(3) dopamine receptor
Retention of sodium (hypertension)	P30518	V2R	Vasopressin V2 receptor
Retention of sodium (hypertension)	P47901	V1BR	Vasopressin V1b receptor
Retention of sodium (hypertension)	P37288	V1AR	Vasopressin V1a receptor
Retention of sodium (hypertension)	P16860	ANFB	Natriuretic peptides B
Retention of sodium (hypertension)	P48048	KCNJ1	ATP-sensitive inward rectifier potassium channel 1
Retention of sodium (hypertension)	P13569	CFTR	Cystic fibrosis transmembrane conductance regulator
Retention of sodium (hypertension)	P55011	S12A2	Solute carrier family 12 member 2
Retention of sodium (hypertension)	O14649	KCNK3	Potassium channel subfamily K member 3
Retention of sodium (hypertension)	Q9NPC2	KCNK9	Potassium channel subfamily K member 9
Retention of sodium (hypertension)	P19634	SL9A1	Sodium/hydrogen exchanger 1
Retention of sodium (hypertension)	P48764	SL9A3	Sodium/hydrogen exchanger 3
Decreased renal excretion of uric acid (hyperuricemia)	Q9NRM0	GTR9	Solute carrier family 2 (Glucose transporter type 9) (GLUT-9)
Decreased renal excretion of uric acid (hyperuricemia)	Q9UNQ0	ABCG2	ATP-binding cassette sub-family G member 2
Decreased renal excretion of uric acid (hyperuricemia)	P07911	UROM	Uromodulin (Tamm-Horsfall urinary glycoprotein) (THP)
Decreased renal excretion of uric acid (hyperuricemia)	Q96S37	S22AC	Solute carrier family 22 member 12
Decreased renal excretion of uric acid (hyperuricemia)	Q9NSA0	S22AB	Solute carrier family 22 member 11
Decreased renal excretion of uric acid (hyperuricemia)	Q13113	PDZ1I	PDZK1-interacting protein 1
Decreased renal excretion of uric acid (hyperuricemia)	O14745	NHRF1	Na(+)/H(+) exchange regulatory cofactor NHE-RF1
Decreased renal excretion of uric acid (hyperuricemia)	O00476	NPT4	Sodium-dependent phosphate transport protein 4 (Na(+)
Decreased renal excretion of uric acid (hyperuricemia)	Q8N695	SC5A8	Sodium-coupled monocarboxylate transporter 1
Decreased renal excretion of uric acid (hyperuricemia)	Q1EHB4	SC5AC	Sodium-coupled monocarboxylate transporter 2
Decreased renal excretion of uric acid (hyperuricemia)	Q8TCC7	S22A8	Solute carrier family 22 member 8 (Organic anion transporter 3)

Decreased renal excretion of uric acid (hyperuricemia)	Q4U2R8	S22A6	Solute carrier family 22 member 6
Decreased renal excretion of uric acid (hyperuricemia)	O15439	MRP4	Multidrug resistance-associated protein 4
Decreased renal excretion of uric acid (hyperuricemia)	Q8WWT9	S13A3	Solute carrier family 13 member 3
Decreased renal excretion of uric acid (hyperuricemia)	Q13183	S13A2	Solute carrier family 13 member 2
Hyperphagia and dysregulated appetite (obesity)	P01258	CALC	Calcitonin
Hyperphagia and dysregulated appetite (obesity)	P06881	CALCA	Calcitonin gene-related peptide 1
Hyperphagia and dysregulated appetite (obesity)	P10092	CALCB	Calcitonin gene-related peptide 2
Hyperphagia and dysregulated appetite (obesity)	Q16602	CALRL	Calcitonin gene-related peptide type 1 receptor
Hyperphagia and dysregulated appetite (obesity)	P30988	CALCR	Calcitonin receptor
Hyperphagia and dysregulated appetite (obesity)	P08949	NMB	Neuromedin-B
Hyperphagia and dysregulated appetite (obesity)	P28336	NMBR	Neuromedin-B receptor
Hyperphagia and dysregulated appetite (obesity)	P47871	GLR	Glucagon receptor
Hyperphagia and dysregulated appetite (obesity)	P01308	INS	Insulin
Hyperphagia and dysregulated appetite (obesity)	P06213	INSR	Insulin receptor
Hyperphagia and dysregulated appetite (obesity)	P04118	COL	Colipase
Hyperphagia and dysregulated appetite (obesity)	P30874	SSR2	Somatostatin receptor type 2
Hyperphagia and dysregulated appetite (obesity)	Q92847	GHSR	Growth hormone secretagogue receptor type 1
Hyperphagia and dysregulated appetite (obesity)	P10082	PYY	Peptide YY
Hyperphagia and dysregulated appetite (obesity)	Q9UBC7	GALP	Galanin-like peptide
Hyperphagia and dysregulated appetite (obesity)	O43603	GALR2	Galanin receptor type 2

Hyperphagia and dysregulated appetite (obesity)	P22466	GALA	Galanin peptides [
Hyperphagia and dysregulated appetite (obesity)	P47211	GALR1	Galanin receptor type 1
Hyperphagia and dysregulated appetite (obesity)	Q8NG41	NPB	Neuropeptide B
Hyperphagia and dysregulated appetite (obesity)	Q8N729	NPW	Neuropeptide W
Hyperphagia and dysregulated appetite (obesity)	P48145	NPBW1	Neuropeptides B/W receptor type 1
Hyperphagia and dysregulated appetite (obesity)	P28335	5HT2C	5-hydroxytryptamine receptor 2C
Hyperphagia and dysregulated appetite (obesity)	Q16568	CART	Cocaine- and amphetamine-regulated transcript protein
Hyperphagia and dysregulated appetite (obesity)	Q07869	PPARA	Peroxisome proliferator-activated receptor alpha
Hyperphagia and dysregulated appetite (obesity)	Q8NER1	TRPV1	Transient receptor potential cation channel subfamily V member 1
Hyperphagia and dysregulated appetite (obesity)	Q6IQ20	NAPEP	N-acyl-phosphatidylethanolamine-hydrolyzing phospholipase D
Hyperphagia and dysregulated appetite (obesity)	P16671	CD36	Platelet glycoprotein 4
Hyperphagia and dysregulated appetite (obesity)	O00253	AGRP	Agouti-related protein
Hyperphagia and dysregulated appetite (obesity)	Q01726	MSHR	Melanocyte-stimulating hormone receptor (Melanocortin receptor 1)
Hyperphagia and dysregulated appetite (obesity)	P28223	5HT2A	5-hydroxytryptamine receptor 2A (Serotonin receptor 2A)
Hyperphagia and dysregulated appetite (obesity)	P28221	5HT1D	5-hydroxytryptamine receptor 1D
Hyperphagia and dysregulated appetite (obesity)	Q13224	NMDE2	Glutamate receptor ionotropic
Hyperphagia and dysregulated appetite (obesity)	P21964	COMT	Catechol O-methyltransferase
Hyperphagia and dysregulated appetite (obesity)	P14416	DRD2	D(2) dopamine receptor

Hyperphagia and dysregulated appetite (obesity)	P25929	NPY1R	Neuropeptide Y receptor type 1
Hyperphagia and dysregulated appetite (obesity)	Q15761	NPY5R	Neuropeptide Y receptor type 5
Hyperphagia and dysregulated appetite (obesity)	P49146	NPY2R	Neuropeptide Y receptor type 2
Hyperphagia and dysregulated appetite (obesity)	P42785	PCP	Lysosomal Pro-X carboxypeptidase
Hyperphagia and dysregulated appetite (obesity)	Q13258	PD2R	Prostaglandin D2 receptor
Hyperphagia and dysregulated appetite (obesity)	P35408	PE2R4	Prostaglandin E2 receptor EP4 subtype
Hyperphagia and dysregulated appetite (obesity)	Q9HD89	RETN	Resistin
Hyperphagia and dysregulated appetite (obesity)	P20396	TRH	Pro-thyrotropin-releasing hormone
Hyperphagia and dysregulated appetite (obesity)	O75882	ATRN	Attractin (Mahogany homolog)
Hyperphagia and dysregulated appetite (obesity)	P43220	GLP1R	Glucagon-like peptide 1 receptor
Hyperphagia and dysregulated appetite (obesity)	P42127	ASIP	Agouti-signaling protein (ASP) (Agouti switch protein)
Hyperphagia and dysregulated appetite (obesity)	P41145	OPRK	Kappa-type opioid receptor
Hyperphagia and dysregulated appetite (obesity)	P41143	OPRD	Delta-type opioid receptor
Hyperphagia and dysregulated appetite (obesity)	P41146	OPRX	Nociceptin receptor
Hyperphagia and dysregulated appetite (obesity)	P01031	CO5	Complement C5
Hyperphagia and dysregulated appetite (obesity)	P06307	CCKN	Cholecystokinin
Hyperphagia and dysregulated appetite (obesity)	P32239	GASR	Gastrin/cholecystokinin type B receptor
Hyperphagia and dysregulated appetite (obesity)	P32238	CCKAR	Cholecystokinin receptor type A

Hyperphagia and dysregulated appetite (obesity)	P10997	IAPP	Islet amyloid polypeptide (Amylin)
Hyperphagia and dysregulated appetite (obesity)	P32247	BRS3	Bombesin receptor subtype-3
Hyperphagia and dysregulated appetite (obesity)	P01275	GLUC	Glucagon
Hyperphagia and dysregulated appetite (obesity)	P06727	APOA4	Apolipoprotein A-IV
Hyperphagia and dysregulated appetite (obesity)	P41159	LEP	Leptin
Hyperphagia and dysregulated appetite (obesity)	P48357	LEPR	Leptin receptor
Hyperphagia and dysregulated appetite (obesity)	P20382	MCH	Pro-MCH
Hyperphagia and dysregulated appetite (obesity)	Q99705	MCHR1	Melanin-concentrating hormone receptor 1
Hyperphagia and dysregulated appetite (obesity)	Q9UBU3	GHRL	Appetite-regulating hormone
Hyperphagia and dysregulated appetite (obesity)	P01303	NPY	Pro-neuropeptide Y
Hyperphagia and dysregulated appetite (obesity)	P83859	OX26	Orexigenic neuropeptide QRFP
Hyperphagia and dysregulated appetite (obesity)	Q96P65	QRFPR	Pyroglutamylated RFamide peptide receptor
Hyperphagia and dysregulated appetite (obesity)	P50391	NPY4R	Neuropeptide Y receptor type 4
Hyperphagia and dysregulated appetite (obesity)	P32245	MC4R	Melanocortin receptor 4
Hyperphagia and dysregulated appetite (obesity)	P41968	MC3R	Melanocortin receptor 3
Hyperphagia and dysregulated appetite (obesity)	P21554	CNR1	Cannabinoid receptor 1
Hyperphagia and dysregulated appetite (obesity)	O00519	FAAH1	Fatty-acid amide hydrolase 1
Hyperphagia and dysregulated appetite (obesity)	P48546	GIPR	Gastric inhibitory polypeptide receptor

Hyperphagia and dysregulated appetite (obesity)	O60674	JAK2	Tyrosine-protein kinase JAK2
Hyperphagia and dysregulated appetite (obesity)	P03372	ESR1	Estrogen receptor
Hyperphagia and dysregulated appetite (obesity)	P54646	AAPK2	5'-AMP-activated protein kinase catalytic subunit alpha-2
Hyperphagia and dysregulated appetite (obesity)	P23560	BDNF	Brain-derived neurotrophic factor (Abrineurin)
Hyperphagia and dysregulated appetite (obesity)	Q16620	NTRK2	BDNF/NT-3 growth factors receptor
Hyperphagia and dysregulated appetite (obesity)	P31645	SC6A4	Sodium-dependent serotonin transporter
Hyperphagia and dysregulated appetite (obesity)	P08913	ADA2A	Alpha-2A adrenergic receptor
Hyperphagia and dysregulated appetite (obesity)	P18825	ADA2C	Alpha-2C adrenergic receptor
Hyperphagia and dysregulated appetite (obesity)	P18089	ADA2B	Alpha-2B adrenergic receptor
Hyperphagia and dysregulated appetite (obesity)	P35348	ADA1A	Alpha-1A adrenergic receptor
Hyperphagia and dysregulated appetite (obesity)	P35368	ADA1B	Alpha-1B adrenergic receptor
Hyperphagia and dysregulated appetite (obesity)	P08588	ADRB1	Beta-1 adrenergic receptor
Hyperphagia and dysregulated appetite (obesity)	P25100	ADA1D	Alpha-1D adrenergic receptor
Hyperphagia and dysregulated appetite (obesity)	P07550	ADRB2	Beta-2 adrenergic receptor
Hyperphagia and dysregulated appetite (obesity)	P06850	CRF	Corticoliberin
Hyperphagia and dysregulated appetite (obesity)	P30559	OXYR	Oxytocin receptor (OT-R)
Hyperphagia and dysregulated appetite (obesity)	P01213	PDYN	Proenkephalin-B
Hyperphagia and dysregulated appetite (obesity)	P14867	GBRA1	Gamma-aminobutyric acid receptor subunit alpha-1

Hyperphagia and dysregulated appetite (obesity)	P35372	OPRM	Mu-type opioid receptor
Hyperphagia and dysregulated appetite (obesity)	P31644	GBRA5	Gamma-aminobutyric acid receptor subunit alpha-5
Hyperphagia and dysregulated appetite (obesity)	P48169	GBRA4	Gamma-aminobutyric acid receptor subunit alpha-4
Hyperphagia and dysregulated appetite (obesity)	Q16445	GBRA6	Gamma-aminobutyric acid receptor subunit alpha-6
Hyperphagia and dysregulated appetite (obesity)	P47869	GBRA2	Gamma-aminobutyric acid receptor subunit alpha-2
Hyperphagia and dysregulated appetite (obesity)	P34903	GBRA3	Gamma-aminobutyric acid receptor subunit alpha-3
Hyperphagia and dysregulated appetite (obesity)	P28472	GBRB3	Gamma-aminobutyric acid receptor subunit beta-3
Hyperphagia and dysregulated appetite (obesity)	P47870	GBRB2	Gamma-aminobutyric acid receptor subunit beta-2
Hyperphagia and dysregulated appetite (obesity)	P18505	GBRB1	Gamma-aminobutyric acid receptor subunit beta-1
Hyperphagia and dysregulated appetite (obesity)	P35367	HRH1	Histamine H1 receptor
Hyperphagia and dysregulated appetite (obesity)	P01189	COLI	Pro-opiomelanocortin (POMC)
Hyperphagia and dysregulated appetite (obesity)	P34972	CNR2	Cannabinoid receptor 2
Hyperphagia and dysregulated appetite (obesity)	P42345	MTOR	Serine/threonine-protein kinase mTOR
Hyperphagia and dysregulated appetite (obesity)	P01266	THYG	Thyroglobulin (Tg)
Hyperphagia and dysregulated appetite (obesity)	P29120	NEC1	Neuroendocrine convertase 1
Hyperphagia and dysregulated appetite (obesity)	Q9NRF2	SH2B1	SH2B adapter protein 1
Hyperphagia and dysregulated appetite (obesity)	P81133	SIM1	Single-minded homolog 1
Hyperphagia and dysregulated appetite (obesity)	Q9BXC9	BBS2	Bardet-Biedl syndrome 2 protein

Hyperphagia and dysregulated appetite (obesity)	Q96RK4	BBS4	Bardet-Biedl syndrome 4 protein
Hyperphagia and dysregulated appetite (obesity)	Q9NPJ1	MKKS	McKusick-Kaufman/Bardet-Biedl syndromes putative chaperonin
Hyperphagia and dysregulated appetite (obesity)	Q86TI0	TBCD1	TBC1 domain family member 1
Hyperphagia and dysregulated appetite (obesity)	Q9C0B1	FTO	Alpha-ketoglutarate-dependent dioxygenase FTO
Hyperphagia and dysregulated appetite (obesity)	P78415	IRX3	Iroquois-class homeodomain protein IRX-3
Hyperphagia and dysregulated appetite (obesity)	O15118	NPC1	Niemann-Pick C1 protein
Hyperphagia and dysregulated appetite (obesity)	P41161	ETV5	ETS translocation variant 5
Hyperphagia and dysregulated appetite (obesity)	Q7Z3B1	NEGR1	Neuronal growth regulator 1
Hyperphagia and dysregulated appetite (obesity)	Q5NUL3	FFAR4	Free fatty acid receptor 4
Hyperphagia and dysregulated appetite (obesity)	Q6VAB6	KSR2	Kinase suppressor of Ras 2
Hyperphagia and dysregulated appetite (obesity)	Q99932	SPAG8	Sperm-associated antigen 8
Hyperphagia and dysregulated appetite (obesity)	P04150	GCR	Glucocorticoid receptor
Hyperphagia and dysregulated appetite (obesity)	P01375	TNFA	Tumor necrosis factor (Cachectin) (TNF-alpha)
Hyperphagia and dysregulated appetite (obesity)	P40763	STAT3	Signal transducer and activator of transcription 3
Hyperphagia and dysregulated appetite (obesity)	O14543	SOCS3	Suppressor of cytokine signaling 3
Hyperphagia and dysregulated appetite (obesity)	O14920	IKKB	Inhibitor of nuclear factor kappa-B kinase subunit beta
Hyperphagia and dysregulated appetite (obesity)	O95352	ATG7	Ubiquitin-like modifier-activating enzyme
White adipose tissue formation (obesity)	P37231	PPARG	Peroxisome proliferator-activated receptor gamma
White adipose tissue formation (obesity)	P17931	LEG3	Galectin-3

White adipose tissue formation (obesity)	Q15672	TWST1	Twist-related protein 1
White adipose tissue formation (obesity)	Q9NZC2	TREM2	Triggering receptor expressed on myeloid cells 2
White adipose tissue formation (obesity)	O60240	PLIN1	Perilipin-1
Cardiomyocyte cell death (heart failure)	P35228	NOS2	Nitric oxide synthase, inducible
Cardiomyocyte cell death (heart failure)	O00165	HAX1	HCLS1-associated protein X-1
Cardiomyocyte cell death (heart failure)	P30405	PPIF	Peptidyl-prolyl cis-trans isomerase F, mitochondrial; Cyclophilin D
Cardiomyocyte cell death (heart failure)	P21796	VDAC1	Voltage-dependent anion-selective channel protein 1
Cardiomyocyte cell death (heart failure)	P45880	VDAC2	Voltage-dependent anion-selective channel protein 2
Cardiomyocyte cell death (heart failure)	Q9Y277	VDAC3	Voltage-dependent anion-selective channel protein 3
Cardiomyocyte cell death (heart failure)	P12235	ADT1	ADP/ATP translocase 1
Cardiomyocyte cell death (heart failure)	P05141	ADT2	ADP/ATP translocase 2
Cardiomyocyte cell death (heart failure)	P12236	ADT3	ADP/ATP translocase 3
Cardiomyocyte cell death (heart failure)	Q9H0C2	ADT4	ADP/ATP translocase 4
Cardiomyocyte cell death (heart failure)	P49841	GSK3B	Glycogen synthase kinase-3 beta
Cardiomyocyte cell death (heart failure)	P25445	TNR6	Tumor necrosis factor receptor superfamily member 6
Cardiomyocyte cell death (heart failure)	P48023	TNFL6	Tumor necrosis factor ligand superfamily member 6
Cardiomyocyte cell death (heart failure)	P50591	TNF10	Tumor necrosis factor ligand superfamily member 10
Cardiomyocyte cell death (heart failure)	Q13158	FADD	FAS-associated death domain protein
Cardiomyocyte cell death (heart failure)	Q15628	TRADD	Tumor necrosis factor receptor type 1-associated DEATH domain protein
Cardiomyocyte cell death (heart failure)	Q14790	CASP8	Caspase-8
Cardiomyocyte cell death (heart failure)	P42574	CASP3	Caspase-3
Cardiomyocyte cell death (heart failure)	P10415	BCL2	Apoptosis regulator Bcl-2
Cardiomyocyte cell death (heart failure)	Q07812	BAX	Apoptosis regulator BAX
Cardiomyocyte cell death (heart failure)	Q99683	M3K5	Mitogen-activated protein kinase kinase kinase 5
Cardiomyocyte cell death (heart failure)	P31152	MAPK4	Mitogen-activated protein kinase 4
Cardiomyocyte cell death (heart failure)	Q16659	MAPK6	Mitogen-activated protein kinase 6
Cardiomyocyte cell death (heart failure)	P55957	BID	BH3-interacting domain death agonist
Cardiomyocyte cell death (heart failure)	P98170	XIAP	E3 ubiquitin-protein ligase XIAP

Cardiomyocyte cell death (heart failure)	Q13490	BIRC2	Baculoviral IAP repeat-containing protein 2
Cardiomyocyte cell death (heart failure)	O15392	BIRC5	Baculoviral IAP repeat-containing protein 5 / survivin
Cardiomyocyte cell death (heart failure)	Q9NR28	DBLOH	Diablo homolog, mitochondrial
Cardiomyocyte cell death (heart failure)	O43464	HTRA2	Serine protease HTRA2, mitochondrial
Cardiomyocyte cell death (heart failure)	Q811U4	MFN1	Mitofusin-1
Cardiomyocyte cell death (heart failure)	Q07820	MCL1	Induced myeloid leukemia cell differentiation protein Mcl-1
Cardiomyocyte cell death (heart failure)	Q92934	BAD	Bcl2-associated agonist of cell death
Cardiomyocyte cell death (heart failure)	P04637	P53	Cellular tumor antigen p53
Cardiomyocyte cell death (heart failure)	P29466	CASP1	Caspase-1
Cardiomyocyte cell death (heart failure)	P13473	LAMP2	Lysosome-associated membrane glycoprotein 2
Cardiomyocyte cell death (heart failure)	Q9H1Y0	ATG5	Autophagy protein 5
Cardiomyocyte cell death (heart failure)	O75385	ULK1	Serine/threonine-protein kinase ULK1
Cardiomyocyte cell death (heart failure)	P49815	TSC2	Tuberin
Cardiomyocyte cell death (heart failure)	Q8N122	RPTOR	Regulatory-associated protein of mTOR
Cardiomyocyte cell death (heart failure)	Q14457	BECN1	Beclin-1
Cardiomyocyte cell death (heart failure)	Q12983	BNIP3	BCL2/adenovirus E1B 19 kDa protein-interacting protein 3
Cardiomyocyte cell death (heart failure)	O00429	DNM1L	Dynamin-1-like protein
Cardiomyocyte cell death (heart failure)	P12644	BMP4	Bone morphogenetic protein 4
Cardiomyocyte cell death (heart failure)	O95140	MFN2	Mitofusin-2
Heart hypertrophy (heart failure)	Q9UBK2	PRGC1	Peroxisome proliferator-activated receptor gamma coactivator 1-α
Heart hypertrophy (heart failure)	P06396	GELS	Gelsolin
Heart hypertrophy (heart failure)	P49238	CX3C1	CX3C chemokine receptor 1
Heart hypertrophy (heart failure)	P78423	X3CL1	Fractalkine
Heart hypertrophy (heart failure)	P49116	NR2C2	Nuclear receptor subfamily 2 group C member 2
Heart hypertrophy (heart failure)	P63098	CANB1	Calcineurin subunit B type 1
Heart hypertrophy (heart failure)	Q96LZ3	CANB2	Calcineurin subunit B type 2
Heart hypertrophy (heart failure)	P00533	EGFR	epidermal growth factor receptor
Heart hypertrophy (heart failure)	P09038	FGF2	Fibroblast growth factor 2 / Basic fibroblast growth factor

Heart hypertrophy (heart failure)	Q14571	ITPR2	Inositol 1,4,5-trisphosphate receptor type 2
Heart hypertrophy (heart failure)	P03956	MMP1	Matrix metalloproteinase-1
Heart hypertrophy (heart failure)	P28482	MAPK1	Mitogen-activated protein kinase 1
Heart hypertrophy (heart failure)	P27361	MAPK3	Mitogen-activated protein kinase 3
Heart hypertrophy (heart failure)	Q99836	MYD88	Myeloid differentiation primary response protein MyD88
Heart hypertrophy (heart failure)	P29474	NOS3	Nitric oxide synthase, endothelial
Heart hypertrophy (heart failure)	O95644	NFAC1	Nuclear factor of activated T-cells 1
Heart hypertrophy (heart failure)	Q13469	NFAC2	Nuclear factor of activated T-cells 2
Heart hypertrophy (heart failure)	Q12968	NFAC3	Nuclear factor of activated T-cells 3
Heart hypertrophy (heart failure)	Q14934	NFAC4	Nuclear factor of activated T-cells 4
Heart hypertrophy (heart failure)	P61296	HAND2	Heart- and neural crest derivatives-expressed protein 2
Heart hypertrophy (heart failure)	P05121	PAI1	Plasminogen activator inhibitor 1
Heart hypertrophy (heart failure)	Q15418	KS6A1	Ribosomal protein S6 kinase alpha-1 (p90RSK)
Heart hypertrophy (heart failure)	Q15349	KS6A2	Ribosomal protein S6 kinase alpha-2 (p90RSK)
Heart hypertrophy (heart failure)	P51812	KS6A3	Ribosomal protein S6 kinase alpha-3 (p90RSK)
Heart hypertrophy (heart failure)	Q08209	PP2BA	Serine/threonine-protein phosphatase 2B catalytic subunit α isoform
Heart hypertrophy (heart failure)	P16298	PP2BB	Serine/threonine-protein phosphatase 2B catalytic subunit βisoform
Heart hypertrophy (heart failure)	P48454	PP2BC	Serine/threonine-protein phosphatase 2B catalytic subunit γ isoform
Heart hypertrophy (heart failure)	Q9UBN4	TRPC4	Short transient receptor potential channel 4
Heart hypertrophy (heart failure)	P32418	NAC1	Sodium/calcium exchanger 1
Heart hypertrophy (heart failure)	P30556	AGTR1	Type-1 angiotensin II receptor
Inflammation (heart failure)	P13500	CCL2	C-C motif chemokine 2
Inflammation (heart failure)	P16581	LYAM2	E-selectin
Inflammation (heart failure)	P05362	ICAM1	Intercellular adhesion molecule 1
Inflammation (heart failure)	P01584	IL1B	Interleukin 1 beta
Inflammation (heart failure)	Q14116	IL18	Interleukin 18
Inflammation (heart failure)	P05231	IL6	Interleukin 6
Inflammation (heart failure)	P19320	VCAM1	Vascular cell adhesion protein 1
Inflammation (heart failure)	P04275	VWF	von Willebrand factor
Oxidative stress (heart failure)	Q9NSA1	FGF21	Fibroblast growth factor 21
Oxidative stress (heart failure)	P04839	CY24B	NADPH oxidase 2
Oxidative stress (heart failure)	Q9NPH5	NOX4	NADPH oxidase 4

Oxidative stress (heart failure)	Q15848	ADIPO	Adiponectin
Inefficient myocardial fuel metabolism (heart failure)	O14734	ACOT8	Acyl-coenzyme A thioesterase 8
Inefficient myocardial fuel metabolism (heart failure)	O75521	ECI2	Enoyl-CoA delta isomerase 2, mitochondrial
Inefficient myocardial fuel metabolism (heart failure)	Q03181	PPARD	Peroxisome proliferator-activated receptor delta
Inefficient myocardial fuel metabolism (heart failure)	Q8NCC3	PAG15	Group XV phospholipase A2
Inefficient myocardial fuel metabolism (heart failure)	P24752	THIL	Acetyl-CoA acetyltransferase, mitochondrial
Inefficient myocardial fuel metabolism (heart failure)	P55809	SCOT1	Succinyl-CoA:3-ketoacid coenzyme A transferase 1, mitochondrial
Inefficient myocardial fuel metabolism (heart failure)	Q02338	BDH	D-beta-hydroxybutyrate dehydrogenase, mitochondrial

Supplementary Table 9. List of all the proteins included in the analysis. A total of 280 proteins have been included in the prediction of the mechanism of action of empagliflozin. Each protein has a Uniprot ID code associated to standardize the nomenclature.

Transcript	*Forward primer (5' – 3')*	*Reverse primer (5' – 3')*
BIRC5	GCATAGGAAGCACTCCCCTG	CCTGGAAAGCTGGGACAAGT
XIAP	TATGACGCACGGATCGTTAC	CACCCTGGATACCACTTAGC
36B4	GTTGCCTCAGTGCCTCACTC	GCAGCCGCAAATGCAGATGG

Supplementary Table 10. List of primers used in this study.

MoA PROTEIN A		MoA PROTEIN B		REFERENCE
Entry name	Uniprot code	Entry name	Uniprot code	
BIRC5	O15392	Heart failure		PMID: 19919994
NHE1	P19634	Heart failure		PMID: 23909633 PMID: 24080184 PMID: 23429007
NHE1	P19634	Heart failure		PMID: 22803959
NHE1	P19634	AKT1	P31749	PMID: 19028724
NHE1	P19634	AKT2	P31751	PMID: 19028724
NHE1	P19634	AKT3	Q9Y243	PMID: 19028724
MAPK3	P27361	NHE1	P19634	PMID: 11807182
MAPK3	P27361	NOS2	P35228	PMID: 16283237
MAPK3	P27361	RPTOR	Q8N122	PMID: 21071439
MAPK1	P28482	NHE1	P19634	PMID: 11807182
MAPK1	P28482	NOS2	P35228	PMID: 16283237
NOS2	P35228	Heart failure		PMID: 29311992
XIAP	P98170	Heart failure		PMID: 19919994
BIRC2	Q13490	BIRC5	O15392	PMID: 15665297
BIRC2	Q13490	XIAP	P98170	PMID: 18414036
RPTOR	Q8N122	Heart failure		PMID: 24859226
EMPAGLIFLOZIN		NHE1	P19634	Drug target
AKT1	P31749	MAPK3	P27361	KEGG: map04371
AKT2	P31751	MAPK3	P27361	KEGG: map04371
AKT3	Q9Y243	MAPK3	P27361	KEGG: map04371
AKT1	P31749	MAPK1	P28482	KEGG: map04371
AKT2	P31751	MAPK1	P28482	KEGG: map04371
AKT3	Q9Y243	MAPK1	P28482	KEGG: map04371
AKT1	P31749	NOS2	P35228	PMID: 28067899
AKT2	P31751	NOS2	P35228	PMID: 28067899
AKT3	Q9Y243	NOS2	P35228	PMID: 28067899
AKT1	P31749	BIRC2	Q13490	KEGG: map01524 PMID: 29769618
AKT2	P31751	BIRC2	Q13490	PMID: 29769618
AKT3	Q9Y243	BIRC2	Q13490	PMID: 29769618
AKT1	P31749	RPTOR	Q8N122	PMID: 21339740 PMID: 26160839 KEGG: map04211
AKT2	P31751	RPTOR	Q8N122	PMID: 21339740 PMID: 26160839 KEGG: map04211
AKT3	Q9Y243	RPTOR	Q8N122	PMID: 21339740 PMID: 26160839 KEGG: map04211
MAPK1	P28482	RPTOR	Q8N122	PMID: 21071439
MAPK1	P28482	LEP	A4D0Y8	PMID: 19688109
MAPK3	P27361	LEP	A4D0Y8	PMID: 19688109
LEP	A4D0Y8	NOS2	P35228	PMID: 19688109
CaN	Q08209	CaM	P0DP23	PMID: 22100452
CaM	P0DP23	CaMKII	Q96RR4	PMID: 14722083
NOS2	P35228	CaMKII	Q96RR4	PMID: 24498331
CaN	Q08209	Heart Failure		PMID: 15336966 PMID: 12015416 PMID: 10086361
CAMKII	Q96RR4	Heart Failure		PMID: 23877259 PMID: 21276796 PMID: 18218981

Supplementary Table 11. Description of each link depicted in Figure 24. MoA Protein A refers to the mechanism

Funding

Oriol Iborra Egea performed his thesis thanks to a public competitive grant, State Program for the Promotion of Talent, supported by the Spanish Ministry of Economy and competitiveness-MINECO (SAF2014-59892-R), reference BES-2015-074991-FPI GRANT 2015-2019.

The group is, or has been, supported in part by multiple agencies that provide funding for research purposes: Spanish Ministry of Economy and competitiveness-MINECO (SAF2014-59892-R and SAF2017-84324-C2-1-R), Fundació La MARATÓ de TV3 (201502-30 and 201516-10), CIBER Cardiovascular (CB16/11/00403), as part of the Plan Nacional de I+D+I, and co-funded by ISCIII-Subdirección General de evaluación and the Fondo Europeo de Desarrollo Nacional (FEDER), “La Caixa” banking foundation, Sociedad Española de Cardiologia, Societat Catalana de Cardiologia, SGR programme from the Generalitat de Catalunya (2017-SGR-483), , Instituto de Salut Carlos III: FIS grants (PI14/01682 and PI17/01487), the Redes temáticas de investigación cooperativa en salud (RETICS): Red de Terápia Celular-TerCel (RD12/0019/0029 and RD16/00111/0006). This work has been developed in the context of CERCA Programme (Generalitat de Catalunya) and AdvanceCat, with the support of ACCIÓ (Catalonia Trade &Investment; Generalitat de Catalunya).

List of publications

Publications are listed by chronological order, sorted by most recent. Of these, there is one complementary work performed during the PhD that is not included directly in the thesis but is worth being highlighted. This accounts for the discovery and molecular exploration of the CS4P score using advanced proteomics, which is extensively discussed in **molecular signature of cardiogenic shock**.

1. Oriol Iborra-Egea, Ferran Rueda, Cosme García-García, Eva Borràs, Eduard Sabidó, Antoni Bayes-Genis. **Molecular Signature of Cardiogenic Shock.** European Heart Journal 2019. *Accepted for publication.*

2. Oriol Iborra-Egea, Evelyn Santiago-Vacas, Salva R. Yurista, Josep Lupón, Milton Packer, Stephane Heymans, Faiez Zannad, Javed Butler, Domingo Pascual-Figal, Antonio Lax, Julio Núñez, Rudolf A. de Boer, Antoni Bayés-Genís. **Unravelling the molecular mechanism of action of empagliflozin in heart failure with reduced ejection fraction with or without diabetes.** JAAC: Basic to Translational Science. *Accepted for publication 2019.*

3. Ferran Rueda, Eva Borràs, Cosme García-García, Oriol Iborra-Egea, Elena Revuelta-López, Veli-Pekka Harjola, Germán Cediel, Johan Lassus, Tuukka Tarvasmäki, Alexandre Mebazaa, Eduard Sabidó, Antoni Bayés-Genís. **Protein-based cardiogenic shock patient classifier.** European Heart Journal 40 (32); 2684–2694, 21 August 2019. doi: 10.1093/eurheartj/ehz294

In this work, we used mass spectrometry analysis of 2654 proteins for screening in the Barcelona discovery cohort (n = 48). Subsequently, we employed targeted quantitative proteomics analyses (n = 51 proteins) in the independent CardShock cohort (n = 97) to derive and cross-validate the

protein classifier. Thus we discovered that the combination of four circulating proteins (Cardiogenic Shock 4 proteins—CS4P), discriminated patients with low and high 90-day risk of mortality. To our enthusiasm, CS4P improved predictive metrics in combination with contemporary risk scores, which may guide clinicians in selecting patients for advanced therapies in the near future.

4. Oriol Iborra-Egea, Ferran Rueda, Päivi Lakkisto, Veli-Pekka Harjola, Cosme García-García, Antoni Bayes-Genis. **Circulating MiRNA Dynamics in ST-Segment Elevation Myocardial Infarction-driven Cardiogenic Shock.** Revista Española de Cardiología 72 (9); 783-786, September 2019. doi: 10.1016/j.rec.2018.10.008.

5. Isaac Perea-Gil, Carolina Gálvez-Montón, Cristina Prat-Vidal, Ignasi Jorba, Cristina Segú-Vergés, Santiago Roura, Carolina Soler-Botija, Oriol Iborra-Egea, Elena Revuelta-López, Marco A. Fernández, Ramon Farré, Daniel Navajas, Antoni Bayes-Genis. **Head-to-head comparison of two engineered cardiac grafts for myocardial repair: From scaffold characterization to pre-clinical testing.** Scientific Reports 8(1); 6708, April 30 2018. doi: 10.1038/s41598-018-25115-2.

6. Carolina Galvez-Monton, Isaac Perea-Gil, Carolina Soler-Botija, Cristina Prat-Vidal, Idoia Díaz-Güemes, Oriol Iborra-Egea, Verónica Crisóstomo, Francisco M.Sánchez-Margallo, Santiago Roura, Antoni Bayes-Genis. **P2562 Comparison between two different natural decellularized scaffolds after myocardial**

infarction in swine. European Heart Journal 38(suppl_1), August 2017, ehx502.P2562. doi: 10.1093/eurheartj/ehx502.P2562.

7. Cristina Prat-Vidal, Isaac Perea-Gil, Ignasi Jorba, Carolina Galvez-Monton, Carolina Soler-Botija, Oriol Iborra-Egea, Elena Revuelta-Lopez, Santiago Roura, Ramon Farre, Daniel Navajas, Antoni Bayes-Genis. **P4464 An acellular myocardial scaffold optimal for cardiac recovery: proteomic, structural and mechanical characterization.** European Heart Journal 38(suppl_1), August 2017, ehx504.P4464. doi: 10.1093/eurheartj/ehx504.P4464

8. Carolina Gálvez-Montón, Carolina Soler-Botija, Oriol Iborra-Egea, Idoia Díaz-Güemes, Mercè Martí, Olalla Iglesias-García, Cristina Prat-Vidal, Veronica Crisóstomo V, Aida Llucià-Valldeperas, Isaac Perea-Gil, Santiago Roura, Francisco M. Sánchez-Margallo, Ángel Raya, Antoni Bayes-Genis. **Preclinical Safety Evaluation of Allogeneic Induced Pluripotent Stem Cell-Based Therapy in a Swine Model of Myocardial Infarction.** Tissue Engineering Part C Methods (11):736-744, 23 November 2017. doi: 10.1089/ten.TEC.2017.0156

9. Santiago Roura, Carolina Gálvez-Montón, David de Gonzalo-Calvo, Ana Gámez Valero, Paloma Gastelurrutia, Elena Revuelta-López, Cristina Prat-Vidal, Carolina Soler-Botija, Aida Llucià-Valldeperas, Isaac Perea-Gil, Oriol Iborra-Egea, Francesc E. Borràs, Josep Lupón, Vicenta Llorente-Cortés, Antoni Bayes-Genis. **Extracellular vesicles do not contribute to higher circulating levels of soluble LRP1 in idiopathic dilated cardiomyopathy.** Journal of Cellular and Molecular Medicine (11):3000-3009, 29 May 2017. doi: 10.1111/jcmm.13211.

10. Oriol Iborra-Egea, Carolina Gálvez-Montón, Santiago Roura, Isaac Perea-Gil, Cristina Prat-Vidal, Carolina Soler-Botija, Antoni Bayes-Genis. **Mechanisms of action of sacubitril/valsartan on cardiac remodeling: a systems biology approach.** Nature Systems Biology and Applications 3: 12, 18 April 2017. doi: 10.1038/s41540-017-0013-4.

11. Isaac Perea-Gil, Cristina Prat-Vidal, Carolina Gálvez-Montón, Santiago Roura, Aida Llucià-Valldeperas, Carolina Soler-Botija, Oriol Iborra-Egea, Idoia Díaz-Güemes, Verónica Crisóstomo, Francisco M.Sánchez-Margallo, Antoni Bayes-Genis. **A Cell-Enriched Engineered Myocardial Graft Limits Infarct Size and Improves Cardiac Function: Pre-Clinical Study in the Porcine Myocardial Infarction Model.** JACC: Basic to Translational Science 1(5); 360-372, 29 August 2016. doi: 10.1016/j.jacbts.2016.06.005.

Manuscripts submitted or under review

1. Oriol Iborra-Egea, Carolina Gálvez-Montón, Cristina Prat-Vidal, Santiago Roura, Carolina Soler-Botija, Elena Revuelta-López, Adriana Cserkoova, Pol Gomez-Puchades, Paloma Gastelurrutia, Antoni Bayes-Genis. **Evolution of post-myocardial infarction remodeling towards heart failure: a complete molecular characterization.** *Submitted.*
2. Alexander Heyde, Jeffrey M. Gerold, David Rohde, Friedrich F. Hoyer, David Cheek, Katrien Vandoorne, Oriol Iborra-Egea, Christian Muñoz-Guijosa, Antoni Bayes-Genis, Johannes Reiter, Morgan Craig, Matthias Nahrendorf, Martin A. Nowak, KamilaNaxerova. **Atherosclerosis accelerates clonal hematopoiesis by increasing stem cell turnover.** *Subbmitted.*

Congress Communications

- Iborra-Egea, O et al. Descobrint el mecanisme d'acció molecular de l'empagliflozina en insuficiència cardíaca amb fracció d'ejecció reduïda amb o sense diabetis. 31st Congress of the Catalan Society of Cardiology 2019, Barcelona, Spain.
- Iborra-Egea, O et al. Unravelling the molecular mechanism of action of empagliflozin in heart failure with reduced ejection fraction with or without diabetes. HOMAGE annual meeting 2019, Barcelona, Spain.
- Iborra-Egea, O et al. Protein-based molecular panel for cardiogenic shock. B-debate clinical proteomics: towards personalized medicine and health, October 2018, Barcelona, Spain.
- Iborra-Egea, O et al. Evaluation of the inflammatory response induced by engineered bioscaffolds of allogeneic porcine iPS implanted in a swine model of myocardial infarction. Baltic Conference Series 2017, Stockholm, Sweden and Helsinki, Finland
- Gálvez-Montón, C et al. Head-to-head comparison of two biological acellular scaffolds for myocardial repair: a pre-clinical myocardial infarction swine model. Baltic Conference Series 2017, Stockholm, Sweden and Helsinki, Finland.
- Prat-Vidal, C et al. An acellular myocardial scaffold optimal for cardiac recovery: proteomic, structural and mechanical characterization. European Society of Cardiology Congress 2017, Barcelona, Spain.
- Gálvez-Montón, C et al. Head-to-head comparison of two biological acellular scaffolds for myocardial repair: a pre-clinical myocardial infarction swine model. European Society of Cardiology Congress 2017, Barcelona, Spain.

- Iborra-Egea, O et al. Mechanisms of action of sacubitril/valsartan on cardiac remodeling: a systems biology approach. 24th Molecular Biology Meeting 2017, Catalan Society of Biology, Barcelona, Spain.
- Iborra-Egea, O et al. Mechanisms of action of sacubitril/valsartan on cardiac remodeling: a systems biology approach. 4th World Congress on Acute Heart Failure, 2017, Paris, France.
- Roura, S et al. Idiopathic dilated cardiomyopathy shows increased circulating levels of soluble low-density lipoprotein receptor-related protein 1. 4th World Congress on Acute Heart Failure, 2017, Paris, France.
- Gálvez-Montón, C et al. Head-to-head comparison of two biological acellular scaffolds for myocardial repair: a pre-clinical myocardial infarction swine model. 4th World Congress on Acute Heart Failure, 2017, Paris, France.
- Iborra-Egea, O et al. Mecanisme d'acció de sacubitril/valsartan en el remodelat cardíac: un estudi de biologia de sistemes. 29th Congress of the Catalan Society of Cardiology, Barcelona, Spain.
- Gálvez-Montón et al. Anàlisi Comparativa de dos matrius acel·lulars per a la reparació miocardíaca en el model pre-clínic d'infart de miocardi. 29th Congress of the Catalan Society of Cardiology, Barcelona, Spain.
- Iborra-Egea, O et al. Mechanisms of action of sacubitril/valsartan on cardiac remodeling: a systems biology approach. 4th Bioinformatics and Genomics Symposium, 2016, Barcelona, Spain.
- Iborra-Egea, O et al. Evaluation of the inflammatory response induced by engineered bioscaffolds of allogeneic porcine iPS implanted in a swine model of myocardial infarction. 23th Molecular Biology Meeting 2016, Catalan Society of Biology, Barcelona, Spain.

Seminars and Workshops

- CRISPR innovation: to take you to the next level, September 2017. ThermoFisher scientific, Barcelona, Spain
- Barcelona Biotech Breakfast: Applying AI in drug discovery and development. June 2019, Barcelona, Spain.

National and International Scientific congresses

- 23th Molecular Biology Meeting, June 2016, Catalan Society of Biology, Barcelona, Spain.
- 4th Bioinformatics and Genomics Symposium, December 2016, Barcelona, Spain.
- European Society of Cardiology Congress, May 2017, Barcelona, Spain.
- 29th Congress of the Catalan Society of Cardiology, June 2017, Barcelona, Spain.
- 24th Molecular Biology Meeting, June 2017, Catalan Society of Biology, Barcelona, Spain.
- Baltic Conference Series, October 2017, Stockholm, Sweden and Helsinki, Finland.
- Reunión Anual de la Red de Terapia Celular (TerCel), November 2017, ISCIII Madrid, Spain.
- 30th Congress of the Catalan Society of Cardiology June 2018, Barcelona, Spain.
- B-debate clinical proteomics: towards personalized medicine and health, October 2018, Barcelona, Spain.
- Reunión Anual de la Red de Terapia Celular (TerCel), November 2018, Pamplona, Spain.
- HOMAGE annual meeting May 2019, Barcelona, Spain.

- 31st Congress of the Catalan Society of Cardiology June 2019, Barcelona, Spain.

Memberships

- Chief Executive and Board of Directors at the Catalan Society of Biology
- Member of RETICS (Cell Therapy Network) TERCEL (RD12/0019/0029) January 2016 – Present
- Member of ADVANCE(CAT)

  January 2016 – Present
- Member of the International Association of Advanced Materials (IAAM) (nº9110311343110)

  October 2017- Present

Awards

- Immunotools Special Award 2017
- Young Scientist Award at the BCS 2017 in Sweden and Finland
- 3rd Best poster at the 4th Bioinformatics and Genomics Symposium (2016)

Patents

- European priority patent (EP 19382126.1), 20 February 2019.

Teaching Activities

- Helena López Martínez. Rewiring the heart. Might endogenous nanocarriers be the ultimate tool to achieve *in vivo* cardiac reprogramming? Bachelor's Degree in Medicine, Final Project – Class 2012 – 2018 Universitat Autònoma de Barcelona.
- Marta Clos Sansalvador. Extracció i sembra de cèl·lules mesenquimals de teixit adipós cardíac de porc (cATMSCs) i aïllament d'exosomes. Bachelor's Degree in Biology, Final Project – Class 2014 – 2018 Universitat de Barcelona.

Clàudia Valls Masoliver. Caracterització de vesícules extracel·lulars de cèl·lules pluripotents induïdes per a la reparació cardíaca. Treball de Recerca 2018